UNIVERSITY OF CALIFORNIA,

IRVINE

# Sexually Dimorphic Synaptic Plasticity: Development and Consequences for Episodic Memory

DISSERTATION

Submitted in partial satisfaction of the requirements

for the degree of

DOCTOR OF PHILOSOPHY

In Biomedical Sciences

By

Aliza Alien Le

Dissertation Committee:

Professor Gary Lynch, Chair

Professor Christine M. Gall

Assistant Professor Lulu Chen

Assistant Professor Javier Diaz Alonso

2023

# DEDICATION

Gửi đến Ba Mẹ, Nguyễn Tố Uyên và Lê Mười:

Sự hy sinh bao la của Ba Mẹ đã ban cho con cơ hội khám phá rất vĩ đại và đưa ngành khoa học thần kinh tiến lên theo cách mà không ai ngờ tới.

And to my brothers, Afelix, Alexan, and Alen who were pivotal to my experiences, which shaped my decisions leading to this dissertation and the findings that will follow.

# TABLE OF CONTENTS

# LIST OF FIGURES

# ACKNOWLEDGEMENTS

To my committee chair and PI, Dr. Gary Lynch: everything that you have taught cannot be contained within this acknowledgement page and is beyond my vocabulary, and it would be insulting to try. I learned so much about science and history, but more importantly, you taught me to understand the past, appreciate the present, and how to be excited about the future. I believe that you are the embodiment of how passion and interest can lead to the bottom of science's Pandora box. You are truly a lover of humanity and nature, for all the good and bad things it has to offer, and I hope to inherit an iota of your genius and personality.

To Dr. Christine Gall: If you hadn't responded to the e-mail or answered the phone back in 2015, I really don't know where I would've been. Maybe in a better or worse future, but I wouldn't trade my experiences here for anything else. Thank you for supporting me at my best and worst and for providing feedback to help me improve on writing and speaking. You are as intensely strict as you are kind, and I am truly honored to work with and be mentored by the 614th best female scientist in the world.

Conor D. Cox: the first person I talked to in lab when I arrived (even before Dr. Gall). He asked if I needed help, and I responded "No I don't need help, thanks." In trying to be independent, it revealed that my bad habit of trying shoulder the responsibilities in lab alone which would ultimately become counter-productive. He became my best moral support through the times in lab and even after he left the lab. I am deeply indebted to him.

Carley Karsten and Kathleen Wang: While Dr. Gall got me in, you convinced me to stay. You were the most interesting and unique people I have ever met, and I had so much fun. Much of my fondest memories were my time working under you two as an undergraduate, and I am so grateful for these memories. Experiences with you have improved me as a person and were one of the driving forces that lead me to today.

Brittney M. Cox: You have such an amazing personality, and I learned how to be more assertive and confident. Despite your brief time in the lab, you have made an impact on everyone you've met, including myself. I am thrilled that you moved on from the addiction field you came from and worked with us. You have carved a future for yourself that makes you happy, and I aspire to be where you are.

Julie Lauterborn: You are a wise and knowledgeable person and have been a phenomenal help and maybe more patient with me than I deserved. I was initially hesitant to accept help because you just seemed so above me, but working with you taught me that the process will go faster and that I can improve faster if I was not so afraid of feedback.

Julian Quintanilla: I was not expecting to have someone joining me in the Lynch lab when I started, but I'm glad you joined us. It was almost uncanny at how similar our backgrounds were, as well as our love for movies and TV shows. I'm grateful to have you as part of my daily life. We were productive and shared a lot of happiness and frustration in the past few years.

Jasmine Chavez: I'm happy you decided to join us, and I am so excited for your journey here. Your arrival felt timely because I felt very jaded and almost forgot what it was like to be excited about things. You have been very enriching to me and the lab environment. I have faith that you have the same (if not better) positive experiences that I did, and you will undoubtedly surpass me and our predecessors.

Lucy Yao: When I joined as an undergrad, I believe we worked together a lot, so it felt like you were there for every step of it. Thank you for being helpful for much of the process-- you are truly indispensable to me and the lab. You're a very sweet and talented person, and I'm happy your 'big boy' and 'little boy' are doing well.

Yousheng Jia: I appreciate all the mentorship you gave me out of your free time (even before I became a graduate student), and I got the impression that you were always looking out for me. Thank you for your help on my projects, and I look forward for future collaborations.

Additional thanks to Linda Palmer, Sandra Gattas, Weisheng Wang, and Mohammad Amani for the collaborations. I also thank my undergraduate students Elaine Nguyen, Elaine Tran, and Giulianna Zelaya for the work you've done for me, and countless others that crossed my path. And thanks to Peter Ju who helped me recently and helped me with tedious tasks (including formatting this document) that saved me so much time. Each of you gave me some insight or habit that I have engrained into my personality.

I also thank my graduate school friends, Thai Nguyen, Elena Dominguez, and Xiaoxiao Lin for being awesome and supportive during my time here.

Financial Support: I thank the NIMH T32 (MH119049-01/ -02), UCI Chancellor's Award, and the Rose Hill Foundation for generously giving me funding which contributed to the completion of this dissertation. Relatedly, thank you Leora Fellus and Manuella Yassa for helping me obtain these fellowships and for giving me some important advice during harder times.

Portions of Chapter 1 are a modification of the material as it appears in Sex Differences in Synaptic Plasticity Underlying Learning, used with permission from the Journal of Neuroscience Research, accessible at https://doi.org/10.1002/jnr.24844. The co-authors listed in this publication are Christine M. Gall and Gary Lynch.

The text from Chapter 2 is a reprint of the material as it appears in Memory-related synaptic plasticity is sexually dimorphic in rodent hippocampus, published by CC BY 4.0 from the Journal of Neuroscience, accessible at https://doi.org/10.1523/JNEUROSCI.0801-18.2018. The co-authors included Weisheng Wang, Bowen Hou, Julie Lauterborn, Conor D. Cox, Ellis Levin, Gary Lynch, and Christine M. Gall. Weisheng Wang directed and supervised research which forms the basis for the dissertation.

The text from Chapter 3 is a reprint of the material as it appears in Prepubescent female rodents have enhanced hippocampal LTP and learning relative to males, reversing in adulthood as inhibition increases, used with permission from Nature Neuroscience, accessible at https://doi.org/10.1038/s41593-021-01001-5. The co-authors included Julie Lauterborn, Yousheng Jia, Weisheng Wang, Conor D. Cox, Christine M. Gall, and Gary Lynch.

# VITA

## Aliza Alien Le

### EDUCATION

2015 Bachelors of Science, Biological Sciences, University of California, Irvine
2023 Doctor of Philosophy, Biomedical Sciences, University of California, Irvine
Advisor: Dr. Gary Lynch, Professor, Departments of Anatomy and Neurobiology and Psychology

### HONORS & AWARDS

2019-2021 NIMH training grant T32 MH119049-01/ -02
2021 UCI Chancellor's Award
2021 SOM Outstanding Graduate Student Research Award (Basic Science)
2021 Anatomy & Neurobiology Grad Day, 1st Place, Graduate Student Research Presentation
2021-22 Rose Hill Foundation Science & Engineering Fellowship

### PUBLICATIONS (* indicates co-authorship)

**Le AA**, Lauterborn JC, Jia Y, Wang W, Cox CD, Gall CM, Lynch G (2022) Prepubescent female rodents have enhanced hippocampal LTP and learning relative to males, reversing in adulthood as inhibition increases. Nat Neurosci 25:180-190.
Selected for Journal Cover and Invited Commentary in Journal Issue:
Tronson, N.C., Puberty reverses sex differences in learning. *Nature Neuroscience.* 2022.

*Wang W, *Cox BM, Jia Y, **Le AA**, Cox CD, Jung KM, Hou B, Piomelli D, Gall CM, Lynch G (2018) Treating a novel plasticity defect rescues episodic memory in Fragile X model mice. Mol Psychiatry 23:1798-1806.

Wang W, **Le AA**, Hou B, Lauterborn JC, Cox CD, Levin ER, Lynch G, Gall CM (2018) Memory-Related Synaptic Plasticity Is Sexually Dimorphic in Rodent Hippocampus. J Neurosci 38:7935-7951.
(Featured for editorial comment in "This week in the Journal" by *J. Neurosci.* Selected as F1000 Prime recommended as being of special significance.)
Selected for the Journal Club feature article:
Baumler E, Strickland L, Privitera L. Molecular Underpinnings of Estradiol-Mediated Sexual Dimorphism of Synaptic Plasticity in the Hippocampus of Rodents. (2019) J Neurosci. 39(12):2160-2. doi: 10.1523/JNEUROSCI.2894-18.2019

Lauterborn JC, Schultz MN, **Le AA**, Amani M, Friedman AE, Leach PT, Gall CM, Lynch GS, Crawley JN (2019) Spaced training improves learning in Ts65Dn and Ube3a mouse

models of intellectual disabilities. Translational Psychiatry 9:166.

*Cox BM, *Cox CD, *Gunn BG, **Le AA**, Inshishian VC, Gall CM, Lynch G (2019) Acquisition of temporal order requires an intact CA3 commissural/associational (C/A) feedback system in mice. Commun Biol 2:251.

Seese RR, **Le AA**, Wang K, Cox CD, Lynch G, Gall CM (2020) A TrkB agonist and ampakine rescue synaptic plasticity and multiple forms of memory in a mouse model of intellectual disability. Neurobiol Dis 134:104604.

Kilinc M, Arora V, Creson TK, Rojas C, **Le AA**, Lauterborn J, Wilkinson B, Hartel N, Graham N, Reich A, Gou G, Araki Y, Bayés À, Coba M, Lynch G, Miller CA, Rumbaugh G (2022) Endogenous Syngap1 alpha splice forms promote cognitive function and seizure protection. Elife 11.

*Amani M, *Lauterborn JC, ***Le AA**, Cox BM, Wang W, Quintanilla J, Cox CD, Gall CM, Lynch G (2021) Rapid Aging in the Perforant Path Projections to the Rodent Dentate Gyrus. J Neurosci 41:2301-2312

Gall CM, **Le AA**, Lynch G (2021) Sex differences in synaptic plasticity underlying learning. J Neurosci Res.

**Le AA**, Quintanilla J, Amani M, Piomelli D, Lynch G, Gall CM (2022) Persistent sexually dimorphic effects of adolescent THC exposure on hippocampal synaptic plasticity and episodic memory in rodents. Neurobiol Dis 162:105565.

Quintanilla J, Jia Y, Lauterborn JC, Pruess BS, **Le AA**, Cox CD, Gall CM, Lynch G, Gunn BG (2022) Novel types of frequency filtering in the lateral perforant path projections to dentate gyrus. J Physiol 600:3865-3896.

Gattas S, **Le AA**, Abadchi JK, Pruess B, Shen Y, Swindlehurst A, Yassa MA, Lynch GS (2022) Signal Transformations and New Timing Rules of Hippocampal CA3 to CA1 Synapses. bioRxiv. 2022.05.26.493588.

Chavez J, **Le AA**, Quintanilla J, Tagne AM, Piomelli D, Lynch G, Gall CM (2022) Microglia Depletion Selectively Eliminates a Singular Form of Hippocampal Long-Term Potentiation. bioRxiv 2022.07.29.501926.

## MEETING PRESENTATIONS

**Le, A.A.,** Quintanilla, J., Amani, M., Piomelli, D., Gall C.M., Lynch, G. Sexually Dimorphic Effects of Adolescent THC on Long-Term Potentiation in Hippocampus. Global Connectome. 2020.

**Le, A.A**. Pubertal Changes in Inhibitory Currents affects Learning Thresholds in Female Rodents. Progress in Neuroscience. 2020.

Cox, B.M., Quintanilla, J., **Le, A.A.**, Mahler, S.V., Gall, C.M., Lynch, G. Cannabinoid (THC) exposure during adolescence has enduring effects on hippocampal plasticity and learning

in females. Program No. 162.21. 2019 Neuroscience Meeting Planner. Chicago, IL: Society of Neuroscience, 2018. Online.

Gall, C.M., Cox, B.M., **Le, A.A.**, Gunn, B.G., Quintanilla, J., Cox, C.D., Lynch, G. Hippocampal field CA3 is necessary for encoding temporal order: A proposed 'when' component of episodic memory. Program No. 689.06. 2019 Neuroscience Meeting Planner. Chicago, IL: Society of Neuroscience, 2018. Online.

**Le, A.A.** Oxytocin rescues hippocampal long-term potentiation and learning in Fmr1-KO mice. UCI Department of Anatomy & Neurobiology Grad Day 2019. May 2019.

**Le, A.A.** Sex and Puberty Influence Synaptic Plasticity and Spatial Learning. UCI CNLM 2019 Spring Conference. April 2019.

**Le, A.A.** Development and sexual dimorphism affects synaptic plasticity in hippocampus. UCI Neuroblitz Talk. March 2019.

**Le, A.A.**, Wang, W., Cox, CD., Lauterborn, JC., Levin, ER., Lynch, G., Gall, CM. Mechanisms of hippocampal long-term potentiation (LTP) are sexually dimorphic in rodents. Program No. 374.14. 2018 Neuroscience Meeting Planner. San Diego, CA: Society for Neuroscience, 2018. Online.

Cox, BM., **Le, A.A.**, Gunn, BG., Cox C.D., Hadidi NR., Quintanilla J., Lynch G., Gall CM. Identification of hippocampal subfields responsible for components of episodic memory. Program No. 324.09. 2018 Neuroscience Meeting Planner. San Diego, CA: Society for Neuroscience, 2018. Online.

**Le, A.A.**, Wang, W., Cox, CD., Lauterborn, JC., Lynch, G., Gall, CM. Mechanisms of hippocampal long-term potentiation (LTP) are sexually dimorphic in rodents. School of Medicine Graduate Day. 2018.

**Le, A.A.** Sexual Dimorphism in Rodent Hippocampus. UCI Neuroblitz Talk. June 2019.

**Le, A.A.**, Cox, BM., Lauterborn, JC., Hsu, E., Crawley, JN., Lynch, G., Gall, CM. Society for Neuroscience Annual Meeting. 2016.

Cox, BM., Wang, W., **Le, A.A.**, Aghazagah, L., Hou, J., Lynch, G., Gall, CM. Fragile X model mice show deficit in a novel episodic memory task. Society for Neuroscience Annual Meeting. 2016.

Karsten, CA., Cox, CD., Wang, K., **Le, A.A.**, Lynch, G., Gall, CM. Abstract. Differences in network activation patterns may underlie learning enhancement with spaced training. Society for Neuroscience Annual Meeting. 2014. 91.09/RR16.

**Le, A.A.,** 7,8-Dihydroxyflavone rescues social learning in Fragile-X mouse model. Talk and Poster for Research of Excellence Symposium. May 2015.

# ABSTRACT OF THE DISSERTATION

Sexually Dimorphic Synaptic Plasticity: Development and Consequences for Episodic Memory

by

Aliza Alien Le

Doctor in Philosophy in Biomedical Sciences

University of California, Irvine, 2022

Professor Gary Lynch, Chair

Studies dating back to the late 19$^{th}$ century have described distinct sex-biased advantages in various facets of memory: men show superiority in spatial memory, whereas females excel in verbal memory and facial recognition. While it is tempting to relate such sex differences to cultural and societal factors, much of these observations have also been consistent across rodents and other mammals. Further investigations over the past three decades have linked steroids, like estradiol, with synaptic plasticity thereby providing a convenient explanation for sex differences in cognition and learning. Research described in this dissertation evaluated the cellular mechanisms underlying sex differences in synaptic plasticity in rodent hippocampus and how this affects the threshold for enduring synaptic plasticity and learning. The first set of studies, described in *Chapter Two,* demonstrated that adult female, but not male, rodents use local estrogen and estrogen receptor α (ERα) for the induction of hippocampal long-term potentiation (LTP) and encoding of spatial memory. This sexual dimorphism was accompanied by a somewhat higher threshold for both synaptic plasticity and

spatial learning in females as compared to males. Evidence pointed towards estrogen and synaptic estrogen receptors as the primary elements thresholding LTP.

Given that estrogen levels are low prior to puberty we reasoned that sex differences in plasticity and learning might be absent in prepubescent animals. There have been many studies of structural and neurochemical changes in hippocampus up to the fourth post-natal week, but relatively little was known about possible changes in synaptic function over ages of puberty (~weeks 4 to 8) in either sex. As described in *Chapter Three* we found robust sex differences prior to puberty but differences were reversed from before to after puberty. Thus, prior to puberty LTP is more robust in females than in males whereas the opposite is true after puberty. These studies also identified a mechanism underlying the puberty-related decrease in female LTP: there is a substantial increase in the feedforward IPSCs that shunt the depolarization produced by the theta bursts used to induce LTP. This inhibition is governed by the levels of α5-$GABA_A$ receptors and studies showed that increases in α5 levels and function account for the lower facility for LTP with maturation in females.

Finally, *Chapter Four* describes processes which account for the reduction in LTP threshold with late maturation in males. Specifically, in distinction from females, we found males rely on previously uncharacterized metabotropic functions of the NMDA receptor. This reliance on the metabotropic NMDA receptor, as with females, is reflected in behavior and appears to reflect sex-specific specializations in different facets of episodic-like memory. Overall, work in this dissertation has identified sexually dimorphic LTP mechanisms, how they affect LTP threshold at critical stages in life (pre- and post-puberty), and, concurrently, how they contribute to sex-biased advantages in specific episodic memory components that describe the content, spatial location, and temporal context.

# CHAPTER ONE: Introduction and Overview of the Dissertation

**Sex differences in learning.**

Investigations into possible sex differences in memory began with the late 19th century monograph by Havelock Ellis (Ellis, 1894). Among a broad array of biological variables, this seminal work included a chapter on intellectual operations in which Ellis suggested that the then available body of work pointed to a female superiority in verbal but not other forms of memory. Numerous studies followed such that by 1974, Maccoby and Jacklin, in a groundbreaking book (Maccoby and Jacklin, 1974), were able to summarize results from nearly 1600 papers on psychological differences between the sexes. They concluded that females are superior in verbal learning whereas males perform better on visual-spatial problems. Subsequent experimental work has for the most part confirmed these male-female differences (see (Andreano and Cahill, 2009) and (Koss and Frick, 2017) for reviews). However, it has been argued from meta-analyses of these results, along with those for other psychological variables, that differences between the sexes are generally small with regard to effect sizes (Hyde, 2005). Evaluation is further complicated by the somewhat arbitrary descriptions of spatial learning and verbal fluency. The phenomena in the real-world lack self-evident measurements and in practice are largely defined by the paradigms used to test them. That said, reasonable though by no means complete agreement across an impressively diverse array of experimental designs supports the general idea that males outperform females on problems that involve spatial relationships (Gagnon et al., 2018; Piber et al., 2018; Fernandez-Baizan et al., 2019; Siedlecki et al., 2019; Wierenga et al., 2019). Whether this reflects sex differences in a particular type of memory processing or instead arises from other variables that affect outcomes on spatial problems is open to question. It has for example been argued that the apparent sexual dimorphism can be traced to different strategies (allocentric vs. egocentric) employed by women vs. men when dealing with cues about current and future locations (Lawton, 1994; Dabbs Jr. et al., 1998; Sandstrom et al., 1998; Cherney et al., 2008; Piber et al., 2018). Notably, the use of

such strategies is dependent on memory and there remains the possibility that each sex selects a behavioral strategy that aligns best with dimorphisms in the encoding and retrieval of information.

The female advantage on verbal problems summarized by Maccoby and Jacklin (1974) has been confirmed in numerous subsequent studies. Women reliably score higher than men when asked to recall words belonging to a particular category (first letter, animals, etc.), suggesting that they have better and/or more readily accessible long-term memory for semantic items. They also perform at a higher level when asked to recall words from a recently presented list (Youngjohn et al., 1991; Berenbaum et al., 1997; Kramer et al., 1997), as expected for superior encoding and retrieval of the original material. Importantly, women also outscore men in tests using faces rather than words (Rehnman and Herlitz, 2007). It is therefore possible that the female advantage is evident in tasks involving serial presentation of items of intrinsic interest rather than being restricted to verbal material. Finally, there are reasons to assume that sex differences in verbal vs. spatial memory are manifested in everyday life. Support for this comes from work on episodic memory, an autobiographical form of encoding that incorporates the identity of serial cues, their relative positions, and the order in which they occur (i.e., what, where and when information) (Tulving, 1972; Dickerson and Eichenbaum, 2010; Eacott and Easton, 2010). Recall of commonplace events, essentially within an episode, is often used to probe the accuracy and completeness of memory. A recent meta-analysis of hundreds of studies published over a 40-year period concluded that women do well in aspects of episodic memory that are verbal in nature or require recall of faces or odors. Men are reportedly superior in those aspects that place heavy demands on spatial memory (Asperholm et al., 2019).

There has been considerable discussion about the origins of sexual dimorphisms in memory and, in particular, whether they result from different life histories as opposed to being the consequence of selective pressures for sex roles (e.g., males as hunters would benefit from

enhanced spatial processing) (Ellis, 2011). Relatedly, a number of studies indicate that spatial learning by animals is superior in males relative to females (Koss and Frick, 2017) and that the variations in allocentric/egocentric strategies are also present (Hamilton et al., 2007; Vorhees et al., 2008; Vorhees and Williams, 2014). The collection of findings from such work suggests that for spatial learning the male advantage may be common to mammals as a group (Silverman and Eals, 1992; Jones et al., 2003). If so, the sexual dimorphism observed in humans could reflect the retention of a sex-linked feature that arose more than two hundred million years ago. Whether this dimorphic feature pertains to exploration of extended environments, and thus relates naturally to observed differences in spatial learning, is a challenging and unresolved problem. In any event, the animal research strongly suggests that neurobiological as opposed to experiential variables are responsible for sex differences in spatial learning. These findings accordingly opened the way to experimental work on brain systems that might account for such differences.

Research to date has not described animal effects that might relate to the female advantage in verbal learning paradigms. Indeed, to our knowledge, there is no evidence that female rodents *consistently* outperform males on any type of memory problem although there are mixed findings for object recognition tasks and evidence that females in proestrus, the high circulating estrogen stage of the estrous cycle, perform better than non-proestrus females and, in some studies, males (Koss and Frick, 2017). The absence of reliable evidence for a female advantage in animal studies of different forms of learning could simply reflect the relative absence of studies searching for such effects, as well as the obvious difficulty of establishing animal analogues of semantic cues. Moreover, human studies rarely involve the practice sessions typically used in animal research to shape behavior towards low variance endpoints. However, we have found that rodents remember individual odors from a recently sampled sequence and do so without training or overt rewards (Otto et al., 1991b; Wang et al., 2018b;

Cox et al., 2019). Odors are of innate interest to rodents and sequence tests of the type just noted might be analogous to the face recognition problems in which women are superior to men (faces are inherently interesting to humans). Sequential olfactory paradigms are accordingly a plausible starting point for investigations into potential female advantages in memory processing by rodents. We have developed versions of the olfactory paradigms that use multiple olfactory cues to sample the three basic elements of episodic memory (cue identity, temporal order, location) and, as in human studies, do not entail repetition or overt rewards (Cox et al., 2019). There is thus the possibility of testing if rodents parallel humans with regard to which aspects of an episode are more easily acquired between the sexes.

**Synaptic substrates for memory storage.**

The mechanisms used by the brain to lay down memory traces constitute a reasonable starting point for investigations into the causes for the sex differences summarized above. It had been suspected since the time of Ramón y Cajal that use-dependent modifications to synapses underlie memory encoding and the discovery of Long-term Potentiation (LTP) confirmed that connections in brain possess the requisite plasticity (Bliss and Lomo, 1973). LTP is a process wherein brief trains of high frequency or rhythmic neuronal activity can enhance transmission at individual synapses (Lynch, 2003; Bliss et al., 2007; Nicoll, 2017). It has been described for excitatory glutamatergic synapses throughout the CNS (e.g., cortex, striatum, amygdala, spinal cord) and is particularly well characterized for intrinsic circuitry within hippocampus. Like memory, LTP develops very quickly yet is both extraordinarily persistent and synapse specific; thus, it satisfies the constraints of a putative information storage mechanism imposed by the unusual properties of memory including its enormous capacity (Lynch, 2003; Morris, 2003; Lynch, 2004b; Nicoll, 2017). Initial tests of the hypothesis that LTP underlies memory showed that selective pharmacological suppression of potentiation blocks spatial learning without affecting acquisition of simple cue-response associations (Morris et al., 1986; Staubli et al.,

1989). There are now many reports showing that disruption of LTP similarly disrupts memory formation (Lynch, 1998; Rex et al., 2005; Rex et al., 2010) and that facilitation of potentiation enhances memory (Lynch, 2002, 2004a; Wang et al., 2018b). It was then found that learning is accompanied by LTP in the same synapses critical for encoding the information. This was first demonstrated for the system that conveys olfactory cues into the cortex (Roman et al., 1987). The pertinent experiments used discrete 5Hz (the sniffing frequency) stimulation of the lateral olfactory tract as a positive or negative cue in a two-odor discrimination paradigm. The monosynaptic responses generated in piriform (olfactory) cortex by the stimulation pulses underwent a lasting increase in amplitude as a rat learned that the 'electric odor' was either correct or incorrect. Now several studies have shown that synaptic potentiation occurs with learning (Whitlock et al., 2006; Cohen et al., 2008). Together, these findings provide compelling evidence that LTP is the synaptic mechanism for encoding many forms of memory.

Early investigations into the cellular mechanisms that induce and express enduring LTP focused on hippocampus and showed that potentiation of the glutamatergic CA3 to CA1 intrahippocampal connections required an increase in postsynaptic calcium (Dunwiddie and Lynch, 1979; Lynch et al., 1983; Wang et al., 2016b). This result meshed well with the discovery that LTP induction is dependent on calcium permeable NMDA-type glutamate receptors (Muller et al., 1988; Park et al., 2014). The search for an LTP expression mechanism generally also focused on hippocampal field CA1 pyramidal cells as representative of neurons through the cortical telencephalon. These studies revealed that in association with LTP there is a change in the size and shape of postsynaptic dendritic spines (Lee et al., 1980; Harris et al., 2003), a finding subsequently confirmed in numerous studies using progressively more sophisticated techniques (Matsuzaki et al., 2004; Yang et al., 2008), as well as an increase in the size of the postsynaptic density (PSD) area (Chen et al., 2007). Despite intense interest in the possibility of new spine formation, studies generally indicate that changes in spine and synapse size occur

without a significant increase in numbers of postsynaptic elements in the field of potentiation (Chen et al., 2007; Harris, 2020). Given that PSD size is highly correlated with the amount of the neurotransmitter receptor pool, PSD expansion provided a straightforward explanation for the enhanced excitatory postsynaptic currents that define LTP. Related experiments demonstrated that in CA1, LTP expression does not affect transmitter release but instead is associated with a selective increase in the ionic currents gated by the postsynaptic AMPA-type glutamate receptors that produce the excitatory postsynaptic currents (Kauer et al., 1988; Muller and Lynch, 1988, 1989; Nicoll, 2003). Although these studies focused on male rodents, there is as yet no evidence that fundamental LTP expression mechanisms differ between the sexes.

Having established that CA1 LTP was due to postsynaptic changes, the next hurdle was to identify the cell biological steps that occur between the rapid triggers for LTP and the structural changes to synapses that express the effect. As early as 1984, Lynch and Baudry had proposed what is now known as the “calpain hypothesis” in which learning related patterns of activity raise calcium levels in depolarized spines and this activates the protease calpain which then degrades spectrin, a protein that forms a scaffold to maintain the cytoskeletal structure of spine, resulting in an expansion of the glutamatergic receptor pool in PSDs (Lynch and Baudry, 1984). Consistent with the hypothesis, more recent work using a novel microscopic approach developed by our group to visualize filamentous (F-) actin within large numbers of dendritic spines (Lin et al., 2005; Kramar et al., 2006) showed that induction of CA1 LTP was quickly followed by a reorganization of the subsynaptic actin cytoskeleton, and that preventing this effect caused potentiation to rapidly decay back to baseline. Pertinent to the LTP-memory association, disruption of the actin cytoskeleton has been shown to interfere with memory (Rudy, 2015; Lamprecht, 2016). Other studies using quantitative immunofluorescence identified within dendritic spines a collection of small GTPase-initiated signaling cascades that lead from the very rapid synaptic events that induce LTP to the slower formation and stabilization of actin

networks within dendritic spines (Chen et al., 2007; Rex et al., 2009; Rex et al., 2010; Seese et al., 2012). This signaling is positively modulated by the neurotrophin brain derived neurotrophic factor (BDNF) that is released during afferent activity and acts through postsynaptic Tropomyosin receptor kinase B (TrkB) receptors, and depressed by adenosine acting on postsynaptic adenosine A1 receptors (Rex et al., 2009). Importantly, as discussed below, estrogen also modulates actin regulatory signaling at excitatory synapses (Kramar et al., 2009; Wang et al., 2018a) and these actions have proven critical for sex differences in LTP and learning.

**LTP as an explanatory construct for memory phenomenology.**

The identification of synaptic elements controlling the activity-dependent remodeling of the actin cytoskeleton that support LTP has provided insight into the neurobiological basis of several well-known memory phenomena. In particular, the characterization of these synaptic mechanisms in male hippocampal field CA1 has identified constraints on aspects of synaptic plasticity that suggest explanations for the links between memory and particular cortical rhythms, the temporal properties of memory consolidation, and the efficacy of spaced training. Moreover, identification of synaptic substrates for encoding has provided markers for analyses of the engrams for different forms of learning.

*Cortical rhythms are associated with learning*: Progress towards identifying the cellular events underlying the production of stable synaptic potentiation substantially increased the explanatory power of the hypothesis that brain networks use LTP to encode new memories. It had been known for some time that many forms of learning are associated with oscillatory activity in brain, and in particular the 4-7 Hz theta rhythm (Hasselmo et al., 2002; Sakimoto and Sakata, 2020), but the reasons for this were obscure. The situation was clarified by the discovery that afferent stimulation with brief high frequency bursts spaced apart by the period of

the theta wave (i.e., 200 msec between bursts; theta burst stimulation, TBS) is near optimal for inducing robust and stable LTP (Larson et al., 1986; Larson and Munkacsy, 2015). The reasons for this curious link between an EEG rhythm and structural modifications to synapses center on the efficacy of TBS in engaging a mechanism for suppressing the feedforward inhibitory transmission that prevents opening of voltage-sensitive NMDA receptors (NMDARs), that are critical for LTP, at glutamatergic synapses (Larson and Lynch, 1988).

*The rapid phase of memory consolidation*: LTP research has also been informative with regard to the much-discussed topic of memory consolidation. The idea that newly acquired information passes through a stabilization period before transferring to long-term storage dates to the late 19$^{th}$ century. Analyses of the effect under controlled conditions became possible with the advent of electroconvulsive shock therapy (Duncan, 1949) and suggested means for studying it in animals (Misanin et al., 1968; Popik et al., 1994). The resultant memory consolidation literature is both large and contentious with regard to potential mechanisms (Lynch et al., 2007; Babayan et al., 2012). The discovery that low frequency stimulation erases LTP when applied within 15 to 30 minutes of induction led to novel insights into the processes underlying the rapid phase of both LTP and memory consolidation (Larson et al., 1993; Staubli and Scafidi, 1999; Lynch et al., 2007). Considering cytoskeletal contributions to consolidation provided even greater understanding. In particular, evidence was obtained that the actin filaments that form shortly after LTP-inducing TBS are dynamic (treadmilling) until being stabilized by components of the signaling cascades noted earlier. Low frequency stimulation gives rise to increases in extracellular adenosine that engages postsynaptic adenosine A1 receptors which, in turn, suppress actin regulatory signaling (Arai et al., 1990; Abraham and Huggett, 1997; Huang et al., 1999; Rex et al., 2009). If this occurs prior to new F-actin stabilization, then the newly formed filaments are lost leading to a rapid decay of potentiation (Kramar et al., 2006). These results help explain why conditions such as electroconvulsive

shock and anoxia, that increase extracellular adenosine, cause retrograde amnesia (Huang and Hsu, 2001).

*Engrams*: Nineteenth century investigators hypothesized that learning results in associations between “nervous elements,” and thus a memory trace, or “engram,” connecting different brain regions (as described by (Schacter, 1982)). The search for engrams has largely involved physiological methods and various forms of conditioning (Swain and Thompson, 1993), and analysis of neuronal activation patterns (Govindarajan et al., 2006; Tonegawa et al., 2015) but the description of molecular substrates of LTP suggested a means for mapping the distribution of *synapses* associated with encoding of new memories. A first study of this type asked if exploration of a novel environment produces LTP-related synaptic changes in field CA1, a region important to spatial learning. Numbers of 3-D reconstructed synapses containing an LTP marker (i.e., the transiently phosphorylated (p) protein cofilin) were low in control animals and about 30% higher in the exploration group (Fedulov et al., 2007). Moreover, PSDs associated with p-cofilin were substantially larger than those that were not. For reasons discussed earlier, it can be assumed that p-cofilin-positive synapses were stronger (potentiated) relative to their neighbors. Injections of an NMDAR antagonist, which disrupts LTP, blocked the increase in both synaptic p-cofilin levels and learning in the exploration group. Together these findings indicate that synapses exhibiting increases in p-cofilin with training are undergoing LTP as part of the memory trace. Importantly, only a very small percentage (<1%) of field CA1 synapses contained elevated levels of p-cofilin after training, a finding consistent with the view that a memory system using LTP rules will have the large capacity needed for a lifetime of interactions with dynamic and complex circumstances. Subsequent studies using a different behavioral paradigm found that the increases in synapses associated with an LTP marker occur in discrete subfields of hippocampus rather than being widely distributed (Cox et al., 2014).

Extension of this strategy to analyses of neocortex could result in maps of synaptic changes occurring there in association with learning and thus visualization of a cortical engram.

**Estrogen promotes LTP and Learning.**

There is an extensive body of evidence that estrogen promotes the growth of dendritic spines and enhances functional synaptic plasticity in rodent hippocampus (Gould et al., 1990; Foy et al., 1999; Foy et al., 2008; Luine and Frankfurt, 2013; Frick et al., 2015; Frick et al., 2018; Luine and Frankfurt, 2020). This is clearly the case for both ovariectomized (Cordoba Montoya and Carrer, 1997; Frye et al., 2007) and gonadally intact females (Woolley et al., 1990; Warren et al., 1995); a smaller collection of reports indicate that estrogen infusion improves spatial memory and synaptic plasticity in males as well (Luine and Rodriguez, 1994; Kampen and Sherwin, 1996; Frick et al., 2015; Kato et al., 2020). Although the high circulating estrogen stage of the estrous cycle is positively correlated with the magnitude of field CA1 LTP (Warren et al. 1995; Bi et al. 2001), it is not known if estrogen effects on spine counts, in particular, contribute to rapid effects of the steroid on synaptic plasticity. Pertinent to this, it is noteworthy that estrogen-induced increases in spine number are NMDAR-dependent, require genomic activity, and in the short term (<1 day), do not entail changes in AMPA receptor currents (Woolley and McEwen, 1994; Smith and McMahon, 2005). This contrasts with the rapid effects of estradiol (E2), the primary form of estrogen, on synaptic responses that have been described in many brain regions (Kelly et al., 1976; Nabekura et al., 1986; Wong and Moss, 1991): These occur within minutes, do not depend on protein synthesis or NMDAR function, and reflect increases in AMPA receptor currents (Wong and Moss, 1992; Kramar et al., 2009; Zadran et al., 2009). *Chapter Two* describes how estrogen also influences synaptic GTPase and kinase signaling activities that are required for induction of LTP (Kramar et al. 2009; Hasegawa et al. 2015;

Wang et al. 2016, 2018), and results suggest that these processes might account for the rapid effects of estrogen on synaptic potentiation.

In line with estrogen effects on transmission and dendritic spines, the preponderance of findings point to the conclusion that performance on certain learning tasks fluctuates across stages of the human menstrual and rodent estrous cycles. For example, women exhibit better verbal memory when circulating estrogen levels are high, but during the same periods perform more poorly in spatial tasks (Hampson and Kimura, 1988; Hampson, 1990; Epting and Overman, 1998). Studies in rodent initially agreed with evidence for the negative effects of estrogen on spatial learning: rats in proestrus (high-estrogen state) reportedly performed worse in spatial (Morris Water Maze, radial arm maze) tasks than rats in low estrogen phases (Frye, 1995; Stackman et al., 1997; Warren and Juraska, 1997). However, in object-based spatial tasks, cycling females perform better in the high-estrogen state (Frye et al., 2007; Paris and Frye, 2008). The seemingly conflicting results, for performance in spatial vs object-based tasks, raise the possibility that stress, which is heightened in Morris Water Maze (spatial) tasks, may influence the response to estrogen (Rubinow et al., 2004). Alternatively, there may be different brain regions critical for learning object-based as opposed to distant-reference tasks (Luine, 2015) and the nature of estrogen effects may be region-specific (Gould et al., 1990; Woolley et al., 1990; Qi et al., 2016).

As described in *Chapter Two*, my studies describe an unambiguous case in which estrogen enhances Object Location Memory (OLM), a CA1-dependent, object-based spatial task. An important feature of the study was that the training period (initial cue sampling time) of ~5 min was at threshold levels for male acquisition and long-term memory (Stefanko et al., 2009). Using this threshold training time, females mice outside of proestrus (i.e., in low circulating estrogen states) did not recognize the new object location in a retention trial conducted 24 hours after training whereas males had high retention scores. Notably, the non-

proestrus females did successfully encode the location of the objects when given a longer training session, indicating that their deficit relates to the speed at which spatial relationships are learned (unpublished observation). Very different results were obtained with females trained in proestrus: these mice performed as well as males when given 5-min OLM training. Importantly, the amount of time spent sampling the objects during training was not detectably affected by estrous cycle stage, a result suggesting that higher estrogen levels during proestrus improved learning by enhancing encoding and not by influencing attention to the cues.

Analogous results are reported for estrogen effects on LTP in hippocampal field CA1, a critical region for OLM. Tests using threshold levels of stimulation for inducing robust and stable synaptic potentiation in males (i.e., 5 paired theta bursts) failed to generate reliable LTP in hippocampal slices from young adult females. However, a full-length train of 10 theta bursts elicited comparable LTP in males and females. Moreover, in hippocampal slices (ex vivo), infusion of E2 (the most potent and prevalent estrogen in brain) at concentrations (1 nM) comparable to those in hippocampus during proestrus (Hojo et al., 2009; Mukai et al., 2010) potently enhanced LTP (Kramar et al., 2009). Relatedly, E2 rapidly and reversibly increased the amplitude of AMPA receptor-gated synaptic field excitatory postsynaptic potentials (fEPSPs) elicited in male CA1 by single pulse afferent stimulation; as with LTP, this effect of E2 infusion did not require involvement, or increase the size, of NMDAR-mediated synaptic responses (Kramar et al., 2009). In both sexes the facilitatory effects of infused E2 were blocked by antagonists of estrogen receptor β (ERβ) but not affected by antagonists for the other two classes of brain estrogen receptors ERα and G-protein coupled estrogen receptor 1 (GPER1) (Kramar et al., 2009; Wang et al., 2016a). These observations raised the question of whether exogenous E2 activates the actin signaling machinery that leads to LTP. Indeed, pretreatment with a toxin (latrunculin) that selectively interferes with actin polymerization eliminated E2-induced enhancement of synaptic responses. Moreover, brief E2 infusion activated the small

GTPase RhoA and RhoA-associated kinase (ROCK) and increased phosphorylation of cofilin, a downstream target of ROCK. Cofilin is a constitutively active protein that severs newly formed actin filaments, but when it is phosphorylated cofilin is inactivated thereby allowing elongation of actin filaments to occur. As expected from these results, E2 treatment increased spine F-actin, an effect that reversed upon washout of the hormone (Kramar et al., 2009). ROCK inhibition prevented both actin polymerization and facilitation of synaptic responses by E2. In all, brief treatments with physiological concentrations of estradiol activated, through ERβ, one the key signaling cascades (RhoA>ROCK>cofilin>actin polymerization) that is engaged by TBS and critical for shifting synapses into their potentiated state. Importantly, in these studies of males, brief E2 treatment failed to activate a second signaling pathway engaged by TBS that involves the small GTPases Rac and Cdc42 and their effector PAK. Available evidence suggests that the Rac/Cdc42-to-PAK cascade serves to stabilize and elaborate the actin networks assembled in response to stimulation of the RhoA-ROCK system by TBS (Rex et al., 2009). The absence of the Rac/Cdc42 response after a short exposure to low levels of E2 helps explain why actin polymerization and EPSP enhancement induced by the steroid reverses after washout in marked contrast to the persistence of synaptic potentiation after TBS.

Links between synaptic (i.e., membrane-associated) estrogen receptors and actin regulatory signaling could be reasonably direct because these receptors activate Src, a tyrosine kinase that influences the activity of small GTPases engaged with LTP (Bunda et al., 2014; Luo et al., 2017). However, recent work indicates that more complex molecular interactions are involved. Specifically, E2 infusion causes β1-family integrins to shift into their activated configuration (Wang et al., 2016a), an event that is critical for TBS-induced actin polymerization and LTP (Kramar et al., 2006). Moreover, suppressing β1 integrin function prevented E2 effects on synaptic responses. Integrins are activated in many circumstances by neighboring receptors via a process referred to as inside-out signaling or, in other fields, ligand-independent

transactivation (Lee et al., 2002; Rajagopal and Chao, 2006). While this process could be involved, it is also the case that inhibitors of matrix metalloproteinases (MMPs), extracellular enzymes that generate integrin ligands from the extracellular matrix, block the effects of E2 on baseline synaptic transmission (Wang et al., 2016a). Thus, estrogen receptor activation may cause the release of factors controlling MMPs and, consequently, ligation of the synaptic integrins. There is evidence that this MMP-integrin sequence is required for the production of LTP (Nagy et al., 2006; Babayan et al., 2012; Wang et al., 2016a).

It should be noted that E2 infusion also activates synaptic TrkB receptors for the neurotrophin BDNF. This involves ligand-free transactivation as sequestration of released BDNF does not prevent TrkB activation by the hormone (Wang et al., 2016a). However, neither BDNF sequestration nor pretreatment with a TrkB antagonist detectably influences E2's facilitation of excitatory synaptic responses. A potential explanation for the latter result is that TrkB transactivation by estradiol is incomplete and, in particular, fails to initiate TrkB signaling to the GTPases. Alternatively, direct signaling from the estrogen receptor (or estrogen receptors), independent of TrkB, is both sufficient for actin remodeling and functionally occludes further contributions from TrkB.

In summary, exogenous E2 activates some but not all of the actin management systems used to support enduring LTP and thereby produces a weak and transient form of synaptic potentiation. This effect could serve to prime synaptic mechanisms activated by neuronal activity and in particular by TBS in the experimental context, and thereby result in the greatly augmented potentiation that occurs in the presence of estradiol (Kramar et al., 2009). Building on these findings my research tested if this complex synaptic machinery differs between adult male and female rodents (Chapter Two), and if such sex differences change with development from before to after puberty (Chapter Three).

**The substrates for LTP are sexually dimorphic.**

Although circulating estrogens pass the blood brain barrier to influence neuronal activity in the CNS, estrogen and related steroids are also synthesized by forebrain neurons including those in hippocampus (Hojo et al., 2009). Cytochrome P450 aromatase (AROM), the rate limiting enzyme for E2 synthesis, is present at surprisingly high concentrations in hippocampus and localized to axon terminals (Peterson et al., 2005; Tabatadze et al., 2014). Reflecting local neurosteroid synthesis, E2 levels are several-fold higher in hippocampus than in blood *in both sexes*, and hippocampal neurons release estrogen (Hojo et al., 2009; Mukai et al., 2010; Kato et al., 2013; Tabatadze et al., 2014). Nevertheless, blocking estrogen production with AROM inhibitors in adults caused a marked reduction in LTP in females only (Vierk et al., 2012; Bender et al., 2017; Wang et al., 2018a).

Studies described in *Chapter Two* investigated the mechanisms underlying this striking example of sexual dimorphism and began with the assumption that locally produced and released estrogen engages the same signaling pathways as exogenous E2. This did not prove to be the case. Antagonists of ERβ (e.g., PHTPP), present at concentrations that blocked the effects of *applied* E2 on synaptic responses in males (Wang et al., 2016), did not disturb female LTP whereas an antagonist of ERα (MPP) prevented stable potentiation in females only. Tests using mice with a point mutation that prevents palmitoylation of ERα, and thus insertion of the receptor into membranes, demonstrated a nearly complete loss of stable LTP in females but normal potentiation in males. In comparison, mutant females lacking *nuclear* ERα expressed normal LTP (Wang et al. 2018). These results indicate that membrane signaling, as opposed to transcriptional effects, of the estrogen receptors is critical for potentiation at least through the first hour after stimulation. This contrasts with the well described dimorphic effects of E2 on spine integrity (Brandt et al., 2013) and on spinogenesis and NMDAR currents (Woolley and McEwen, 1994; Woolley et al., 1997; Smith et al., 2009), which reportedly depend on new

protein synthesis and are slower to emerge. Genetic manipulations that prevent AROM expression in hippocampus lead to reductions in neuronal arbors and synaptic density as well as disruption of LTP and memory in both sexes (Lu et al., 2019). However, we found that with briefer manipulations (e.g., AROM inhibition for a few days) synaptic populations were not disturbed and both LTP and memory were impaired in females only (Wang et al., 2018a). These results indicate that in females, but not males, links in the signaling sequences set in motion by TBS are dependent on locally produced and released estrogen acting though ERα.

Further studies of the basis of sexual dimorphism in field CA1 LTP evaluated the physiological response to LTP-inducing TBS. The composite postsynaptic response to the stimulation pulses that comprise a single theta burst was not detectably affected by estrogen receptor antagonists or downregulation of surface ERα. The pronounced facilitation of burst responses that normally occurs during a TBS train was also intact after these manipulations (Wang et al., 2018a). These results rule out the possibility that local neurosteroid estrogen and ERα influence neurotransmitter release or the complex events, including NMDAR activation, that together constitute the postsynaptic response to TBS. However, suppressing ERα function blocked TBS-induced activation of the LTP-critical kinases Src and ERK in females while having no effect on these kinases in males. These enzymes are present in the postsynaptic element and activated by TBS in an NMDAR-dependent fashion in males, evidently without contribution from locally derived estrogen. In agreement with others, we found the TBS-NMDAR route for kinase activation is operative in females as well but, from the results described, this process appears to require a 'boost' from locally produced estrogen. As concluded in Chapter Two, this argument implies that one (or more) feature of NMDAR function is better developed in males so as to not require supplemental estrogen receptor contributions for kinase activation and LTP. This idea was specifically examined in *Chapter Three* studies that evaluated ionotropic and metabotropic NMDAR function in both males and females, from before to after puberty.

Brief strings of theta bursts, as used in the LTP threshold studies, resemble conditions occurring during learning (Otto et al., 1991a) suggesting these results are plausibly related to sex differences in the threshold for encoding long term memory. To further understand actions of exogenous, and thus circulating, estrogen on synaptic actin regulatory signaling we evaluated effects of E2 infusion at low doses on the postsynaptic kinases. The steroid activated postsynaptic ERK and Src in both sexes (Bi et al., 2000; Wang et al., 2018a). In males these responses were largely dependent upon ERβ with no evident contribution from ERα (Wang et al., 2018a). In females, however, the effects of E2 infusion were reduced by about half in the presence of ERα antagonist MPP, indicating that complete kinase activation by applied or circulating E2 requires binding to both classes of estrogen receptor. Evidence that in females the same ERα antagonist significantly attenuated TBS-induced activation of ERK/Src whereas an ERβ blocker had little if any effect (Wang et al., 2018a) indicates that in females *locally derived* estrogen, released during induction of LTP, acts via synaptic ERα alone without contribution from ERβ. The partial efficacy of the ERβ blocker with regard to *infused* E2 raises the possibility that in vivo the two avenues of estradiol action promote LTP during proestrus when both locally derived and circulating hormone levels are high and, specifically, that locally derived and circulating estrogen act through ERα and ERβ, respectively, to engage the same downstream effector kinases. This conclusion likely accounts for the superior spatial learning seen in proestrus females.

There remains the question of why males don't use locally produced estrogen and ERα to boost NMDAR signaling and promote LTP. One possibility is suggested by the observation that males have substantially lower concentrations of synaptic ERα as compared to females (Wang et al., 2018a). An alternative but not exclusive possibility is that signaling from ERα to various effectors is less effective in males, in which case dimorphism would involve sexually differentiated coupling between the two types of receptors (ERα and NMDARs) and downstream

kinases. Of interest in this regard are recent reports that NMDAR-mediated Src activation involves non-ionic signaling (Nabavi et al., 2013; Dore et al., 2016); a metabotropic route is also suggested to be important for NMDAR-dependent ERK activation (Weilinger et al., 2016). It is therefore possible that non-ionic coupling between the NMDARs and LTP-related kinases is sexually dimorphic, and specifically more potent in males, thereby removing the need for the boost from E2/ERα for induction of LTP. This scenario would suggest that females, like males, retain the dependency of LTP on the ionic (calcium signaling) functions of the NMDARs. We propose that in females the dependence on a local estrogen/ERα step for kinase activation may account for the higher activity threshold for induction of LTP described above (Wang et al., 2018a). *Chapter Four* tests for this non-ionic feature in NMDA receptors following TBS in male and female rodents.

Sex differences in LTP, at least for field CA1, may be restricted to the events just described. As detailed in *Chapter Two*, many of the mechanisms previously found to be required for LTP in males (Wang et al., 2018a) are also engaged and required in females. Thus, in both sexes, TBS activates β1-integrins and TrkB receptors and both steps are essential for LTP consolidation; TrkB autophosphorylation (activation) is dependent on integrin activation (Wang et al., 2016a) and antagonism of the β1 integrins blocks LTP. Additionally, theta bursts activate signaling to p-cofilin in both females and males, and inhibition of ROCK, the upstream kinase for cofilin phosphorylation, effectively suppresses LTP consolidation in both sexes. However, activation of synaptic TrkB and β1 integrin is disrupted by ERα antagonists in females only indicating that dimorphism in activities of the membrane receptors account for the majority of sex differences in signaling thus far identified.

The above results led us to conclude that NMDAR coupling to the signaling cascades that produce LTP in young adults is less potent in females than males and therefore require a ‘boost’ from estrogen receptors in the former. Our most recent work suggests a substantial

revision to this idea. Specifically, it appears that reorganization of the subsynaptic actin cytoskeleton initiated during induction of male LTP is driven by non–ionic (metabotropic) NMDAR signaling rather than by elevated calcium as previously assumed. Remarkably, our data strongly suggest that females substitute local estrogen signaling for metabotropic NMDAR operations (they do however have the same dependency on NMDAR gate ionic fluxes as in males). The sex difference in LTP substrates is thus more profound than originally envisioned.

These sex differences in metabotropic NMDAR and estrogen receptor signaling raise the question of whether there might be an adaptive advantage to the more complex, higher threshold LTP mechanism used by young adult females. We explored this using by comparing three basic elements of episodic memory in the sexes and found that female mice outperform males on episodic 'what' and 'when' while males have a clear advantage on episodic 'where'. Why an elevated threshold for LTP might lead to superior performance on a cognition critical-form of memory will be discussed.

In summary, this dissertation will address the following issues regarding sex and LTP:

- Thresholds for induction in the two sexes;
- Differences in the machinery that stabilizes LTP: metabotropic NMDARs in males and local estrogen/ERα in females;
- Evidence that sex differences in LTP are reversed prior to puberty;
- Reasons why the female threshold for LTP increases across puberty;
- Consequences of sex-differences in LTP for acquisition of episodic memories.

**References**


Abraham WC, Huggett A (1997) Induction and reversal of long-term potentiation by repeated high-frequency stimulation in rat hippocampal slices. Hippocampus 7:137-145.

Andreano JM, Cahill L (2009) Sex influences on the neurobiology of learning and memory. Learn Mem 16:248-266.

Arai A, Kessler M, Lynch G (1990) The effects of adenosine on the development of long-term potentiation. Neurosci Lett 119:41-44.

Asperholm M, Hogman N, Rafi J, Herlitz A (2019) What did you do yesterday? A meta-analysis of sex differences in episodic memory. Psychol Bull 145:785-821.

Babayan AH, Kramar EA, Barrett RM, Jafari M, Haettig J, Chen LY, Rex CS, Lauterborn JC, Wood MA, Gall CM, Lynch G (2012) Integrin dynamics produce a delayed stage of long-term potentiation and memory consolidation. J Neurosci 32:12854-12861.

Bender RA, Zhou L, Vierk R, Brandt N, Keller A, Gee CE, Schafer MK, Rune GM (2017) Sex-dependent regulation of aromatase-mediated synaptic plasticity in the basolateral amygdala. J Neurosci 37:1532-1545.

Berenbaum SA, Baxter L, Seidenberg M, Hermann B (1997) Role of the hippocampus in sex differences in verbal memory: memory outcome following left anterior temporal lobectomy. Neuropsychol 11:585-591.

Bi R, Broutman G, Foy MR, Thompson RF, Baudry M (2000) The tyrosine kinase and mitogen-activated protein kinase pathways mediate multiple effects of estrogen in hippocampus. Proc Natl Acad Sci U S A 97:3602-3607.

Bliss T, Collingridge GL, Morris RGM (2007) Synaptic Plasticity in the Hippocampus. In: The Hippocampus Book (Anderson P, Morris R, Amaral D, Bliss T, O'Keefe J, eds), pp 343-374. New York: Oxford University Press.

Bliss TVP, Lomo T (1973) Long-lasting potentiation of synaptic transmission in the dentate area of the anesthetized rabbit following stimulation of the perforant path. J Physiol 232:334-356.

Brandt N, Vierk R, Rune GM (2013) Sexual dimorphism in estrogen-induced synaptogenesis in the adult hippocampus. The International journal of developmental biology 57:351-356.

Bunda S, Heir P, Srikumar T, Cook JD, Burrell K, Kano Y, Lee JE, Zadeh G, Raught B, Ohh M (2014) Src promotes GTPase activity of Ras via tyrosine 32 phosphorylation. Proc Nat Acad Sci U S A 111:E3785-E3794.

Chen LY, Rex CS, Casale MS, Gall CM, Lynch G (2007) Changes in synaptic morphology accompany actin signaling during LTP. J Neurosci 27:5363-5372.

Cherney ID, Brabec CM, Runco DV (2008) Mapping out spatial ability: sex differences in way-finding navigation. Percept Mot Skills 107:747-760.

Cohen Y, Reuveni I, Barkai E, Maroun M (2008) Olfactory learning-induced long-lasting enhancement of descending and ascending synaptic transmission to the piriform cortex. J Neurosci 28:6664-6669.

Cordoba Montoya DA, Carrer HF (1997) Estrogen facilitates induction of long term potentiation in the hippocampus of awake rats. Brain Res 778:430-438.

Cox BM, Cox CD, Gunn BG, Le AA, Inshishian VC, Gall CM, Lynch G (2019) Acquisition of temporal order requires an intact CA3 commissural/associational (C/A) feedback system in mice. Commun Biol 2:251.

Cox CD, Rex CS, Palmer LC, Babayan AH, Pham DT, Corwin SD, Trieu BH, Gall CM, Lynch G (2014) A map of LTP-related synaptic changes in dorsal hippocampus following unsupervised learning. J Neurosci 34:3033-3041.

Dabbs Jr. JM, Chang EL, Strong RA, Milun R (1998) Spatial ability, navigation strategy, and geographic knowledge among men and women. Evol Human Behav 19:89-98.

Dickerson BC, Eichenbaum H (2010) The episodic memory system: neurocircuitry and disorders. Neuropsychopharm 35:86-104.
Dore K, Aow J, Malinow R (2016) The Emergence of NMDA Receptor Metabotropic Function: Insights from Imaging. Frontiers in synaptic neuroscience 8:20.
Duncan CP (1949) The Retroactive Effect of Electroshock on Learning. J Comp Physiol Psychol 42:32-44.
Dunwiddie TV, Lynch G (1979) The relationship between extracellular calcium concentrations and the induction of hippocampal long-term potentiation. Brain Res 169:103-110.
Eacott MJ, Easton A (2010) Episodic memory in animals: remembering which occasion. Neuropsychologia 48:2273-2280.
Ellis H (1894) Man and woman; A study of human secondary sexual characteristics. London, UK: A&C Black Ltd.
Ellis L (2011) Identifying and explaining apparent universal sex differences in cognition and behavior. Personality and Individual Differences 51:552-561.
Epting LK, Overman WH (1998) Sex-sensitive tasks in men and women: a search for performance fluctuations across the menstrual cycle. Behav Neurosci 112:1304-1317.
Fedulov V, Rex CS, Simmons DA, Palmer L, Gall CM, Lynch G (2007) Evidence that long-term potentiation occurs within individual hippocampal synapses during learning. J Neurosci 27:8031-8039.
Fernandez-Baizan C, Arias JL, Mendez M (2019) Spatial memory in young adults: Gender differences in egocentric and allocentric performance. Behav Brain Res 359:694-700.
Foy MR, Baudry M, Diaz Brinton R, Thompson RF (2008) Estrogen and hippocampal plasticity in rodent models. Journal of Alzheimer's disease : JAD 15:589-603.
Foy MR, Xu J, Xie X, Brinton RD, Thompson RF, Berger TW (1999) 17beta-estradiol enhances NMDA receptor-mediated EPSPs and long-term potentiation. J Neurophysiol 81:925-929.
Frick KM, Kim J, Tuscher JJ, Fortress AM (2015) Sex steroid hormones matter for learning and memory: estrogenic regulation of hippocampal function in male and female rodents. Learning & Memory 22:472-493.
Frick KM, Tuscher JJ, Koss WA, Kim J, Taxier LR (2018) Estrogenic regulation of memory consolidation: A look beyond the hippocampus, ovaries, and females. Physiol Behav 187:57-66.
Frye CA (1995) Estrus-associated decrements in a water maze task are limited to acquisition. Physiol Behav 57:5-14.
Frye CA, Duffy CK, Walf AA (2007) Estrogens and progestins enhance spatial learning of intact and ovariectomized rats in the object placement task. Neurobiol Learn Mem 88:208-216.
Gagnon KT, Thomas BJ, Munion A, Creem-Regehr SH, Cashdan EA, Stefanucci JK (2018) Not all those who wander are lost: Spatial exploration patterns and their relationship to gender and spatial memory. Cognition 180:108-117.
Gould E, Woolley CS, Frankfurt M, McEwen BS (1990) Gonadal steroids regulate dendritic spine density in hippocampal pyramidal cells in adulthood. J Neurosci 10:1286-1291.
Govindarajan A, Kelleher RJ, Tonegawa S (2006) A clustered plasticity model of long-term memory engrams. Nat Rev Neurosci 7:575-583.
Hamilton DA, Akers KG, Weisend MP, Sutherland RJ (2007) How do room and apparatus cues control navigation in the Morris water task? Evidence for distinct contributions to a movement vector. J Exp Psychol Anim Behav Process 33:100-114.
Hampson E (1990) Estrogen-related variations in human spatial and articulatory-motor skills. Psychoneuroendocrinology 15:97-111.
Hampson E, Kimura D (1988) Reciprocal effects of hormonal fluctuations on human motor and perceptual-spatial skills. Behav Neurosci 102:456-459.

Harris KM (2020) Structural LTP: from synaptogenesis to regulated synapse enlargement and clustering. Curr Opin Neurobiol 63:189-197.
Harris KM, Fiala JC, Ostroff L (2003) Structural changes at dendritic spine synapses during long-term potentiation. Philos Trans R Soc Lond B Biol Sci 358:745-748.
Hasselmo ME, Bodelon C, Wyble BP (2002) A proposed function for hippocampal theta rhythm: Separate phases of encoding and retrieval enhance reversal of prior learning. Neural Computation 14:793-817.
Hojo Y, Higo S, Ishii H, Ooishi Y, Mukai H, Murakami G, Kominami T, Kimoto T, Honma S, Poirier D, Kawato S (2009) Comparison between hippocampus-synthesized and circulation-derived sex steroids in the hippocampus. Endocrinology 150:5106-5112.
Huang CC, Hsu KS (2001) Progress in understanding the factors regulating reversibility of long-term potentiation. Rev Neurosci 12:51-68.
Huang CC, Liang YC, Hsu KS (1999) A role for extracellular adenosine in time-dependent reversal of long-term potentiation by low-frequency stimulation at hippocampal CA1 synapses. J Neurosci 19:9728-9738.
Hyde JS (2005) The gender similarities hypothesis. Am Psychol 60:581-592.
Jones CM, Braithwaite VA, Healy SD (2003) The evolution of sex differences in spatial ability. Behav Neurosci 117:403-411.
Kampen DL, Sherwin BB (1996) Estradiol is related to visual memory in healthy young men. Behav Neurosci 110:613-617.
Kato A, Hojo Y, Higo S, Komatsuzaki Y, Murakami G, Yoshino H, Uebayashi M, Kawato S (2013) Female hippocampal estrogens have a significant correlation with cyclic fluctuation of hippocampal spines. Frontiers in neural circuits 7:149.
Kato AC, Murakami G, Hojo Y, Horie S, Kawato S (2020) Rapid Effects of Estradiol on Dendritic Spines and Synaptic Plasticity in the Male and Female Hippocampus. In: Estrogens and Memory: Basic Research and Clinical Implications, pp 38-47: Oxford University Press.
Kauer JA, Malenka RC, Nicoll RA (1988) A persistent postsynaptic modification mediates long-term potentiation in the hippocampus. Neuron 1:911-917.
Kelly MJ, Moss RL, Dudley CA (1976) Differential sensitivity of preoptic-septal neurons to microelectrophoresed estrogen during the estrous cycle. Brain Res 114:152-157.
Koss WA, Frick KM (2017) Sex differences in hippocampal function. J Neurosci Res 95:539-562.
Kramar EA, Lin B, Rex CS, Gall CM, Lynch G (2006) Integrin-driven actin polymerization consolidates long-term potentiation. Proc Natl Acad Sci U S A 103:5579-5584.
Kramar EA, Chen LY, Brandon NJ, Rex CS, Liu F, Gall CM, Lynch G (2009) Cytoskeletal changes underlie estrogen's acute effects on synaptic transmission and plasticity. J Neurosci 29:12982-12993.
Kramer JH, Delis DC, Kaplan E, O'Donnell L, Prifitera A (1997) Developmental sex differences in verbal learning. Neuropsychology 11:577-584.
Lamprecht R (2016) The Role of Actin Cytoskeleton in Memory Formation in Amygdala. Front Mol Neurosci 9:23.
Larson J, Lynch G (1988) Role of N-methyl-D-aspartate receptors in the induction of synaptic potentiation by burst stimulation patterned after the hippocampal theta-rhythm. Brain Res 441:111-118.
Larson J, Munkacsy E (2015) Theta-burst LTP. Brain Res 1621:38-50.
Larson J, Wong D, Lynch G (1986) Patterned stimulation at the theta frequency is optimal for the induction of hippocampal long-term potentiation. Brain Res 368:347-350.
Larson J, Xiao P, Lynch G (1993) Reversal of LTP by theta frequency stimulation. Brain Res 600:97-102.
Lawton CA (1994) Gender Differences in Way-Finding Strategies - Relationship to Spatial Ability and Spatial Anxiety. Sex Roles 30:765-779.

Lee FS, Rajagopal R, Chao MV (2002) Distinctive features of Trk neurotrophin receptor transactivation by G protein-coupled receptors. Cytokine Growth Factor Rev 13:11-17.
Lee K, Schottler F, Oliver M, Lynch G (1980) Brief bursts of high-frequency stimulation produce two types of structural changes in rat hippocampus. J Neurophysiol 44:247-258.
Lin B, Kramar EA, Bi X, Brucher FA, Gall CM, Lynch G (2005) Theta stimulation polymerizes actin in dendritic spines of hippocampus. J Neurosci 25:2062-2069.
Lu Y, Sareddy GR, Wang J, Wang R, Li Y, Dong Y, Zhang Q, Liu J, O'Connor JC, Xu J, Vadlamudi RK, Brann DW (2019) Neuron-Derived Estrogen Regulates Synaptic Plasticity and Memory. J Neurosci 39:2792-2809.
Luine V (2015) Recognition memory tasks in neuroendocrine research. Behavioural Brain Research 285:158-164.
Luine V, Rodriguez M (1994) Effects of estradiol on radial arm maze performance of young and aged rats. Behav Neural Biol 62:230-236.
Luine V, Frankfurt M (2013) Interactions between estradiol, BDNF and dendritic spines in promoting memory. Neuroscience 239:34-45.
Luine V, Frankfurt M (2020) Estrogenic regulation of memory: The first 50 years. Hormones and behavior 121.
Luo WF, Janostiak R, Tolde O, Ryzhova LM, Koudelkova L, Dibus M, Brabek J, Hanks SK, Rosel D (2017) ARHGAP42 is activated by Src-mediated tyrosine phosphorylation to promote cell motility. J Cell Sci 130:2382-2393.
Lynch G (1998) Memory and the brain: unexpected chemistries and a new pharmacology. Neurobiol Learn Mem 70:82-100.
Lynch G (2002) Memory enhancement: the search for mechanism-based drugs. Nat Neurosci 5 Suppl:1035-1038.
Lynch G (2003) Long-term potentiation in the Eocene. Philos Trans R Soc Lond B Biol Sci 358:625-628.
Lynch G (2004a) AMPA receptor modulators as cognitive enhancers. Curr Opin Pharmacol 4:4-11.
Lynch G, Baudry M (1984) The biochemistry of memory: a new and specific hypothesis. Science 224:1057-1063.
Lynch G, Rex CS, Gall CM (2007) LTP consolidation: substrates, explanatory power, and functional significance. Neuropharmacology 52:12-23.
Lynch G, Larson J, Kelso S, Barrionuevo G, Schottler F (1983) Intracellular injections of EGTA block induction of hippocampal long-term potentiation. Nature 305:719-721.
Lynch MA (2004b) Long-term potentiation and memory. Physiol Rev 84:87-136.
Maccoby EE, Jacklin CN (1974) The psychology of sex differences. Stanford, CA: Stanford Univ. Press.
Matsuzaki M, Honkura N, Ellis-Davies GC, Kasai H (2004) Structural basis of long-term potentiation in single dendritic spines. Nature 429:761-766.
Misanin JR, Miller RR, Lewis DJ (1968) Retrograde amnesia produced by electroconvulsive shock after reactivation of a consolidated memory trace. Science 160:554-555.
Morris RG (2003) Long-term potentiation and memory. Philos Trans R Soc Lond B Biol Sci 358:643-647.
Morris RG, Anderson E, Lynch GS, Baudry M (1986) Selective impairment of learning and blockade of long-term potentiation by an N-methyl-D-aspartate receptor antagonist, AP5. Nature 319:774-776.
Mukai H, Kimoto T, Hojo Y, Kawato S, Murakami G, Higo S, Hatanaka Y, Ogiue-Ikeda M (2010) Modulation of synaptic plasticity by brain estrogen in the hippocampus. Biochim Biophys Acta 1800:1030-1044.
Muller D, Lynch G (1988) Long-term potentiation differentially affects two components of synaptic responses in hippocampus. Proc Natl Acad Sci U S A 85:9346-9350.

Muller D, Lynch G (1989) Evidence that changes in presynaptic calcium currents are not responsible for long-term potentiation in hippocampus. Brain Res 479:290-299.
Muller D, Joly M, Lynch G (1988) Contributions of quisqualate and NMDA receptors to the induction and expression of LTP. Science 242:1694-1697.
Nabavi S, Kessels HW, Alfonso S, Aow J, Fox R, Malinow R (2013) Metabotropic NMDA receptor function is required for NMDA receptor-dependent long-term depression. Proc Natl Acad Sci U S A 110:4027-4032.
Nabekura J, Oomura Y, Minami T, Mizuno Y, Fukuda A (1986) Mechanism of the rapid effect of 17 beta-estradiol on medial amygdala neurons. Science 233:226-228.
Nagy V, Bozdagi O, Matynia A, Balcerzyk M, Okulski P, Dzwonek J, Costa RM, Silva AJ, Kaczmarek L, Huntley GW (2006) Matrix metalloproteinase-9 is required for hippocampal late-phase long-term potentiation and memory. J Neurosci 26:1923-1934.
Nicoll RA (2003) Expression mechanisms underlying long-term potentiation: a postsynaptic view. Philos Trans R Soc Lond B Biol Sci 358:721-726.
Nicoll RA (2017) A Brief History of Long-Term Potentiation. Neuron 93:281-290.
Otto T, Eichenbaum H, Wiener SI, Wible CG (1991a) Learning-related patterns of CA1 spike trains parallel stimulation parameters optimal for inducing hippocampal long-term potentiation. Hippocampus 1:181-192.
Otto T, Schottler F, Staubli U, Eichenbaum H, Lynch G (1991b) Hippocampus and olfactory discrimination learning: effects of entorhinal cortex lesions on olfactory learning and memory in a successive-cue, go-no-go task. Behav Neurosci 105:111-119.
Paris JJ, Frye CA (2008) Estrous cycle, pregnancy, and parity enhance performance of rats in object recognition or object placement tasks. Reproduction 136:105-115.
Park P, Volianskis A, Sanderson TM, Bortolotto ZA, Jane DE, Zhuo M, Kaang BK, Collingridge GL (2014) NMDA receptor-dependent long-term potentiation comprises a family of temporally overlapping forms of synaptic plasticity that are induced by different patterns of stimulation. Philos Trans R Soc Lond B Biol Sci 369:20130131.
Peterson RS, Yarram L, Schlinger BA, Saldanha CJ (2005) Aromatase is pre-synaptic and sexually dimorphic in the adult zebra finch brain. Proceedings Biological sciences / The Royal Society 272:2089-2096.
Piber D, Nowacki J, Mueller SC, Wingenfeld K, Otte C (2018) Sex effects on spatial learning but not on spatial memory retrieval in healthy young adults. Behav Brain Res 336:44-50.
Popik P, Mamczarz J, Vetulani J (1994) The effect of electroconvulsive shock and nifedipine on spatial learning and memory in rats. Biol Psychiatry 35:864-869.
Qi XQ, Zhang K, Xu T, Yamaki VN, Wei ZS, Huang MF, Rose GM, Cai X (2016) Sex Differences in Long-Term Potentiation at Temporoammonic-CA1 Synapses: Potential Implications for Memory Consolidation. Plos One 11.
Rajagopal R, Chao MV (2006) A role for Fyn in Trk receptor transactivation by G-protein-coupled receptor signaling. Mol Cell Neurosci 33:36-46.
Rehnman J, Herlitz A (2007) Women remember more faces than men do. Acta Psychol (Amst) 124:344-355.
Rex CS, Kramar EA, Colgin LL, Lin B, Gall CM, Lynch G (2005) Long-term potentiation is impaired in middle-aged rats: regional specificity and reversal by adenosine receptor antagonists. J Neurosci 25:5956-5966.
Rex CS, Chen LY, Sharma A, Liu J, Babayan AH, Gall CM, Lynch G (2009) Different Rho GTPase-dependent signaling pathways initiate sequential steps in the consolidation of long-term potentiation. J Cell Biol 186:85-97.
Rex CS, Gavin CF, Rubio MD, Kramar EA, Chen LY, Jia Y, Huganir RL, Muzyczka N, Gall CM, Miller CA, Lynch G, Rumbaugh G (2010) Myosin IIb regulates actin dynamics during synaptic plasticity and memory formation. Neuron 67:603-617.

Roman F, Staubli U, Lynch G (1987) Evidence for synaptic potentiation in a cortical network during learning. Brain Res 418:221-226.
Rubinow MJ, Arseneau LM, Beverly JL, Juraska JM (2004) Effect of the estrous cycle on water maze acquisition depends on the temperature of the water. Behav Neurosci 118:863-868.
Rudy JW (2015) Actin dynamics and the evolution of the memory trace. Brain Res 1621:17-28.
Sakimoto Y, Sakata S (2020) The role of the hippocampal theta rhythm in non-spatial discrimination and associative learning task. Neurosci and Biobehav Rev 110:92-99.
Sandstrom NJ, Kaufman J, Huettel SA (1998) Males and females use different distal cues in a virtual environment navigation task. Brain Res Cogn Brain Res 6:351-360.
Schacter DL (1982) Stranger Behind the Engram: Theories of Memory and the Psychology of Science. Hillsdale NJ: Erlbaum Associates.
Seese RR, Babayan AH, Katz AM, Cox CD, Lauterborn JC, Lynch G, Gall CM (2012) LTP induction translocates cortactin at distant synapses in wild-type but not Fmr1 knock-out mice. J Neurosci 32:7403-7413.
Siedlecki KL, Falzarano F, Salthouse TA (2019) Examining Gender Differences in Neurocognitive Functioning Across Adulthood. Journal of the International Neuropsychological Society : JINS 25:1051-1060.
Silverman I, Eals M (1992) Sex differences in spatial abilities: Evolutionary theory and data. In: The adapted mind: Evolutional psychology and the generation of culture. (Barkow JH, Cosmides L, Tooby J, eds), pp 533-549. Oxford, UK: Oxford University Press.
Smith CC, McMahon LL (2005) Estrogen-induced increase in the magnitude of long-term potentiation occurs only when the ratio of NMDA transmission to AMPA transmission is increased. J Neurosci 25:7780-7791.
Smith CC, Vedder LC, McMahon LL (2009) Estradiol and the relationship between dendritic spines, NR2B containing NMDA receptors, and the magnitude of long-term potentiation at hippocampal CA3-CA1 synapses. Psychoneuroendocrinology 34 Suppl 1:S130-142.
Stackman RW, Blasberg ME, Langan CJ, Clark AS (1997) Stability of spatial working memory across the estrous cycle of Long-Evans rats. Neurobiol Learn Mem 67:167-171.
Staubli U, Scafidi J (1999) Time-dependent reversal of long-term potentiation in area CA1 of the freely moving rat induced by theta pulse stimulation. J Neurosci 19:8712-8719.
Staubli U, Thibault O, DiLorenzo M, Lynch G (1989) Antagonism of NMDA receptors impairs acquisition but not retention of olfactory memory. Behav Neurosci 103:54-60.
Stefanko DP, Barrett RM, Ly AR, Reolon GK, Wood MA (2009) Modulation of long-term memory for object recognition via HDAC inhibition. Proc Natl Acad Sci U S A 106:9447-9452.
Swain RA, Thompson RF (1993) In search of engrams. Ann N Y Acad Sci 702:27-39.
Tabatadze N, Sato SM, Woolley CS (2014) Quantitative analysis of long-form aromatase mRNA in the male and female rat brain. PLoS One 9:e100628.
Tonegawa S, Pignatelli M, Roy DS, Ryan TJ (2015) Memory engram storage and retrieval. Cur Opin Neurobiol 35:101-109.
Tulving E (1972) Episodic and semantic memory. In: Organization of Memory (Tulving E, Donaldson W, eds), pp 381-403. New York: Academic Press.
Vierk R, Glassmeier G, Zhou L, Brandt N, Fester L, Dudzinski D, Wilkars W, Bender RA, Lewerenz M, Gloger S, Graser L, Schwarz J, Rune GM (2012) Aromatase inhibition abolishes LTP generation in female but not in male mice. J Neurosci 32:8116-8126.
Vorhees CV, Williams MT (2014) Assessing spatial learning and memory in rodents. ILAR J 55:310-332.
Vorhees CV, Herring NR, Schaefer TL, Grace CE, Skelton MR, Johnson HL, Williams MT (2008) Effects of neonatal (+)-methamphetamine on path integration and spatial learning in rats: effects of dose and rearing conditions. Int J Dev Neurosci 26:599-610.

Wang W, Kantorovich S, Babayan AH, Hou B, Gall CM, Lynch G (2016a) Estrogen's effects on excitatory synaptic transmission entail integrin and TrkB transactivation and depend upon β1-integrin function. Neuropsychopharmacology 41:2723-2732.
Wang W, Le AA, Hou B, Lauterborn JC, Cox CD, Levin ER, Lynch G, Gall CM (2018a) Memory-related synaptic plasticity is sexually dimorphic in rodent hippocampus. J Neurosci 38:7935-7951.
Wang W, Cox BM, Jia Y, Le AA, Cox CD, Jung KM, Hou B, Piomelli D, Gall CM, Lynch G (2018b) Treating a novel plasticity defect rescues episodic memory in Fragile X model mice. Mol Psychiatry 23:1798-1806.
Wang W, Trieu BH, Palmer LC, Jia Y, Pham DT, Jung KM, Karsten CA, Merrill CB, Mackie K, Gall CM, Piomelli D, Lynch G (2016b) A primary cortical input to hippocampus expresses a pathway-specific and endocannabinoid-dependent form of long-term potentiation. eNeuro 3.
Warren SG, Juraska JM (1997) Spatial and nonspatial learning across the rat estrous cycle. Behav Neurosci 111:259-266.
Warren SG, Humphreys AG, Juraska JM, Greenough WT (1995) LTP varies across the estrous cycle: enhanced synaptic plasticity in proestrus rats. Brain Res 703:26-30.
Weilinger NL, Lohman AW, Rakai BD, Ma EM, Bialecki J, Maslieieva V, Rilea T, Bandet MV, Ikuta NT, Scott L, Colicos MA, Teskey GC, Winship IR, Thompson RJ (2016) Metabotropic NMDA receptor signaling couples Src family kinases to pannexin-1 during excitotoxicity. Nat Neurosci 19:432-442.
Whitlock JR, Heynen AJ, Shuler MG, Bear MF (2006) Learning induces long-term potentiation in the hippocampus. Science 313:1093-1097.
Wierenga LM, Bos MGN, van Rossenberg F, Crone EA (2019) Sex Effects on Development of Brain Structure and Executive Functions: Greater Variance than Mean Effects. J Cogn Neurosci 31:730-753.
Wong M, Moss RL (1991) Electrophysiological evidence for a rapid membrane action of the gonadal steroid, 17 beta-estradiol, on CA1 pyramidal neurons of the rat hippocampus. Brain Res 543:148-152.
Wong M, Moss RL (1992) Long-term and short-term electrophysiological effects of estrogen on the synaptic properties of hippocampal CA1 neurons. J Neurosci 12:3217-3225.
Woolley CS, McEwen BS (1994) Estradiol regulates hippocampal dendritic spine density via an N-methyl-D-aspartate receptor-dependent mechanism. J Neurosci 14:7680-7687.
Woolley CS, Gould E, Frankfurt M, McEwen BS (1990) Naturally occurring fluctuation in dendritic spine density on adult hippocampal pyramidal neurons. J Neurosci 10:4035-4039.
Woolley CS, Weiland NG, McEwen BS, Schwartzkroin PA (1997) Estradiol increases the sensitivity of hippocampal CA1 pyramidal cells to NMDA receptor-mediated synaptic input: correlation with dendritic spine density. J Neurosci 17:1848-1859.
Yang Y, Wang XB, Frerking M, Zhou Q (2008) Spine expansion and stabilizaiton associated with long-term potentiation. J Neurosci 28:5740-5751.
Youngjohn JR, Larrabee GJ, Crook TH (1991) First-last names and the grocery list selective reminding test: Two computerized measures of everyday verbal learning. Arch Clin Neuropsychol 6:287-300.
Zadran S, Qin Q, Bi X, Zadran H, Kim Y, Foy MR, Thompson R, Baudry M (2009) 17-Beta-estradiol increases neuronal excitability through MAP kinase-induced calpain activation. Proc Natl Acad Sci U S A 106:21936-21941.

# CHAPTER TWO: Memory-Related Synaptic Plasticity is Sexually Dimorphic

**Abstract**

Men are generally superior to women in remembering spatial relationships whereas the reverse holds for semantic information, but the neurobiological bases for these differences are not understood. Here we describe striking sexual dimorphism in synaptic mechanisms of memory encoding in hippocampal field CA1, a region critical for spatial learning. Studies of acute hippocampal slices from adult rats and mice show that for excitatory Schaffer-Commissural projections, the memory-related LTP effect depends upon endogenous estrogen and membrane estrogen receptor α (ERα) in females but not in males; there was no evident involvement of nuclear ERα in females, or of ERβ or GPER1 in either sex. Quantitative immunofluorescence showed that stimulation-induced activation of two LTP related kinases (Src, ERK1/2) and of postsynaptic TrkB required ERα in females only, and that postsynaptic ERα levels are higher in females than males. Several downstream signaling events involved in LTP were comparable between the sexes. In contrast to endogenous estrogen effects, infused estradiol facilitated LTP and synaptic signaling in females via both ERα and ERβ. The estrogen dependence in females was associated with a higher threshold for both inducing LTP and acquiring spatial information. These results indicate that the observed sexual dimorphism in hippocampal LTP reflects differences in synaptic kinase activation including both a weaker association with NMDA receptors and greater ERα-mediated kinase activation in response locally produced estrogen in females. We propose that male/female differences in mechanisms and threshold for field CA1 LTP contribute to differences in encoding specific types of memories.

## Introduction

Much has been learned about synaptic mechanisms of memory encoding and the neuronal activity patterns that engage them. This includes the particularly intriguing finding that memory-related LTP of excitatory transmission in hippocampus (Vierk et al., 2012) and amygdala (Bender et al., 2017) is dependent upon locally synthesized estrogen in females but not in males. Hippocampal and other forebrain neurons express cytochrome p450 aromatase, the final enzyme in the production of estradiol (E2), the most prevalent and potent estrogen in brain, and this enzyme is concentrated in hippocampal axon terminals in both sexes (Hojo et al., 2004; Hojo et al., 2011; Kato et al., 2013; Tabatadze et al., 2014). Resultant E2 levels are substantially higher in hippocampus than in plasma and somewhat surprisingly higher in males than in females (Mukai et al., 2010; Ooishi et al., 2012). Nevertheless, blocking local E2 production has been shown to eliminate LTP in females while having little if any effect on potentiation in males (Vierk et al., 2012; Bender et al., 2017). This is all the more surprising in that exogenous E2 applied at physiological concentrations is an extremely potent enhancer of glutamatergic transmission and hippocampal LTP in both sexes (Woolley, 2007; Kramar et al., 2009). These findings raise a number of fundamental questions concerning sex differences in plasticity of excitatory synaptic transmission. Where in the complex signaling cascades that produce LTP does the neurosteroid exert its effects in females? Why don't the high levels of local estrogen in males contribute to LTP? And, regarding functional outcome, does the addition of an estrogen step in the production of enduring changes in synaptic strength in females affect the threshold levels of synaptic activity needed for inducing stable LTP, a point with evident implications for learning?

To address these issues the present studies first evaluated the type of estrogen receptor (ER) required for LTP of the glutamatergic, Schaffer-Commissural (S-C) afferents to hippocampal field CA1 in adult female rats and mice. Although contributions of multiple ERs to

synaptic responses have been described for hippocampal synapses (Smejkalova and Woolley, 2010; Kumar et al., 2015; Oberlander and Woolley, 2016), we anticipated this would be ERβ because infusion of agonists for this receptor enhances synaptic AMPA receptor responses and facilitate field CA1 LTP whereas ERα agonists do not (Kramar et al., 2009; Smejkalova and Woolley, 2010). However, the receptor critical for S-C LTP in females proved to be ERα and, more specifically, membrane-associated as opposed to nuclear ERα. Subsequent analyses identified an unexpected mode of action for ERα in females and, in particular, sexually dimorphic regulation of the NMDAR-regulated kinases Src, Erk1/2, and TrkB which each play critical roles in consolidating newly induced LTP. The studies also identified markedly lower levels of synaptic ERα in males as compared to females, suggesting a reason why males don't use local estrogen to enhance plasticity.

The above results provided a neurobiological perspective from which to consider the much-discussed question of sex differences in learning (Andreano and Cahill, 2009). In *in vivo* studies of gonadally intact females the problem is complicated by variations in levels of the circulating estrogen associated with phases of the estrus cycle. Using hippocampal slices from females, we found that infused E2, acting through both ERα and ERβ, engages the same kinases activated by local estrogen through ERα during the induction of LTP and, further, that contributions of local estrogen offset a higher activity-threshold for stable potentiation in females as compared to males. Studies of field CA1-dependent spatial (object location) learning during the high vs. low estrogen stages of the estrus cycle confirmed predictions from the LTP work regarding activation of synaptic kinases and memory encoding.

**Materials and Methods**

*Animals.* Experiments were conducted using naïve adult (2-4 months of age) rats and mice of both sexes that were group housed (4 rats or 5 mice per cage) with food and water *ad libitum*.

All animals were on a 12 hr on / 12 hr off light cycle. Experiments were initiated from 8-10 AM for electrophysiology and treatments for biochemical measures; animals were euthanized from 10-11 AM for studies involving immunofluorescence analysis alone. Experiments were conducted in accordance with NIH Guidelines for the Care and Use of Animals and protocols approved by the UCI Institutional Care and Use.

*Estrous staging of female rats and mice.* For all females used, estrous cycle was evaluated using vaginal lavage and Nissl staining (McLean et al., 2012). For electrophysiological studies estrous state was determined from samples collected at the time of sacrifice and evaluated after analysis of electrophysiological recordings. Results are reported separately for cases within proestrus (i.e., with smears showing mostly nucleated cells) as compared to those outside proestrus including estrus (mostly cornified cells), and diestrus (mostly leukocytes and some cornified cells) (McLean et al., 2017; Kato et al. 2013). As circulating estrogen levels are low in the latter states relative to proestrus (Kato et al., 2013), results for animals at these stages are pooled as 'non-proestrus' for electrophysiological and signaling analyses. For behavioral experiments, vaginal smears were collected and evaluated for several days prior to experimental use in order to select animals for training when in a specific estrous state. These animals were coded and run for behavioral analysis blind to that state.

*Hippocampal slice electrophysiology.* Extracellular field recordings were collected from hippocampal slices prepared from, in both sexes, 40-50 day old rats (Sprague Dawley; Harlan Laboratories, Indianapolis, IN) and 3-4 month mice. The latter included mutant mice engineered to prevent trafficking of ERα to the nucleus (membrane only ERα, MOER) or the plasma membrane (nucleus only ERα, NOER) (Pedram et al., 2014) and were compared with age, sex and background strain (C57BL6N) matched wild type (WT) mice. Some studies used conditional β1-integrin KOs (cKOs) and paired WTs (Wang et al., 2016a). The β1 cKOs were generated by

crossing mice homozygous for a floxed β1-exon 3 with mice expressing Cre via CaMKII promoter thus generating progeny in which β1 integrin expression was knocked down in excitatory hippocampal and cortical neurons beginning at about 3 weeks of age.

Acute hippocampal slices were prepared as described (Trieu et al., 2015; Wang et al., 2016b), collected into chilled high magnesium artificial cerebral spinal fluid (aCSF) containing (in mM): 124 NaCl, 3 KCl, 1.25 $KH_2PO_4$, 5.0 $MgSO_4$, 26 $NaHCO_3$ and 10 dextrose and then transferred to an interface recording chamber at 31 ± 1°C with 60-70 ml/hr infusion of oxygenated aCSF containing (in mM): 124 NaCl, 3 KCl, 1.25 $KH_2PO_4$, 1.5 $MgSO_4$, 26 $NaHCO_3$, 2.5 $CaCl_2$, and 10 dextrose (Wang et al., 2016b). Experiments began 1.5 hr after sacrifice. To study responses of S-C innervation of field CA1b st. radiatum (SR), stimulating electrodes were placed in CA1a and CA1c SR (**Fig. 2.1**) and a glass recording electrode (2 M NaCl filled, 2-3 MΩ) was positioned in CA1b SR at the midpoint between the two stimulating electrodes; all electrodes were equidistant from the pyramidal cell layer (offset by ~100 µm) to optimize recording responses to stimulation of the S-C projection which courses parallel to that cell layer. Stimulation intensity was set to elicit fEPSPs that were 50-60% of the maximum spike free response. fEPSP initial slopes and peak amplitudes were measured using NACGather 2.0 (Theta Burst Corp. Irvine, CA). Baseline stimulation was applied as single pulses at 3/min. Unless specified, LTP was induced with a single train of theta burst stimulation (TBS: 10 bursts of 4 pulses at 100 Hz, 200 ms between bursts) applied via one electrode. In abbreviated stimulation protocols, parameters of the individual stimulation bursts were the same, burst pairs and triplets were presented with 200 ms inter-burst, and there was a 2 min gap between sets (i.e., pairs or triplets). In experiments involving TBS, control slices received low frequency stimulation (LFS) of 3 pulses/min. Group comparisons of LTP magnitude considered the mean response during the last 5 minutes of the recordings relative to baseline recordings. For immunofluorescence analyses of synaptic signaling associated with LTP, single 10 burst trains of TBS were applied to each of the two stimulating electrodes (**Fig. 2.1**) with 30 sec in between.

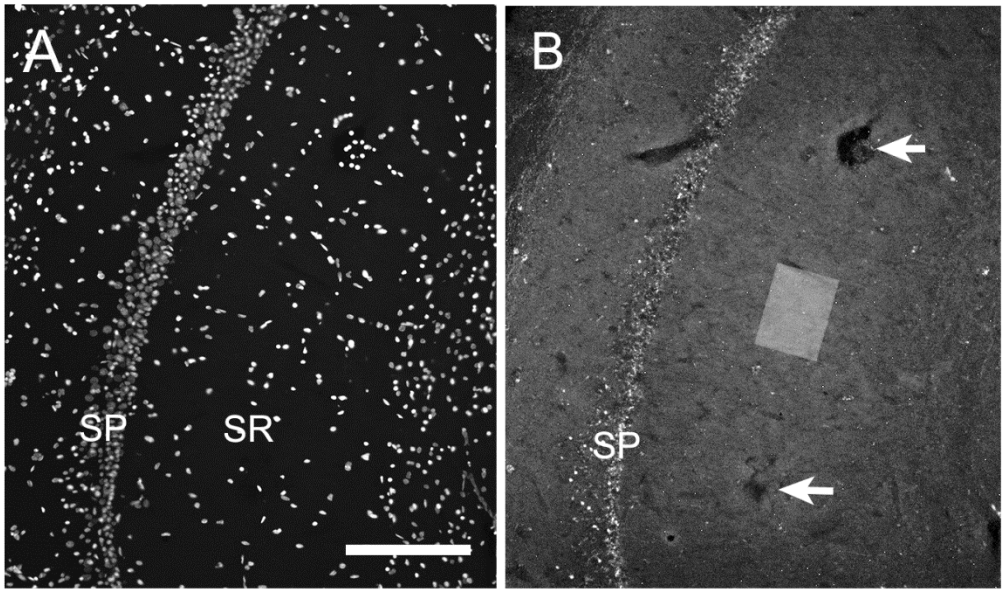


**Figure 2.1. Electrode and image sample field placement in CA1 stratum radiatum.** Images show at low magnification (**A**) DAPI-labeled cellular nuclei and (**B**) immunofluorescence for PSD95 in the same CA1 field of a hippocampal slice to illustrate the position of the stimulating electrodes (arrows indicate areas of visible electrode damage) and of image z-stack collection (rectangle drawn to the scale of the sample field). In this case, the electrodes were lowered deep within the tissue to create visible damage for illustration purposes. SR, stratum radiatum. SP, stratum pyramidale. Bar = 200 µm for A and B.

*Drug Application.* For hippocampal slice studies, antagonists were introduced to the ACSF perfusion line using a syringe pump whereas E2 was added directly to the perfusion ACSF reservoir. Effects of vehicle and experimental reagent infusion were evaluated in parallel, on separate recording chambers, using slices from the same animal. The following reagents and final treatment concentrations were used: ERα antagonist MPP (3 μM); ERβ antagonist 4-[2-phenyl-5,7-*bis*(trifluoromethyl)pyrazolo[1,5-*a*] pyrimidin-3-yl]phenol (PHTPP, 3 μM); β-estradiol (E2, 1 nM); ANA-12 (750 nM) and ROCK inhibitor H1152 dihydrochloride (100 nM) all from Tocris Bioscience (Bristol, UK); and selective G protein coupled estrogen receptor (GPER1) antagonist G15 (500 nM, Cayman Chemical, Ann Arbor, MI). All compounds were prepared in 100% dimethylsulfoxide (DMSO) with the latter diluted to a final concentration in the ACSF bath of <0.01% for both experimental and vehicle infusions. Echistatin (10μM; Sigma-Aldrich, St. Louis, MO) was diluted in ACSF and applied locally by pressure ejection (Picospritzer; General Valve, Fairfield, NJ) (Kramar et al., 2006). For studies of the effects of hippocampal estrogen depletion, mice were given systemic injections of formestane (2 mg/kg subcutaneous, Tocris Bioscience) daily for 7 days with the last treatment 1 day prior to experimental use. For behavioral experiments, mice were given intraperitoneal injections of the following drugs (or vehicle): MPP or PHTPP (0.6 mg/kg, 60 min prior to behavior) dissolved in saline with 5% dimethylsulfoxide (Labouesse et al., 2015; Li et al., 2017).

*Immunostaining and Fluorescence Deconvolution Tomography (FDT).* Hippocampal slices were immersion fixed in 4% paraformaldehyde, sectioned at 20 μM and then the slide mounted tissue sections were processed for dual immunofluorescence and FDT as described (Seese et al., 2013; Seese et al., 2014). Primary antisera cocktails included rabbit antisera to pTrkB Y515 (Wang et al., 2016a) (1:500 Novus Biochem, Littleton, CO; NB100-92656, RRID AB1218205), the activated (Act) conformation of β1 integrin (Wang et al., 2016a) (1:400, EMD Millipore, Burlington, MA; MAB2259Z, RRID AB94616), pFAK Y397 (Bock and Herz, 2003) (1:500,

ThermoFisher Scientific, Waltham, MA; 44-624G, RRID AB2533701), pCofilin Ser3 (Lauterborn et al., 2016a) (1:500, Abcam, Cambridge, MA; ab12866, RRID AB299488), pERK1/2 Thr202/Tyr204 (Seese et al., 2014) (1:500, Cell Signaling, Danvers, MA; 4370, RRID AB2315112), pSrc Tyr418 (Chen et al., 2010) (1:500, ThermoFisher Scientific; 44–660G, RRID AB1500523), ERα (1:700, Santa Cruz Biotechnology, Dallas TX; sc-542, RRID AB631470), or GPER1 (1:1000, Abcam ab39742, RRID AB1141090) in combination with mouse anti-PSD-95 (1:1000, ThermoFisher Scientific, MA1-045, RRID AB325399 or Abcam, ab12093, RRID AB298846), or mouse anti-ERβ (1:700, Santa Cruz Biotechnology, sc-390243, RRID AB2728765) in combination with goat anti-PSD-95 (1:1000, Abcam, ab12093, RRID AB298846). Secondary antisera included AlexaFluor 594 anti-rabbit IgG with either AlexaFluor 488 anti-mouse IgG or anti-goat IgG, or AlexaFluor 594 anti-mouse IgG with AlexaFluor 488 anti-goat IgG (1:1000, Life Technologies, Carlsbad, CA).

For measures of synaptic immunolabeling, epifluorescence images were collected at 63X using a Leica DM6000B microscope equipped with a Ludl stage with a BioPrecision Stepper motor driven by Volocity 4.0 software (Perkin Elmer, Waltham, MA): Image z-stacks were collected in 200 nm steps through a depth of 2µm from CA1b SR for a total sample field of 136 µm x 105 µm x 2 µm (28,560 $\mu m^3$). An individual z-stack was collected from CA1b SR from each of 4 to 5 tissue sections through each hippocampal slice. For image collection from slices having received S-C stimulation, the z-stack was collected from the mid-point between the positions of the two stimulation electrodes (evident by slight tissue damage) and at comparable distance from the cell layer (**Fig. 2.1**). Thus, the image-sample field was approximately 200 µm from each of the stimulation electrodes. Briefly, images were processed through restorative deconvolution (99% confidence, Volocity 4.0) and individual z-stacks were used to construct a 3-dimensional (3D) montage of each sample field; within that field, objects were detected using threshold image segmentation across each channel separately. An image was normalized and thresholded at a given intensity threshold, erosion and dilation was used to fill holes and remove

background pixels, and objects were segmented based on connected pixels above a threshold using in house software (using C, Java, Matlab, and Perl). All immunofluorescent elements meeting size constraints of synapses, and detected across multiple intensity thresholds, were quantified using automated systems (Seese et al., 2014; Wang et al., 2016a). This resulted in analysis of ~30,000 reconstructed PSD-95 immunoreactive (IR) elements (i.e., PSDs) per sample field and over 100,000 PSDs per slice. The PSD-95-IR elements were considered double-labeled for the second antigen if there was contact or overlap in fields of the two fluorophores as assessed in 3D. The quantification of synaptic immunolabeling is presented graphically in two ways. First, using automated systems, the density of immunoreactivity to the antigen co-localized with PSD-95 was measured for each double-labeled PSD and the numbers of such elements within a particular density range was expressed as a percent of all double-labeled PSDs (i.e., double-labeled, PSD-95-IR elements) within the full 28,560 $\mu m^3$ sample field. These results were used to construct line graph, immunolabeling density frequency distributions wherein elements with lower levels immunoreactivity (e.g., for pSrc) are plotted toward the left and those with dense immunoreactivity are plotted toward the right on the x-axis; for these data significance was determined using RM-ANOVA. Second, to provide an index of the proportion of PSD-95-IR synapses densely labeled for the second antigen, bar graphs show the numbers of synapses for which immunolabeling for the second antigen was above a specific density threshold (≥90 density units) normalized to the control group (vehicle or LFS) mean for that particular experiment; for these analysis significance was determined using 2-tailed *t*-test (2 groups) or 1 way ANOVA with post hoc comparisons (≥3 groups).

To illustrate the synaptic localization of ERα, image z-stacks of dual ERα and PSD-95 immunolabeling (in tissue processed as described) were collected at Nyquist rate (1.3 µm steps through a depth of 2 µm) using a ThorLabs 2-photon microscope (Newton, New Jersey) with a 63X (NA1.4) objective, deconvolved with AutoQuant (Media Cybernetics, Rockville MD) and constructed into a 3D montage using Imaris (Bitplane; Concord MA) (Lauterborn et al., 2016b).

*Object location memory (OLM).* As detailed elsewhere (Seese et al., 2014), C57BL6/J mice at 8-10 weeks of age were handled for 2 min daily for 5 days and then habituated to white (24×30×30 cm) plexiglas chamber for 5 min/day for at least 5 days. For the training trial the following day, mice were placed in the chamber containing identical small glass funnels in two adjacent corners of the apparatus for 5 or 10 min. For retention testing, mice were returned to the chamber 24 hr post-training, with either the left or right funnel being displaced toward the chamber center, and allowed to explore for 5 min. Animal movements within the chamber were video recorded using an overhead camera for all training and test sessions. Movements were scored from the videos by an observer that was blind to experimental group and treatment. Object exploration was scored in seconds when the animal was facing towards and sniffing the object (funnel) within ~0.5 cm. Interaction was not scored when the animal climbed over the object or when they were within the zone but not addressing the objects (i.e. turning head). Discrimination index was calculated as $100 \times (t_{novel} - t_{familiar})/ (t_{novel} + t_{familiar})$ and total object exploration time was the total-sum time of interactions with both objects.

*Experimental Design and Statistical Analyses.* Execution of experimental procedures and analyses were arranged in order to enhance rigor and avoid experimenter bias. Specifically, for analyses of electrophysiological responses in NOER and MOER mice, hippocampal slices from age matched mutant and wild type mice were run simultaneously on parallel electrophysiology rigs using the same ACSF and reagent solutions. For studies of effects of sex and estrogen receptor antagonism on synaptic signaling, acute hippocampal slices from the same animal were run on parallel rigs to first assess the effect of the test reagent (e.g., MPP, rig #1) versus vehicle (rig #2) on synaptic responses in the same animal. The slices were then fixed and processed for immunostaining in batches that included groups to be compared for that particular analysis (e.g., male vs female, with MPP vs without MPP). Immunofluorescent labeling was

photographed blind to group, and quantification of synaptic labeling was accomplished using automated systems which avoid potential effects of experimenter bias.

Group sizes for the different analyses were selected on the basis of past experience and to be equal to or exceed dictates of power analyses. For electrophysiological studies, power analysis determined that with the typical effect size and profile (i.e., LTP magnitude entailing a 50% increase in the fEPSP; sigma = 15; alpha = 0.05; power = 0.80) the minimal sample size to determine the significance of a 20% change in LTP magnitude would be 5 slices/group. For immunofluorescence analyses the power analysis determined that, for typical effect sizes from similar studies (Wang et al., 2016a), we needed an '*n'* of at least 4 slices/group. For behavior experiments similar calculations determined with an effect size (i.e., Discrimination index, DI) of 30% (sigma = 10%; alpha = 0.05; power = 0.80) the minimal sample size to detect a 10% difference in the DI would be 3/group. Throughout the text, *n* values denote numbers of hippocampal slices per group unless otherwise indicated. For electrophysiological studies slices were obtained from ≥ 4 animals. For behavioral experiments the analyses of movements were made from video recordings by an investigator blind to estrus state and experimental group.

The results are presented as group mean ± SEM values. Statistical significance (i.e., $p \leq 0.05$) was evaluated using two-tailed Student's *t*-test unless otherwise specified; some experiments used one- and two-way ANOVA (GraphPad Prism, San Diego, CA) as indicated. In graphs asterisks denote the level of significance (*$p \leq 0.05$; **$p \leq 0.01$; ***$p \leq 0.001$).

## Results

*LTP consolidation in female CA1 requires endogenous estrogen acting on membrane ERα.*

Prior work had shown that in rats depletion of estrogen levels using the aromatase inhibitor letrozole, given *in vivo* in several daily systemic injections prior to acute slice preparation or in bath treatments of cultured hippocampal slices, impairs LTP in the Schaffer-

commissural (S-C) projections to field CA1 of females but not males (Vierk et al., 2012). We tested for similar sex-specific effects of estrogen depletion on theta burst stimulation (TBS)-induced S-C LTP in mice using *in vivo* pretreatment (7 daily IP injections) with the structurally different aromatase inhibitor formestane (Wei et al., 2014). In acute hippocampal slices from formestane-pretreated female mice, TBS applied to the S-C projections elicited normal initial potentiation but this failed to stabilize with responses decaying to control levels over the hour post-TBS; in contrast, potentiation in females pretreated with vehicle, LTP was stable and robust (**Fig. 2.2A*, left***). Infusion of 1 nM E2 largely restored LTP in slices from formestane pretreated female mice (**Fig. 2.2A, *right***). Formestane pretreatment had no effect on S-C potentiation in slices from males ($p$=0.69, $t_{(14)}$=0.41; veh $n$=7, formestane $n$=9). Together with prior results, these experiments demonstrate that in females but not in males field CA1 LTP is dependent upon local estrogen action.

Next, we used selective receptor antagonists to evaluate which of the principle estrogen receptors expressed in hippocampus (ERα, ERβ, and GPER1) (Hara et al., 2015) mediates the effects of endogenous estrogen on LTP. Infusion of the ERαantagonist MPP (3μM) markedly reduced S-C potentiation in slices from females but not males (**Fig. 2.2B**). Bath treatment with antagonists for ERβ (PHTPP, 3μM) or the third estrogen receptor in hippocampus GPER1 (Almey et al., 2015; Kumar et al., 2015; Waters et al., 2015) (G15, 500 nM) had no effect on LTP in females (**Fig. 2.2C,D**). Similarly, PHTPP infusion had no effect on S-C LTP in males ($p$=0.74, $t_{(14)}$=0.23, $n$=8/group); this despite the finding that E2 infusion facilitates LTP in males via ERβ (Kramar et al., 2009; Wang et al., 2016a). We conclude that effects of local estrogen on LTP depends on ERα in females only.

In slices from females, the composite response to the first theta burst in a train (**Fig. 2.2E**) and the well-known within-train facilitation of burst responses (Kramar et al., 2009) (**Fig. 2.2F**) were comparable to responses in slices from males, and were similarly not affected by MPP treatment. Within-train facilitation reflects suppression of feedforward inhibitory

postsynaptic potentials and associated increases in NMDAR-mediated depolarization (Larson and Lynch, 1986). Thus, these findings indicate that the initial triggering steps for LTP are similar in CA1 of males and females and are not influenced by estrogen acting through ERα. Note also that the initial S-C potentiation produced by TBS, a variable that is strongly dependent on NMDARs (Larson and Lynch, 1986), was comparable in males and females and unaffected by MPP (**Fig. 2.2B**).

To further test the conclusion that ERα is critical for S-C LTP in adult females, we assessed potentiation in transgenic mice selectively lacking either membrane or nuclear variants of the receptor. 'Nucleus only ERα' (NOER) mice have a point mutation that prevents ERα-palmitoylation and, as a consequence, plasma membrane trafficking (Pedram et al., 2014). The mutants have impaired reproductive tract development like full ERα knockouts (Pedram et al., 2014), but hippocampal structure and basic synaptic physiology are normal. Input/output (I/O) curves for field EPSPs (fEPSPs) were comparable for slices from NOER and wild type (WT) female mice (**Fig. 2.2G, *left***). However, despite normal initial potentiation, LTP failed to stabilize in female NOERs (**Fig. 2.2G, *right***). In contrast, in slices from female mice that express the membrane-associated, but lack nuclear, ERα ('membrane only ER' or MOER mice) (Pedram et al., 2013) the S-C I/O curve and LTP were normal (**Fig. 2.2H**). In distinction from females, the male NOER mice were indistinguishable from WTs with regard to both the S-C I/O curve and LTP (**Fig. 2.2I**). These results reinforce the conclusion that ERα is needed for LTP in female but not male hippocampal field CA1 and further show that nuclear ERα does not contribute to the I/O curve or to LTP in either sex.

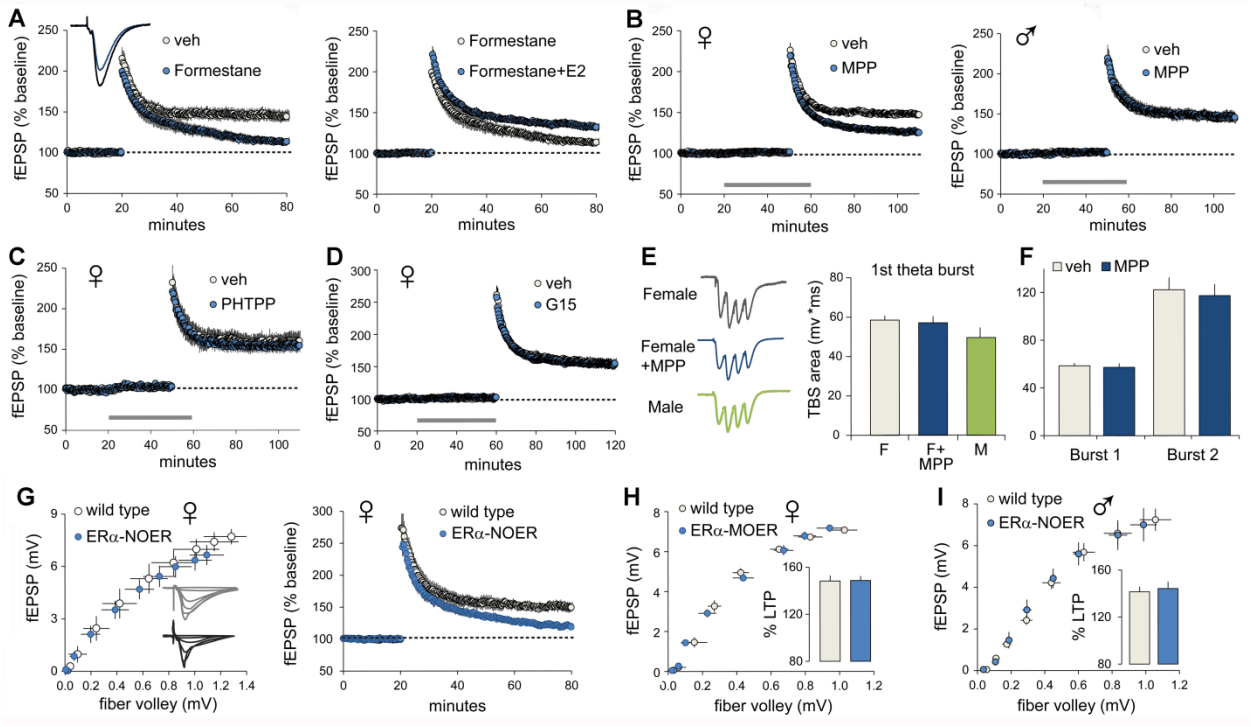


**Figure 2.2. Local estrogen promotes LTP via membrane ERα in female hippocampus.** LTP was induced by TBS of Schaffer-commissural (S-C) projections and fEPSPs were recorded from CA1 SR. (**A**, *left*) In vivo formestane pretreatment severely impaired LTP in slices from female rats ($p$=0.0026, $t_{(10)}$=3.98 for vehicle (veh) vs formestane during last 5 min of recordings, $n$=6/group). (**A**, *right*) E2 (1 nM) perfusion initiated 30 min prior to TBS rescued LTP in slices from formestane-pretreated females ($p$=0.017, $t_{(17)}$=2.65; formestane $n$=6, formestane+E2 $n$=13). (**B**) ERα antagonist MPP blocked LTP in female (*left*; $p$<0.0001, $t_{(26)}$=5.55; $n$=14/group) but not male (*right*; $p$=0.87, $t_{(16)}$=0.16, $n$=9/group) slices. (**C, D**) Neither ERβ antagonist PHTPP (C; $p$=0.70, $t_{(10)}$=0.39; $n$=6/group) nor GPER1 antagonist G15 (D; $p$=0.84, $t_{(17)}$=0.21; veh $n$=10, G15 $n$=9) influenced S-C LTP in females. (**E**) The size (area) of the first theta burst response was not different between slices from female, female+MPP, or male slices ($p$=0.20, $F_{(2,26)}$=1.70, one-way ANOVA; male $n$=7, other groups $n$=10). (**F**) MPP did not influence the theta burst response enhancement between the first and second burst in females ($p$=0.77, $F_{(1,18)}$=0.09, 2-way ANOVA; $n$=10/group). (**G**) The fiber volley to fEPSP amplitude relationship (I/O curve) for female NOER mice was comparable to that of female wild types (WTs) ($p$=0.61, $F_{(9,90)}$=0.81, 2-way ANOVA; $n$=6/group) but S-C LTP failed to stabilize ($p$=0.0006, $t_{(14)}$=4.39 vs WT; WT $n$=6, NOER $n$=10). (**H**) For female MOER mice, both the I/O curve ($p$=0.21, $F_{(8,144)}$=1.37, 2-way RM-ANOVA; WT $n$=10, MOER $n$=12) and S-C LTP (insert bar graph, $p$=0.99, $t_{(20)}$=0.01; WT $n$=10, MOER $n$=12) were comparable to measures from female wild types. (**I**) For male NOER mice, both the I/O curve ($p$=0.93, $F_{(7,77)}$=0.36, 2-way ANOVA; WT $n$=7, NOER $n$=6) and S-C LTP (insert bar graph, $p$=0.77, $t_{(23)}$=0.30; WT $n$=9, NOER $n$=16) were comparable to measures from male wild types.

*Females require ERα for TBS-activation synaptic kinases critical for LTP.*

Activation of synaptic NMDARs is already evident on the second burst in a TBS train, and this is among the first steps in the induction of S-C LTP (Lynch et al., 2013). It is quickly followed by activation of postsynaptic kinases including the Src family kinases (Src) and extracellular signal-regulated protein kinase 1/2 (ERK1/2) (Wang et al., 2007; El Gaamouch et al., 2012; Weilinger et al., 2016). Src kinases then phosphorylate the cytoplasmic tail of NMDAR subunit NR2B, further increasing calcium influx (Salter and Kalia, 2004; Trepanier et al., 2012). These secondary signaling events support LTP stabilization and memory formation (Lu et al., 1998; Giovannini et al., 2001; Bozon et al., 2003; Giovannini, 2006; Yamazaki et al., 2006; Patterson et al., 2010) and, for Src, promote activation of other synaptic receptors required for LTP stabilization including the neurotrophin receptor TrkB (Chen et al., 2010) and β1 integrins (Babayan et al., 2012; Wang et al., 2016a). Membrane ERα signals to both Src and ERK1/2 in various cell types including neurons (Song et al., 2005; Fu and Simoncini, 2008; Micevych et al., 2017). We therefore used immunofluorescence to test if ERα modulates TBS-driven increases in synaptic Src and ERK1/2 phosphorylation at specific activation sites in hippocampal slices from male and female rats. Dual immunofluorescence and Fluorescence Deconvolution Tomography (FDT) were used to generate digital 3D reconstructions of synapses immunolabeled for the target phosphoprotein and the excitatory synapse, postsynaptic density protein PSD-95 (Petersen et al., 2003) in the field surrounding the LTP recording electrode (**Fig. 2.3A**). FDT supports quantification of over 30,000 double-labeled synapses per 136 x 105 x 2 µm image z-stack and over 100,000 synapses per hippocampal slice (Seese et al., 2012). We first confirmed the finding (Chen et al., 2010) that a single TBS train increases the proportion of PSDs associated with dense concentrations of phosphorylated (p) Src Y418 in male slices: In slices receiving TBS, as compared to those receiving low frequency stimulation (LFS), the density frequency distribution for pSrc immunoreactivity co-localized with PSD-95 exhibited a

greater skew to the right (**Fig. 2.2B**, left), and the proportion of double-labeled synapses containing high levels of pSrc immunoreactivity (≥ 90 units on the frequency distribution) was greater (**Fig. 2.3B, right**). Infusion of the ERα blocker MPP did not attenuate either effect in males (**Fig. 2.3B**) and the ERβ antagonist PHTPP was similarly ineffective (not shown; $p>0.999$, $F_{(19,418)}=0.113$, $n=12$/group for frequency distributions in TBS vs TBS+PHTPP groups).

Strikingly different results were obtained with slices from young adult females. For the CA1 SR recording field, TBS increased both the rightward skew in the pSrc density frequency distribution (**Fig. 2.3C, left**) and the percentage of PSDs with high concentrations of pSrc immunoreactivity (**Fig. 2.3C,** right); in contrast to results in males, the ERα antagonist MPP significantly reduced both effects in females. As previously reported for males, TBS causes a robust increase in synaptic pERK1/2 Thr202/Tyr204 (Seese et al., 2012). This effect of TBS was also present in slices from females but was also markedly reduced by MPP (**Fig. 2.3A, 2.3D**). Thus, two early NMDAR-dependent steps in the production of S-C LTP require ERα function in females but not in males.

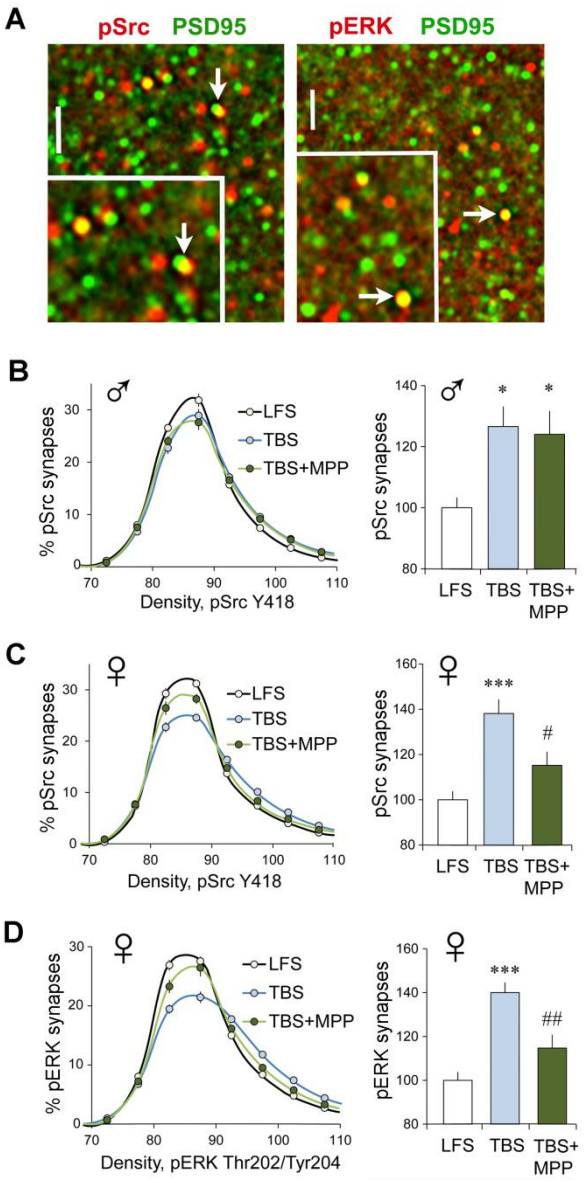


**Figure 2.3. TBS-driven increases in synaptic pSrc and pERK are ERα-dependent in females.** Fluorescence deconvolution tomography was used to assess effects of S-C stimulation on synaptic immunolabeling at 3-4 min post-TBS. Line graphs show immunolabeling density frequency distributions for the phosphoprotein at all double-labeled (phosphoprotein-IR + PSD-95-IR) synapses (see Methods); treatment effects on frequency distributions were assessed using two-way RM-ANOVA. Bar graphs show the proportion of double-labeled synapses containing dense immunolabeling for the phosphoprotein (≥90 density units) with group mean values normalized to the mean for control (low frequency stimulation, LFS) slices. (**A**) Deconvolved images show punctate localization of PSD-95-IR (green) in combination with that for pSrc (red, left) and pERK1/2 (red, right); yellow indicates double-labeled elements (arrows) (bar: 10 µm for large image, 2 µm for insets). (**B**) In slices from males, TBS caused a greater rightward skew in the pSrc density frequency distribution (thus an increase in the

proportion of synapses with dense pSrc immunoreactivity) as compared to the curve for slices receiving LFS ($p$<0.0001, $F_{(19,323)}$=5.348; LFS $n$=9, TBS $n$=10, TBS+MPP $n$=10); this effect was not influenced by ERα antagonist MPP ($p$=0.917, $F_{(19,342)}$=0.585). Bar graph shows that in males TBS increased numbers of PSD95-IR synapses with dense pSrc-IR relative to measures from slices receiving LFS and that this effect was not altered by MPP ($p$=0.0135, $F_{(2,28)}$=5.11, Bonferroni's test for post-hoc comparisons: LFS vs. TBS: $p$<0.05, LFS vs. TBS +MPP: $p$<0.05; TBS vs. TBS+MPP: n.s.). (**C**) In females, TBS also caused a greater rightward skew in the pSrc immunolabeling density frequency distribution relative to that for LFS slices (left; $p$<0.0001, $F_{(19,342)}$=24.56; $n$=10/group); MPP substantially reduced the effect ($p$<0.0001, $F_{(19,342)}$=5.981). Bar graph shows that in females the proportion of PSDs with dense pSrc-IR was increased by TBS and this increase was substantially reduced by MPP ($p$=0.0002, $F_{(2,29)}$=12.33, post-test: LFS vs. TBS: $p$<0.001, TBS vs. TBS+MPP: $^{\#}p$<0.02; LFS vs. TBS + MPP: n.s.). (**D**) TBS caused a greater rightward skew in the density frequency distribution for synaptic pERK-IR in female slices ($p$<0.0001, $F_{(19,361)}$=34.62; LFS $n$=10, TBS $n$=11, TBS+MPP $n$=8); MPP substantially reduced this effect ($p$<0.0001, $F_{(19,323)}$=10.01); bar graph shows that the TBS-driven increase in numbers of densely pERK-IR synapses was similar in magnitude to that for pSrc and attenuated by MPP ($p$<0.0001, $F_{(2,28)}$=19.68; LFS vs. TBS: $p$<0.0001, TBS vs. TBS+MPP: $^{\#\#}p$<0.01).

*Sexually dimorphic effects of infused estradiol on synaptic kinase activation.*

The essential contribution of ERα to LTP in females (but not males) could involve facilitation of NMDAR-gated synaptic currents or a direct action of ERα on Src and ERK1/2. As described above (**Fig. 2.2E,F**), the ERα antagonist MPP, infused beginning 30 min prior to TBS, had no effect on the NMDAR-mediated within-train increase in the size of the composite fEPSP response, an observation that argues against an influence of ERα on NMDAR function during the induction of LTP. Estrogen receptors signal directly to both ERK1/2 and Src in various cell preparations (Fu and Simoncini, 2008) and we found that bath perfusion of 1 nM E2 rapidly increased phosphorylation of synaptic ERK1/2 in hippocampal slices from females, as evidenced by an increase in the percentage of PSD-95-IR synapses associated with high concentrations of pERK1/2. This effect was substantially reduced by either ERα blocker MPP (**Fig. 2.4A**) or ERβ blocker PHTPP (**Fig. 2.4B**). Similar results were obtained for pSrc: in female slices E2 infusion increased the rightward skew in the density frequency distribution for synaptic pSrc-IR (**Fig. 2.4C**) and increased the proportion of PSDs associated with dense pSrc-IR (**Fig. 2.4D**); both of these effects were attenuated by MPP (**Fig. 2.4C,D**). These results confirm that in females E2 acting through ERα directly promotes intermediary steps (kinase activation) between the NMDARs and the actin remodeling underlying LTP (Lynch et al., 2013) at hippocampal synapses. The results further show that in contrast to effects of endogenous estrogen, in females infused E2 influences these kinases through both ERα and ERβ.

We tested for similar regulation of the synaptic kinases in slices from male rats and found that E2 infusion robustly increased the proportion of PSD-95-IR excitatory synapses with dense pERK1/2 immunoreactivity but, in contrast to effects in females, this increase was not influenced by ERα blocker MPP (**Fig. 2.4E**). In males the ERβ antagonist PHTPP reduced E2-driven increases in synaptic pERK1/2 (**Fig. 2.4F**). This result aligns with our previous observation that ERβ is critical for LTP enhancement by exogenous E2 in male hippocampus with negligible contribution from ERα (Kramar et al., 2009).

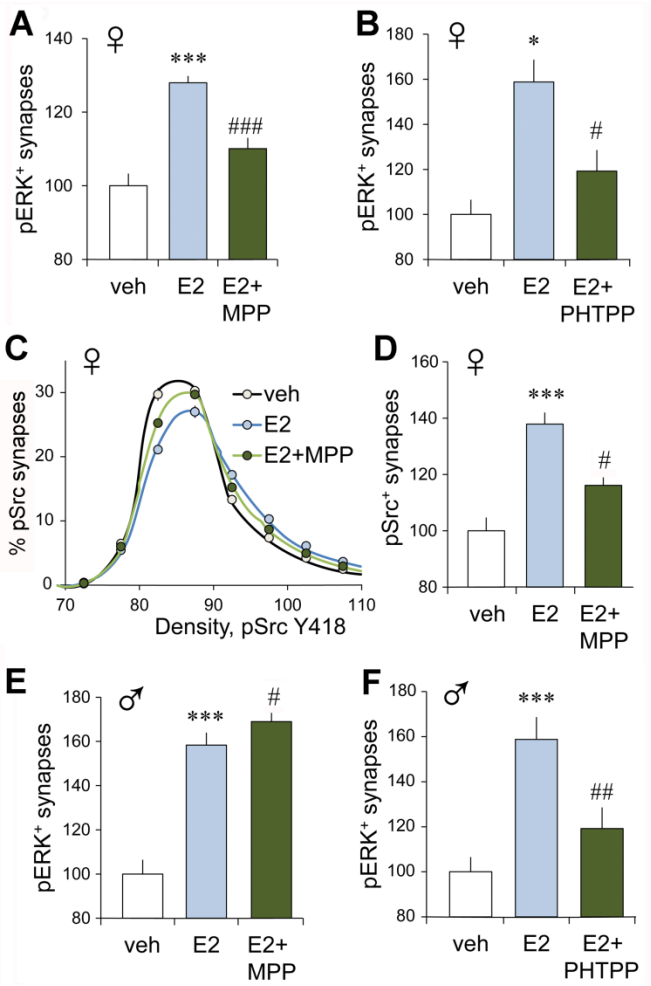


**Figure 2.4. Estradiol infusion increases synaptic ERK1/2 and Src phosphorylation.** (**A**) Estradiol (E2) perfusion alone increased the percent of synapses with dense concentrations of synaptic pERK1/2-IR in female slices relative to vehicle (veh) treatment; the effect was reduced by MPP ($p$<0.0001, $F_{(2,35)}$=26.21, post-hoc tests: veh vs. E2: ***$p$<0.0001, E2 vs. E2+MPP: $^{\#\#\#}p$<0.001, $n$=10/group; quantitative FDT analysis). (**B**) Additional experiments confirmed that E2 increased synaptic pERK1/2-IR and further showed that the ERβ antagonist PHTPP reduced the effect ($p$=0.0002, $F_{(2,28)}$=12.27, post-hoc tests: veh vs. E2: *$p$<0.05, E2 vs. E2+PHTPP: $^{\#}p$<0.05; veh $n$=10, E2 and E2+PHTPP $n$=11). (**C**) E2 increased the rightward skew in the density frequency distribution for pSrc-IR co-localized with PSD-95 (vs. vehicle, $p$<0.0001, $F_{(19,418)}$=33.42); MPP blocked most of this effect ($p$<0.0001, $F_{(19,418)}$=12.32; $n$=12/group). (**D**) E2 treatment of female slices produced the predicted, MPP-sensitive increase in the proportion of doubled-labeled synapses with dense pSrc-IR relative to vehicle controls ($p$=0.0002, $F_{(2,29)}$=12.33, Bonferroni's post-test: veh vs. E2: ***$p$<0.0001, E2 vs. E2+MPP: #$p$<0.05; $n$=12/group). (**E**) In male slices, E2 infusion increased the percentage of synapses with dense pERK1/2-IR but the increase was not affected by MPP ($p$<0.0001, $F_{(2,29)}$=37.51, post-hoc tests: veh vs. E2: ***$p$<0.001, E2 vs. E2+MPP: $^{\#}p$>0.05, $n$=10/group). (**F***)* Separate experiments replicated the E2-induced increase in synaptic pERK1/2 in male slices and determined this was suppressed in the presence of PHTPP ($p$=0.0002, $F_{(2,26)}$=12.27, post-hoc tests: veh vs. E2: ***$p$=0.0001, E2 vs. E2+PHTPP: $^{\#\#}p$=0.01, veh and E2 $n$=10, E2+PHTPP $n$=9).

*Synaptic ERα concentrations are higher in females than males.*

The preceding results provide evidence that exogenous and local estrogens both activate synaptic kinases via ERα–dependent mechanisms in females but not in males. We used dual immunofluorescence for PSD-95 and ERα (**Fig. 2.5A**), and FDT, to determine if this sex difference reflects differences in the abundance of synaptic ERα. First, there was no effect of sex on numbers or density of PSD-95-IR contacts ($p$=0.12, $t_{(22)}$ = 1.603; 6 male, 12 female slices). In contrast, the density frequency distribution for synaptic (PSD-95 colocalized) ERα had a greater rightward skew for females than for males (**Fig. 2.5B**), resulting in a higher proportion of synapses with dense ERα-IR (i.e., density units ≥90; **Fig. 2.5C**). This effect was similar between females that were or were not in proestrus. We then assessed if there are similar effects of sex on ERβ and GPER1 immunoreactivities. Both ERβ and GPER1 were predominantly localized to synapse-sized puncta scattered across the sample field CA1 SR and some were clearly colocalized with PSD-95 (**Fig. 2.5F**). The frequency distributions for synaptic ERβ were slightly different between males and females due to a somewhat greater proportion of synapses with low density ERβ-IR in males (**Fig. 2.5D**). The frequency distribution for GPER1-IR was similar between sexes (**Fig. 2.5E**). In contrast to ERα, there were no significant male-female differences in the proportion of PSDs with dense immunoreactivity for ERβ (p = 0.12, $t_{(22)}$ =1.6) or GPER1 (p=0.69, $t_{(22)}$ =0.4). As with prior cohorts, there were no effects of sex on numbers of PSD-95-IR synapses in the CA1 SR sample field ($p$=0.20, $t_{(22)}$ =1.32; $n$=12/sex).

Sex differences in concentrations of ERs have been described in brain (Brown et al., 1992), and greater total numbers of extranuclear ERα-IR elements (ie., dendrites, glia, spines and boutons) have been described for field CA1 of diestrus female vs. male mice (Mitterling et al., 2010) but the present results constitute novel evidence for significant sex differences at excitatory hippocampal synapses independent of female estrous state. The marked dimorphism in synaptic ERα levels described provides a plausible explanation for at least some of the sex differences in the contributions of neurosteroid estrogen to hippocampal LTP.

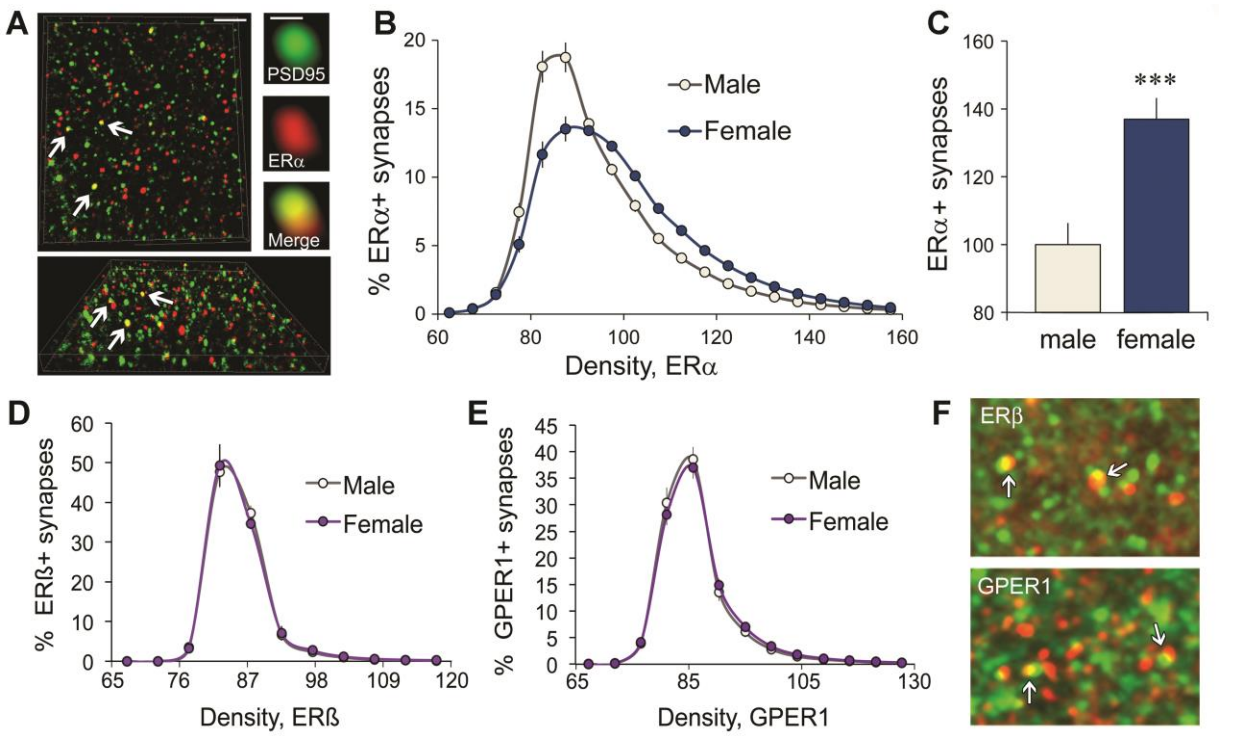


**Figure 2.5. ERα is present at higher concentrations in female than in male CA1 synapses.** (**A**) *Top left*. Deconvolved 2-photon microscopic images of immunofluorescent labeling were used to construct a 3D montage of the CA1 sample field (shown); one can see that a subpopulation of PSD-95-IR contacts (green) also contain ERα immunoreactivity (double labeling appears yellow). Scale bar: 2 µm. *Top right*: Image of a single double-labeled PSD shows the spatial relationship of areas occupied by PSD-95 (green) and ERα (red) immunoreactivities and the extent of overlap (merge, yellow). Scale bar: 0.1 µm. *Bottom*: Image shows the montage from the same z-stack illustrated in the upper left but with the top of that panel rotated away from the viewer to show double labeling of the same puncta (arrows) from a different 3D viewpoint. (**B**) The density frequency distribution for ERα-IR (co-localized with PSD-95) shows a greater rightward skew in females relative to males ($p$<0.0001, $F_{(19,646)}$=17.28; Male $n$=12, Female $n$=24). (**C***)* Bar graph shows the percent of double-labeled synapses with high concentrations of ERα immunolabeling (density units of 90 and above) normalized to the mean male value shows that there were far more densely ERα-IR synapses in females than in males (***$p$=0.0001, $t_{(34)}$=4.40). (**D,E**) Density frequency distributions for all synapse-sized clusters of ERβ- (**D**) and GPER1- (**E**) immunoreactivities colocalized with PSD-95 in the CA1 SR sample field ($n$=12/group, females in diestrus). For ERβ-IR (D) there was a significant interaction between sex and immunolabeling density (p=0.0005, $F_{(21,462)}$ =2.4) due to a slightly greater proportion of synapses with low density ERβ-IR (density units 83-88) in males than in females. There was no effect of sex on numbers of densely ERβ-IR synapses (density units ≥90; $p$ =0.12, $t_{(22)}$=1.6). For GPER1-IR there were no group differences (GPER1 $p$=0.89 $F_{(20,440)}$=0.33). (F) Deconvolved epifluorescence images shows ERβ and GPER1 (red) are both localized to synapse-sized puncta in CA1 SR and that some of those are colocalized with PSD-95 (green; doubles appear yellow; bar = 2µm).

*Downstream LTP stabilization mechanisms are comparable in the sexes.*

β1-integrins. We tested if sex differences extend to elements known to regulate the cytoskeletal reorganization that consolidates LTP in males (Rex et al., 2009; Babayan et al., 2012; Lynch et al., 2013; Rudy, 2015) beginning with an analysis of TBS effects on synaptic β1 integrins. In male field CA1, TBS activates postsynaptic integrins containing the β1 subunit and integrin-dependent signaling to actin, a sequence that is required for stable LTP (Kramar et al., 2006; Babayan et al., 2012; Wang et al., 2016a). Antisera that is specific for the activated (Act) form of β1 integrin labels discrete puncta in field CA1 SR, a subset of which are colocalized with PSD-95 (**Fig. 2.6A**). Using FDT to evaluate effects of S-C stimulation on levels of the activated integrin showed that TBS increases synaptic levels of Act-β1 immunoreactivity in female slices as assessed 3-4 min later (**Fig. 2.6B, C**). The magnitude of this effect was comparable to that reported previously and confirmed here for males ($p$<0.0001, $F_{(21,588)}$=6.80 for the intensity frequency distribution and $p$=0.046, $t_{(28)}$=2.08 for the proportion of synapses with dense Act-β1-IR, respectively; LFS vs TBS, $n$=15 slices/group).

Integrin signaling to actin is mediated in part by focal adhesion kinase (FAK), a synaptic tyrosine kinase that is robustly activated by TBS in male field CA1 (Babayan et al., 2012). Using FDT to evaluate stimulation effects on synaptic pFAK Y397-IR (**Fig. 2.6D**), we found S-C TBS induced a comparable increase in females but in this case the ERα antagonist MPP blocked TBS effects on both greater rightward skew in the pFAK immunolabeling density frequency distribution and the proportion of PSDs with dense pFAK immunoreactivity (**Fig. 2.6E,F**). We then tested if in females, as in males, β1 integrin engagement is required for LTP in experiments using slices from conditional knockout (cKO) mice in which expression of β1 integrin by excitatory forebrain neurons is reduced beginning at ~3 weeks of age (Chan et al., 2006; Huang et al., 2006; Wang et al., 2016a). For female β1 integrin cKOs, as previously determined for males (Wang et al., 2016a), the S-C I/O curves and baseline synaptic responses were not

detectably different from those of WTs (**Fig. 2.6G**). Nevertheless, LTP stabilization was severely impaired in the cKOs (**Fig. 2.6H**). β1-family integrins fall into two groups, distinguished by whether or not they bind matrix ligands containing the amino acid sequence arg-gly-asp (RGD) (Humphries et al., 2006). We found that the potent disintegrin echistatin, a toxin that inhibits RGD-binding integrins, disrupted LTP stabilization in females (**Fig. 2.6I**) as previously shown for males (Kramar et al., 2006).

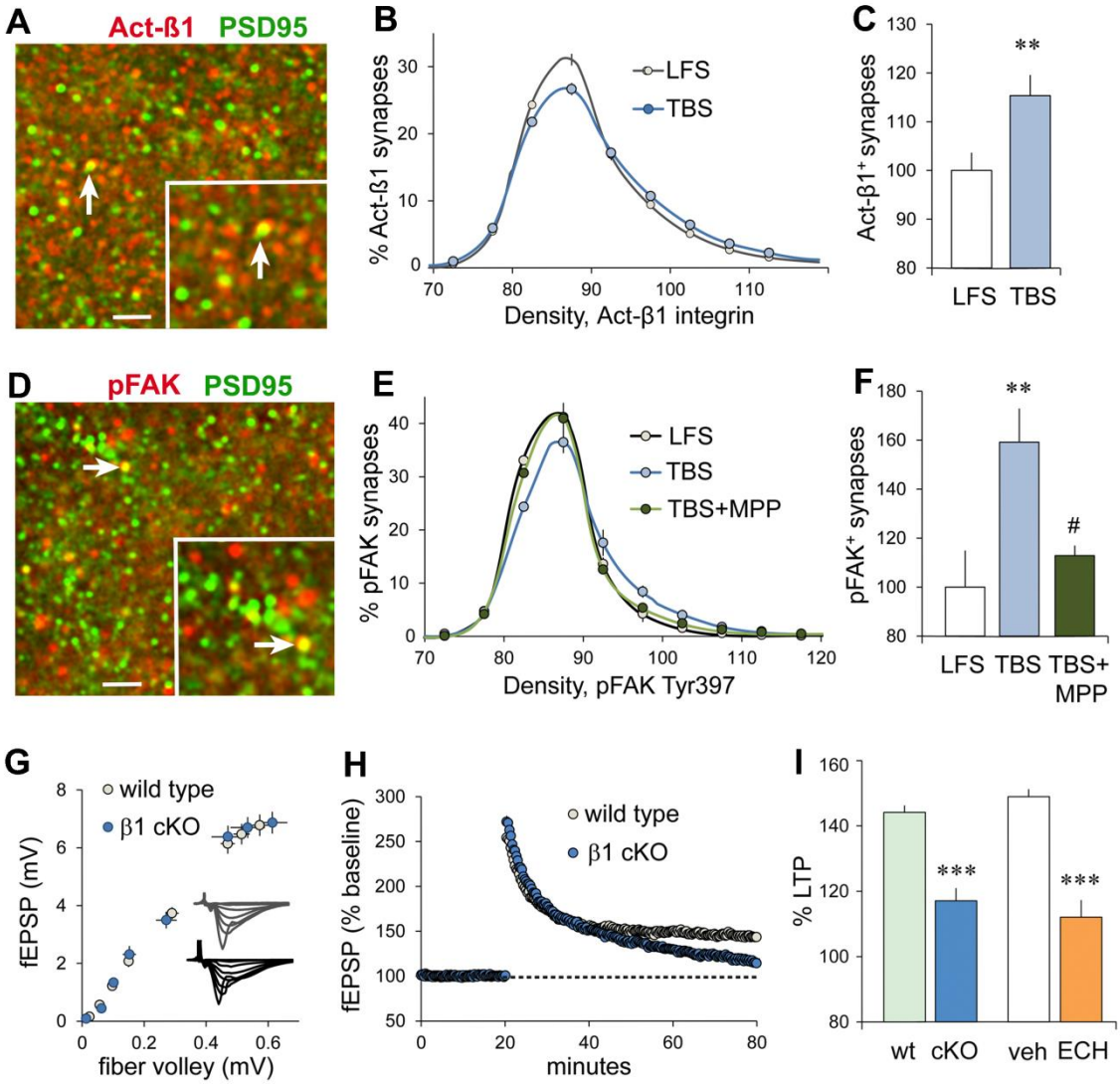


**Figure 2.6. Female S-C LTP depends on an RGD-binding, β1 integrin.** (**A**) Image shows dual immunolabeling for activated (Act-) β1 integrin (red) and PSD-95 (green) in CA1 SR; inset shows the area surrounding a double-labeled PSD (arrow) at higher magnification (bars for A and D: 10 µm for larger image, 2 µm for insert). (**B**) Plot shows the immunolabeling density frequency distributions for Act-β1-IR colocalized with PSD-95 in CA1 SR in female slices that received low frequency (LFS) or theta burst (TBS) stimulation of S-C projections; with TBS, as compared to LFS, there was a greater rightward skew in the Act-β1 density frequency distribution indicating an increase in the proportion of synapses with dense Act-β1-IR ($p$<0.0001, $F_{(21,882)}$=7.91; $n$=22/group). (**C**) The percent of double-labeled PSDs with dense Act-β1-IR (>90 units on B), normalized to the mean of the LFS control group, showed that TBS increased numbers of Act-β1 enriched synapses (**$p$=0.009, $t_{(42)}$=2.75). (**D**) Deconvolved image shows colocalization of pFAK (red) and PSD-95 (green) immunoreactivities; double labeling appears yellow (arrows); inset shows the area surrounding a double-labeled PSD (arrow) at higher magnification. (**E**) TBS increased the rightward skew in the density frequency distribution for synaptic (PSD-95 colocalized) pFAK-IR ($p$<0.0001, $F_{(19,323)}$=6.294) that was largely

eliminated by ERα antagonist MPP ($p$<0.0001, $F_{(19,285)}$=7.514; LFS $n$=10, TBS $n$=9, TBS+MPP $n$=8). (**F**) The percent of double-labeled synapses with high concentrations of pFAK (>90 units), normalized to LFS control slices, was increased by TBS; MPP blocked this pFAK increase ($p$=0.0037, $F_{(2,26)}$=7.13, Bonferroni's post-test: LFS vs. TBS: **$p$<0.01, TBS vs. TBS+MPP: $^{\#}p$<0.05). (**G**) The fiber volley amplitude vs. fEPSP amplitude relationship (I/O curve) for female wild type and conditional β1 integrin KO (cKO) mice were comparable ($p$=1.0, $F_{(7,126)}$=0.01; $n$=9/group). (**H**) Plot of fEPSP slopes (expressed as a percent of the mean baseline response) shows that in female mice TBS (applied at 20 min) induced robust LTP in wild types whereas, in β1 cKOs, potentiation declined toward baseline over 60 min. (**I**) The percent LTP measured at 55-60 min post-TBS was greatly reduced in female β1 cKO mice relative to wild types (wt). A similarly pronounced suppression of female LTP was produced by RGD-binding β1 integrin blocker echistatin (ECH) infused for 40 min before TBS ($p$<0.0001, $F_{(3,27)}$=24.01; post-hoc tests: wt vs. cKO and veh vs. ECH: ***$p$<0.001; $n$=9/group).

BDNF signaling. The neurotrophin BDNF, acting on synaptic TrkB receptors, is critical for TBS-induced dendritic spine actin polymerization and the production of stable LTP in male hippocampus (Figurov et al., 1996; Kramar et al., 2004; Rex et al., 2007; Minichiello, 2009). Using dual immunolabeling for PSD-95 and pTrkB Y515 (**Fig. 2.7A**) in combination with FDT, we determined that TBS-induced increases in synaptic pTrkB are ERα-dependent (i.e., fully blocked by MPP) in females as evident in both immunolabeling density frequency distributions and analyses of the proportions of PSDs containing dense pTrkB-IR (**Fig 2.7A).** In contrast, in males the similarly robust TBS-induced increases in postsynaptic pTrkB-IR were unaffected by ERα antagonism (**Fig. 2.7B**). We then confirmed that TrkB is critical for LTP in females, as in males, using the inhibitor ANA-12 (Zhang et al., 2015) (**Fig. 2.7C**). We previously showed that, in male field CA1, E2-induced TrkB activation requires β1 integrin function (Wang et al., 2016a), a finding consistent with reports that integrins enable activities of neighboring transmembrane receptors in many circumstances (Meng et al., 2011; Munger and Sheppard, 2011). We tested for similar receptor cross talk of female LTP by evaluating TBS effects on TrkB in the presence and absence of functioning β1 integrins: the increase in synaptic pTrkB levels produced by a single TBS train in slices from female WT mice was absent in age-matched female β1 cKOs (**Fig. 2.7D**) thereby showing that in females synaptic TrkB activation was β1 integrin dependent.

Actin signaling. Both β1 integrin and TrkB engage actin regulatory signaling involving the small GTPase RhoA and its effectors Rho-associated coiled-coil protein kinase (ROCK), LIM kinase, and cofilin. These events are critical for production of stable S-C LTP in males (Rex et al., 2009; Lynch and Gall, 2013). Similar signaling was identified in females: females exhibited TBS increased levels of synaptic pCofilin (Ser3)-IR (**Fig. 2.7E**), as described for males (Chen et al., 2007), and that infusion of the ROCK inhibitor H1152 eliminated LTP (**Fig. 2.7F**).

In all, we found no evidence for sex differences in the complex, downstream signaling events required for LTP consolidation other than the dependency on ERα in females.

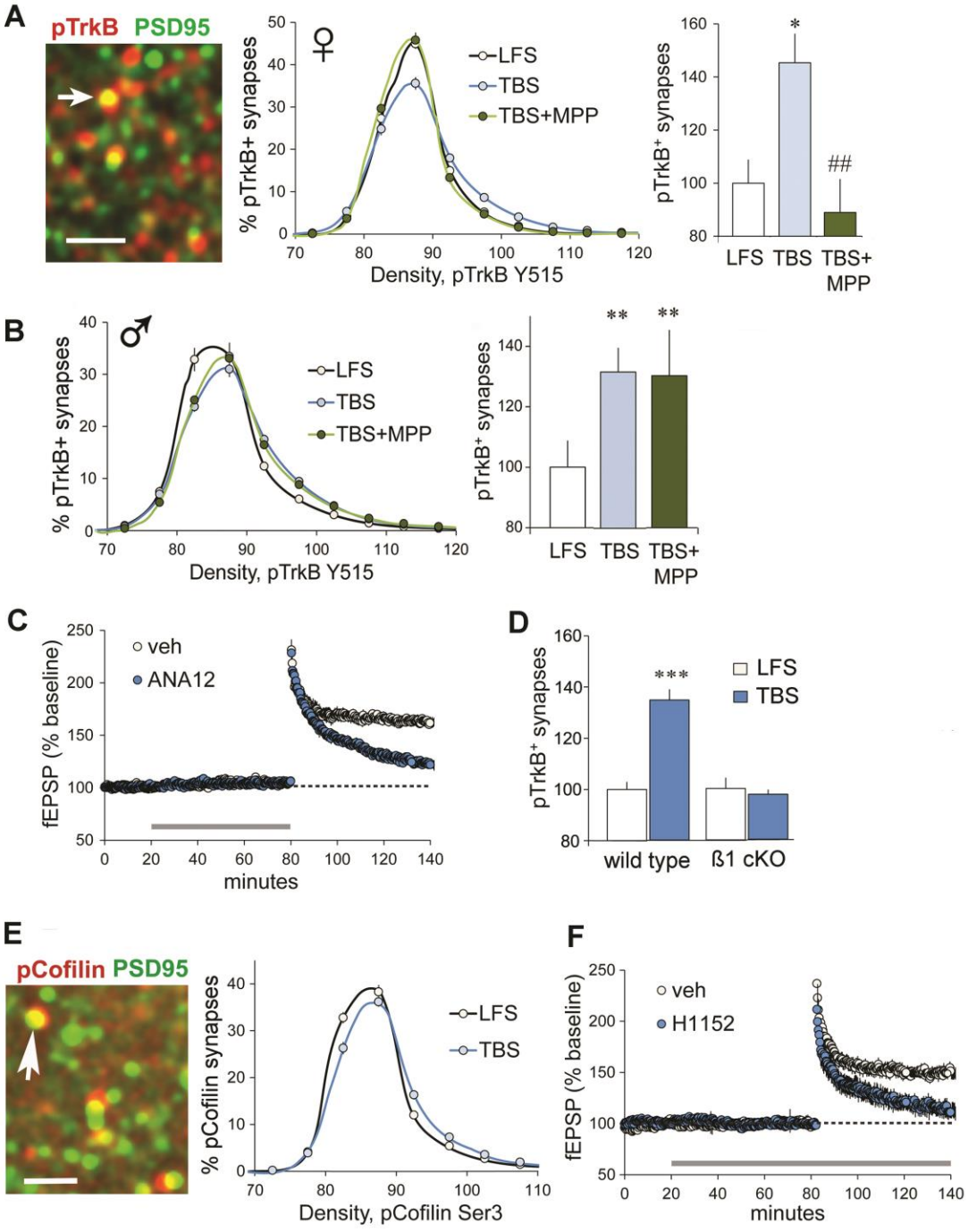


**Figure 2.7. Synaptic TrkB activation depends on ERα and β1 integrin, and is required for LTP in females.** (**A**) Deconvolved image shows punctate localization of pTrkB Y515 (red) and PSD-95 (green); yellow indicates double labeling (arrow; bar: 2 µm). Line graph shows that TBS, as compared to LFS, caused a greater rightward skew in the density frequency distribution for pTrkB-IR colocalized with PSD-95 ($p$<0.0001, $F_{(19,342)}$=10.44) and MPP substantially reduced this effect ($p$<0.0001, $F_{(19,342)}$=10.66; $n$=10/group). *(right)* The percent of double-labeled synapses with dense pTrkB-IR (≥ 90 units) was elevated after TBS in vehicle- but not MPP-treated female slices (groups means normalized to LFS group mean; $p$=0.0025, $F_{(2,29)}$=7.55;

post-hoc tests: LFS vs. TBS: *$p$<0.05, TBS vs. TBS+MPP: $^{\#\#}p$<0.01). (**B**) In slices from male rats, TBS increased both (*left*) the rightward skew in the synaptic pTrkB-IR density frequency distribution (vs LFS, $p$<0.0001; $F_{(19,342)}$ = 6.794) that was not influenced by MPP ($p$=0.939; $F_{(19,342)}$=0.549, $n$=10/group) and (*right*) the percent of PSD-95-IR synapses associated with dense pTrkB-IR (≥90 units), also not influenced by MPP ($p$=0.009, $F_{(2,29)}$=5.68, Bonferroni's post-test: **p<0.01 vs LFS). (**C**) TrkB blocker ANA-12 (750 nM) disrupted stabilization of CA1 LTP in female slices ($p$<0.0001, $t_{(10)}$=8.36; $n$=6/group). (**D**) S-C TBS produced a marked increase in the percentage of PSDs associated with dense pTrkB-IR in wild type mice but not in β1 integrin cKOs ($p$<0.0001, $F_{(3,36)}$=25.55; post-hoc tests: LFS vs. TBS for wild types: ***$p$<0.0001, LFS $n$=9, TBS $n$=8; LFS vs TBS for β1 cKOs: n.s., $n$=10/group). (**E**) Image shows pCofilin-IR co-localized with PSD-95 in female CA1 SR. (*right*) In females S-C TBS increased the rightward skew in the density frequency distribution for synaptic pCofilin (relative to LFS; $p$<0.0001, $F_{(19,399)}$=7.69; LFS $n$=12, TBS $n$=11). (**F**) The selective ROCK inhibitor H1152 (100 nM, 160 min) blocked S-C LTP in female slices ($p$=0.0013, $t_{(9)}$=4.57; veh $n$=6, H1152 $n$=5).

**Sexual dimorphism in LTP and learning threshold.**

TBS, which mimics cell firing during learning (Otto et al., 1991), is near optimal for inducing LTP in males (Larson et al., 1986) and generates a similar degree of potentiation in females (Kramar et al., 2009). In accord with previous work (Bi et al., 2001), the percent LTP induced by a 10 burst TBS train was slightly higher in slices collected from proestrus (high circulating estrogen levels) than non-proestrus females (52.0 ± 4.1% vs. 37.9± 4.5%, respectively; $p$=0.047; proestrus $n$=7, non-proestrus $n$=5). Nevertheless, we observed substantial sex differences in LTP threshold: five pairs of theta bursts, delivered at 2 min intervals, produced significant S-C LTP in slices from males, as described (Larson et al., 1993), but not in those from female rats (**Fig. 2.8A**). Differences were evident after the first three burst pairs; male responses continued to increase with subsequent bursts whereas female responses did not (**Fig. 2.8B**). We next tested if the threshold for LTP corresponds to that for activating synaptic ERK1/2: the minimum condition for inducing potentiation was sufficient to cause a robust increase in synaptic pERK1/2-IR in males but not in females (**Fig. 2.8C**). In contrast to effects of paired theta bursts, we found that four sets of three bursts, separated by 2 minutes, generated robust LTP in females (**Fig. 2.8D**) with individual fEPSPs progressively increasing in size after each triplet (**Fig. 2.8E**). These results constitute the first evidence that adult females have a higher threshold for S-C potentiation than do males.

Bath infusion of 1 nM E2 lowered the LTP threshold (to paired bursts) in females to the level found in untreated males. As predicted from the above kinase studies, antagonists to either ERα or ERβ significantly attenuated the enhancing effects of E2 infusion on female LTP (**Fig. 2.8F**).

The LTP threshold results predict that females will require measurably more training than males to encode memories that are dependent on plasticity in field CA1. We tested this using object location (a.k.a. object placement) memory (OLM) (**Fig. 2.8G**), which depends on

synaptic plasticity in CA1 (Barrett et al., 2011; Babayan et al., 2012) and is facilitated by E2 action in hippocampus (Inagaki et al., 2010; Boulware et al., 2013). OLM in males requires five minutes of training, is associated with elevated synaptic pERK1/2, and requires □1 integrin function (Babayan et al., 2012; Seese et al., 2014). Tests in females showed that one 5-minute training trial supports long-term OLM for mice in proestrus (**Fig. 2.8H**) but not for those outside proestrus, although the total time spent exploring cues did not differ across cycle stages during training or testing (training $p$=0.95, t(18)=0.06; testing $p$=0.57, $t_{(18)}$=0.58, 2-tail $t$ test; proestrus $n$=8, nonproestrus $n$=12). Peripheral injections of either ERα antagonist MPP or ERβ antagonist PHTPP blocked long-term OLM (assessed 24 hr after training; **Fig. 2.8I**) by proestrus females also without effect on exploratory behavior (training $p$=0.99, F(2,17)=0.003; testing $p$=0.97, F(2,17)=0.032, veh $n$=6, MPP $n$=5, PHTPP $n$=7; one way ANOVA). Neither inhibitor affected OLM by males ($p$=0.99, F(2,3)=0.64; veh $n$=7, MPP and PHTPP $n$=6 each; one way ANOVA).

Finally, we asked if learning object location depends upon ERα-dependent engagement of signaling through kinases associated with LTP. Proestrus females were given a 5 min OLM training trial and then immediately euthanized for pERK1/2 immunofluorescence. FDT analyses of synaptic immunolabeling the CA1 dendritic lamina evaluated in LTP studies (**Fig. 2.8J**) identified an elevated proportion of PSDs associated with dense pERK1/2-IR relative to similarly staged control female mice. The ERα antagonist MPP blocked training-induced increases in synaptic pERK1/2 (**Fig. 2.8K**). Finally, 5 min OLM training did not increase synaptic pERK-IR in non-proestrus females (**Fig. 2.8L**), a result that accords with the absence of learning in these mice.

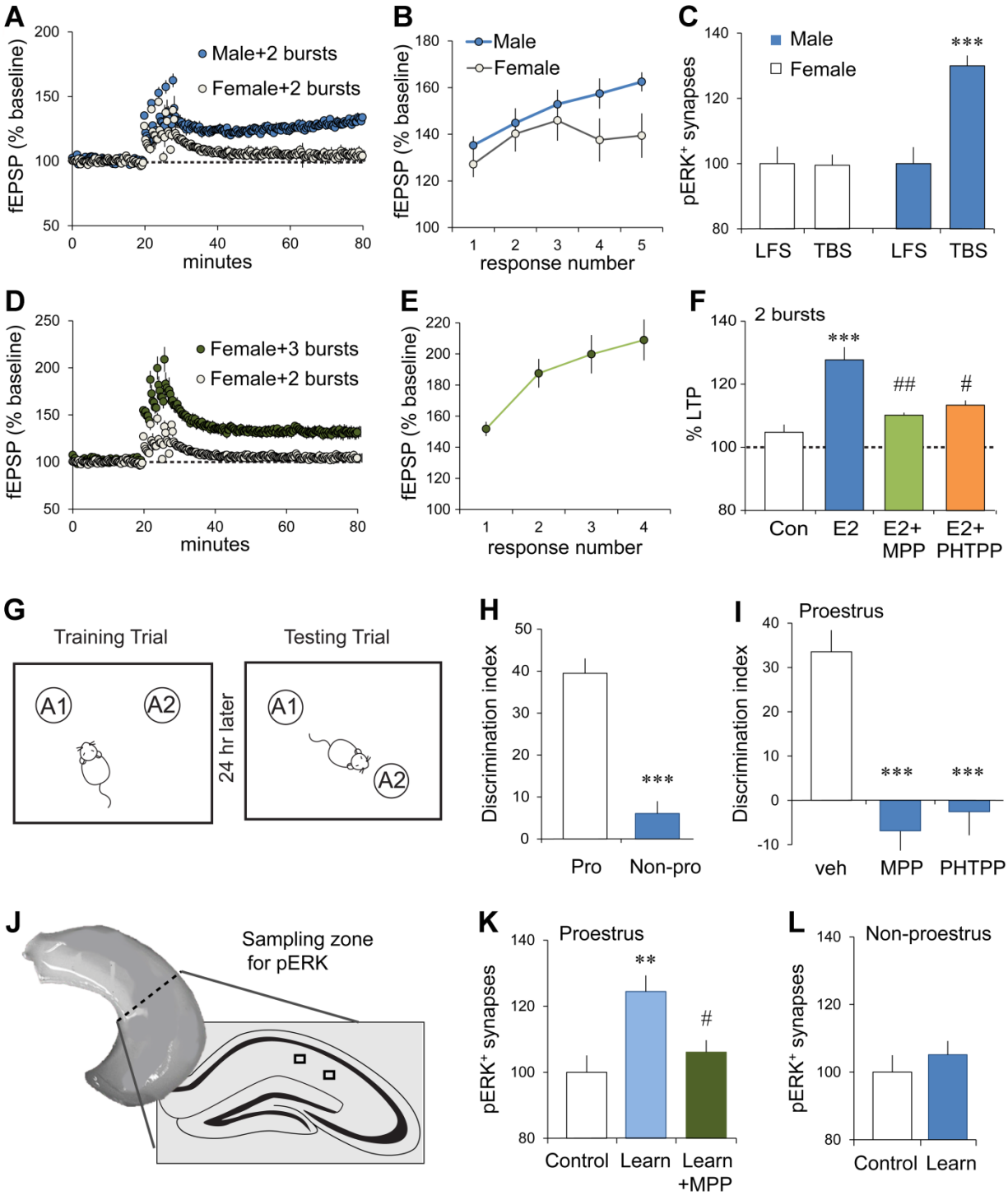


**Figure 2.8. Sex differences in thresholds for LTP and spatial learning.** (**A**) Five pairs of two theta bursts produced significant S-C LTP in male but not female CA1 ($p$=0.0005, $t_{(11)}$=4.86; Female $n$=7, Male $n$=6). (**B**) The S-C fEPSP slope immediately after each burst pair increased steadily across the first three pairs for both sexes but diverged for the last two pairs ($p$=0.045, $F_{(4,44)}$=2.666). (**C**) Five pairs of two theta bursts increased the percentage of CA1 SR synapses with dense pERK1/2-IR in male but not female slices (Values normalized to the mean of their

respective LFS groups; one–way ANOVA: $p<0.0001$, $F_{(3,56)}=11.28$; post-hoc tests: male TBS vs. each other group: ***$p\leq0.0001$; 14-16 slices/group). *(***D**) Four sets of TBS triplets (3 bursts, 200 ms between bursts, 2 min between triplets) produced significant LTP in female slices ($p=0.0025$, $t_{(11)}=3.91$ vs 2 burst group; $n=6$/group). (**E**) The fEPSP slope immediately after each burst triplet steadily increased (~150% to 209% of baseline). (**F**) E2 (1 nM), perfused for 10 min before collecting baseline responses and continued 30 min more, increased LTP magnitude in females (five pairs of theta bursts); this enhancement was significantly attenuated by either ERα antagonist MPP or ERβ antagonist PHTPP applied 30 min before and during E2 application ($p=0.0001$, $F_{(3,25)}=9.52$, one way ANOVA; post-hoc tests: con vs E2: ***$p=0.0001$, E2 vs. E2+MPP: $^{\#\#}p=0.003$, E2 vs. E2+PHTPP: $^{\#}p<0.02$, con vs E2+ MPP or E2+PHTPP: $p>0.35$). (**G**) For object location memory (OLM) training mice explored the chamber containing two identical objects (A1 and A2); for testing 24 hr later they returned to the chamber with one of the objects moved to a novel location. (**H**) With 5 min training, OLM was greater for proestrus (Pro) than non-proestrus (Non-pro) mice (signified by Discrimination Index (DI); ***$p<0.0001$, $t_{(18)}=7.27$; Pro $n= 8$, Non-pro $n=12$). (**I**) MPP or PHTPP (0.6 mg/kg) blocked OLM in proestrus mice ($p<0.0001$, $F_{(2,17)}=28.94$, post-hoc tests: veh vs. MPP: ***$p<0.001$, veh vs. PHTPP: ***$p<0.001$, veh $n=6$, MPP $n=5$, PHTPP $n=7$). (**J**) Location of CA1 fields for measures of pERK-IR. (**K**) After 5 min OLM training in proestrus, numbers of densely pERK1/2-IR PSDs were increased in mice that sampled the objects relative to those that explored an empty chamber; this effect was blocked by MPP ($p=0.003$, $F_{(2,23)}=7.78$; Control vs. Learn: **$p<0.01$, Learn vs. Learn+MPP: $^{\#}p<0.05$, $n=8$/group; normalized to control mean). (**L**) 5 min OLM training did not affect the numbers of densely pERK1/2-IR PSDs in non-proestrus mice ($p=0.44$, $t_{(23)}=0.79$; Control $n=13$, Learn $n=12$).

## Discussion

Sexual dimorphisms in brain and their contributions to male/female differences in learning are topics of broad and increasing interest (Scharfman and MacLusky, 2008; Andreano and Cahill, 2009; Luine, 2014). The present results point to striking yet unexpectedly discrete sex differences in functional plasticity of excitatory synapses, within a hippocampal field critical for memory formation, that are likely to be centrally involved in the encoding of spatial information.

We previously showed that the well described facilitation of synaptic responses produced by exogenous E2 in adult male field CA1 (Woolley, 2007) is due to partial and reversible activation of postsynaptic actin-regulatory signaling required for LTP consolidation (Kramar et al., 2009). Not surprisingly, infused E2 also markedly lowered the threshold and increased the magnitude of LTP in males. Using selective agonists we determined that these effects of applied E2 were initiated by ERβ, with no evident contribution from ERα or GPER1 (Kramar et al., 2009; Wang et al., 2016a). The most upstream ERβ-initiated events identified in those experiments included activation of synaptic β1 integrins and integrin-dependent transactivation of TrkB (Wang et al., 2016a); these two receptors are critical for LTP-related actin remodeling in dendritic spines (Kramar et al., 2006; Rex et al., 2007; Bramham, 2008; Wang et al., 2008). Here we identified still earlier events set in motion by E2 application in CA1 of females only: ERα contributes to the engagement of NMDAR-associated kinases ERK1/2 and Src, which in turn regulate β1 integrin and TrkB function (Fincham et al., 2000; Chen et al., 2010). Results further show that in females E2 infusion lowers the threshold for LTP but - unlike the case for males - both ERα and ERβ contribute to this effect. We conclude that exogenous E2 mobilizes ERβ signaling at excitatory S-C synapses in both sexes but triggers significant contributions from ERα in females only. Quantitative immunofluorescence uncovered a plausible explanation for this synaptic dimorphism: in CA1 SR the proportion of excitatory synapses

containing high concentrations of ERα was substantially greater in females than in males whereas numbers of synapses enriched in ERβ (or GPER1) were comparable between the sexes. Figures 2.9A and 2.9B summarize these findings.

Activation of synaptic Src, ERK1/2 and TrkB are critical early steps in the production of LTP as extensively characterized in male field CA1 (Figurov et al., 1996; Sweatt, 2001; MacDonald et al., 2006; Chen et al., 2010; Seese et al., 2012). Surprisingly, the present experiments using selective ER antagonists showed that with TBS, postsynaptic activation of each of these kinases, and induction of LTP itself, depends on ERα in females but not in males. We found no evidence for contributions of ERβ to TBS-induced signaling responses or LTP in either sex. The critical involvement of ERα in LTP in females only was further demonstrated in studies of NOER and MOER mice that express only the nuclear or membrane variant of ERα, respectively; these studies further showed that in females LTP depends upon membrane-associated ERα. Although the classical mechanism of ER action entails nuclear transport and transcriptional regulation, our results align with the growing body of evidence that signal transduction, including rapid kinase activation in neurons, can originate from the membrane receptor (Grove-Strawser et al., 2010; Roepke et al., 2011; Almey et al., 2015; Levin and Hammes, 2016; Micevych et al., 2017) and that some of this membrane signaling is sexually dimorphic (Boulware et al., 2005; Boulware et al., 2007; Huang and Woolley, 2012).

Evidence that local estrogen effects on synaptic signaling and LTP in females depend on membrane ERα suggests that the absence of endogenous estrogen effects on LTP in males is due, at least in part, to lower postsynaptic ERα levels. That said, a lack of a contribution from estrogen signaling through ERβ in males is surprising. Responses to applied E2 and specific ER ligands show that both ERα and ERβ can facilitate S-C LTP (present results) and learning (Boulware et al., 2013). Thus sex differences in the contributions of local estrogens could reflect the somewhat lower affinity of the neurosteroids for ERβ relative to ERα (Kuiper et al., 1997; Perkins et al., 2017), which may be important in the context of the presumably brief estrogen

release event associated with TBS, or sex differences in signaling properties of neuronal ERs and associated proteins as considered elsewhere (Boulware et al., 2005).

The dependence in females on ERα for activation of at least two NMDAR- and LTP-related kinases with TBS highlights a second aspect of synaptic dimorphism: Estrogen-independent mechanisms for activation of these kinases by patterned afferent activity must be weaker in females than in males, and this is compensated for by stronger signaling to the enzymes from local ERα in females (**Figs 2.9C and 2.9D**). This effect does not seem to be due to differences in NMDAR activation between the sexes. Blocking ERα in females did not affect NMDAR-influenced physiological responses to TBS: there was no effect on initial LTP magnitude or the facilitation of burst responses across the theta train. Why then are the depolarizing potentials (absent ERα signaling) insufficient to activate synaptic ERK1/2 and Src or to induce LTP in females when they are clearly adequate in males? One possibility involves links between NMDARs and the kinases. With induction of LTP, ERK1/2 activation is NMDAR-dependent (Wang et al., 2007). Mechanisms of Src activation are more complex, with contributions from NMDARs, integrins and ephrinB receptors among others (Salter and Kalia, 2004). Recent work has shown that NMDARs can activate Src via non-ionic, signalosome type interactions (Weilinger et al., 2016). We propose that such non-ionic relationships between the NMDARs and submembrane elements (Dore et al., 2017) may be stronger in males than in females. This idea further suggests that the relatively weaker kinase regulation by non-ionic NMDAR function in females requires a boost from ERα signaling to initiate downstream events necessary for LTP. Tests of this idea will be an important next step in describing the substrates for sex differences in synaptic plasticity.

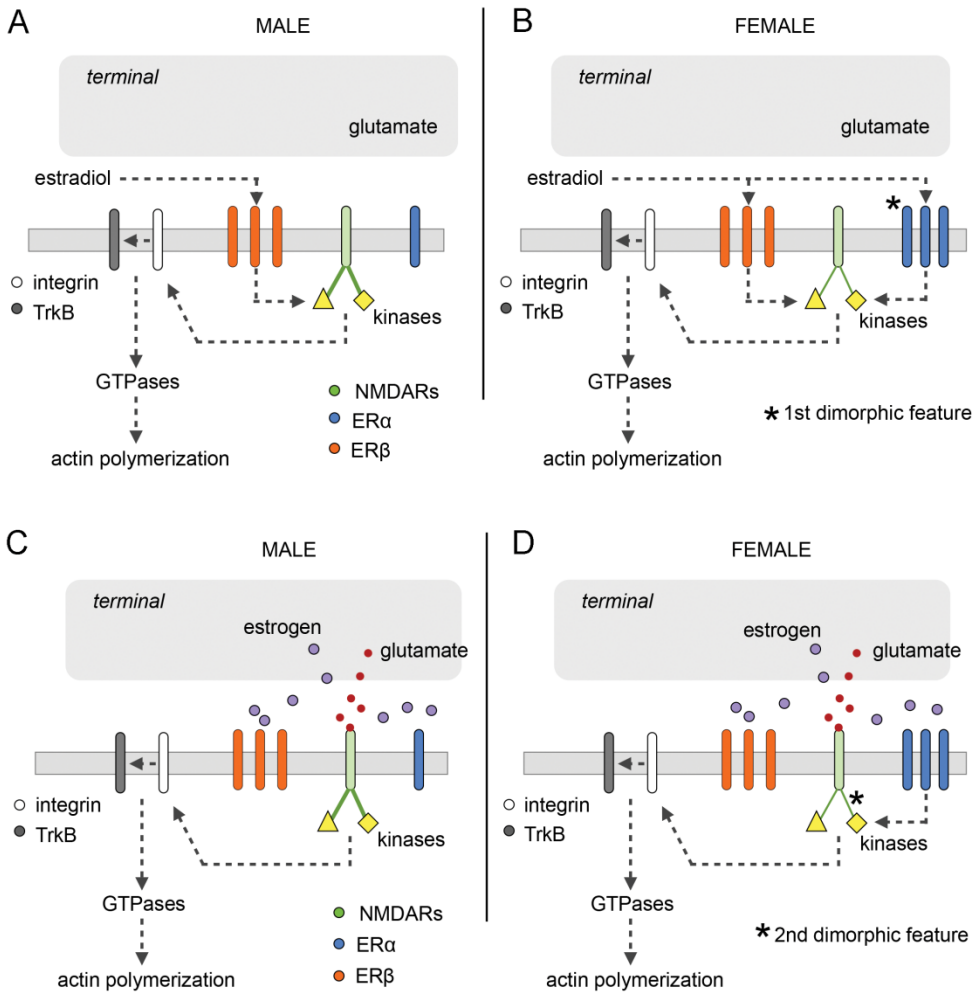


**Figure 2.9. A two-factor hypothesis for sexual dimorphism at hippocampal synapses.** (**A**) Prior studies showed that, in male hippocampus, infused E2 acts via ERβ to stimulate modulatory receptors (β1 integrins, TrkB) leading to actin signaling and transiently enhanced baseline synaptic responses. Experiments described here demonstrate that E2 engages two NMDAR associated kinases (ERK1/2, Src) that are upstream from these events; in males this effect is mediated by ERβ with no detectable contribution from ERα. (**B**) E2 application also activates the two kinases but in females the response to exogenous E2 is mediated by both ERα and ERβ. It is proposed that this sex difference reflects the greater concentration of ERα in female synapses (first dimorphic feature). (**C**) Induction of LTP in males activates the two NMDAR-related kinases and downstream signaling events that stabilize the potentiated state. These downstream steps, and LTP itself, do not depend on local estrogen, ERα or ERβ. (**D**) LTP induction in females also activates ERK1/2 and Src but, in contrast to males, the effect is dependent upon ERα. We propose that the functional links between NMDARs and the kinases are weaker in females than in males (second dimorphic feature), and so kinase activation requires a boost from released estrogen and stimulation of ERα. The dependency upon local estrogen is accompanied by a higher threshold for LTP in females, an effect that can be offset by exogenous estradiol acting via mechanisms described in panel ‘A’.

The sexually dimorphic synaptic features identified here appeared to be discrete: a number of LTP-related signaling events downstream from NMDAR and kinase activation (Lynch et al., 2013; Wang et al., 2016a) were comparable between the sexes except for the anticipated dependency on ERα in females. These events included activity-dependent β1 integrin and TrkB activation, integrin regulation of TrkB activation, TBS-induced increases in pCofilin and dependence of LTP on the actin regulatory signaling through ROCK. Thus, although the substrate map for shifting synapses into their potentiated state is still better understood for males (Lynch et al., 2013), the available data indicate that sexual dimorphisms influencing the generation of S-C LTP are limited to early stages in NMDAR-associated signaling and synaptic ERα levels.

The convergence of ERα and ERβ signaling on LTP-associated synaptic kinases suggests that effects of circulating and local estrogen will be additive with regard to plasticity. Tests of this argument generated novel evidence that females have a higher activity-threshold for induction of LTP as compared to males, and that this sex difference is eliminated by infusion of E2 in the concentration-range of circulating E2 (Mukai et al., 2010). Antagonists of either ER prevented the threshold lowering of female LTP by infused E2. These results give rise to predictions as to the basis and pharmacology of sex differences in the acquisition of spatial memory, a process that is known to involve field CA1. Specifically, we expected that during diestrus, when circulating and hippocampal estrogens are low (Kato et al., 2013), females will have a higher threshold than males and proestrus females for field CA1-dependent object location memory and this proved to be the case. This finding aligns with human studies showing that encoding spatial relationships is sexually differentiated (Kimura, 1996; Andreano and Cahill, 2009).

Are there adaptive advantages associated with sex differences in the threshold for learning-related synaptic modifications? There is no *a priori* reason to assume that a single

optimal encoding threshold applies across circumstances: certain types of signals might be effectively acquired with brief sampling and short theta burst trains while more elaborate information would be best acquired with longer trains. From this perspective, evolutionary pressures towards synaptic dimorphism would reflect male vs. female probabilities for having to deal with different aspects of the environment. It will be interesting in future studies to test for sex differences in learning and associated firing patterns in the afferents of CA1, in animals exposed to complex environments that contain the semantic, spatial, and temporal elements of episodic memory which rely on distinct components of hippocampal circuitry.

## References


Almey A, Milner TA, Brake WG (2015) Estrogen receptors in the central nervous system and their implication for dopamine-dependent cognition in females. Horm Behav 74:125-138.

Andreano JM, Cahill L (2009) Sex influences on the neurobiology of learning and memory. Learn Mem 16:248-266.

Babayan AH, Kramar EA, Barrett RM, Jafari M, Haettig J, Chen LY, Rex CS, Lauterborn JC, Wood MA, Gall CM, Lynch G (2012) Integrin dynamics produce a delayed stage of long-term potentiation and memory consolidation. J Neurosci 32:12854-12861.

Barrett RM, Malvaez M, Kramar E, Matheos DP, Arrizon A, Cabrera SM, Lynch G, Greene RW, Wood MA (2011) Hippocampal focal knockout of CBP affects specific histone modifications, long-term potentiation, and long-term memory. Neuropsychopharmacology 36:1545-1556.

Bender RA, Zhou L, Vierk R, Brandt N, Keller A, Gee CE, Schafer MK, Rune GM (2017) Sex-Dependent Regulation of Aromatase-Mediated Synaptic Plasticity in the Basolateral Amygdala. J Neurosci 37:1532-1545.

Bi R, Foy MR, Vouimba RM, Thompson RF, Baudry M (2001) Cyclic changes in estradiol regulate synaptic plasticity through the MAP kinase pathway. Proc Natl Acad Sci U S A 98:13391-13395.

Bock HH, Herz J (2003) Reelin activates SRC family tyrosine kinases in neurons. Curr Biol 13:18-26.

Boulware MI, Kordasiewicz H, Mermelstein PG (2007) Caveolin proteins are essential for distinct effects of membrane estrogen receptors in neurons. J Neurosci 27:9941-9950.

Boulware MI, Heisler JD, Frick KM (2013) The memory-enhancing effects of hippocampal estrogen receptor activation involve metabotropic glutamate receptor signaling. J Neurosci 33:15184-15194.

Boulware MI, Weick JP, Becklund BR, Kuo SP, Groth RD, Mermelstein PG (2005) Estradiol activates group I and II metabotropic glutamate receptor signaling, leading to opposing influences on cAMP response element-binding protein. J Neurosci 25:5066-5078.

Bozon B, Kelly A, Josselyn SA, Silva AJ, Davis S, Laroche S (2003) MAPK, CREB and zif268 are all required for the consolidation of recognition memory. Philos Trans R Soc Lond B Biol Sci 358:805-814.

Bramham CR (2008) Local protein synthesis, actin dynamics, and LTP consolidation. Curr Opin Neurobiol 18:524-531.

Brown TJ, Naftolin F, Maclusky NJ (1992) Sex differences in estrogen receptor binding in the rat hypothalamus: effects of subsaturating pulses of estradiol. Brain Res 578:129-134.

Chan CS, Weeber EJ, Zong L, Fuchs E, Sweatt JD, Davis RL (2006) Beta 1-integrins are required for hippocampal AMPA receptor-dependent synaptic transmission, synaptic plasticity, and working memory. J Neurosci 26:223-232.

Chen LY, Rex CS, Casale MS, Gall CM, Lynch G (2007) Changes in synaptic morphology accompany actin signaling during LTP. J Neurosci 27:5363-5372.

Chen LY, Rex CS, Sanaiha Y, Lynch G, Gall CM (2010) Learning induces neurotrophin signaling at hippocampal synapses. Proc Natl Acad Sci U S A 107:7030-7035.

Dore K, Stein IS, Brock JA, Castillo PE, Zito K, Sjostrom PJ (2017) Unconventional NMDA Receptor Signaling. J Neurosci 37:10800-10807.

El Gaamouch F, Buisson A, Moustie O, Lemieux M, Labrecque S, Bontempi B, De Koninck P, Nicole O (2012) Interaction between alphaCaMKII and GluN2B controls ERK-dependent plasticity. J Neurosci 32:10767-10779.

Figurov A, Pozzo-Miller LD, Olafsson P, Wang T, Lu B (1996) Regulation of synaptic responses to high-frequency stimulation and LTP by neurotrophins in the hippocampus. Nature 381:706-709.
Fincham VJ, James M, Frame MC, Winder SJ (2000) Active ERK/MAP kinase is targeted to newly forming cell-matrix adhesions by integrin engagement and v-Src. EMBO J 19:2911-2923.
Fu XD, Simoncini T (2008) Extra-nuclear signaling of estrogen receptors. IUBMB Life 60:502-510.
Giovannini MG (2006) The role of the extracellular signal-regulated kinase pathway in memory encoding. Rev Neurosci 17:619-634.
Giovannini MG, Blitzer RD, Wong T, Asoma K, Tsokas P, Morrison JH, Iyengar R, Landau EM (2001) Mitogen-activated protein kinase regulates early phosphorylation and delayed expression of Ca2+/calmodulin-dependent protein kinase II in long-term potentiation. J Neurosci 21:7053-7062.
Grove-Strawser D, Boulware MI, Mermelstein PG (2010) Membrane estrogen receptors activate the metabotropic glutamate receptors mGluR5 and mGluR3 to bidirectionally regulate CREB phosphorylation in female rat striatal neurons. Neuroscience 170:1045-1055.
Hara Y, Waters EM, McEwen BS, Morrison JH (2015) Estrogen Effects on Cognitive and Synaptic Health Over the Lifecourse. Physiol Rev 95:785-807.
Hojo Y, Higo S, Kawato S, Hatanaka Y, Ooishi Y, Murakami G, Ishii H, Komatsuzaki Y, Ogiue-Ikeda M, Mukai H, Kimoto T (2011) Hippocampal synthesis of sex steroids and corticosteroids: essential for modulation of synaptic plasticity. Front Endocrinol (Lausanne) 2:43.
Hojo Y, Hattori TA, Enami T, Furukawa A, Suzuki K, Ishii HT, Mukai H, Morrison JH, Janssen WG, Kominami S, Harada N, Kimoto T, Kawato S (2004) Adult male rat hippocampus synthesizes estradiol from pregnenolone by cytochromes P45017alpha and P450 aromatase localized in neurons. Proc Natl Acad Sci U S A 101:865-870.
Huang GZ, Woolley CS (2012) Estradiol acutely suppresses inhibition in the hippocampus through a sex-specific endocannabinoid and mGluR-dependent mechanism. Neuron 74:801-808.
Huang Z, Shimazu K, Woo NH, Zang K, Muller U, Lu B, Reichardt LF (2006) Distinct roles of the beta 1-class integrins at the developing and the mature hippocampal excitatory synapse. J Neurosci 26:11208-11219.
Humphries JD, Byron A, Humphries MJ (2006) Integrin ligands at a glance. J Cell Sci 119:3901-3903.
Inagaki T, Gautreaux C, Luine V (2010) Acute estrogen treatment facilitates recognition memory consolidation and alters monoamine levels in memory-related brain areas. Horm Behav 58:415-426.
Kato A, Hojo Y, Higo S, Komatsuzaki Y, Murakami G, Yoshino H, Uebayashi M, Kawato S (2013) Female hippocampal estrogens have a significant correlation with cyclic fluctuation of hippocampal spines. Front Neural Circuits 7:149.
Kimura D (1996) Sex, sexual orientation and sex hormones influence human cognitive function. Curr Opin Neurobiol 6:259-263.
Kramar EA, Lin B, Rex CS, Gall CM, Lynch G (2006) Integrin-driven actin polymerization consolidates long-term potentiation. Proc Natl Acad Sci U S A 103:5579-5584.
Kramar EA, Lin B, Lin CY, Arai AC, Gall CM, Lynch G (2004) A novel mechanism for the facilitation of theta-induced long-term potentiation by brain-derived neurotrophic factor. J Neurosci 24:5151-5161.
Kramar EA, Chen LY, Brandon NJ, Rex CS, Liu F, Gall CM, Lynch G (2009) Cytoskeletal changes underlie estrogen's acute effects on synaptic transmission and plasticity. J Neurosci 29:12982-12993.

Kuiper GG, Carlsson B, Grandien K, Enmark E, Haggblad J, Nilsson S, Gustafsson JA (1997) Comparison of the ligand binding specificity and transcript tissue distribution of estrogen receptors alpha and beta. Endocrinology 138:863-870.
Kumar A, Bean LA, Rani A, Jackson T, Foster TC (2015) Contribution of estrogen receptor subtypes, ERalpha, ERbeta, and GPER1 in rapid estradiol-mediated enhancement of hippocampal synaptic transmission in mice. Hippocampus.
Labouesse MA, Langhans W, Meyer U (2015) Effects of selective estrogen receptor alpha and beta modulators on prepulse inhibition in male mice. Psychopharmacology (Berl) 232:2981-2994.
Larson J, Lynch G (1986) Induction of synaptic potentiation in hippocampus by patterned stimulation involves two events. Science 232:985-988.
Larson J, Wong D, Lynch G (1986) Patterned stimulation at the theta frequency is optimal for the induction of hippocampal long-term potentiation. Brain Res 368:347-350.
Larson J, Xiao P, Lynch G (1993) Reversal of LTP by theta frequency stimulation. Brain Res 600:97-102.
Lauterborn JC, Kramar EA, Rice JD, Babayan AH, Cox CD, Karsten CA, Gall CM, Lynch G (2016a) Cofilin Activation Is Temporally Associated with the Cessation of Growth in the Developing Hippocampus. Cereb Cortex.
Lauterborn JC, Palmer LC, Jia Y, Pham DT, Hou B, Wang W, Trieu BH, Cox CD, Kantorovich S, Gall CM, Lynch G (2016b) Chronic Ampakine Treatments Stimulate Dendritic Growth and Promote Learning in Middle-Aged Rats. J Neurosci 36:1636-1646.
Levin ER, Hammes SR (2016) Nuclear receptors outside the nucleus: extranuclear signalling by steroid receptors. Nat Rev Mol Cell Biol 17:783-797.
Li XM, Yang Q, Li XB, Cheng Q, Zhang K, Han J, Zhao JN, Liu G, Zhao MG (2017) Estrogen-like neuroprotection of isopsoralen against spinal cord injury through estrogen receptor ERalpha. Metab Brain Dis 32:259-265.
Lu YM, Roder JC, Davidow J, Salter MW (1998) Src activation in the induction of long-term potentiation in CA1 hippocampal neurons. Science 279:1363-1367.
Luine VN (2014) Estradiol and cognitive function: past, present and future. Horm Behav 66:602-618.
Lynch G, Gall CM (2013) Mechanism based approaches for rescuing and enhancing cognition. Front Neurosci 7:143.
Lynch G, Kramar EA, Babayan AH, Rumbaugh G, Gall CM (2013) Differences between synaptic plasticity thresholds result in new timing rules for maximizing long-term potentiation. Neuropharmacology 64:27-36.
MacDonald JF, Jackson MF, Beazely MA (2006) Hippocampal long-term synaptic plasticity and signal amplification of NMDA receptors. Crit Rev Neurobiol 18:71-84.
McLean AC, Valenzuela N, Fai S, Bennett SA (2012) Performing vaginal lavage, crystal violet staining, and vaginal cytological evaluation for mouse estrous cycle staging identification. J Vis Exp:e4389.
Meng R, Tang HY, Westfall J, London D, Cao JH, Mousa SA, Luidens M, Hercbergs A, Davis FB, Davis PJ, Lin HY (2011) Crosstalk between integrin alphavbeta3 and estrogen receptor-alpha is involved in thyroid hormone-induced proliferation in human lung carcinoma cells. PLoS One 6:e27547.
Micevych PE, Mermelstein PG, Sinchak K (2017) Estradiol Membrane-Initiated Signaling in the Brain Mediates Reproduction. Trends Neurosci 40:654-666.
Minichiello L (2009) TrkB signalling pathways in LTP and learning. Nat Rev Neurosci 10:850-860.
Mitterling KL, Spencer JL, Dziedzic N, Shenoy S, McCarthy K, Waters EM, McEwen BS, Milner TA (2010) Cellular and subcellular localization of estrogen and progestin receptor immunoreactivities in the mouse hippocampus. J Comp Neurol 518:2729-2743.

Mukai H, Kimoto T, Hojo Y, Kawato S, Murakami G, Higo S, Hatanaka Y, Ogiue-Ikeda M (2010) Modulation of synaptic plasticity by brain estrogen in the hippocampus. Biochim Biophys Acta 1800:1030-1044.
Munger JS, Sheppard D (2011) Cross talk among TGF-beta signaling pathways, integrins, and the extracellular matrix. Cold Spring Harb Perspect Biol 3:a005017.
Oberlander JG, Woolley CS (2016) 17beta-Estradiol Acutely Potentiates Glutamatergic Synaptic Transmission in the Hippocampus through Distinct Mechanisms in Males and Females. J Neurosci 36:2677-2690.
Ooishi Y, Kawato S, Hojo Y, Hatanaka Y, Higo S, Murakami G, Komatsuzaki Y, Ogiue-Ikeda M, Kimoto T, Mukai H (2012) Modulation of synaptic plasticity in the hippocampus by hippocampus-derived estrogen and androgen. J Steroid Biochem Mol Biol 131:37-51.
Otto T, Eichenbaum H, Wiener SI, Wible CG (1991) Learning-related patterns of CA1 spike trains parallel stimulation parameters optimal for inducing hippocampal long-term potentiation. Hippocampus 1:181-192.
Patterson MA, Szatmari EM, Yasuda R (2010) AMPA receptors are exocytosed in stimulated spines and adjacent dendrites in a Ras-ERK-dependent manner during long-term potentiation. Proc Natl Acad Sci U S A 107:15951-15956.
Pedram A, Razandi M, Lewis M, Hammes S, Levin ER (2014) Membrane-localized estrogen receptor alpha is required for normal organ development and function. Dev Cell 29:482-490.
Pedram A, Razandi M, O'Mahony F, Harvey H, Harvey BJ, Levin ER (2013) Estrogen reduces lipid content in the liver exclusively from membrane receptor signaling. Sci Signal 6:ra36.
Perkins MS, Louw-du Toit R, Africander D (2017) A comparative characterization of estrogens used in hormone therapy via estrogen receptor (ER)-alpha and -beta. J Steroid Biochem Mol Biol 174:27-39.
Petersen JD, Chen X, Vinade L, Dosemeci A, Lisman JE, Reese TS (2003) Distribution of postsynaptic density (PSD)-95 and Ca2+/calmodulin-dependent protein kinase II at the PSD. J Neurosci 23:11270-11278.
Rex CS, Lin CY, Kramar EA, Chen LY, Gall CM, Lynch G (2007) Brain-derived neurotrophic factor promotes long-term potentiation-related cytoskeletal changes in adult hippocampus. J Neurosci 27:3017-3029.
Rex CS, Chen LY, Sharma A, Liu J, Babayan AH, Gall CM, Lynch G (2009) Different Rho GTPase-dependent signaling pathways initiate sequential steps in the consolidation of long-term potentiation. J Cell Biol 186:85-97.
Roepke TA, Ronnekleiv OK, Kelly MJ (2011) Physiological consequences of membrane-initiated estrogen signaling in the brain. Front Biosci (Landmark Ed) 16:1560-1573.
Rudy JW (2015) Actin dynamics and the evolution of the memory trace. Brain Res 1621:17-28.
Salter MW, Kalia LV (2004) Src kinases: a hub for NMDA receptor regulation. Nat Rev Neurosci 5:317-328.
Scharfman HE, MacLusky NJ (2008) Estrogen-growth factor interactions and their contributions to neurological disorders. Headache 48 Suppl 2:S77-89.
Seese RR, Wang K, Yao YQ, Lynch G, Gall CM (2014) Spaced training rescues memory and ERK1/2 signaling in fragile X syndrome model mice. Proc Natl Acad Sci U S A 111:16907-16912.
Seese RR, Babayan AH, Katz AM, Cox CD, Lauterborn JC, Lynch G, Gall CM (2012) LTP induction translocates cortactin at distant synapses in wild-type but not Fmr1 knock-out mice. J Neurosci 32:7403-7413.
Seese RR, Chen LY, Cox CD, Schulz D, Babayan AH, Bunney WE, Henn FA, Gall CM, Lynch G (2013) Synaptic abnormalities in the infralimbic cortex of a model of congenital depression. J Neurosci 33:13441-13448.

Smejkalova T, Woolley CS (2010) Estradiol acutely potentiates hippocampal excitatory synaptic transmission through a presynaptic mechanism. J Neurosci 30:16137-16148.
Song RX, Zhang Z, Santen RJ (2005) Estrogen rapid action via protein complex formation involving ERalpha and Src. Trends Endocrinol Metab 16:347-353.
Sweatt JD (2001) The neuronal MAP kinase cascade: a biochemical signal integration system subserving synaptic plasticity and memory. J Neurochem 76:1-10.
Tabatadze N, Sato SM, Woolley CS (2014) Quantitative analysis of long-form aromatase mRNA in the male and female rat brain. PLoS One 9:e100628.
Trepanier CH, Jackson MF, MacDonald JF (2012) Regulation of NMDA receptors by the tyrosine kinase Fyn. FEBS J 279:12-19.
Trieu BH, Kramar EA, Cox CD, Jia Y, Wang W, Gall CM, Lynch G (2015) Pronounced differences in signal processing and synaptic plasticity between piriform-hippocampal network stages: a prominent role for adenosine. J Physiol 593:2889-2907.
Vierk R, Glassmeier G, Zhou L, Brandt N, Fester L, Dudzinski D, Wilkars W, Bender RA, Lewerenz M, Gloger S, Graser L, Schwarz J, Rune GM (2012) Aromatase inhibition abolishes LTP generation in female but not in male mice. J Neurosci 32:8116-8126.
Wang JQ, Fibuch EE, Mao L (2007) Regulation of mitogen-activated protein kinases by glutamate receptors. J Neurochem 100:1-11.
Wang W, Kantorovich S, Babayan AH, Hou B, Gall CM, Lynch G (2016a) Estrogen's effects on excitatory synaptic transmission entail integrin and TrkB transactivation and depend upon β1-integrin function. Neuropsychopharmacology 41:2723-2732.
Wang W, Trieu BH, Palmer LC, Jia Y, Pham DT, Jung KM, Karsten CA, Merrill CB, Mackie K, Gall CM, Piomelli D, Lynch G (2016b) A primary cortical input to hippocampus expresses a pathway-specific and endocannabinoid-dependent form of long-term potentiation. eNeuro 3.
Wang XB, Bozdagi O, Nikitczuk JS, Zhai ZW, Zhou Q, Huntley GW (2008) Extracellular proteolysis by matrix metalloproteinase-9 drives dendritic spine enlargement and long-term potentiation coordinately. Proc Natl Acad Sci U S A 105:19520-19525.
Waters EM, Thompson LI, Patel P, Gonzales AD, Ye HZ, Filardo EJ, Clegg DJ, Gorecka J, Akama KT, McEwen BS, Milner TA (2015) G-protein-coupled estrogen receptor 1 is anatomically positioned to modulate synaptic plasticity in the mouse hippocampus. J Neurosci 35:2384-2397.
Wei J, Yuen EY, Liu W, Li X, Zhong P, Karatsoreos IN, McEwen BS, Yan Z (2014) Estrogen protects against the detrimental effects of repeated stress on glutamatergic transmission and cognition. Mol Psychiatry 19:588-598.
Weilinger NL, Lohman AW, Rakai BD, Ma EM, Bialecki J, Maslieieva V, Rilea T, Bandet MV, Ikuta NT, Scott L, Colicos MA, Teskey GC, Winship IR, Thompson RJ (2016) Metabotropic NMDA receptor signaling couples Src family kinases to pannexin-1 during excitotoxicity. Nat Neurosci 19:432-442.
Woolley CS (2007) Acute effects of estrogen on neuronal physiology. Annu Rev Pharmacol Toxicol 47:657-680.
Yamazaki Y, Jia Y, Wong JK, Sumikawa K (2006) Chronic nicotine-induced switch in Src-family kinase signaling for long-term potentiation induction in hippocampal CA1 pyramidal cells. Eur J Neurosci 24:3271-3284.
Zhang JC, Yao W, Dong C, Yang C, Ren Q, Ma M, Han M, Hashimoto K (2015) Comparison of ketamine, 7,8-dihydroxyflavone, and ANA-12 antidepressant effects in the social defeat stress model of depression. Psychopharmacology (Berl) 232:4325-4335.

# CHAPTER THREE: Prepubescent female rodents have enhanced hippocampal LTP and learning relative to males, reversing in adulthood as inhibition increases

**Abstract**

Multiple studies indicate that male rodents perform better than females on spatial problems and have a lower threshold for long-term potentiation (LTP) in hippocampal, CA3-to-CA1 synapses. We report here that in rodents, prepubescent females rapidly encode spatial information and express low threshold LTP, while age-matched males do not. The loss of low threshold LTP across female puberty was associated with three inter-related changes: increased densities of α5 subunit-containing $GABA_A$Rs at inhibitory synapses, greater shunting of burst responses used to induce LTP, and a reduction of NMDAR-mediated synaptic responses. A negative allosteric modulator of α5-$GABA_A$Rs increased burst responses to a greater degree in adult than in juvenile females and markedly enhanced both LTP and spatial memory in adults. The reasons for the gain of functions with male puberty do not involve these mechanisms. In all, puberty has opposite consequences for plasticity in the two sexes, albeit it through different routes.

## Introduction

There is considerable evidence for sex differences in learning: Among adults, men generally score higher on spatial problems whereas women are frequently better on semantic tests (Andreano and Cahill, 2009; Koss and Frick, 2017). Although for some tasks, differences have been shown to reflect sex-specific learning strategies and influences including task familiarity, the mode of testing, and task demands (Voyer et al., 1995; Seurinck et al., 2004; Voyer et al., 2017; Yagi and Galea, 2019; Bocchi et al., 2021; Tascón et al., 2021), the disparity in spatial learning has been reported for diverse species of mammals suggesting it may be a characteristic feature of the class (Jones et al., 2003). Relatedly, sex differences in forms of synaptic plasticity underlying learning have been described. In hippocampal field CA1, Long-Term Potentiation (LTP) is dependent on locally synthesized estrogen in females but not in males (Vierk et al., 2012). The rate limiting enzyme (p450 aromatase) for synthesis of estradiol (E2), the most prevalent and potent estrogen in brain, is present at high levels in hippocampus and localized to axon terminals (Hojo et al., 2004; Kato et al., 2013; Tabatadze et al., 2014), and E2 levels are several-fold higher in hippocampus than in blood in both sexes (Mukai et al., 2010; Ooishi et al., 2012). However, blocking E2 synthesis disrupts LTP only in females (Vierk et al., 2012; Wang et al., 2018). Moreover, at hippocampal CA3-CA1 synapses released estrogen acts through estrogen receptor α (ERα) to activate the LTP critical kinases ERK1/2 and Src, and BDNF receptor TrkB, in females but not males (Wang et al., 2018). It thus appears that females require locally produced estrogen to induce critical synaptic modifications whereas males do not. Parallel studies found that the minimum afferent stimulation needed to elicit LTP (the LTP threshold) is greater in adult females than males (Wang et al., 2018), an effect that is plausibly related to the addition of an estrogen-dependent step in the sequence for inducing potentiation. Given the central role of hippocampus in spatial learning, the higher female LTP threshold helps

explain why in rodents adult females require more training to learn object location than age-matched males (Wang et al., 2018).

The present studies tested if the elevated LTP and learning thresholds identified in female rodents are products of late development. Puberty is a critical landmark in brain maturation and results in a wide array of sex differences in behavior (Sisk and Zehr, 2005; Juraska and Willing, 2017; Kight and McCarthy, 2020) but little is known about how it affects the substrates for memory encoding. Past studies showed that in male rats the magnitude of LTP reaches adult levels by the end of the fourth postnatal week and thus in advance of puberty (Baudry et al., 1981; Muller et al., 1989; Figurov et al., 1996). However, these studies did not assess LTP threshold, which is more closely related to neuronal activity occurring during behavior. Studies addressing developmental changes in LTP in female rodents are rare (Shen et al., 2010), and none have compared the sexes. Thus, it is possible that the sex differences described above are absent or different in prepubertal animals. Such sexually differentiated adjustments during puberty are known to occur in certain psychological domains; anxiety attacks and depression, which occur more frequently in post-pubescent girls than boys, are prominent examples (Romeo, 2003; Pattwell et al., 2013; Smith, 2013). Results described here indicate that the transition from pre- to post-pubertal life causes strikingly different and indeed opposite male vs. female changes in LTP and associated spatial learning. They also describe synaptic mechanisms related to the marked developmental changes that occur in females.

**Materials and Methods**

*Animals.* The studies used postnatal day (P) 21-26 and 2-4 month old male and female mice (FVB129 background) and P21-28 and 2-3 month old Sprague Dawley male and female rats. We used rats for most of the electrophysiological (excepting the use of mice for analysis in Fig.

5c) and all of the immunolabeling experiments because their larger hippocampus allowed for greater precision in aligning zones used in the imaging methods with those sampled during recording studies. Mice were used in all behavior experiments to allow for larger sample size and because tasks have been validated in mice. Animals were on a 12 hr light/dark cycle with lights on at 6:30AM and food and water *ad libitum*. Mice were grouped by 3-5 littermates and rats by 2-4 littermates per cage in rooms maintained at 68°F and 55% humidity. Experiments were conducted in accord with NIH guidelines for the Care and Use of Laboratory Animals and protocols approved by the Institutional Animal Care and Use Committee at University of California, Irvine. All adult females were estrous staged using vaginal lavage as described (Caligioni, 2009; Cora et al., 2015) and identified as proestrus (presence of nucleated cells) and non-proestrus (cornified cells for estrus stage and leukocytes for metestrus/diestrus). Prepubescent females were defined as P21-26 in mice and P21-P28 in rats to reflect differences on puberty onset, as defined visually by vaginal canal opening in both species (Bell, 2018). Prepubescent male rats and mice were age-matched to conspecific females.

*Object Location Memory (a.k.a., object placement).* Behavioral experiments were performed as described (Seese et al., 2014; Wang et al., 2018) in FVB129 mice. Animals were handled for two minutes per day for two days and then habituated to an empty arena (30x25cm floor, 21.5 cm walls) for 5 min on each of the 4 days. For training, mice were returned to the arena containing two identical glass funnels that were 1 cm away from two adjacent corners, were allowed to explore for 5 or 10 minutes, and then were returned to their home cage. After a specified time delay, the mice were placed in the same arena with one funnel displaced towards the center and allowed to explore for 5 minutes.

Adult female mice were monitored for estrous cycling for at least 7 days prior to the training day to ensure normal cycling. On the training day animals were separated into proestrus vs non-proestrus (estrus, metaestrus, diestrus were pooled) groups (Kato et al., 2013).

Prepubescent mice were P25 at training and did not show evidence of vaginal opening on training or testing days. For studies with L655,708, adult female mice were randomly assigned to the drug or vehicle group on the training day.

For these and other behavioral paradigms, the animal's movements within the test chamber were recorded by overhead camera during both training and testing. Videos were hand-scored by individuals blind to group, and sampling time was recorded when the animal's nose sniffed the object within 0.5cm. Sampling was not noted if the animal's nose was in the same zone while turning their head but not attending to the object. A discrimination index (DI) was calculated by $100*(t_{\text{novel object}} - t_{\text{familiar object}})/(t_{\text{novel object}} + t_{\text{familiar object}})$.

*Episodic "Where" Task.* Studies used FVB129 mice as previously described (Cox et al., 2019) . The mice were handled one day prior to the task. On training day, the mice were then placed into a plexiglas arena (60x60 cm floor, 30 cm walls) containing four empty glass cups (5.25 cm diameter x 5 cm height) with a metal lid with a single hole (~1. 5 cm diameter). The cups were removed from the chamber, and the animal rested undisturbed for 5 minutes. For the training session, the four cups were re-introduced with each containing one of the following odorants dissolved in mineral oil (final concentration of 0.1 Pascals): (A) (+)-Limonene (≥97% purity, Sigma-Aldrich), (B) Cyclohexyl ethyl acetate (≥97%, International Flavors & Fragrances Inc.), (C) (+)-Citronellal (~96% Alfa Aesar), and (D) Octyl Aldehyde (~99%, Acros Organics). The animal's behavior was monitored over 5 minutes of odor exposure, and then they were returned to their home cage for 24 hours. For testing, the animals were allowed to explore the chamber with either odorant pairs (A:D) or (B:C) switched in position for 5 minutes.

*Episodic "What" Task.* The task followed the same set up as in the episodic "Where" task, but, for training, the animals were exposed to odorant B, C, D, and E (Anisole; ~99%, Acros

Organics) for 5 minutes. The next day, the animals returned to the chamber with odorant A replacing odorants B or D and were allowed to explore the arena for 5 minutes.

For Episodic Where and What tasks, video recording of behavior were hand-scored by observers that were blind to odors and groups. Cue sampling time was designated as the time the animal's nose was oriented towards the odor hole and within a 0.5 cm radius. The DI for the "Where" task was calculated as follows: $100*(t_{\text{MEAN OF SWITCHED PAIR}}-t_{\text{MEAN OF STATIONARY PAIR}})/(t_{\text{TOTAL SAMPLING}})$. For the "What" task, DI was: $100*(t_{\text{NOVEL}}-t_{\text{MEAN FAMILIARS}})/(t_{\text{TOTAL SAMPLING}})$.

*Extracellular Hippocampal Slice Recording.* Transverse rat hippocampal slices (370µm thick) were prepared using the McIllwain chopper and then transferred to an interface recording chamber, with constant oxygenated artificial cerebrospinal fluid (aCSF) perfusion (60-70mL/hr; 31±1°C) as described (Wang et al., 2018). The aCSF was composed of (in mM): 124 NaCl, 26 $NaHCO_3$, 3 KCl, 1.25 $KH_2PO_4$, 2.5 $CaCl_2$, 1.5 $MgSO_4$ and 10 dextrose (pH 7.4, 300-310 mOsm). Recordings started 1.5-2 hours after slice preparation. Field EPSPs were elicited using a twisted nichrome wire stimulating electrode and recorded with glass pipette electrode (2M NaCl, R=2-3MΩ). These electrodes were placed in dorsal CA1b stratum radiatum equidistant from the CA1 stratum pyramidale. Single pulse baseline stimulation was applied at 0.05Hz with baseline intensity set to 50-60% of the maximum population-spike free fEPSP amplitude. All recordings were digitized at 20kHz using an AC amplifier (A-M Systems, Model 1700) and sweeps of 1.5 seconds duration were recorded every 20 seconds using NAC 2.0 Neurodata Acquisition System (Theta Burst Corp. Irvine, CA). After baseline recording and additional drug infusion, LTP was induced by applying 10 bursts of TBS (4 bursts at 100 Hz, 200 ms interval between bursts) or threshold TBS (4 triplets of theta bursts with 200 ms interval between bursts within the triplet and 90 seconds between triplets), and the recording to baseline (0.05Hz) stimulation resumed for 1 hour. Female rat vaginal smears for estrous monitoring were collected post-mortem at time of slice preparation, and only non-proestrus animals were included in LTP

experiments. Experiments using APV included all stages as there were no statistical differences between proestrus and non-proestrus stages. For all electrophysiology experiments, multiple slices from at least 4 rats were used, and the N reported was number of slices.

*Whole-Cell Voltage Current Clamp Recording.* Hippocampal slices were prepared on the horizontal plane at a thickness of 350 µm from 4- and 8-week-old mice and rats using a Leica vibrating tissue slicer (Model: VT1000S). Slices were placed in a submerged recording chamber and continuously perfused at 2 mL/min with oxygenated (95% $O_2$/5% $CO_2$) aCSF at 32°C. Whole-cell recordings (Axopatch 200A amplifier: Molecular Devices) were made with 4–7 MΩ recording pipettes filled with a solution containing (in mM): 140 $CsMeSO_3$, 8 CsCl, 10 HEPES, 0.2 EGTA, 2 QX-314, 2 Mg-ATP, 0.3 Na-GTP. Osmolarity was adjusted to 290–295 mOsm and pH 7.4. Bipolar stimulating electrodes were placed in CA1 stratum radiatum, 100-150 µm from the recording cell. EPSCs were recorded by clamping the pyramidal cell at −50 mV in the presence of 50 µM APV. Data was collected using Clampex 10.6 and analyzed with Clampfit 10.6 (Molecular Devices).

*Drug Application.* For hippocampal slice recording, the compounds were infused into the aCSF bath via an independent perfusion line (6mL/hr). Final aCSF bath concentrations: APV (100 µM; Hello Bio #HB0225), bicuculline (20 µM; Tocris Bioscience #0130), L655,708 (field electrophysiology: 150 nM, whole-cell electrophysiology: 50 nM; Tocris Bioscience #1327), MPP dihydrochloride (3 µM; Tocris Bioscience #1991) were dissolved in DMSO (<0.01%). For the Object Location Memory task, vehicle (0.1% DMSO) or L655,708 (0.5mg/kg in 0.1% DMSO) was injected intraperitoneally 30 min prior to training.

*Fluorescence Deconvolution Tomography (FDT).* Prepubescent female and male rats were sacrificed on P25; all adult female rats were sacrificed during the diestrus stage of the estrous cycle (P57-59), and adult male rats were age-matched. Slide-mounted, fresh frozen tissue

sections (25 µm; coronal) from mid-septotemporal hippocampus (same region used for electrophysiological studies) were immersion-fixed in 4% paraformaldehyde and processed for dual immunofluorescence as previously described (Rex et al., 2009; Babayan et al., 2012; Seese et al., 2013; Seese et al., 2014) with incubation in primary antisera at 4°C for 24 hours and in secondary antisera at room temperature for 2 hours. After the secondary incubation, sections were washed in 0.1M phosphate buffer and cover-slipped using VectaShield with DAPI (Vector Labs).

Primary antisera cocktails included rabbit anti-gephyrin (1:2000, Abcam #ab32206; RRID: AB_1860490) combined with either guinea pig anti-β1-$GABA_AR$ (1:500, Synaptic Systems #224705; RRID: AB_2619940) or mouse anti-α2-$GABA_AR$ (1:500, Abcam #ab193311; RRID: AB_2890213); mouse anti-gephyrin (1:1500, Synaptic Systems #147021; RRID: AB_2232546) combined with either guinea pig anti-vGAT (1:2000; Synaptic Systems #131004; RRID: AB_887873) or rabbit anti-α5-$GABA_AR$ (1:800, Abcam #ab10098; RRID: AB_296840); rabbit anti-ERα (1:700; Santa Cruz Biotechnology; #sc-542; RRID: AB_631470) combined with mouse anti-PSD95 (1:1000, Thermo Fisher #MA1-045; RRID: AB_325399); and mouse anti-ERβ (1:700, Santa Cruz Biotechnology #sc-390243; RRID: AB_2728765) combined with goat anti-PSD-95 (1:1000; Abcam #ab12093; RRID: AB_298846). Secondary antibodies (all at 1:1000 dilution) included donkey anti-rabbit Alexa Fluor 594 (Invitrogen, Thermo Fisher Scientific #A-21207; RRID: AB_141637), goat anti-guinea pig Alexa Fluor 488 (Invitrogen, Thermo Fisher Scientific #A-11073; RRID: AB_2534117), donkey anti-goat Alexa Fluor 488 (Invitrogen, Thermo Fisher Scientific #A-11055; RRID: AB_2534102), and donkey anti-mouse Alexa Fluor 488 (Invitrogen, Thermo Fisher Scientific # A-21202; RRID: AB_141607).

FDT was conducted as described (Rex et al., 2009; Babayan et al., 2012; Seese et al., 2014; Wang et al., 2018). Under 63x magnification image z-stacks (136x105x2 µm) were collected using 200 nm steps from CA1 stratum radiatum; for each case images were collected

from ≥5 sections spaced by 250 μm on the septotemporal axis of hippocampus. The images were processed for iterative deconvolution (99% confidence, Volocity 4.0). Individual stacks were used to construct 3-D montages of each sample field. Labeled objects were detected using threshold image segmentation across each channel separately; an image was normalized and thresholded at a given intensity threshold, erosion and dilation were used to fill holes and remove background pixels, and objects were segmented based on connected pixels above a threshold using in-house software (using C99, Java (openJDK IcedTea6.1.12.6), Matlab R2019b, PuTTY 0.74, and Perl v5.30.0). All immunofluorescent elements meeting size constraints of synapses, and detected across multiple intensity thresholds, were quantified using automated systems. The gephyrin and PSD-95-immunoreactive elements were considered to be double-labeled for the second antigen if there was contact or overlap in fields of the two fluorophores as assessed in 3-D. Using this approach, ~30,000 inhibitory or excitatory synapses were reconstructed per sample field, and >150,000 were analyzed per rat.

*Statistics.* Results are presented as mean±SEM. For LTP studies significance was determined by comparing the within-slice normalized mean response over the last 5 minutes of the experiment between groups using 2-tailed unpaired t-test or two-way ANOVA with post-hoc Tukey test. Significance in STP and burst pulse analyses was determined using repeated-measure (RM) ANOVA with Bonferroni post-hoc test. Whole-cell recordings and input-output curves were analyzed using 2-tailed unpaired and paired t-test and linear regression, respectively. Behavioral data was analyzed with two-way ANOVA with post-hoc test Tukey for age and sex comparisons, or unpaired or paired 2-tailed Student's t-test for two group comparisons. For FDT density frequency distributions, significance was determined using 2-way RM-ANOVA; for statistical comparison of mean data between two groups a Student's t-test was used, and for age and sex comparisons a two-way ANOVA was used followed by post-hoc Tukey test. All analyses were performed using Prism 6.0 (GraphPad).

## Results

*Hippocampal LTP threshold before vs. after puberty*. We used theta burst stimulation (TBS) to induce potentiation of Schaffer-Commissural (S-C) afferents to field CA1 in acute hippocampal slices from prepubescent (postnatal day (P) 21-28) and young adult (2-3 month old) rats. The amplitudes of field excitatory postsynaptic potentials (fEPSPs) elicited in the CA1 apical dendrites by single pulse stimulation of S-C projections were tightly related to the amplitudes of the preceding fiber volley. Input/output (fiber volley vs. fEPSP amplitude) curves were similar between ages and sex (**Fig. 3.1a**). Prior studies using multiple short trains of three bursts, a protocol that is near threshold for eliciting stable potentiation (Larson and Lynch, 1986), identified a marked sex difference in S-C LTP threshold (Wang et al., 2018). We compared effects of four such triplets, applied at 90-sec intervals, on pre- vs. post-pubertal slices. LTP was obtained in adult males but not females (**Fig. 3.1b**); the percent potentiation at 55-60 minutes post-induction was 35.0±6.1% and 8.1±4.4%, respectively ($p$=0.0038, unpaired t-test). The sex difference was also present in short-term potentiation (STP) recorded during the 90 seconds after each triplet ($F_{3,33}$=7.40, $p$=0.0006, R-M ANOVA; **Fig. 3.1c**). After the last triplet, potentiation steadily decayed to baseline in females but not in males (**Fig. 3.1d**).

Results for the prepubescent groups were dramatically different than those for adults: theta burst triplets induced robust LTP in females (29.2±4.6% at 55-60 min post-induction) but not in males (3.9±2.7%; unpaired t-test $p$=0.0005) (**Fig. 3.1e**). Sex differences were also evident for STP ($F_{3,42}$=4.181, $p$=0.01, R-M ANOVA; **Fig. 3.1f**). Potentiation was sustained over the subsequent 40 min in females whereas the smaller effect in males quickly fell to baseline (**Fig. 3.1g**). In all, theta bursts produced a more pronounced initial potentiation in prepubescent females than in age-matched males and is reflected in the magnitude and stability of subsequent LTP.

Results above indicate that, with age, S-C LTP threshold changes in opposite directions for males vs. females. The difference in percent potentiation at 55-60 min post-induction for pre- vs. post-puberty groups was highly significant for both sexes (2-way ANOVA: $F_{1,25}$=36.35, $p$<0.0001; Tukey's post-hoc: female: $p$=0.0015; male: $p$=0.0004) (**Fig. 3.1h**). Burst triplets produced substantially greater STP before than after puberty in females (R-M ANOVA: $F_{3,48}$=11.57, $p$<0.0001) (**Fig. 3.1i, right**). In contrast, STP in males tended to be smaller before than after puberty but this was not statistically significant ($F_{3,33}$=1.78, $p$=0.17; **Fig. 3.1i, left**). These results raise the possibility that the brief postsynaptic depolarization produced by theta bursts decreases with female puberty resulting in an increase in the number of bursts needed to produce LTP and that male changes across puberty are likely to involve other types of mechanisms.

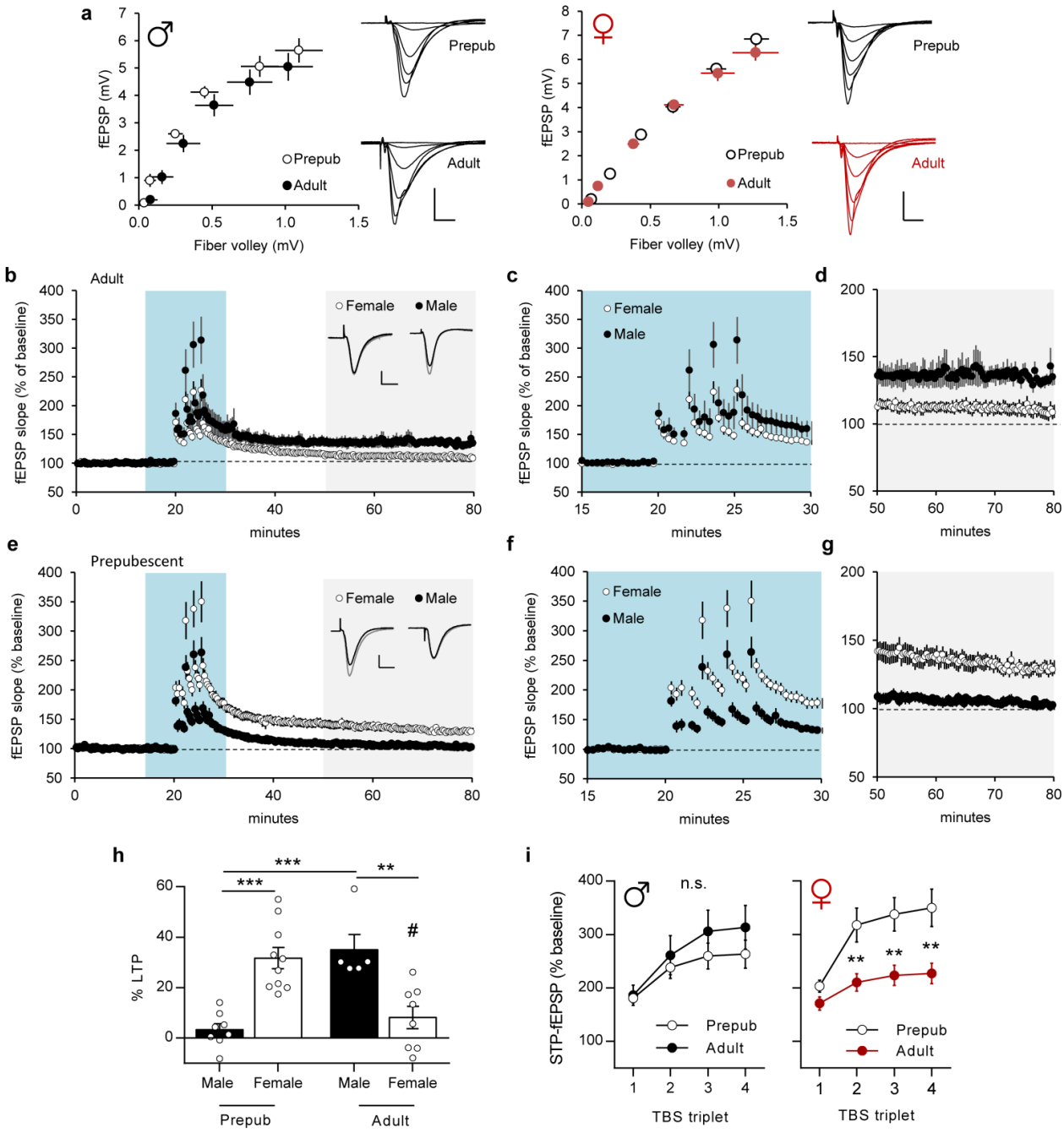


**Figure 3.1. Sex differences in adult rat LTP thresholds are reversed before puberty.** fEPSPs elicited by stimulation of the Schaffer-commissural (S-C) projections were recorded in CA1 stratum radiatum in acute hippocampal slices from prepubertal ('Prepub'; 3-4 week) and adult (8-10 week) rats of both sexes. (**a**) Input-output curves were comparable across age and sex ($p$=0.46, $F_{3,124}$=0.86, linear regression). Representative traces on right. Bars: 2mV, 5ms. (**b**) Four theta burst 'triplets', spaced by 90 seconds, were delivered to S-C axons after 20 minutes of baseline. Each triplet included three bursts (1 burst: 4 pulses at 100Hz) separated by 200ms. After the triplets, single pulse responses in adult females decayed steadily to baseline whereas

those in males fell to a stable plateau just above baseline values. Inset: superimposed traces from baseline (black) and the end of the recording session (gray). Bars: 1mV, 10ms. (**c**) Stretched x-axis (minutes 15-30 of panel 'b') to illustrate single pulse responses during the 90 seconds after each triplet; male fEPSPs were elevated above those of females, indicating a sex difference in short-term potentiation (STP). (**d**) Stretched axes (minutes 50-80 of 'b') show that adult males had a lasting increase in fEPSPs after TBS whereas females did not. (**e-g**) Same format as that for panels b-d but for prepubescent rats: Responses recorded for 90 seconds after each triplet are much larger in females than males (**f**), the reverse of the pattern recorded in adults, and females expressed robust LTP whereas males did not (**g**). (**h**) Summary of LTP (55-60 minutes) for both age groups and sexes (Two-way ANOVA Interaction: $F_{1,25}$=36.35, $p$=0.00005; Tukey Post-hoc: ***$p$<0.001, **$p$<0.01, #$p$=0.0015 for adult female vs prepub female). (**i**) Averaged responses (percent baseline) collected following each of the four theta burst triplets. There was no reliable difference for STP in prepubescent vs. adult male slices (2-way RM-ANOVA: $F_{3,33}$=1.781, $p$=0.17), but STP was larger in prepubescent female vs. adult female slices ($F_{3,42}$=11.57, $p$=8.44x$10^{-6}$; Bonferroni post-hoc: **$p$<0.01). For all panels, N=5-10. Mean±SEM values shown.

*Spatial learning thresholds before vs. after puberty*. The LTP threshold data (above) lead to the striking prediction that the male-female differences in minimum cue exposure required for spatial memory in young adults would be reversed prior to puberty. We tested this using threshold duration training in the Object Location Memory (OLM) task (**Fig. 3.2a**), a paradigm in which memory is CA1-dependent and facilitated by E2 (Inagaki et al., 2010; Barrett et al., 2011; Boulware et al., 2013).

Prepubescent (P25) and adult (2-3 months) male and female mice were given an initial 5-min exposure to two identical objects ("training" session) and, 24 hours later, a 5-min "testing" session during which they re-explored the arena with one object displaced towards the center. Despite lacking high levels of circulating estrogen (Bell, 2018), prepubescent females preferentially explored the novel-location object during testing, as indicated by high Discrimination Index (DI) scores, whereas adult females trained during low-estrogen states ("non-proestrus") showed no preference (low DI scores) (**Fig. 3.2b**). The opposite developmental pattern held for males: adults performed significantly better than pre-pubertal mice. When comparing sexes in age-matched mice ($F_{1,56}$=27.07, $p$<0.0001, interaction 2-way ANOVA), adult males outperformed adult females ($p$=0.003, Tukey's post-hoc), whereas prepubescent females scored better than prepubescent males ($p$=0.002). As predicted from the DI scores, prepubescent females and adult males both explored the novel-location object more than the familiar-location object (paired t-tests: $p$=0.0001 for females, $p$=0.0006 for males), whereas adult, non-proestrus females and prepubescent males did not ($p$=0.21, $p$=0.73, respectively; **Extended Data Fig. 3.1a**). As described (Wang et al., 2018), adult females trained during the high-estrogen stage (proestrus) showed a marked preference for the novel-location object ($p$=0.004; **Extended Data Fig. 3.1b**).

In contrast to the above, adult females given 10 (as opposed to 5) minutes of training discriminated the novel-location object during testing ($p$=0.01), indicating that they require

longer training than prepubescent females to encode spatial memory. Surprisingly, prepubescent males given extended (10-min) training still did not discriminate the moved object ($p$=0.46, **Extended Data Fig. 3.1b**).

Next we tested if the lower facility for rapid spatial learning in prepubescent males and adult females involve problems relating to initial acquisition of cue locations as opposed to later consolidation of the information. Mice were given 5-minute training session and tested for OLM 15-minutes later (**Fig. 3.2a**). The DI for non-proestrus adult females was near zero, indicating that they failed to develop short-term memory for object location. In contrast, although prepubescent males did not encode long-term memory for cue location as assessed at 24h, they had excellent DIs after the short delay (adult female vs prepubescent male; $p$=0.0002; unpaired t-test) (**Fig. 3.2c; Extended Data Fig. 3.1c**). These data reinforce the conclusion from the STP analyses in the physiological experiments that the reversal of sex differences across puberty is due to different types of changes in female vs. male plasticity.

Total cue sampling times (both objects) during OLM training and testing were greater for adult than prepubescent mice (females: P≤0.0002, males: P≤0.0012) but did not differ between the sexes at either age (**Supplementary Fig. 3.1a,b**). Thus, the absence of long-term memory in adult females was not due to a failure to investigate the objects and their locations. Inattention could however have been a factor in the poor performance by prepubescent males (but see below). There were no evident differences between groups in locomotor activity in the behavioral sessions (**Supplementary Fig. 3.1c**).

The above findings raise the question of whether differences in spatial learning are specific to simple tasks such as OLM or instead occur in the same subgroups in more complex circumstances. We tested this using a paradigm in which mice freely sampled four distinct and equally salient odors for 5 minutes and were tested for preferences 24 hours later with positions

of two of the odors swapped ('Where' task; **Fig. 3.2d**). Note that the animals sequentially investigate a collection of cues under these circumstances and that recognition of changes requires encoding of both cue location and identity. Thus the task is considerably more challenging than OLM and incorporates both 'what' and 'where' features of episodic memory. The animals sampled the four odors to similar degree during training with no evident differences between groups (**Extended Data Fig. 3.1d**). The DI indicated that adult, non-proestrus females did not discriminate the novel-location cues at testing whereas prepubescent females spent more time with moved odors (**Fig. 3.2e**) ($p$=0.008, paired t-test, **Extended Data Fig. 3.1e**). Males exhibited the opposite pattern: prepubescent males had a DI near zero whereas adults preferentially attended to the moved cues (**Fig. 3.2e**). A two-way ANOVA ($F_{1,34}$=21.38, $p$<0.0001) of the four groups showed that the adult females and prepubescent males performed worse than the other two groups (P≤0.043, Tukey's post-hoc).

In contrast to the OLM results, there were no age or sex differences in the total time investigating the four odors during training or testing for the episodic 'where' task (**Supplementary Fig. 3.1d,e**). Thus, the absence of long-term memory in post-pubescent females and prepubescent males cannot be attributed to different sampling times. There were no evident differences in locomotion during behavioral sessions (**Supplementary Fig. 3.1f**).

We then tested additional groups to determine if there are sex or age differences in a version of the multi-cue task with a minimal spatial component (episodic "What" test). Mice were allowed to sample four odors for 5 minutes and were tested 24 hours later with one of the cues replaced by a novel odor (**Fig. 3.2d; Extended Data Fig. 3.1f**). In contrast to results for the combined cue identity/location problem, all four groups showed a clear preference for the novel odor at testing (**Fig. 3.2f; Extended Data Fig. 3.1g**). Total sampling times were similar to those for OLM in that adult males and females sampled the cues longer than their prepubescent counterparts (**Supplementary Fig. 3.1h**), but this did not appear to influence retention scores.

Locomotor activity was similar between groups (**Supplementary Fig. 3.1i**). These findings establish that sex and age do not significantly affect encoding cue identity, but that changes across puberty produce opposite effects on female vs. male learning when a spatial component is introduced.

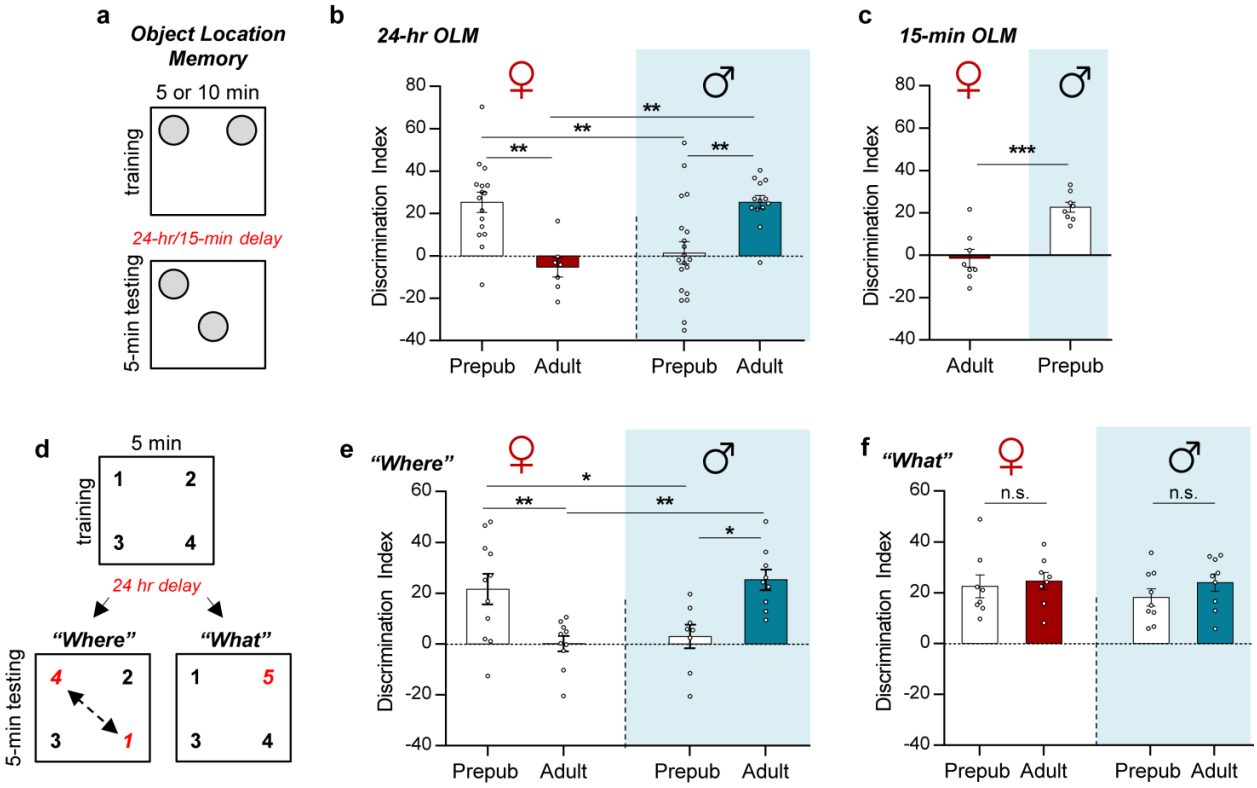


**Figure 3.2. Adult sex differences in spatial learning are reversed prior to puberty.** (**a**) Object Location Memory (OLM) paradigm. Mice were exposed to two identical objects for 5 minutes ('training'). After a delay, mice were returned to the chamber for 5 minutes with one object displaced ('testing'). (**b**) With a 24 hour delay, prepubescent ("Prepub") females (N=16) discriminated the displaced whereas adult females (N=7) (2-way ANOVA (Interaction of sex and age): $F_{1,56}$=27.07, $p$=2.9x10$^{-6}$; Tukey's post-hoc: **$p$=0.0034) and prepubescent males (N=20) (**$p$=0.002) did not. Conversely, adult males (N=17) better discriminated the moved object than prepubescent males (**$p$=0.0016) and adult female mice (**$p$=0.003). (**c**) When tested 15 minutes post-training, adult females performed significantly worse in the task than prepubescent males (2-tailed unpaired t-test: ***$p$=0.0002, N=8/group). (**d**) Episodic "Where" and "What" task schematic. Mice were exposed to four different odors for 5 minutes (training); 24 hours later, the animals explored the chamber with either the two objects switched in position ("Where") or one odor replaced by a novel odor ("What"). (**e**) In the "Where" task, prepubescent females better discriminated the switched odor pairs than did adult females ($F_{1,34}$=21.38, $p$=5.25x10$^{-5}$. post-hoc: **$p$=0.0091) and prepubescent males (*$p$=0.043). Adult males better discriminated switched odors compared to prepubescent males (*$p$=0.016) and adult females (**$p$=0.003) (N=8-11/group). (**f**) In the "What" task, all groups preferentially explored the novel odor vs the familiar odors at testing ($F_{1,30}$=0.26, $p$=0.61. N=8-9/group). Mean±SEM values shown.

*Factors relating to the developmental changes in female LTP.* The STP results described above could reflect age- and sex-differences in the depolarizing responses produced by theta burst triplets and thus the likelihood of triggering the initial steps leading to LTP. Comparisons of the composite response to a single four-pulse theta burst in rat slices confirmed that the amplitudes of the 2$^{nd}$ through 4$^{th}$ fEPSP were substantially larger in females before vs. after puberty ($F_{3,90}$=24.40, $p$=5.38x10$^{-12}$; RM-ANOVA) (**Fig. 3.3a**). These results are suggestive for underlying mechanisms. Afferents from CA3 monosynaptically innervate both CA1 pyramidal cells and local interneurons, some of which form inhibitory synapses in the same dendritic field (stratum radiatum) as the excitatory contacts (Alger and Nicoll, 1982). Inhibitory postsynaptic currents (IPSCs) are slower than the fast AMPAR-mediated glutamatergic currents and thus exert their greatest shunting effects on EPSCs triggered by the 3$^{rd}$ and 4$^{th}$ pulses in a theta burst (Ben-Ari et al., 1981; Larson and Munkácsy, 2015).

We tested the possibility of an age-related increase in feedforward IPSCs in females using voltage-clamp recordings to compare effects of the $GABA_AR$ antagonist bicuculline on the size of a burst response in prepubescent and adult rat slices (**Fig. 3.3b**). In agreement with the field recordings, the area of the baseline (pre-drug) burst response, normalized to the amplitude of the first EPSC in the burst, was nearly twice as large in pre-pubertal females (60.6±2.8 pA*msec) as in adult females (31.3±3.6 pA*msec; $p$=0.0002, unpaired t-test). The burst response area tended to decrease with age in males (pre- vs. post-puberty: 61.4±3.5 vs. 51.0±4.3 pA*msec) but this effect did not reach statistical significance ($p$=0.068, unpaired t-test; **Supplementary Fig. 3.2a**). The percent decrease from prepubescence to adulthood was significantly larger in females (-48.3±5.9%) than in males (-16.9 ±7.1%) ($p$=0.004, unpaired t-test). Bicuculline had a larger effect after puberty: in females it increased the area of a single burst response by 82.5±22.9% and 195.8±29.7% in prepubescent and adult animals, respectively ($p$=0.02, unpaired t-test) (**Fig. 3.3c**). The antagonist had a measurably greater effect on normalized burst responses in males than females before ($p$=0.019, unpaired t-test)

but not after ($p$=0.273) puberty. These results indicate that feedforward IPSCs during a burst response increase across puberty in females and thereby more potently shunt the depolarization produced by a burst.

Delivery of two bursts separated by 150-200 msec results in a marked facilitation of the second response due to partial suppression of feedforward IPSPs (Pacelli et al., 1989, 1991). The enhanced and prolonged depolarization unblocks NMDARs and thus initiates the sequence leading to the production of LTP (Larson and Lynch, 1988). We used the selective NMDAR antagonist APV to estimate the magnitude of the NMDAR-component of the burst response before vs. after female puberty. A pair of theta bursts was delivered under control conditions and then again after 30 minutes of APV infusion. As expected from above, the area of the composite potential produced by the first (control) theta burst was substantially larger in slices from prepubertal than adult female rats ($p$<0.0001) (**Fig. 3.3d,e**). Notably, the amplitude of the initial fEPSP within the burst was virtually identical in the two groups (Prepuberty: 2.10±0.02 mV, Adult: 2.11±0.03 mV. $p$=0.64, unpaired t-test) indicating that the age difference in burst responses was due to the $2^{nd}$-$4^{th}$ potentials. The prepubescent cases also had a larger response to the second theta burst than did adults during baseline testing (159.9±4.8 vs. 119.1±4.7 mV*msec respectively, $p$=0.0003) (**Fig. 3.3e**). Following APV infusion, the response to the first of the two theta bursts was not measurably different than that before APV infusion for either age group but the magnitude of the second burst response was reduced in both cases. We subtracted the waveforms of the APV-plus responses from those acquired before APV infusion to quantify the drug effect (**Fig. 3.3f**). This analysis confirmed that the antagonist had no effect on the first burst response but removed a significant component of the second, an effect that was clearly greater in pre- vs. post-puberty slices (-26.4±4.6 vs. -12.1±3.8 mV*msec, respectively. $p$=0.024) (**Fig. 3.3g**). This accord with the prediction that the NMDAR-mediated component of the composite response decreases across puberty.

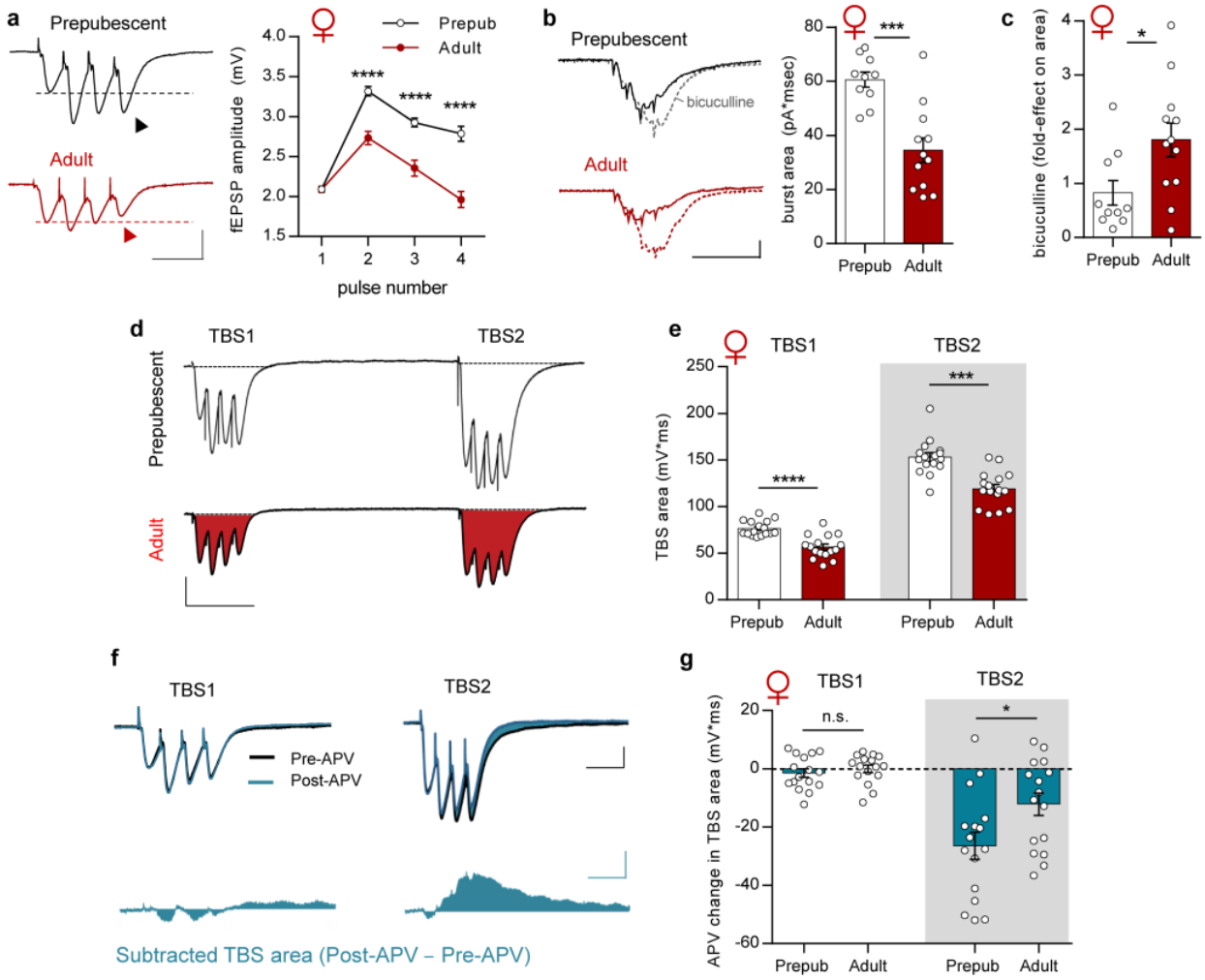


**Figure 3.3. Theta burst responses, feedforward inhibition, and NMDAR-mediated synaptic potentials differ between pre- vs. post-pubescent female rats.** (**a**) Traces of fEPSP responses elicited by a single burst (four pulses,100Hz) delivered to the Schaffer-commissural (S-C) projections and recorded from CA1 stratum radiatum in slices from prepubescent ('Prepub') or adult female rats. Arrowheads mark the fourth fEPSP in the burst response. Bars: 2mV, 20msec. *Right*: Graph shows the four fEPSPs within the burst responses in adult and prepubescent groups (2-way RM-ANOVA: $F_{3,90}$=25.40, $p$=5.38x$10^{-12}$. Asterisks indicate group differences for each fEPSP in the burst response: Bonferroni post-hoc, ****$p$<0.0001). (**b**) Voltage-clamp recordings from CA1 pyramidal cells during delivery of single burst stimulation to S-C projections in slices from a prepubescent or adult female rats before (solid trace) and during (dotted) infusion of bicuculline (20 µM, 10 min). In adults the baseline response is smaller and the $GABA_AR$ antagonist had a greater effect (bars: 100 pA, 50 ms). Graph shows areas of baseline (pre-drug) burst responses for prepubescent (N=10) and adult (N=12) groups: the size of the composite four EPSC responses (normalized to amplitude of the first response) were nearly twice as large in prepubescent vs. adult females (2-tailed unpaired t-test: ***$p$=0.0002). (**c**) Group data for effects of bicuculline before vs. after puberty. The antagonist had

substantially larger effect in slices from the older rats (2-tailed unpaired t-test: *$p$=0.02). (**d**) Traces show S-C responses elicited by two theta bursts (4 pulses at 100 Hz, 200 ms interval) in prepubertal and adult female slices (bars: 1 mV, 50 ms). (**e**) Group data for areas of responses elicited by the first and second theta bursts. As in 'a', the first of these (TBS1) was larger in prepubertal as compared to adult female slices (2-tailed unpaired t-test: **** $p=7.4x10^{-6}$); this was also the case for the composite response to the second burst (TBS2) (***$p$=0.0003). (**f**) Traces show superimposed theta burst responses before and after 30-min infusion of NMDAR antagonist APV (100μM) (bars: 1 mV, 25 ms). The bottom graphs (solid blue) show the results of subtracting the baseline responses to TBS1 and TBS2 from those recorded in the presence of APV (bars: 0.5 mV, 25 ms). Note that APV reduced the later segments of the negative-going response to TBS2 while having minimal effects on that produced by TBS1. (**g**) Summary of group data for effects of APV on the size of responses to two theta bursts: APV did not alter the composite response to TBS1 in prepubescent or adult slices (n.s. $p$=0.46) but reduced the areas of responses to TBS2. The attenuation of the TBS2 response was larger prior to puberty (*$p$=0.024, 2-tailed unpaired t-test). For panels (**a, e, g**): N=16/group. Data are presented as mean values ± SEM.

*$GABA_AR$ synapses before vs. after female puberty.* The above findings indicate that some element of fast ionotropic GABAergic transmission activated by CA3 inputs to CA1 changes during female puberty. We accordingly counted the number of inhibitory synapses in the apical CA1 dendritic subfield evaluated in the physiological studies. Dual immunofluorescence for the postsynaptic scaffolding protein gephyrin and the presynaptic vesicular GABA transporter (VGAT) was used to label inhibitory synapses in female rats; 3-D reconstructions of several thousand individual pre- and post-synaptic elements were created from image z-stacks and quantified using Fluorescence Deconvolution Tomography (Rex et al., 2009; Seese et al., 2013) (FDT) (**Fig. 3.4a**). There was no change in the incidence of inhibitory synapses (**Fig. 3.4b**) or the per-synapse density of gephyrin (**Fig. 3.4c**) or VGAT (not shown) immunoreactivity (-ir) from 4- to 8-weeks of age.

Next, we evaluated specific $GABA_AR$ subunits co-localized with gephyrin beginning with the α5 subunit that has been linked to feedforward inhibition in CA1 (Schulz et al., 2018). Specifically, α5-$GABA_A$Rs are present in inhibitory synapses on CA1 pyramidal cell dendrites where they mediate slow decaying IPSCs. Deletion of α5 decreases the amplitude of spontaneous (synaptic) IPSCs in CA1 and increases paired-pulse facilitation of fEPSPs elicited by S-C stimulation. The latter result constitutes evidence that a significant portion of feedforward inhibition, which shunts the response to the second stimulation pulse, is mediated by α5-$GABA_A$Rs.

The α5 subunit levels at inhibitory (gephyrin-ir) synapses in CA1 stratum radiatum increased markedly from 4- to 8-weeks of age in females (**Fig. 3.4d,e**); this was evident as a right-shift in the immunolabeling density frequency distribution towards higher values in adults relative to juveniles ($F_{50,700}$=14.46, $p$<0.0001, RM-ANOVA) (**Fig. 3.4d**, left). As expected from this, the percentage of synapses associated with high concentrations of α5-ir was more than two-fold greater after puberty (**Fig. 3.4d**, right). This developmental change was not present in males: the frequency distributions for densities of synaptic α5-ir were superimposable for

prepubescent and adult groups ($F_{10,130}$=0.46, $p$=0.91) (**Supplementary Fig. 3.2b**) and the percent of contacts with high concentrations of α5-ir were comparable (pre-puberty: 20.6±1.3%; post-puberty: 20.5±2.2%) (**Fig. 3.4d,** right). Comparisons of males and females identified an interaction between sex and age ($F_{1,26}$=15.30, $p$=0.0006, 2-way ANOVA). The density of synaptic α5-ir increased across female puberty ($p$<0.0001), and pre-pubescent males had higher levels than age-matched females ($p$=0.033). There were no differences between juvenile and adult males ($p$=0.99) or between adult males and females ($p$=0.07). In all, there was a striking difference between the sexes with regard to puberty-related changes in a key element of feedforward GABAergic transmission in CA1 apical dendrites.

We analyzed two additional $GABA_AR$ subunits to test the selectivity of the pre- to post puberty increase in α5 recorded for females. From 4- to 8-weeks of age, the density of immunoreactivity for the α2 subunit at gephyrin-ir synapses was unchanged ($F_{50,700}$=0.17, P>0.99, RM-ANOVA) (**Fig. 3.4f**) and there was a slight shift towards higher densities of β1 subunit-ir but this was not statistically significant ($F_{50,700}$=1.32, $p$=0.07) (**Fig. 3.4g**).

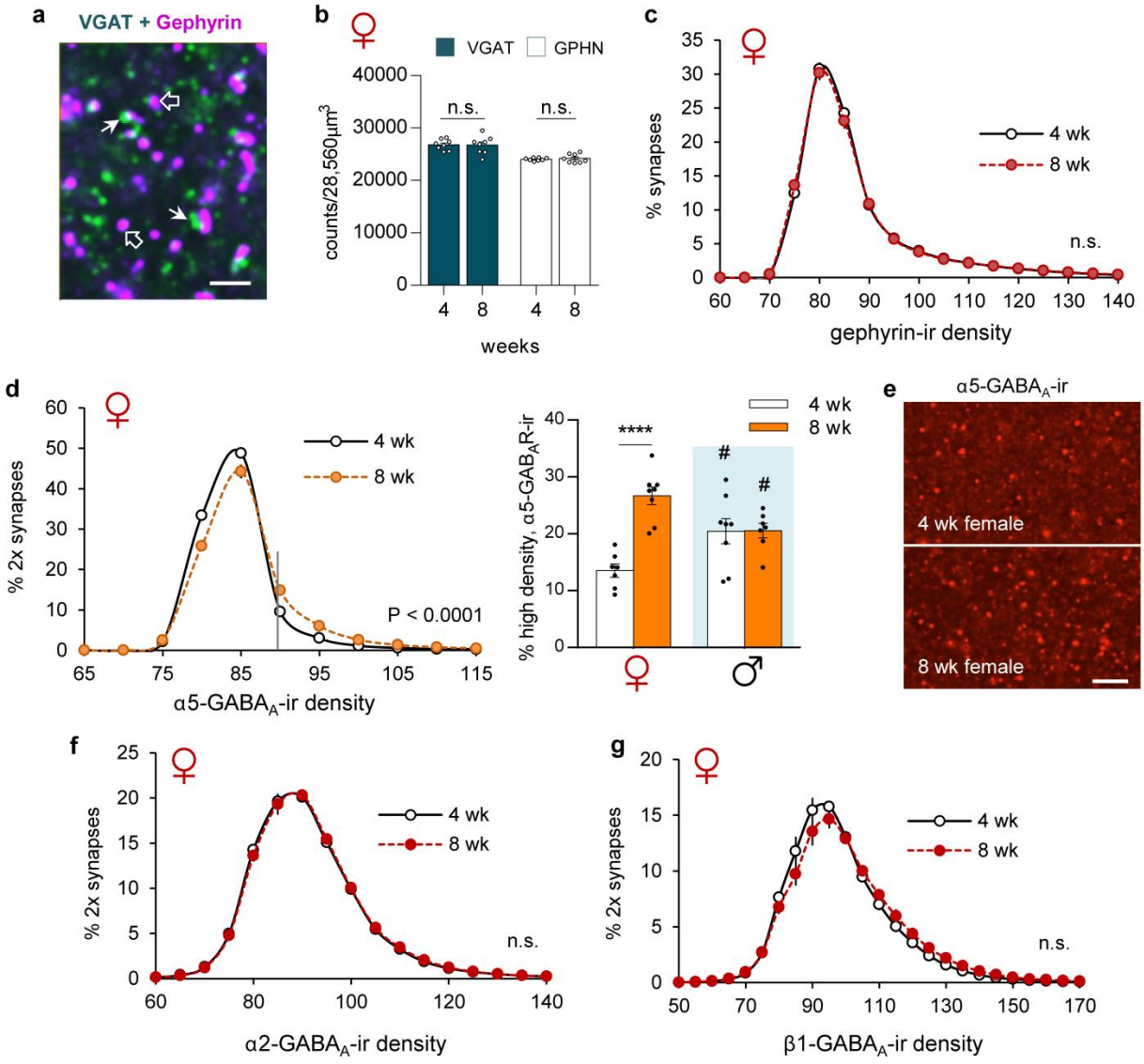


**Figure 3.4. Synaptic levels of GABAAR subunits in pre- vs. post-pubescent female rat.** (**a-c**) Dual immunofluorescence for presynaptic vesicular GABA transporter (VGAT) and postsynaptic gephyrin (GPHN) in CA1 stratum radiatum indicates that numbers of inhibitory synapses are equivalent in the two age groups. (**a**) Image shows immunofluorescence localization of gephyrin (open arrows, magenta) and VGAT (closed arrows, green) in an 8-week old female. Calibration bar: 2 µm. (**b**) Counts of VGAT-immunoreactive (-ir) and GPHN-ir puncta (mean±SEM) were comparable at 4- and 8-weeks of age (2-tailed, unpaired t-test: VGAT, $p$=0.92; GPHN, $p$=0.78). (**c**) Immunolabeling density frequency distributions for gephyrin-ir elements did not differ between groups ($F_{40,560}$=0.58, $p$=0.98). (**d-e**) The density of immunolabeling for the α5 $GABA_AR$ subunit at inhibitory synapses changes from 4 to 8 weeks in females, but not males. (**d**) *Left*. Plot shows the density frequency distributions for α5-ir co-localized with gephyrin ('2x synapses') in females: the curve for the 8-week group was markedly

right-shifted towards higher densities relative to that for the 4-week group ($p$=5.8x10$^{-78}$, $F_{50,700}$=14.46). *Right*. Graphs shows the percentage of double-labeled synapses with dense α5-ir (above vertical cutoff line on the frequency distribution curve) in female and male rats (**Supplementary Fig. 2b** for males frequency distribution): Values were significantly higher in post- vs pre-pubescent females, whereas males showed no change between ages (2-way ANOVA Interaction $F_{1,26}$=15.30, $p$=0.0006; Tukey's post-hoc: ****$p$<0.0001, #$p$<0.05 vs. 4 wk female. $p$=0.99 for 4wk vs 8wk male). (**e**) Photomicrographs of α5-GABA$_A$-ir in CA1 stratum radiatum illustrate the increase in densely-immunolabeled puncta in 8- vs 4 -week old females. Bar: 5 µm. (**f,g**) Density frequency distributions for (**f**) α2-GABA$_A$R-ir and (**g**) β1-GABA$_A$R-ir show that levels of synaptic immunoreactivity (colocalized with gephyrin) did not differ between pre- and post-pubescent females (α2: P>0.99, $F_{50,700}$=0.17; β1: $p$=0.07, $F_{50,700}$=1.32). For all panels N=7-8/group. Statistics on (**c-d, f-g**) performed with 2-way RM-ANOVA (Interaction). Data are presented as mean values ± SEM.

*Effects of blocking α5-GABA$_A$Rs.* We tested the prediction that blocking α5-GABA$_A$Rs with subunit selective negative allosteric modulators (NAMs, a.k.a., inverse agonists) would restore theta burst responses and LTP in adult female rats to levels found before puberty. Infusion of the selective α5-NAM L655,708 (150 nM, 40 minutes), which acts via the benzodiazepine binding site to suppress IPSCs gated by α5-GABA$_A$Rs, had minimal effects on baseline fEPSP amplitude in adult females but caused a clear enhancement of the normalized and raw amplitudes of the 2$^{nd}$-4$^{th}$ potentials in the composite response to a theta burst, as expected for suppression of fast inhibition (**Fig. 3.5a** for normalized values; raw values: 1$^{st}$ pulse, vehicle: 2.75±0.13 mV, L655,708: 3.00±0.11 mV, two-tailed unpaired t-test $p$=0.11; RM-ANOVA across pulses: $p$=0.0048, $F_{3,39}$=5.041). These results constitute the first evidence that α5-GABA$_A$Rs potently affect theta burst responses. We confirmed that theta burst triplets fail to elicit LTP in vehicle-treated adult female rat slices but do produce robust LTP in the presence of L655,708 (9.3±2.9% vs. 48.9±6.7%; $p$=0.0002, at 55-60 min post-TBS, unpaired t-test) (**Fig. 3.5b**). Voltage-clamp recordings in mouse slices revealed that the NAM significantly increased (22.2±4.8%, $p$=0.003; paired t-test) the area of single theta burst responses above pre-treatment baseline in adult females. However, and in accord with the analysis of α5 densities at synapses, the compound had little if any effect (8.3±4.2%, $p$=0.144) on response size in prepubescent female slices (prepubertal vs adult; $p$=0.04, unpaired t-test) (**Fig. 3.5c**). Collectively, these findings indicate that the pronounced increase in synaptic α5-GABA$_A$Rs that occurs over the course of female puberty depresses theta burst responses leading to an increase in LTP threshold.

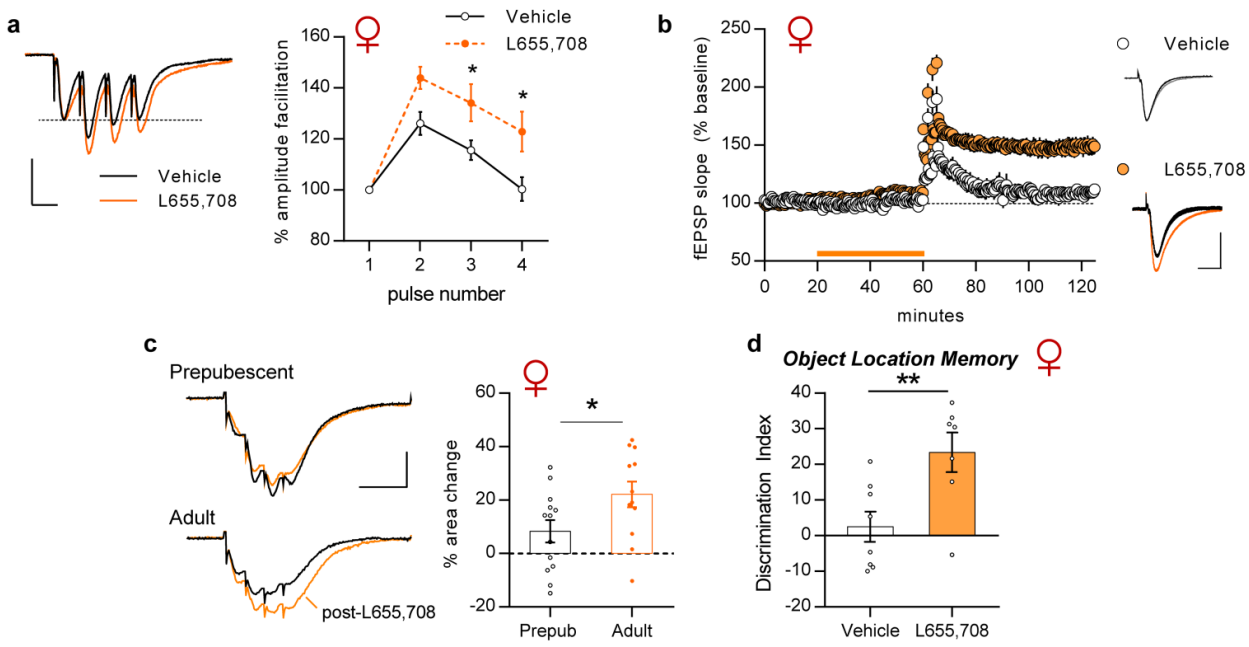


**Figure 3.5. A negative allosteric modulator (L655,708) of the α5-GABAAR subunit increases theta burst responses and facilitates LTP in adult females.** (**a,b**) Baseline responses were collected for 20 min before a 40-min infusion of L655,708 (150 nM) in adult female rat hippocampal slices. Four TBS 'triplets' (90 sec intervals) were applied to induce LTP after drug treatment. (**a**) *Left*. L655,708 increased the size of the response to one theta burst (4 pulses, 100 Hz) relative to vehicle-treatment (bars: 2mV, 10ms). *Right*. Group data (N=7-8/group) for the four fEPSP amplitudes normalized to the first pulse that comprise a single theta burst response (2-way RM-ANOVA: $p$=0.011, $F_{3,39}$=4.21;Bonferroni post-hoc (3$^{rd}$ pulse: *$p$=0.048 and 4$^{th}$ pulse: *$p$=0.012). (**b**) Female slices treated with L655,708 (line bar) express robust LTP whereas those infused with vehicle do not (2-tailed unpaired t-test: $p$=0.0002 at 1 hour post-TBS. N=7/group). Right: Representative superimposed traces. Black: baseline, Orange: post-LTP, bars: 2 mV, 10 ms. (**c**) Voltage-clamp recordings from CA1 neurons elicited by a single theta burst from prepubescent vs adult female mouse slices before (black trace) and during infusion with L655,708 (50 nM, 10 min; bars: 50 pA, 25 ms). Bar graph summarizes results for prepubescent and adult female slices: L655,708 significantly increased the area of the burst response in adult (N=12; $p$=0.003, 2-tailed, paired t-test) but not prepubescent females (N=13; $p$=0.144). The difference in % increase above pre-drug baseline for the two groups was significant (2-tailed, unpaired t-test: *$p$=0.04). (**d**) Adult female mice were intraperitoneally injected with vehicle (0.1% DMSO) or L655,708 (0.5mg/kg) 30 minutes before the 5-minute training trial for Object Location Memory. With a 24 hour delay, adult females given L655,708 showed enhanced discrimination for the displaced object compared to vehicle-treated females (2-tailed unpaired t-test: **$p$=0.0097. Vehicle N=8, L655,708 N=7). Mean±SEM values shown.

As expected from the FDT analysis of synaptic α5 concentrations, L655,708 caused a comparable increase in burst response area in males before and after puberty (% area change: 26.6±3.4 and 29.6±4.7, respectively; $p<0.01$ within groups, paired t-tests. $p=0.649$ between age groups, unpaired t-tests. **Supplementary Fig. 3.2c**).

Next, we tested the prediction that the recovery of low threshold LTP in adult females produced by L655,708 would result in a comparable improvement in spatial learning. Non-proestrus mice were injected with vehicle or the α5-NAM 30 minutes before 5-minute OLM training and were tested for discrimination of the moved object 24 hours later (**Fig. 3.2a**). Vehicle-treated mice had low retention scores whereas the L655,708 group performed at the level of prepubescent females and adult males (vehicle vs. L655,708: $p=0.0097$, unpaired t-test) (**Fig. 3.5d; Extended Data Fig. 3.2a**). The NAM did not influence cue sampling times during training or testing, or locomotor activity (**Extended Data Figs 3.2b,c,d**).

*Contributions of ERα to LTP prior to puberty.* As described, LTP in adult females is dependent on locally synthesized estrogen acting on synaptic ERα (Wang et al., 2018). We investigated the possibility that this requirement emerges with puberty, and associated increases in circulating estrogen (Bell, 2018), and thus is a potential contributor to the elevation of LTP thresholds. The selective ERα antagonist MPP produced a near complete blockade of potentiation induced by a train of 10 theta bursts in slices from 4-week old female rats (Vehicle: 58.9±7.2% at 55-60 min post-TBS; MPP: 12.4±4.5%; $p=0.0006$, unpaired t-test) (**Fig. 3.6a**). The use of a stronger induction paradigm (10 bursts instead of burst–triplets) emphasizes the extent to which prepubescent female LTP is dependent on this estrogen receptor class. Using FDT we determined that ERα levels at PSD-95-ir synapses in CA1 stratum radiatum are dramatically higher in adult than in prepubertal female rats ($F_{19,342}=22.10$, $p<0.0001$) (**Fig. 3.6b**). This result argues against a decline in ERα contributing to the age-related increase in LTP threshold. We previously showed that synaptic ERα levels are substantially higher in adult females than age-

matched males (Wang et al., 2018), but this sex difference was not detected in prepubescent rats (**Supplementary Fig. 3.2d,e**). Moreover, synaptic concentrations of ERβ-ir in prepubertal and adult females were comparable (**Fig. 3.6c**). Together, these findings raise the possibility that the marked and sex-specific change in synaptic ERα levels is a specialization that partially compensates for the reduction in the NMDAR-component of the theta burst response that occurs in female rodents during the transition through puberty.

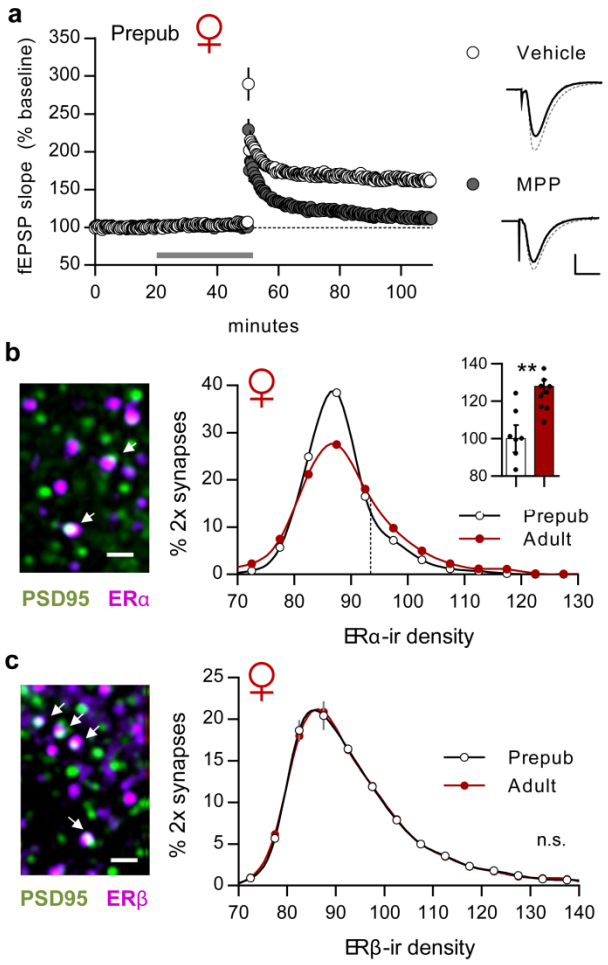


**Figure 3.6. LTP induction in prepubescent female rats is dependent on activation of estrogen receptor α (ERα).** (**a**) Slices from prepubertal female rats were infused for 30 minutes with ERα antagonist MPP or vehicle before S-C stimulation with 10 theta bursts. In the presence of MPP, LTP decayed to baseline within an hour, while vehicle-treated cases exhibited robust and stable LTP (2-tailed unpaired t-test at 55-60 min post-TBS: $p$=0.0006; N=5/group). Traces (right) show superimposed pre- (black) vs. post-TBS (dashed) fEPSPs. Bars: 1 mV, 10 ms. (**b**) Dual immunolabeling for ERα (magenta) and PSD95 (green) in the CA1 lamina used for LTP experiments from prepubertal and adult females (deconvolved images; area of overlap (white) identified in 3D). Arrows highlight double-labeled contacts ('2x synapses'). Line graph summarizes the density frequency distributions for ERα-ir co-localized with PSD95 as determined using Fluorescence Deconvolution Tomography. Adult females show a significant rightward skew towards high densities relative to prepubescent animals (2-way RM-ANOVA: $F_{19,342}$=22.10, $p$=2.17x10$^{-48}$. N=10/group). Inset graph summarizes % higher density contacts (92+ on x-axis) (2-tailed unpaired t-test: **$p$=0.002 for pre- vs. post-puberty). (**c**) Representative image of ERβ (magenta) and PSD-95 (green) double-labeling. Synaptic ERβ density distribution curves were comparable in prepubertal and adult females ($F_{19,323}$=0.16, $p$=0.99. Prepub N=9, Adult N=10). Bar for **b-c**: 1 µm. Mean±SEM values shown.

## Discussion

The above results lead to the surprising conclusion that the polarity of sex differences at hippocampal synapses and related learning reverses from before to after puberty. This occurs because of opposite developmental changes in females vs. males: thresholds for plasticity and encoding spatial information increase in females and decrease in males. We identified a plausible mechanism for the female effect: the depolarizing responses elicited by the short high-frequency stimulation bursts are substantially larger in the prepubertal animals. The bursts produce frequency facilitation of transmitter (glutamate) release at the S-C synapses but the expected enhancement of successive postsynaptic responses is partially shunted by the buildup of di-synaptic feedforward IPSCs. The latter GABAergic responses are due to interneurons engaged by CA3-CA1 projections. Shunting is of considerable functional significance with regard to LTP because enhanced and prolonged depolarization is required to unblock the voltage-dependent, relatively slow NMDARs that initiate the complex sequences leading to synaptic modifications. We found that the shape of the composite response elicited by a four-pulse burst differed significantly between pre- vs. post-pubescent females: responses to later pulses in the burst were larger in prepubertal animals suggesting less inhibition at this age. Clamp recordings demonstrated that feedforward inhibition during the bursts increases dramatically at some point during female puberty.

The facilitation of responses that occurs when two bursts are given sequentially was also greater before than after female puberty. Previous work showed that the enhancement of the second response reflects a partial refractoriness of feedforward inhibition due to–$GABA_BR$ activation on interneuron terminals (Davies et al., 1991; Mott and Lewis, 1991). These metabotropic receptors open potassium channels and thereby reduce GABA release probability with the effect maximized at about the period of the theta wave. We interpret the greater facilitation of the second burst in prepubescent females as resulting from the refractory process

operating on weaker inhibition. This effect is directly related to LTP threshold because the greater and temporally extended depolarization produced by the second burst suffices to open NMDAR channels. We confirmed that the NMDAR-component of the second response is larger before than after puberty in females.

Despite age-related changes in activity-driven IPSCs, we did not detect an increase in the number or density of GABAergic contacts in CA1 stratum radiatum. This finding raised the possibility of developmental changes in the composition of $GABA_A$Rs. The pentameric GABA receptors include one gamma, two alpha, and two beta subunits (Sigel and Steinmann, 2012). The specific α subunits exert differential effects on rate kinetics. Receptors containing α5 are of particular interest in the present context because they generate large and prolonged IPSCs that shunt NMDAR-mediated currents in the apical dendrites of field CA1 (Collinson et al., 2002). Notably, adult hippocampus in rodents and humans has unusually high levels of α5 expression (Sur et al., 1998; Wainwright et al., 2000; Sieghart and Sperk, 2002). Our analyses indicate that α5 levels at inhibitory synapses in apical field CA1 are substantially lower before puberty in females. The developmental difference in α5-$GABA_A$Rs in the same dendritic layer containing the excitatory S-C synapses that generate the theta burst response helps explain why later potentials in those responses are unusually large in prepubescent females. In accord with the above arguments, we found that negative modulation of α5-$GABA_A$Rs restored theta burst responses, LTP thresholds, and spatial learning in adult females to levels found before puberty.

The changes in α5 concentrations could reflect the developmental onset of the estrous cycle, which occurs around P28-30 in rodents (Bell, 2018), as multiple studies have shown this influences the $GABA_A$R subunit composition (Herbison and Fénelon, 1995; Weiland and Orchinik, 1995; Vastagh et al., 2016; Mukherjee et al., 2017). These effects have been related to fluctuations in progesterone and its neurosteroid metabolites (Weiland and Orchinik, 1995). The steroids operate over different time courses and mechanisms including effects on $GABA_A$R

subunit gene expression (Herbison and Fénelon, 1995; Vastagh et al., 2016). These analyses have only recently extended to α5 in rodents (Franco-Enzástiga et al., 2020) and as yet do not provide an interpretation for the present findings. An alternative possibility involves the late maturation of interneurons and their connections. Neuronal activity affects expression of cell-specific transcription factors, including Npas4, that influence the formation of excitatory synapses on somatostatin-positive interneurons (Sim et al., 2013; Spiegel et al., 2014). Relatedly, network activity influences elements of perineuronal nets associated with parvalbumin-positive interneurons, a specialization widely held to alter synaptic connectivity (Spiegel et al., 2014; Shepard et al., 2019). There is also evidence that activity influences the expression of channels by parvalbumin interneurons, including the potassium and voltage-gated Kv1.1, that regulate the excitability and firing characteristics of these cells (Monaghan et al., 2001; Morgan et al., 2019). It is thus possible that the change from pre- to post-pubertal life is associated with changes in interneuron function that alter postsynaptic cells in a manner that shifts the balance of inhibitory synapses in favor of those enriched with α5-$GABA_A$Rs.

The absence of age-related changes in the density of α5-ir at inhibitory synapses in males constitutes one of the more striking sex differences observed in the present studies. It is clear from this, and related observations, that changes in shunting IPSCs and theta burst responses are not responsible for the emergence of low threshold LTP in post-pubertal males. In males, burst responses were if anything reduced from before to after puberty which strongly suggests that NMDAR-gated ionic currents did not increase. There remains the possibility that calcium influx through the receptors, or the subsequent release of the cation from intracellular stores, increases from 4- to 8-weeks of age in males. Alternatively, recent studies raise the possibility that NMDAR-mediated activation of the LTP critical kinase Src involves non-ionic functions; a metabotropic route is also suggested for NMDAR-dependent ERK activation

(Nabavi et al., 2013; Dore et al., 2016). A change in the linkages between the NMDARs and these enzymes during puberty could account for the observed drop in male LTP threshold.

Given the extensive evidence linking LTP to some but not all forms of learning, an increase of the threshold for inducing LTP is likely to have significant consequences for behavior. In accord with this, post-pubescent females did not acquire simple or complex spatial information with a minimal number of trials, tests on which excellent scores were observed prior to puberty. Importantly, pharmacological suppression of α5-$GABA_A$Rs restored LTP and memory encoding in adult females to levels observed prior to puberty. One interpretation of the seemingly deleterious elevation of plasticity and learning thresholds is that the effects are secondary to adaptations for other, unrelated female behaviors. The α5-containing $GABA_A$Rs have been linked to anxiety (Navarro et al., 2002; Clayton et al., 2015; Magnin et al., 2019), a psychological variable that can be strongly affected in a sex-specific manner by puberty (Costello et al., 2011; Altemus et al., 2014; Asher et al., 2017). Possibly, then, an adaptation involving emotional behaviors appropriate to the transition to early adult life affects learning mechanisms as a side effect. Moreover, slower encoding could have advantages in complex real world environments that contain multiple cues and choices, circumstances in which it is necessary to distinguish reliable signals from noise. If so, then adaptive pressures relating to typical mammalian sex differences in the variety and extent of social roles, including extremely complex care of altricial offspring, may have resulted in opposing late developmental adjustments to learning mechanisms.

Finally, evidence that hippocampal LTP threshold changes in opposite directions, between males and females, in the transition to post-pubertal life raise the question of whether there are similar effects in other brain regions. This issue has yet to be addressed but there is reason to expect the hippocampal changes influence broader network function. The hippocampus works in concert with parahippocampal and medial prefrontal cortex in encoding

spatial and episodic memory (Eichenbaum, 2017), and cooperativity with the latter is reportedly critical for realizing estrogen effects on encoding (Tuscher et al., 2019; Schwabe et al., 2020). This suggests that hippocampal changes described here likely influence functions of the larger hippocampal-prefrontal cortical system including behaviors ascribed to the cortical field.

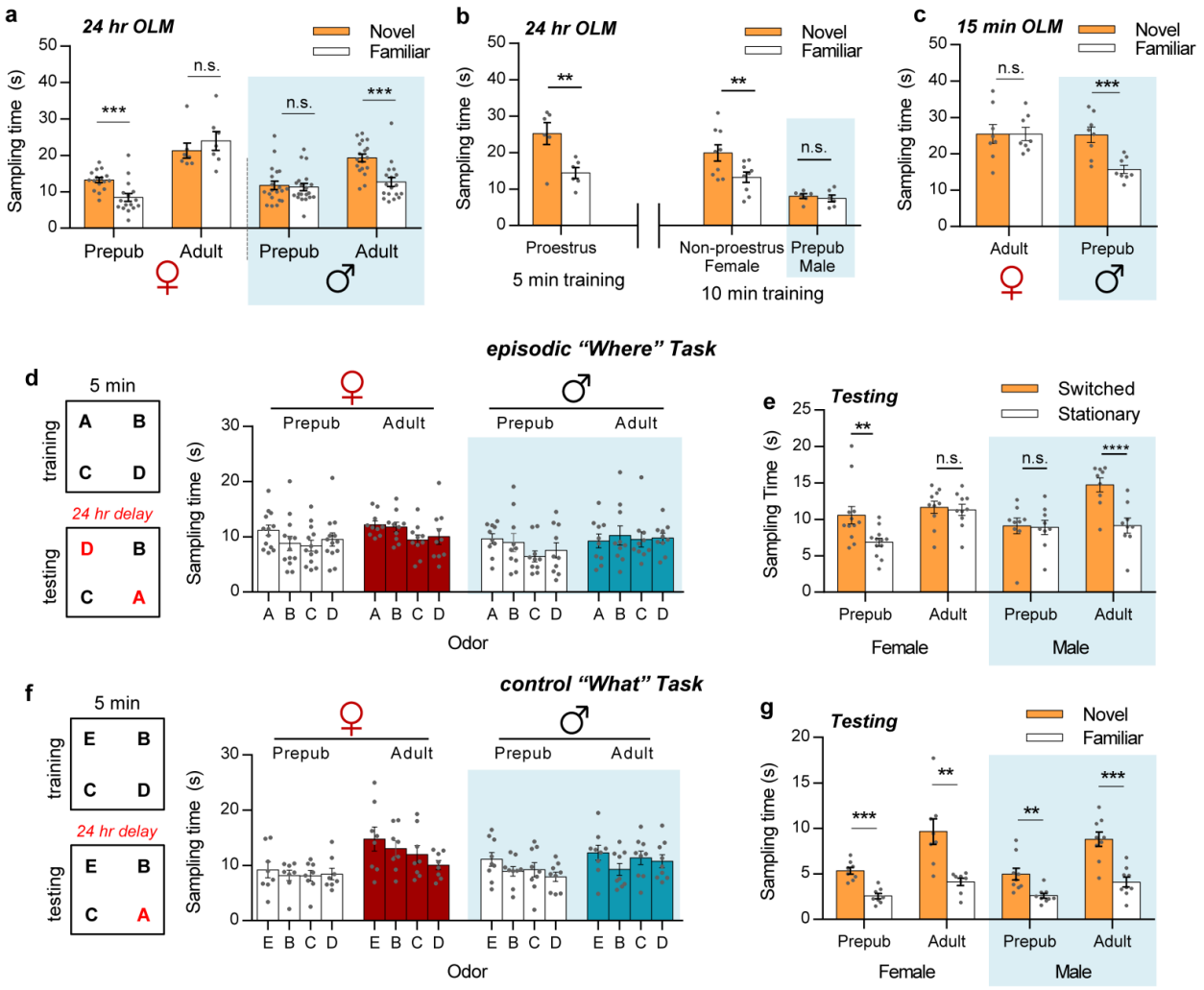


**Extended Data Figure 3.1. Sampling times for each cue in Object Location Memory, "Where", and "What" tasks across age and sex.** (**a**) Object location memory (OLM) (5-min training session, tested 24 hours later): Sampling times of displaced (Novel) vs the stationary (Familiar) objects were compared for male and female mice of prepubescent (Prepub) and adult ages. Prepubescent females and adult males preferentially sampled the displaced object (***$p$=0.0001, ***$p$=0.0006, respectively; 2-tailed paired t-test), whereas non-proestrus adult females and prepubescent males did not (n.s. $p$=0.21, $p$=0.73, respectively; N=7-18/group). (**b**) OLM (5- or 10-min training, tested 24-hours later): Adult females trained for 5 minutes during proestrus stage preferentially sampled the displaced object over the stationary object (**$p$=0.004). Non-proestrus adult females and prepubescent males were trained for 10 minutes. Non-proestrus females preferred the displaced object (**$p$=0.01), but the prepubescent males did not (n.s. $p$=0.46; N=6-9/group). (**c**) OLM (5-min training, 15-min delay): Adult females did not spend more time with the moved object ($p$=0.99), whereas Prepub males preferred the moved object (***$p$=0.0002; N=8/group). (**d**) *Left.* Schematic for episodic "Where" task with four odors (see Methods). *Right*. Sampling times of odors A-D for each group during the 5-minute training trial (One-way ANOVA: P>0.05 within all age groups). (**e**) Sampling times for the "switched" pair (Novel) vs the stationary pair. Prepubescent females and adult males sampled the "switched"

pair more than the stationary pair (2-tailed paired t-test: Prepub female **$p$=0.008, Adult male ****$p$=0.00004). Prepubescent male and adult females showed no preference ($p$=0.65, $p$=0.97, respectfully; N=8-11). **(f)** *Left*. Schematic of the "What" task (see Methods). *Right*: Sampling times for each odor (One-way ANOVA: P>0.05 within all age groups; N=8-9/group). (**g**) Sampling times for novel odor vs mean of the three familiar odors (2-tailed paired t-test: ***$p$<0.001, **$p$<0.01; N=8-9/group). Data are represented as mean±SEM.

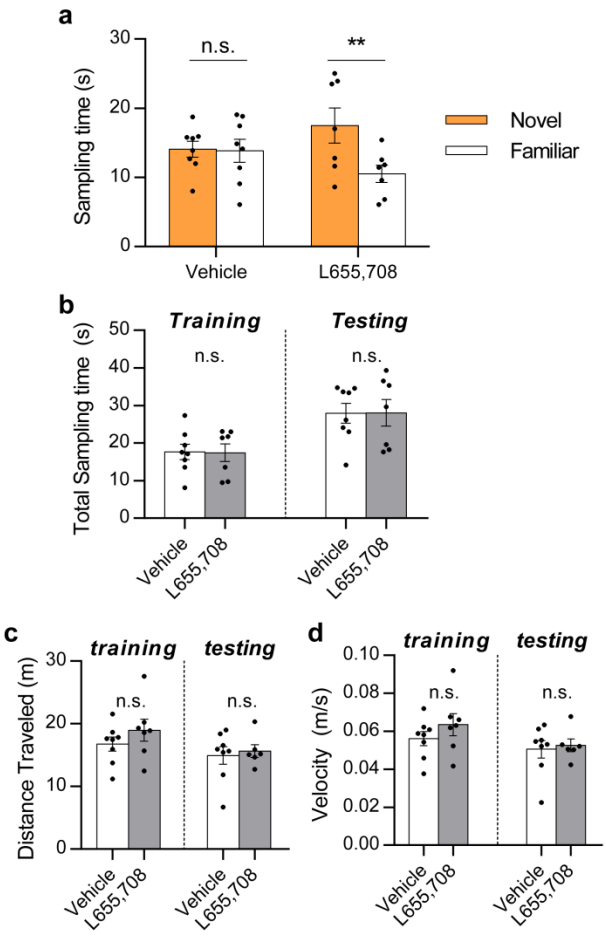


**Extended Data Figure 3.2. Exploration data for 24-hour delay Object Location Memory in adult, non-proestrus female mice given L655,708.** (**a**) Sampling times for displaced (Novel) vs stationary (Familiar) for Vehicle (2-tailed paired t-test: n.s. $p$=0.85) and L655,708 (**$p$=0.009). (**b**) Total sampling times for training and testing were comparable for treated vs. vehicle groups (2-tailed unpaired t-test: n.s. training $p$=0.95, testing $p$=0.98). (**c**) Distance traveled was comparable (2-tailed unpaired t-test: training $p$=0.29, testing $p$=0.71) and (**d**) velocity was similar between treatments (training $p$=0.30, testing $p$=0.73). For all panels, Vehicle N=8, L655,708 N=7. Data presented as mean±SEM.

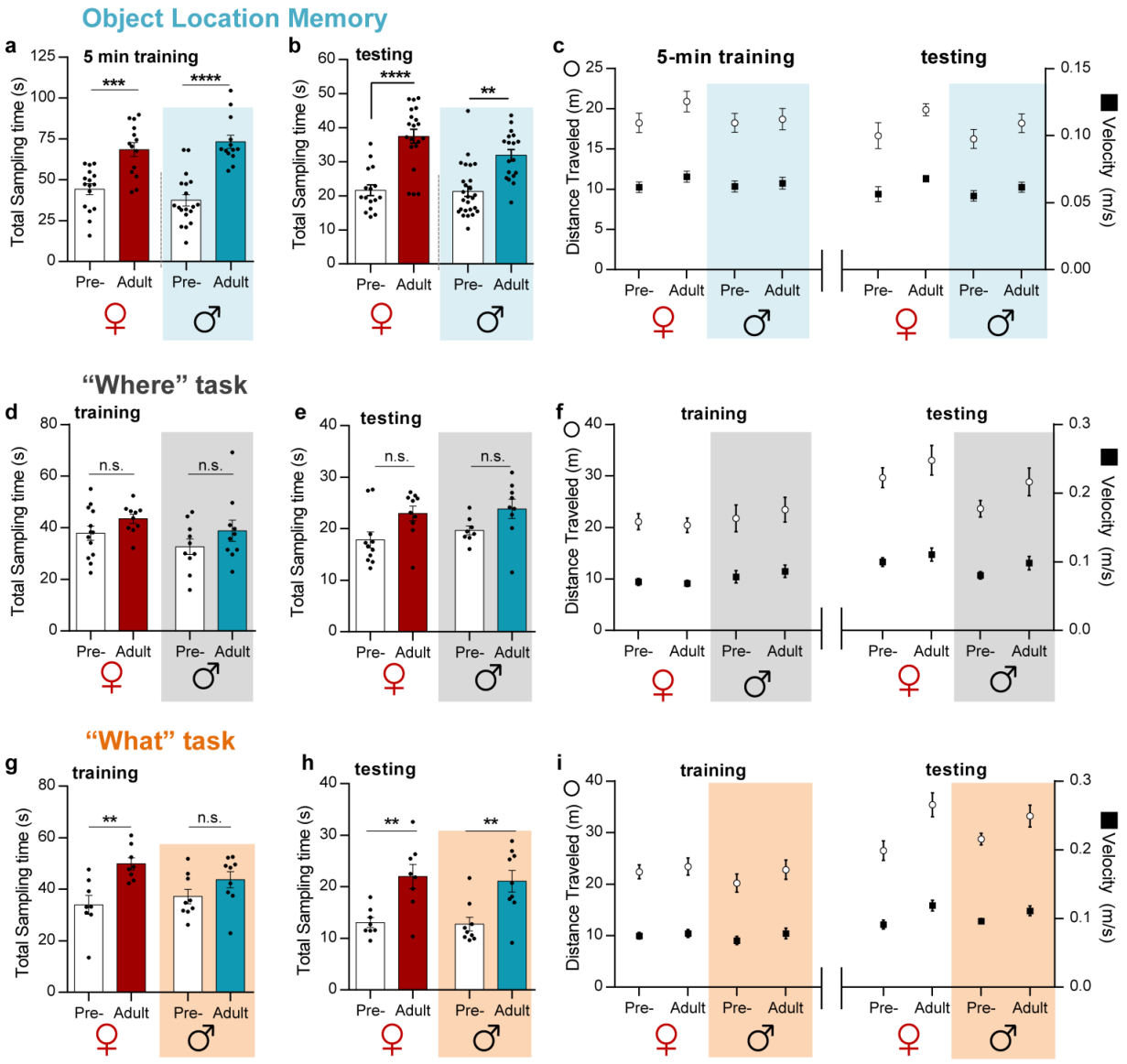


**Supplemental Figure 3.1. Total sampling time during training and testing sessions and locomotor activity for OLM, "Where", and "What" task.** (**a**) Prepubescent (Pre-) mice of both sexes explored significantly less compared to the adult mice when sampling both cues during the OLM 5-minute training (2-way ANOVA (Age effect): $F_{1,58}$= 63.03, $p$=7.75x10$^{-11}$; Tukey post-hoc: *** $p$=0.0002, ****$p$<0.0001) and (**b**) testing trial ($F_{1,62}$=46.51, $p$=4.4x10$^{-9}$, post-hoc: **$p$=0.0012, **** $p$<0.0001). (**c**) Distance traveled (open circles) during training (Interaction: $F_{1,98}$=0.61, $p$=0.44) and testing ($F_{1,98}$=0.26, $p$=0.61). Velocity (closed squares) during training ($F_{1,98}$=0.22, $p$=0.64) and testing ($F_{1,98}$=0.27, $p$=0.61). (**d**) Time spent sampling all four odors in the 'Where' paradigm during training session (Age effect: $F_{1,34}$=4.52, $p$=0.04; post-hoc n.s. P>0.05) and (**e**) testing session ($F_{1,34}$=9.40 $p$=0.0042; post-hoc n.s. P>0.05). (**f**) Distance traveled and velocity (Interaction: P>0.05) during training. Distance traveled and velocity during testing (Interaction: P>0.05). (**g**) Time spent sampling all odors during the "What" training

session (Age effect: $F_{1,30}$=13.72, $p$=0.0009, post hoc: **$p$<0.01, n.s. P>0.05) and (**h**) the testing session (Age effect: $F_{1,30}$=23.49, $p$=3.59x$10^{-5}$, post-hoc: **$p$<0.01). (**i**) Distance traveled during training and testing (Interaction: P>0.05). Velocity during training and testing (Interaction: P>0.05). For panels (**a, b**), proestrus and non-proestrus females were pooled due to similar sampling times (a; $p$=0.34 and b; $p$=0.38, 2-tailed unpaired t-test). Data are represented as mean±SEM.

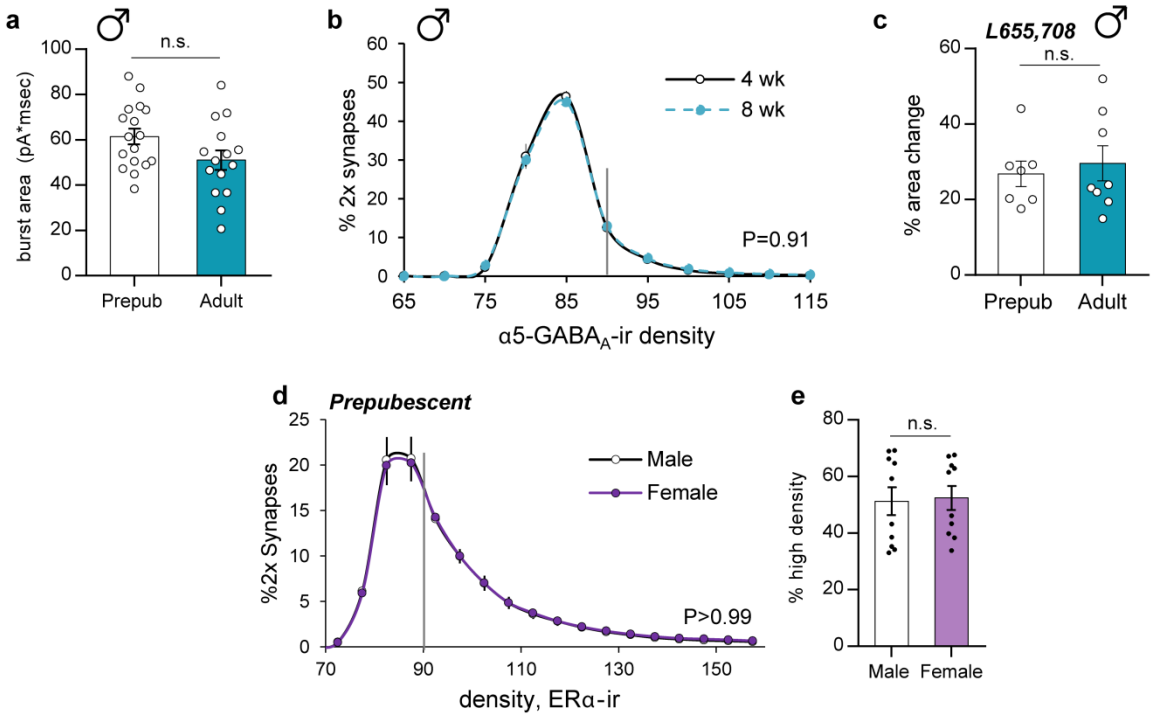


**Supplemental Figure 3.2. GABAergic-related numbers and functions are comparable in prepubescent vs adult males, and prepubescent male and female have similar ERα-ir density distributions.** (**a**) Burst area normalized to initial amplitude response in male prepubescent (N=17) vs adult (N=15) rats in voltage-clamp ($p$=0.068). (**b**) Frequency distribution of the GABA$_A$-α5-immunoreactivity (-ir) colocalized with gephyrin comparing prepubescent (N=8) and adult male rats (N=7) ($F_{10,130}$=0.46, $p$=0.91). (**c**) L655,708 infusion to prepubescent (N=7) and adult male (N=8) mouse slices ($p$=0.65). (**d**) Histogram of ERα-ir comparing male vs female prepubescents (N=10/group; $F_{19,342}$=0.041, P>0.99). (**e**) Bar graph of high density bins (>90) from panel d ($p$=0.86). Statistics performed were 2-tailed unpaired t-test panels (**a,c,e**) and panels (**b,d**) were analyzed using 2-way RM-ANOVA (Interaction). Data shown are mean±SEM.

**References**


Alger BE, Nicoll RA (1982) Feed-forward dendritic inhibition in rat hippocampal pyramidal cells studied in vitro. J Physiol 328:105-123.

Altemus M, Sarvaiya N, Neill Epperson C (2014) Sex differences in anxiety and depression clinical perspectives. Front Neuroendocrinol 35:320-330.

Andreano JM, Cahill L (2009) Sex influences on the neurobiology of learning and memory. Learn Mem 16:248-266.

Asher M, Asnaani A, Aderka IM (2017) Gender differences in social anxiety disorder: A review. Clin Psychol Rev 56:1-12.

Babayan AH, Kramár EA, Barrett RM, Jafari M, Häettig J, Chen LY, Rex CS, Lauterborn JC, Wood MA, Gall CM, Lynch G (2012) Integrin dynamics produce a delayed stage of long-term potentiation and memory consolidation. J Neurosci 32:12854-12861.

Barrett RM, Malvaez M, Kramar E, Matheos DP, Arrizon A, Cabrera SM, Lynch G, Greene RW, Wood MA (2011) Hippocampal focal knockout of CBP affects specific histone modifications, long-term potentiation, and long-term memory. Neuropsychopharmacology 36:1545-1556.

Baudry M, Arst D, Oliver M, Lynch G (1981) Development of glutamate binding sites and their regulation by calcium in rat hippocampus. Brain Res 227:37-48.

Bell MR (2018) Comparing Postnatal Development of Gonadal Hormones and Associated Social Behaviors in Rats, Mice, and Humans. Endocrinology 159:2596-2613.

Ben-Ari Y, Krnjević K, Reiffenstein RJ, Reinhardt W (1981) Inhibitory conductance changes and action of gamma-aminobutyrate in rat hippocampus. Neuroscience 6:2445-2463.

Bocchi A, Palmiero M, Redondo JMC, Tascón L, Nori R, Piccardi L (2021) The Role of Gender and Familiarity in a Modified Version of the Almeria Boxes Room Spatial Task. Brain Sci 11.

Boulware MI, Heisler JD, Frick KM (2013) The memory-enhancing effects of hippocampal estrogen receptor activation involve metabotropic glutamate receptor signaling. J Neurosci 33:15184-15194.

Caligioni CS (2009) Assessing reproductive status/stages in mice. Curr Protoc Neurosci Appendix 4:Appendix 4I.

Clayton T, Poe MM, Rallapalli S, Biawat P, Savić MM, Rowlett JK, Gallos G, Emala CW, Kaczorowski CC, Stafford DC, Arnold LA, Cook JM (2015) A Review of the Updated Pharmacophore for the Alpha 5 GABA(A) Benzodiazepine Receptor Model. Int J Med Chem 2015:430248.

Collinson N, Kuenzi FM, Jarolimek W, Maubach KA, Cothliff R, Sur C, Smith A, Otu FM, Howell O, Atack JR, McKernan RM, Seabrook GR, Dawson GR, Whiting PJ, Rosahl TW (2002) Enhanced learning and memory and altered GABAergic synaptic transmission in mice lacking the alpha 5 subunit of the GABAA receptor. J Neurosci 22:5572-5580.

Cora MC, Kooistra L, Travlos G (2015) Vaginal Cytology of the Laboratory Rat and Mouse: Review and Criteria for the Staging of the Estrous Cycle Using Stained Vaginal Smears. Toxicol Pathol 43:776-793.

Costello EJ, Copeland W, Angold A (2011) Trends in psychopathology across the adolescent years: what changes when children become adolescents, and when adolescents become adults? J Child Psychol Psychiatry 52:1015-1025.

Cox BM, Cox CD, Gunn BG, Le AA, Inshishian VC, Gall CM, Lynch G (2019) Acquisition of temporal order requires an intact CA3 commissural/associational (C/A) feedback system in mice. Commun Biol 2:251.

Davies CH, Starkey SJ, Pozza MF, Collingridge GL (1991) GABA autoreceptors regulate the induction of LTP. Nature 349:609-611.

Dore K, Aow J, Malinow R (2016) The Emergence of NMDA Receptor Metabotropic Function: Insights from Imaging. Front Synaptic Neurosci 8:20.
Eichenbaum H (2017) Prefrontal-hippocampal interactions in episodic memory. Nat Rev Neurosci 18:547-558.
Figurov A, Pozzo-Miller LD, Olafsson P, Wang T, Lu B (1996) Regulation of synaptic responses to high-frequency stimulation and LTP by neurotrophins in the hippocampus. Nature 381:706-709.
Franco-Enzástiga Ú, García G, Murbartián J, González-Barrios R, Salinas-Abarca AB, Sánchez-Hernández B, Tavares-Ferreira D, Herrera LA, Barragán-Iglesias P, Delgado-Lezama R, Price TJ, Granados-Soto V (2020) Sex-dependent pronociceptive role of spinal α. J Neurochem.
Herbison AE, Fénelon VS (1995) Estrogen regulation of GABAA receptor subunit mRNA expression in preoptic area and bed nucleus of the stria terminalis of female rat brain. J Neurosci 15:2328-2337.
Hojo Y, Hattori TA, Enami T, Furukawa A, Suzuki K, Ishii HT, Mukai H, Morrison JH, Janssen WG, Kominami S, Harada N, Kimoto T, Kawato S (2004) Adult male rat hippocampus synthesizes estradiol from pregnenolone by cytochromes P45017alpha and P450 aromatase localized in neurons. Proc Natl Acad Sci U S A 101:865-870.
Inagaki T, Gautreaux C, Luine V (2010) Acute estrogen treatment facilitates recognition memory consolidation and alters monoamine levels in memory-related brain areas. Horm Behav 58:415-426.
Jones CM, Braithwaite VA, Healy SD (2003) The evolution of sex differences in spatial ability. Behav Neurosci 117:403-411.
Juraska JM, Willing J (2017) Pubertal onset as a critical transition for neural development and cognition. Brain Res 1654:87-94.
Kato A, Hojo Y, Higo S, Komatsuzaki Y, Murakami G, Yoshino H, Uebayashi M, Kawato S (2013) Female hippocampal estrogens have a significant correlation with cyclic fluctuation of hippocampal spines. Front Neural Circuits 7:149.
Kight KE, McCarthy MM (2020) Androgens and the developing hippocampus. Biol Sex Differ 11:30.
Koss WA, Frick KM (2017) Sex differences in hippocampal function. J Neurosci Res 95:539-562.
Larson J, Lynch G (1986) Induction of synaptic potentiation in hippocampus by patterned stimulation involves two events. Science 232:985-988.
Larson J, Lynch G (1988) Role of N-methyl-D-aspartate receptors in the induction of synaptic potentiation by burst stimulation patterned after the hippocampal theta-rhythm. Brain Res 441:111-118.
Larson J, Munkácsy E (2015) Theta-burst LTP. Brain Res 1621:38-50.
Magnin E, Francavilla R, Amalyan S, Gervais E, David LS, Luo X, Topolnik L (2019) Input-Specific Synaptic Location and Function of the α5 GABA. J Neurosci 39:788-801.
Monaghan MM, Trimmer JS, Rhodes KJ (2001) Experimental localization of Kv1 family voltage-gated K+ channel alpha and beta subunits in rat hippocampal formation. J Neurosci 21:5973-5983.
Morgan PJ, Bourboulou R, Filippi C, Koenig-Gambini J, Epsztein J (2019) Kv1.1 contributes to a rapid homeostatic plasticity of intrinsic excitability in CA1 pyramidal neurons in vivo. Elife 8.
Mott DD, Lewis DV (1991) Facilitation of the induction of long-term potentiation by GABAB receptors. Science 252:1718-1720.
Mukai H, Kimoto T, Hojo Y, Kawato S, Murakami G, Higo S, Hatanaka Y, Ogiue-Ikeda M (2010) Modulation of synaptic plasticity by brain estrogen in the hippocampus. Biochim Biophys Acta 1800:1030-1044.

Mukherjee J, Cardarelli RA, Cantaut-Belarif Y, Deeb TZ, Srivastava DP, Tyagarajan SK, Pangalos MN, Triller A, Maguire J, Brandon NJ, Moss SJ (2017) Estradiol modulates the efficacy of synaptic inhibition by decreasing the dwell time of GABA. Proc Natl Acad Sci U S A 114:11763-11768.
Muller D, Oliver M, Lynch G (1989) Developmental changes in synaptic properties in hippocampus of neonatal rats. Brain Res Dev Brain Res 49:105-114.
Nabavi S, Kessels HW, Alfonso S, Aow J, Fox R, Malinow R (2013) Metabotropic NMDA receptor function is required for NMDA receptor-dependent long-term depression. Proc Natl Acad Sci U S A 110:4027-4032.
Navarro JF, Burón E, Martín-López M (2002) Anxiogenic-like activity of L-655,708, a selective ligand for the benzodiazepine site of GABA(A) receptors which contain the alpha-5 subunit, in the elevated plus-maze test. Prog Neuropsychopharmacol Biol Psychiatry 26:1389-1392.
Ooishi Y, Kawato S, Hojo Y, Hatanaka Y, Higo S, Murakami G, Komatsuzaki Y, Ogiue-Ikeda M, Kimoto T, Mukai H (2012) Modulation of synaptic plasticity in the hippocampus by hippocampus-derived estrogen and androgen. J Steroid Biochem Mol Biol 131:37-51.
Pacelli GJ, Su W, Kelso SR (1989) Activity-induced depression of synaptic inhibition during LTP-inducing patterned stimulation. Brain Res 486:26-32.
Pacelli GJ, Su W, Kelso SR (1991) Activity-induced decrease in early and late inhibitory synaptic conductances in hippocampus. Synapse 7:1-13.
Pattwell SS, Lee FS, Casey BJ (2013) Fear learning and memory across adolescent development: Hormones and Behavior Special Issue: Puberty and Adolescence. Horm Behav 64:380-389.
Rex CS, Chen LY, Sharma A, Liu J, Babayan AH, Gall CM, Lynch G (2009) Different Rho GTPase-dependent signaling pathways initiate sequential steps in the consolidation of long-term potentiation. J Cell Biol 186:85-97.
Romeo RD (2003) Puberty: a period of both organizational and activational effects of steroid hormones on neurobehavioural development. J Neuroendocrinol 15:1185-1192.
Schulz JM, Knoflach F, Hernandez MC, Bischofberger J (2018) Dendrite-targeting interneurons control synaptic NMDA-receptor activation via nonlinear α5-GABA. Nat Commun 9:3576.
Schwabe MR, Taxier LR, Frick KM (2020) It takes a neural village: Circuit-based approaches for estrogenic regulation of episodic memory. Front Neuroendocrinol 59:100860.
Seese RR, Wang K, Yao YQ, Lynch G, Gall CM (2014) Spaced training rescues memory and ERK1/2 signaling in fragile X syndrome model mice. Proc Natl Acad Sci U S A 111:16907-16912.
Seese RR, Chen LY, Cox CD, Schulz D, Babayan AH, Bunney WE, Henn FA, Gall CM, Lynch G (2013) Synaptic abnormalities in the infralimbic cortex of a model of congenital depression. J Neurosci 33:13441-13448.
Seurinck R, Vingerhoets G, de Lange FP, Achten E (2004) Does egocentric mental rotation elicit sex differences? Neuroimage 23:1440-1449.
Shen H, Sabaliauskas N, Sherpa A, Fenton AA, Stelzer A, Aoki C, Smith SS (2010) A critical role for alpha4betadelta GABAA receptors in shaping learning deficits at puberty in mice. Science 327:1515-1518.
Shepard R, Heslin K, Hagerdorn P, Coutellier L (2019) Downregulation of Npas4 in parvalbumin interneurons and cognitive deficits after neonatal NMDA receptor blockade: relevance for schizophrenia. Transl Psychiatry 9:99.
Sieghart W, Sperk G (2002) Subunit composition, distribution and function of GABA(A) receptor subtypes. Curr Top Med Chem 2:795-816.
Sigel E, Steinmann ME (2012) Structure, function, and modulation of GABA(A) receptors. J Biol Chem 287:40224-40231.

Sim S, Antolin S, Lin CW, Lin Y, Lin YX, Lois C (2013) Increased cell-intrinsic excitability induces synaptic changes in new neurons in the adult dentate gyrus that require Npas4. J Neurosci 33:7928-7940.
Sisk CL, Zehr JL (2005) Pubertal hormones organize the adolescent brain and behavior. Front Neuroendocrinol 26:163-174.
Smith SS (2013) The influence of stress at puberty on mood and learning: role of the α4βδ GABAA receptor. Neuroscience 249:192-213.
Spiegel I, Mardinly AR, Gabel HW, Bazinet JE, Couch CH, Tzeng CP, Harmin DA, Greenberg ME (2014) Npas4 regulates excitatory-inhibitory balance within neural circuits through cell-type-specific gene programs. Cell 157:1216-1229.
Sur C, Quirk K, Dewar D, Atack J, McKernan R (1998) Rat and human hippocampal alpha5 subunit-containing gamma-aminobutyric AcidA receptors have alpha5 beta3 gamma2 pharmacological characteristics. Mol Pharmacol 54:928-933.
Tabatadze N, Sato SM, Woolley CS (2014) Quantitative analysis of long-form aromatase mRNA in the male and female rat brain. PLoS One 9:e100628.
Tascón L, Di Cicco C, Piccardi L, Palmiero M, Bocchi A, Cimadevilla JM (2021) Sex Differences in Spatial Memory: Comparison of Three Tasks Using the Same Virtual Context. Brain Sci 11.
Tuscher JJ, Taxier LR, Schalk JC, Haertel JM, Frick KM (2019) Chemogenetic Suppression of Medial Prefrontal-Dorsal Hippocampal Interactions Prevents Estrogenic Enhancement of Memory Consolidation in Female Mice. eNeuro 6.
Vastagh C, Rodolosse A, Solymosi N, Liposits Z (2016) Altered Expression of Genes Encoding Neurotransmitter Receptors in GnRH Neurons of Proestrous Mice. Front Cell Neurosci 10:230.
Vierk R, Glassmeier G, Zhou L, Brandt N, Fester L, Dudzinski D, Wilkars W, Bender RA, Lewerenz M, Gloger S, Graser L, Schwarz J, Rune GM (2012) Aromatase inhibition abolishes LTP generation in female but not in male mice. J Neurosci 32:8116-8126.
Voyer D, Voyer S, Bryden MP (1995) Magnitude of sex differences in spatial abilities: a meta-analysis and consideration of critical variables. Psychol Bull 117:250-270.
Voyer D, Voyer SD, Saint-Aubin J (2017) Sex differences in visual-spatial working memory: A meta-analysis. Psychon Bull Rev 24:307-334.
Wainwright A, Sirinathsinghji DJ, Oliver KR (2000) Expression of GABA(A) receptor alpha5 subunit-like immunoreactivity in human hippocampus. Brain Res Mol Brain Res 80:228-232.
Wang W, Le AA, Hou B, Lauterborn JC, Cox CD, Levin ER, Lynch G, Gall CM (2018) Memory-Related Synaptic Plasticity Is Sexually Dimorphic in Rodent Hippocampus. J Neurosci 38:7935-7951.
Weiland NG, Orchinik M (1995) Specific subunit mRNAs of the GABAA receptor are regulated by progesterone in subfields of the hippocampus. Brain Res Mol Brain Res 32:271-278.
Yagi S, Galea LAM (2019) Sex differences in hippocampal cognition and neurogenesis. Neuropsychopharmacology 44:200-213.

# CHAPTER FOUR: Sex Differences in NMDAR Signaling Are Reflected in Episodic Memory

**Abstract**

NMDARs are generally viewed as coincidence detectors with their contributions to synaptic plasticity being gated by voltage-dependent ion channel properties. We show here that blocking the NMDAR channel with MK801 prevents induction of CA3-CA1 long-term potentiation (LTP) in adult male rodents but leaves intact complex postsynaptic events (signaling, actin polymerization) that stabilize the potentiated state. However, F-actin assembly and LTP were both disrupted by a compound (Ro25-6981) that blocks the NMDAR GluN2B subunit and thereby suppresses non-ionic (metabotropic) NMDAR signaling. MK801 also produced the peculiar 'consolidation without LTP expression' condition in females but, in contrast to males, Ro25-6981 did not attenuate actin polymerization or LTP. Rather, an antagonist of estrogen receptor alpha suppressed the LTP consolidation machinery in females. We evaluated the functional significance of these sex differences in LTP substrates using tests for distinct elements of episodic memory. Females were superior in encoding cue identity and temporal order whereas males excelled in the spatial task. In accord with LTP results, Ro25-6981 interfered with acquisition in males only. We conclude that properties of an everyday, cognition critical form of memory are linked to the type of metabotropic signaling used to stabilize synaptic modifications.

## Introduction

NMDARs are unusual in that opening of their channel requires both ligand binding and prolonged depolarization. These arrangements result in a type of 'coincidence detector' (Seeburg et al., 1995; Dore et al., 2017) that is engaged by co-occurrence of presynaptic (release) and post-synaptic (depolarization) events. This discovery was of great interest because theorists had independently proposed the enormously influential idea that synchronized activity by inputs and target cells strengthens the contacts between them while uncoordinated firing reduces synaptic strength (Hebb, 1949; Lisman, 1989; Lisman et al., 2011; Markram et al., 2011; Baldi and Vershynin, 2021). NMDARs fit naturally into this argument because of their critical contributions to memory related synaptic plasticity. They accomplish this by gating calcium into spines, an event that is essential for shifting synapses into their potentiated state (Lynch et al., 1983; Paoletti et al., 2013; Volianskis et al., 2013; Park et al., 2014; Shipton and Paulsen, 2014). However, an increasing body of work indicates that NMDARs also signal in a metabotropic (non-ionic) manner (Nabavi et al., 2013; Gray et al., 2016; Dore et al., 2017; Stein et al., 2021).

Initial evidence for non-ionic signaling came from reports showing that in rodents use-dependent dephosphorylation (Vissel et al., 2001) and internalization of the NMDARs occurs in the absence of channel opening (Nong et al., 2003). Work by Malinow and colleagues (Nabavi et al., 2013; Nabavi et al., 2014; Dore et al., 2015) described multiple instances of NMDAR-driven effects that occur in the presence of the channel blocker MK801. There is now a rich literature describing metabotropic (m) NMDAR functions (Park et al., 2022) including mediating in excitotoxic damage (Weilinger et al., 2016) and glutamate uncaging-induced changes in spine size (Stein et al., 2020; Stein et al., 2021), with several studies implicating the GluN2B (NR2B) subunit in these processes (Papouin et al., 2012; Kessels et al., 2013; Ferreira et al., 2017). However, efforts to connect mNMDAR actions to long-term potentiation (LTP) or long-term

depression have produced inconsistent results (Nabavi et al., 2014; Gray et al., 2016; Park et al., 2022). Also lacking are data showing that brief, learning-related patterns of afferent activity actually trigger mNMDAR signaling at synapses. In all, while it is clear that calcium flux is required for the production of LTP and related learning, there remains the possibility that non-ionic signaling by the NMDARs also plays an essential but unspecified role.

Much less is known about the occurrence of mNMDAR signaling in females than males, an oversight that is of particular interest because of recent reports documenting surprisingly large sex differences in LTP substrates. While female potentiation is dependent on NMDARs, it also requires locally produced estrogen in rats and mice (Huang and Woolley, 2012; Vierk et al., 2012; Bender et al., 2017; Wang et al., 2018a), acting on synaptic estrogen receptors to trigger the complex events leading to LTP consolidation (Kramár et al., 2009). This mechanism appears to be entirely absent in males (Wang et al., 2018a) and it is thus possible that sexes employ different forms of metabotropic signaling – estrogen receptor- vs. NMDAR-mediated – to engage the elaborate downstream signaling needed to stabilize potentiation.

Likely related to the above, the threshold for LTP induction is significantly higher in females than males (Wang et al., 2018a; Le et al., 2022), a difference that emerges late in postnatal development (Le et al., 2022). This can reasonably be assumed to lead to important sex differences in hippocampus-dependent forms of memory encoding and results support of this. Specifically, and as might be expected from the results for LTP thresholds, males outperform females on learning spatial locations (Koss and Frick, 2017; Le et al., 2022). There is evidence for this effect in humans but women are usually reported to be superior in verbal learning and related elements of episodic memory (Andreano and Cahill, 2009; Koss and Frick, 2017) a form of encoding that depends on the hippocampus (Westmacott et al., 2001; Noulhiane et al., 2007; Dede et al., 2016). Surprisingly, corresponding tests for female advantages in episodic learning by rodents are lacking (Koss and Frick, 2017).

The present studies addressed the question of if and how non-ionic NMDAR functions are involved in the production of male LTP. The results prompted us to test the idea that male and female rats use different forms of metabotropic signaling to produce stable modifications to excitatory synapses. Finally, we investigated the possibility that sex differences in LTP mechanisms are reflected in acquisition of spatial and nonspatial elements of episodic memory.

**Materials and Methods**

*Animals.* Experiments used 2-4 month old Sprague Dawley rats (Charles River) and 2-4 month old sighted-FVB129 mice of both sexes. Animals were group-housed (2-4/cage for rat; 3-5/cage for mice) in rooms (68°F and 55% humidity) with 12-hr light/dark cycle with lights on at 6:30AM, and food/water *ad libitum*. Experiments were conducted in accordance with the National Institutes of Health Guide for the Care and Use for Laboratory Animals and protocols approved by the Institutional Animal Care and Use Committee at the University of California, Irvine. Females were estrous staged via vaginal lavage (Cora et al., 2015) prior to experimentation. For LTP, behavioral, and phalloidin measures, females staged outside of proestrus (estrus /diestrus) were used and pooled together for analyses. For NMDAR subunit comparisons, analyses were exclusively performed in diestrus-females. For all electrophysiology and imaging experiments, each N represents a slice from at least 3 animals per group.

*Field Electrophysiology.* Rat hippocampal slices were prepared using a McIllwain chopper (transverse; 370 µm) and then immediately transferred to an interface recording chamber with oxygenated artificial cerebrospinal fluid perfusion (aCSF; 60-70 mL/hr, 31±1°C, 95% $O_2$/5% $CO_2$) which included (in mM): 124 NaCl, 26 $NaHCO_3$, 3 KCl, 1.25 $KH_2PO_4$, 2.5 $CaCl_2$, 1.5 $MgSO_4$, and 10 dextrose (pH 7.4). Experiments were initiated 2 hours after sacrifice. Field excitatory postsynaptic potentials (fEPSPs) were elicited using a twisted nichrome wire stimulating electrode placed in CA1a or c stratum radiatum (SR) and recording with a glass

pipette electrode filled with 2M NaCl, R=2-3MΩ) placed in CA1b SR. Single-pulse baseline stimulation was applied with fEPSP amplitude at approximately 40-50% of maximum population-spike free amplitude. Responses were digitized at 20kHz using an AC amplifier (A-M Systems, Model 1700) and recorded using NAC2.0 Neurodata Acquisition System (Theta Burst Corporation). For LTP studies, potentiation was induced by applying 10 theta bursts (TBS: four pulses at 100Hz, 200 ms between bursts). For LTP-threshold levels of TBS, theta burst triplets were applied four times at 90 sec intervals (Wang et al., 2018a; Le et al., 2022). For drug studies, all compounds were in the bath 1-3 hr prior to TBS.

*Whole-Cell Voltage Current-Clamp Recording.* Horizontal hippocampal slices (350μm) from 8-week old male mice were prepared using a Leica vibrating tissue slicer (Model: VT1000S). Slices were placed in a submerged recording chamber with constant oxygenated aCSF perfusion (2ml/min) at 32°C. Whole-cell recordings (Axopatch 200A amplifier, Molecular Devices) used 4–7 MΩ glass pipettes filled with (in mM): 140 $CsMeSO_3$, 8 CsCl, 10 HEPES, 0.2 EGTA, 2 QX-314, 2 Mg-ATP, 0.3 Na-GTP. Bipolar stimulating electrodes were placed in the CA1 SR, 100-150 μm from the recorded cell. EPSCs were recorded with the holding potential at +40 mV for NMDAR amplitude (at 50ms from stimulation artifact) in the presence of 50 μM picrotoxin.

*Fluorescence Deconvolution Tomography (FDT).* For measures of basal synaptic protein levels, transverse hippocampal slices (370 μm) sectioned and promptly immersed in cold 4% paraformaldehyde (PFA) overnight. For LTP-related experiments, stimulating electrodes were placed on CA1a and CA1c SR, and recording electrode placed in CA1b, all equidistant from the cell layer. After a stable baseline (~5 min) was recorded, the slices were given a single train of 10 burst TBS for each polarity on each of the stimulating electrodes (pulses at 2x baseline duration). Slices were then harvested after a specified time post-TBS (3 min for pERK (Wang et al., 2018a), 7 min for pSrc (Chen et al., 2010a), and 15 min for pCAMKII (Cox et al., 2014)) and

fixed overnight in 4% PFA. All slices were cyro-protected with 20% sucrose in 0.1M phosphate buffer (PB), sub-sectioned on a sliding microtome (Leica) at 20 µm thickness, and 6-8 sections from the top of each slice (to encompass the depth of electrode placement) were slide-mounted. Tissue was processed for dual immunofluorescence with incubation in primary antisera (4°C, 18 hours) and secondary antisera (room temperature, 2 hours) in 0.1 M PB containing 0.3% Triton-X and 3% normal swine serum. After the PB washes, the slides were cover-slipped with VectaShield containing DAPI (Vector Labs).

The following primary antibodies (concentration; vendor, catalogue number, RRID) were used: goat anti-PSD95 (1:1500; Abcam, ab12093, AB_298846) with either rabbit anti-pCaMKII (Thr286/Thr287) (1:500; Upstate (now Millipore), 06-881, RRID:AB_310282) or rabbit anti-pERK1/2 (Thr202/Tyr204) (1:500; Cell Signaling 4377, AB_331775); Mouse anti-PSD95 (1:1000; Invitrogen, MA1-045, AB_325399) with rabbit anti-pSrc (Tyr419) (1:250; Invitrogen, 44-660G, AB_2533714); Rabbit anti-GluN1 (extracellular) (1:1000; Alamones Labs, AGC-001, AB_2040023), anti-GluN2A (1:500, Alamones Labs, AGC-002, AB_2040025), anti-GluN2B (1:500, Alamones Labs, AGC-003, AB_2040028), or anti-GluN2B Tyr1472 (1:300; PhosphoSolutions, P1516-1472, AB_2492182) with goat anti-PSD95 (1:1500, abcam ab12093; AB_298846). Secondary antibodies (all at 1:1000) included AlexaFluor donkey anti-goat 488 (Invitrogen, A32814, AB_2762838), donkey anti-rabbit 594 (A32754, Invitrogen, AB_2762827), donkey anti-mouse 594 (A21203, AB_141633), and donkey anti-rabbit 488 (A21206, AB_2535792).

FDT analyses were as described (Rex et al., 2009; Babayan et al., 2012; Seese et al., 2014; Wang et al., 2018a). Images were captured using an epifluorescence microscope (Leica DM6000) with a 63x PlanApo objective and CCD camera (ORCA-ER, Hamamatsu). Image z-stacks (136 x 105 x 2 µm, 200 nm steps) were collected from the CA1 SR from 6 or more sections per slice. All image stacks were processed for iterative deconvolution (99% confidence;

Volocity 4.0, PerkinElmer) and then 3-dimensional (3-D) montages of each z-stack was analyzed for synaptic labeling using in-house software (c99, Java (OpenJDK IcedTea 6.1.12.6), Matlab R2019b, PuTTY 0.74, and Perl 5.30.0). First, each image labeling was normalized and thresholded at a given intensity threshold, and erosion and dilation filtering was used to fill holes and remove background pixels to reliably detect edges of both faintly and densely labeled structures. Objects were then segmented based on connected pixels above a threshold across each channel separately. All immunofluorescent elements meeting size constraints of synapses and detected across multiple intensity thresholds were quantified by the system. PSD95-ir elements were considered double-labeled for the second antigen if there was contact or overlap in fields occupied by the two fluorophores as assessed in 3-D. Approximately 20-30 thousand synapses were thus analyzed per z-stack. Finally, based on the maximum intensity of each image, counts of double-labeled puncta were assigned to ascending density (fluorescence intensity) bins and then the data were expressed as frequency distributions. Labeled puncta that fell within bins for immunofluorescence density at ≥95 were considered to be densely labeled. Individual tissue section counts of densely labeled puncta were then averaged with those from other sections for that slice to generate the mean slice value presented.

*F-actin phalloidin immunolabelling.* Alexa Fluor 568-conjugated phalloidin (Invitrogen; A12380) was prepared by diluting the concentrate to 12 µM in water as stock and then to 6 µM in aCSF and 1% DMSO on the day of experimentation. Electrode placement and stimulation was that same as used for FDT analyses. Beginning 3 min post-stimulation, phalloidin (6 µM) was applied topically onto the slice (2 µl) and this was repeated three times at 3 min intervals (Lynch et al., 2007). Three minutes after the last application, the slices were placed in cold 4% PFA and fixed overnight. Slices were subsectioned and tissue was slide-mounted as for FDT; the slides were washed for 10 min in 0.1 M PB, air-dried, and cover-slipped with Vectashield using DAPI (Vector Labs).

Image z-stacks (136 x 105 x 3 µm, 200 nm steps) of phalloidin labeling were captured as for FDT. Because the labeling was in a single channel, images were not processed for deconvolution prior to analyses using the in-house software described above. To quantify spine phalloidin labeling, every image of each z-stack first received a small saturated 1x1 µm reference square to two corners of the image (Python 3.0). The global reference square was used to define a comparable maximum intensity level for all images without significantly altering the background or raw intensity values of each puncta; this step was added because the software assigns the final density values for phalloidin labeling based on the maximum intensity a given image. With the reference squares, the image z-stacks were processed for quantification as described for FDT. Labeled puncta that fell within the density bins of ≥90 were considered to have dense concentrations of F-actin. Counts of densely-labeled puncta were then averaged across tissue sections to generate a mean value per slice. Values from experimental groups were normalized to those of their respective control group.

*Serial 'What' task.* Mice were handled prior to the start of experimentation. Mice were first placed into a Plexiglas arena (30x25 cm floor, 21.5 cm height) containing two empty glass jars (5.25 cm diameter, 5 cm height) with a metal lid with a single hole (1.5 cm diameter) for 5 min. The cups were removed and the animals were allowed to explore the chamber undisturbed for 5 min. Afterwards, the animals were exposed a series of three 3-min trials, each involving exposure to a different identical odor pair including the following odorants dissolved in mineral oil (final concentration in 0.1 Pascals): (A) (+)-Limonene (≥97% purity, Sigma-Aldrich), (B) Cyclohexyl ethyl acetate (≥97%, International Flavors & Fragrances), (C) (+)-Citronellal (~96% Alfa Aesar). There was a 5-min delay between each odor pair. For the test trial, mice were given an odor pair including a familiar odor from the training series (A) and a novel odor (D) Octyl Aldehyde (~99%, Acros Organics). This task was counter-balanced by reversing the order of

cue presentation (D, C, B, A). For the version that tests across four odors in sequence (A, B, C, D), the test compared familiar odor (A) with novel odor (E) Anisole (~99%, Acros Organics).

*Serial 'When' task.* The task followed the same protocol the episodic 'What' task using 4 odor pairs in a sequence (A:A, B:B, C:C, D:D). However, at testing the first and second odors were presented (A vs. B; less vs. more recent). This was counter-balanced by reversing the order of initial odor exposure (testing: B vs. A; less vs. more recent).

*Simultaneous 'What' task.* Mice were allowed to explore the plexiglas arena (60 cm × 60 cm floor, 30-cm walls) containing four empty jars for 5 min. After a 3-min delay, they were allowed to explore the four jars containing odor A, B, C, and D for 5 min. These odors were previously confirmed to be equally salient in males and female mice (Le et al., 2022). They were returned to their home-cage for 48-hours. Mice were reintroduced to the chamber with three familiar (A, B, C) and one novel (E) odor and were allowed to explore the chamber for 5 min. For counterbalance, some mice were initially exposed to odors E, B, C, D, with the testing novel odor being A.

*'Where' task.* This paradigm used the same arena as that in the simultaneous 'what' task. Mice sampled the four empty jars for 5 min, and after a 3-min delay, mice were allowed to sample the four distinct odor jars for either 5 or 10 min. The jars were removed from the chamber and, 3 min later, the odors were reintroduced with the position of two odorant jars switched. The mice were then allowed to explore the chamber for 5 min. For counter-balancing, either odor pair A-D or B-C were switched.

*Behavioral scoring.* For all behavioral tasks, sessions were recorded with an overhead web camera and scored by an observer blind to group. Cue sampling time (t) was collected as the number of seconds the mouse's nose was actively pointed towards the odor hole (~0.5-cm radius). The calculation of the Discrimination Index (DI) across the tasks are as follows: 'Where'

DI = 100 x ($t_{sum\ of\ switched\ pair} - t_{sum\ of\ stationary\ pair}$)/($t_{total\ sampling}$); serial 'What' and 'When' DI = 100 × ($t_{novel} - t_{familiar}$)/($t_{total\ sampling}$); simultaneous 'What' DI = 100 × ($t_{novel} - t_{mean\ familiars}$)/($t_{total\ sampling}$). Z-score calculations were as follows: (mean $DI_{female}$ – mean $DI_{male}$)/(standard $deviation_{male}$).

*Drug Administration.* For electrophysiological recordings, compounds were infused into the aCSF infusion line with a syringe pump (6ml/hr) for the final bath concentrations: MK801 (30μM; Tocris, 0924), APV (100μM; Hello Bio, HB0225), DNQX (20μM, Hello Bio HB0261), picrotoxin (30μM, Sigma-Aldrich, P1675) in water. MPP (3μM; Tocris, 1991) and Ro25-6981 (3μM; Hello Bio, HB0554) were dissolved with DMSO (≤0.01%). For behavior, Ro25-6981 (5mg/kg, saline) was injected intraperitoneally 30 min prior to initial exposure to odors.

*Statistics.* All data are shown as mean ± standard error of the mean (s.e.m.). For electrophysiology, the magnitudes of LTP (averaged fEPSP slopes for last 5 min of recordings) and STP (averaged over 1 min immediately after TBS) were compared via two-tailed unpaired Student's t-test. Two-tailed unpaired Student's t-test were used for comparing significance between two groups, and one-way ANOVA (Interaction) with post-hoc Tukey test was used for comparisons of 3+ groups. TBS area analysis and STP (for threshold TBS) were analyzed with repeated-measures two-way ANOVA (Interaction). For behavioral studies, results were analyzed with either two-tailed unpaired t-test or two-way ANOVA (Interaction) with post-hoc Tukey test. Significance at $p<0.05$ was determined via GraphPad Prism (v6.0).

## Results

### Non-ionic NMDAR signaling activates LTP stabilization machinery in males.

*Blocking the NMDAR channel does not disrupt actin signaling*. We previously showed that the theta burst stimulation (TBS) commonly used to induce LTP in hippocampal CA3-CA1 (Schaffer-commissural; SC) projections causes a rapid and lasting, NMDAR-dependent increase in the density of phalloidin-labeled filamentous (F-) actin in dendritic spines (Lin et al., 2005; Kramár et al., 2006). Latrunculin, a toxin that prevents actin filament assembly, entirely eliminates this phalloidin effect along with LTP (Rex et al., 2009). While subsequent work described kinase signaling pathways that link synaptic responses to actin polymerization and stabilization (Kramár et al., 2006; Chen et al., 2007; Rex et al., 2009), we had not tested the general assumption that calcium influx through the NMDAR channel pore is necessary for the above cytoskeletal remodeling. We tested the point using MK801, which occludes the NMDAR channel and resulting calcium influx. Infusion of 30μM MK801 into hippocampal slices prepared from adult male rats produced a near complete suppression of both short-term potentiation (STP) and LTP (vehicle vs. MK801: STP: 224.3±14.6% vs. 143.6±16.0%, p=0.0043; LTP: 151.6±6.3% vs. 114.1±9.2%, p=0.005, two-tailed unpaired t-tests; **Fig. 4.1a**) without evidence for response depression. Next, we tested if these conditions affect TBS-induced actin polymerization. Two populations of CA3 efferents converging on the apical dendrites of CA1b pyramidal neurons were activated with (i) a train of 10 theta bursts with one of the inputs stimulated 30 sec after the other or (ii) with low frequency stimulation (LFS, control; 3/min) (**Fig. 4.1b**). Alexa Fluor 568-Phalloidin was then topically applied to the hippocampal slice [see Methods] and numbers of densely labeled spines in CA1 stratum radiatum (SR) counted (**Fig. 4.1c,d**). In accord with previous reports (Lin et al., 2005; Rex et al., 2007), TBS caused a marked increase in the numbers of spines containing dense concentrations of F-actin, an effect that was completely abolished by the competitive NMDAR antagonist APV (Rex et al., 2007).

Surprisingly, the MK801 dose that eliminated LTP failed to reduce the F-actin labeling generated by TBS (**Fig. 4.1d**), indicating that actin polymerization requires NMDARs but not calcium influx mediated by those receptors. These data constitute evidence that naturalistic patterns of afferent activity initiate non-ionic (metabotropic) NMDAR signaling in adult synapses and describe a surprising instance in which a critical LTP stabilization event (actin polymerization) occurs in the absence of synaptic potentiation. They also indicate that non-ionic NMDAR-mediated operations – i.e., those blocked by APV but not MK801 – are essential for LTP. These results accord with evidence that local glutamate uncaging-induced spine enlargement reflects non-ionic NMDAR functions (Stein et al., 2021) although uncaging in the absence of calcium influx led to spine shrinkage as typically associated with long term depression. We did not observe response depression in the absence of ionic NMDAR function.

To separate the relative contributions of ionic vs. metabotropic signaling streams, we tested the MK801 sensitivity of three NMDAR-regulated kinases that play important roles in the production of LTP. First, slices were harvested 3 min post-TBS and processed for immunolabeling of phosphorylated (p) ERK1/2 – a kinase involved in actin polymerization and stabilization (Tanimura and Takeda, 2017) and LTP induction (English and Sweatt, 1997; Cammarota et al., 2008) – co-localized with the postsynaptic marker PSD95. Fluorescence Deconvolution Tomography (FDT) was used to make 3-D reconstructions of individual elements that fell within the size constraints of synapses. The density of pERK Thr202/Tyr204-immunoreactivity (ir) at each double-labeled element was measured and the resultant value placed in one of an ascending series of labeling-density bins. This automated process was repeated for 150,000-250,000 synapses per hippocampal slice and the data are expressed as a density frequency distribution (% of the total population vs. density). Consistent with earlier studies (Wang et al., 2018a), TBS markedly skewed the frequency curve of vehicle treated-slices to the right towards greater labeling densities relative to that of control stimulation. MK801

treatment did not attenuate this effect, and the TBS+MK801 curve was nearly superimposed with that for TBS+vehicle (**Fig. 4.1e**). The percent of synapses with high-density pERK-ir, i.e., within greater labeling density bins, was nearly two-fold greater in the TBS vs. LFS (control) groups, and this effect was not attenuated by MK801 (**Fig. 4.1e** inset).

NMDARs are also known to engage Src family kinases, which both phosphorylate the NMDAR C-terminal domain (CTD) and activate TrkB and cortactin, two proteins centrally involved in actin filament assembly (Weaver et al., 2001; Singh and McNiven, 2008; Chen et al., 2010a). We confirmed earlier reports (Chen et al., 2010a; Wang et al., 2018a) that TBS elevates postsynaptic pSrc Tyr419 and the effect is blocked by APV (Chen et al., 2010a). TBS-induced increases in pSrc were not affected by MK801 (**Fig. 4.1f**). Thus, as was the case for ERK1/2, Src activation was not dependent on NMDAR-gated calcium influx.

Lastly, we assessed calcium-calmodulin dependent protein kinase II (CaMKII), an enzyme that is activated by calcium influx and widely held to be critical for the activity-driven transfer of AMPARs into the synapse for expression of LTP (Lisman et al., 2012). TBS increased the percentage of postsynaptic densities associated with dense concentrations of pCaMKII Thr286/Thr287 in vehicle-treated cases but not in slices treated with MK801 (**Fig. 4.1g**).

Taken together, the MK801 results strongly suggest that ionic operations of the NMDARs are required for shifting synapses into the potentiated state but not for signaling activities and actin remodeling critical for LTP-stabilization.

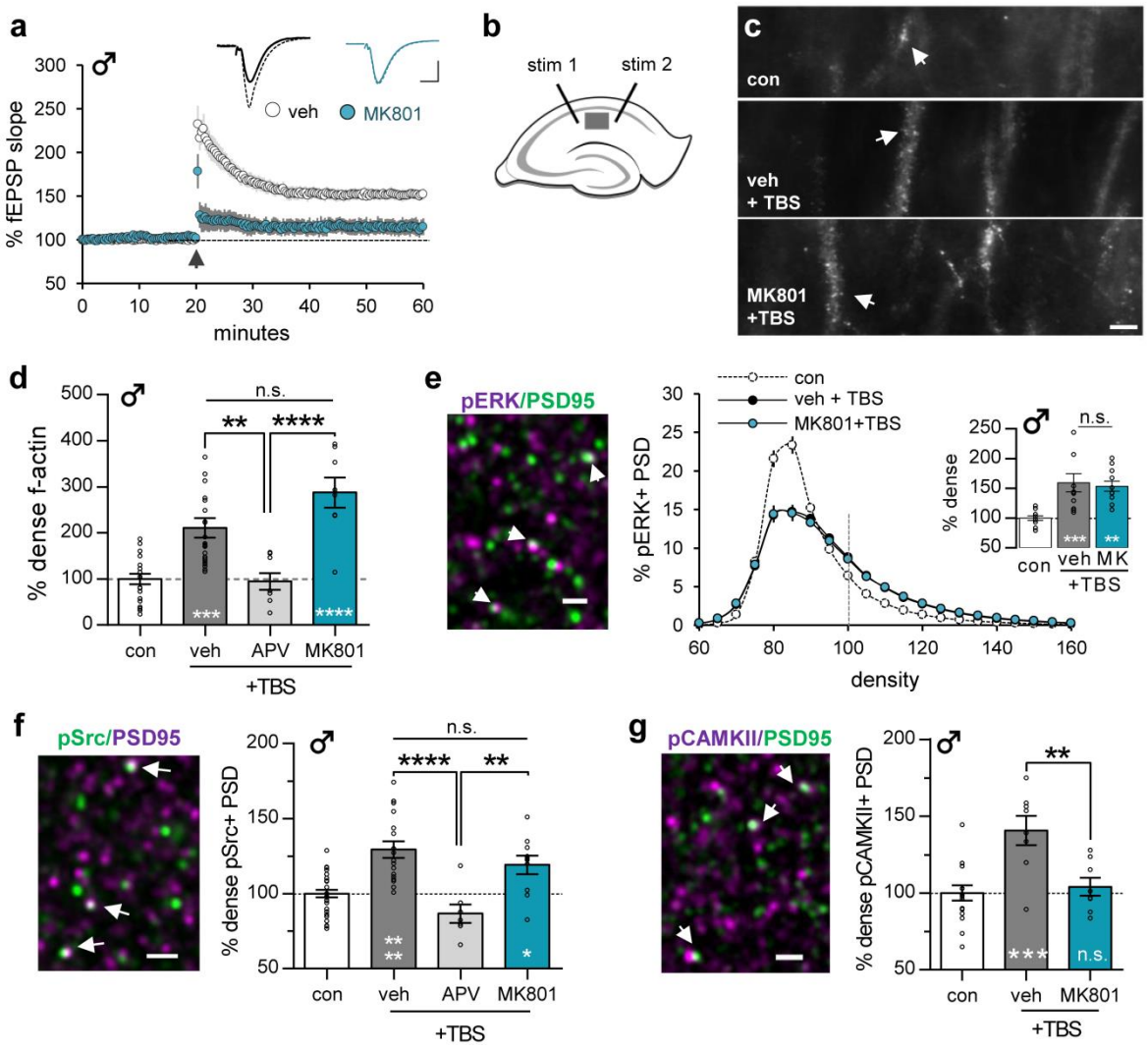


**Figure 4.1. Theta burst stimulation (TBS) elicits non-ionic NMDAR signaling and actin polymerization.** Stimulation was applied to Schaffer-commissural (SC) projections and analyses focused on CA1 stratum radiatum (SR) in slices from adult male rats. **a)** Plot of SC fEPSP slopes shows that TBS (arrow) elicits robust potentiation in vehicle (veh)-treated slices whereas MK801 infusion (30 µM; introduced ~2 hr before TBS) almost completely blocked this effect (% potentiation at 40 min post-TBS: $t_{11}$=3.477, p=0.0052; veh N=8, MK801 N=5). At top, traces from before (solid) and 40 min after (dashed) TBS. **b)** For data shown in c-g, stimulating electrodes (stim 1 and 2) were placed in CA1a and c, and analysis focused on CA1b SR (gray box) and responses after infusion of vehicle, MK801 (30 µM), or APV (100 µM). **c)** Images show phalloidin labeling in CA1b SR of a control (con) slice and slices receiving SC TBS in the presence of veh or APV; Arrows indicate phalloidin-labeled F-actin puncta. **d)** TBS increased the number of densely phalloidin-labeled spines above values recorded after low-frequency (con) stimulation. The TBS-induced increase was blocked by APV, but not MK801 ($F_{3,57}$=15.30, *p*<0.0001; N=8-24). **(e-g)** Fluorescence deconvolution tomography was used to access the

effects of SC-TBS on postsynaptic signaling proteins in the presence and absence of NMDAR antagonists. Deconvolved images from CA1 SR show immunoreactive (-ir) phosphoprotein and PSD95; double labeling appears white (arrowheads). **e)** TBS caused a rightward-skew (towards greater density) in the synaptic pERK density-frequency distribution compared to slices receiving control stimulation ($F_{38,608}$= 18.50, $p$<0.0001; p=0.0048 post-hoc); this TBS effect was unaffected by MK801 treatment (p>0.99 post-hoc). Inset: average numbers of densely pERK-ir spines (≥100 density units, vertical dotted line) normalized to mean control values. TBS produced an equivalent increase in numbers of PSD95-ir synapses with high concentrations of pERK-ir in veh- and MK801-treated slices ($F_{2,32}$=10.33, p=0.0003; N=11-12/group). **f)** Numbers of synapses with dense pSrc (Tyr419)-ir was increased by TBS and this effect was blocked by APV but not MK801 ($F_{3,62}$=15.11, $p$<0.0001; N=7-32/group). **g)** TBS increased synaptic pCaMKII-ir levels and this effect was blocked by MK801 ($F_{2,29}$=10.53, p=0.0004; N=8-16/group). Scale bars: (**a**) 1mV, 10ms; (**c**) 5 µm; (**e, f, g**) 2 µm. Statistics: (**a**) two-tailed unpaired t-test; (**e**) two-way repeated-measures ANOVA (interaction) with Bonferroni post-hoc tests; (**d, e** (inset)**, f, g**) One-way ANOVA with Tukey post-hoc tests. White asterisks inside bars denote significance vs. con stimulation. Black asterisks above bars denote differences between TBS groups. n.s. = not significant, *$p$<0.05, **$p$<0.01, ***$p$<0.001, ****$p$<0.0001. Mean ± s.e.m. values shown.

*An antagonist of the GluN2B subunit blocks actin polymerization.* It is widely agreed that the long cytoplasmic tail of the NMDAR GluN2B subunit mediates metabotropic signaling in pathological conditions (Kessels et al., 2013; Minnella et al., 2018; Warnet et al., 2021) and that GluN2B is also involved in synaptic plasticity (Sun et al., 2018). We accordingly evaluated the effects of Ro25-6981 (Ro25), a selective allosteric antagonist of GluN2B (Fischer et al., 1997; Karakas et al., 2011) on TBS-induced kinase activation, actin polymerization, and LTP. A first set of experiments assessed the extent to which low concentrations of Ro25 (3μM) depress pharmacologically isolated NMDAR-mediated responses in CA1 field recordings. A combination of AMPAR antagonist DNQX (20μM) and GABA receptor antagonist picrotoxin (30μM) eliminated ~90% of the fEPSP amplitude (data not shown). MK801 (30μM) produced a near complete elimination of the residual response thereby confirming that component of the fEPSPs was mediated by NMDARs (**Fig. 4.2a**). Ro25 did not measurably affect these NMDAR-gated fEPSPs (**Fig. 4.2b**). However, Ro25 reduced NMDAR-mediated EPSCs by ~25% in clamp recordings with the membrane potential set to +40mV and GABAergic transmission inhibited ($p=0.027$, two-tailed unpaired t-test; **Fig. 4.2c**). This value agrees with earlier work that also confirmed the exclusively synaptic location of GluN2B in CA1 (Miwa et al., 2008) and is consistent with actions of Ro25 being activity-dependent (Fischer et al., 1997). Theta bursts produce a depolarization that is considerably smaller and briefer than that elicited in the clamp experiments. There will accordingly be substantially less relief from the voltage-sensitive magnesium block of the NMDAR pore in field potential experiments. In agreement with this, the composite areas of fEPSP responses elicited by single bursts in the TBS train were not affected by Ro25 (**Fig. 4.2d**). This, together with slower dissociation of magnesium from GluN2B than GluN2A (Clarke and Johnson, 2006), helps explain why Ro25 had little if any effect on the NMDAR component of fEPSPs. The results also accord with the suggestion that GluN2A di-heterodimeric and tri-heteromeric receptors are present at higher levels in CA1 synapses than are GluN2B di-heteromers (Rauner and Köhr, 2011).

There are conflicting reports of Ro25 effects on LTP, possibly due to age effects or protocol variations (Shipton and Paulsen, 2014). In slices from adult male rats, we induced LTP using a near-threshold stimulation consisting of four triplets of theta bursts delivered at 90-sec intervals. The initial expression of fEPSP potentiation, measured immediately after each triplet, was unaffected by Ro25 ($F_{3,21}$=0.4174, p=0.7423; repeated-measures ANOVA, interaction of STP vs. treatment) but responses failed to stabilize and returned to near baseline levels after 60 min (vehicle: 137.2±9.7%, Ro25: 106.5±1.3%; p=0.011, two-tailed unpaired t-test) (**Fig. 4.2e**). Ro25 also caused a steady decay of LTP induced by a full-length train of 10 theta bursts, although levels were still above baseline by 60 min post-TBS (vehicle vs. Ro25: 152.8±4.3% vs. 126.5±4.8%, p=0.0015) (**Fig. 4.2f**).

Next, we tested if in males Ro25 affects cellular events that stabilize LTP. TBS applied to SC projections in vehicle-treated slices again produced a nearly 2-fold increase in the percentage of spines containing dense F-actin. This effect was entirely blocked by Ro25 (**Fig. 4.2g**), which accords with the drug's actions on LTP consolidation. Unlike results obtained with MK801, Ro25 also eliminated TBS-induced Src phosphorylation at CA1 synapses. It did not however disrupt effects of TBS on synaptic pERK (**Fig. 4.2h**). Prior work showed that NMDARs activate ERK1/2 (Sun et al., 2018) but the above findings indicate that this is not mediated by ionic operations of the NMDARs or metabotropic actions of GluN2B. GluN2A-containing NMDARs, which are known to upregulate ERK phosphorylation (Sun et al., 2018) independent of calcium (Li et al., 2016), could be involved perhaps with support from TrkB (Alonso et al., 2004). Lastly, Ro25 infusion blocked TBS-driven increases in synaptic pCaMKII (**Fig. 4.2h**). This result accords with evidence that CaMKII mediates effects of non-ionic NMDAR signaling on spine size elicited by local glutamate uncaging (Stein et al., 2020). Together our results for Ro25 (**Fig. 4.2h**) and MK801 (**Fig. 4.1g**), describe an instance in which both ionic and non-ionic NMDAR functions are needed to engage an LTP-critical protein.

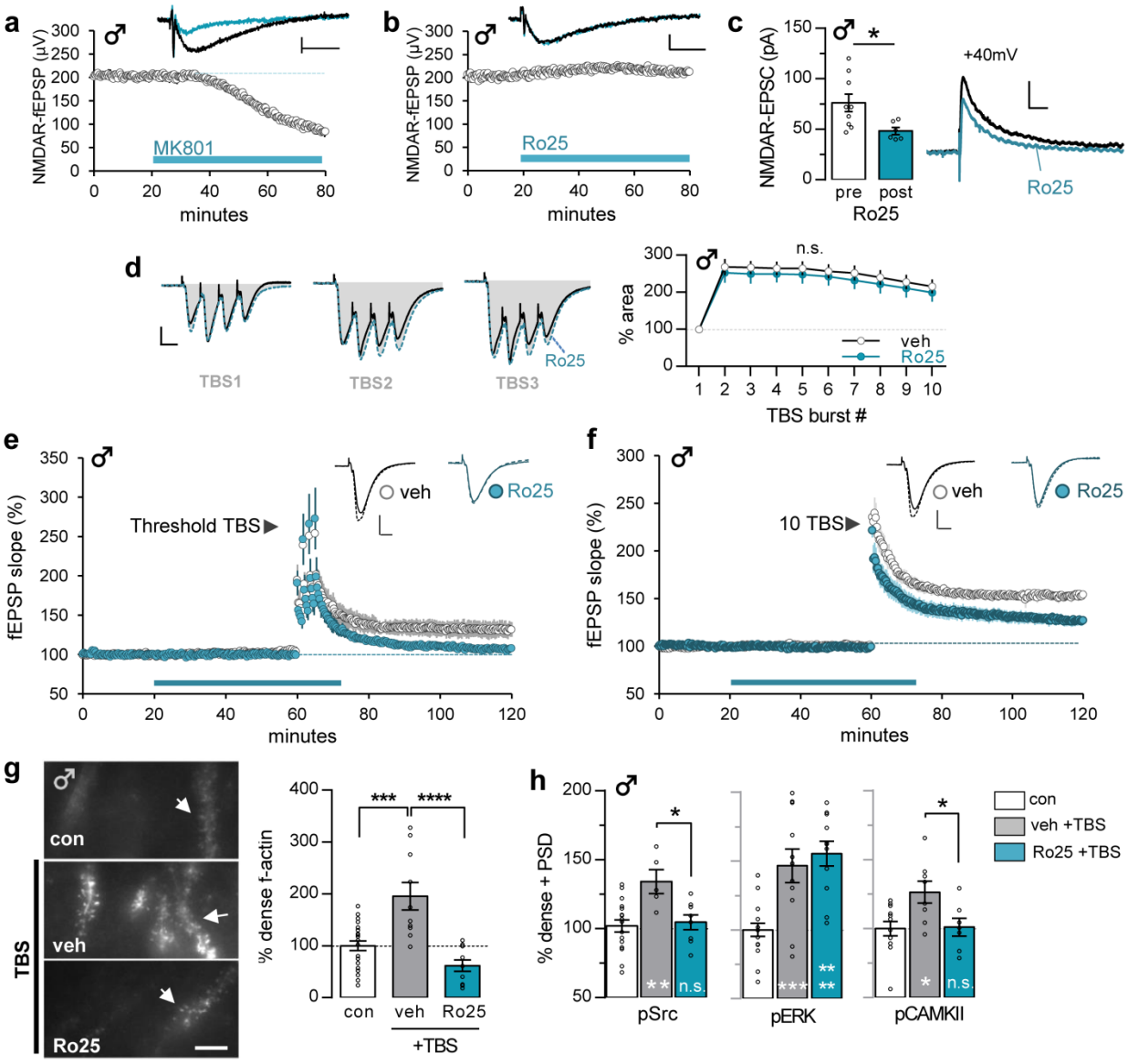


**Figure 4.2. A GluN2B antagonist Ro25-6981 blocks TBS-induced kinase activation, actin polymerization, and LTP consolidation in males. a,b)** The NMDAR-mediated component of CA1 fEPSPs was isolated using AMPAR antagonist DNQX (20 μM) and $GABA_AR$ antagonist picrotoxin (30 μM). **a)** MK801 (30 μM) markedly depressed the residual (isolated) fEPSP amplitude (N=6). **b)** Ro25-6981 (Ro25; 3 μM) did not reduce the isolated response (N=5). **c)** Voltage-clamp recording from adult mouse CA1 pyramidal cells held at +40mV show that Ro25 infusion decreased NMDAR-EPSC amplitude ($t_{13}$=2.493, p=0.027; pre-Ro25 N=9, post-Ro25 N=6). **d**) Ro25 infusion did not reduce the area of fEPSP responses to TBS ($F_{9,189}$=0.2407, p=0.9880; vehicle (veh) N=14, Ro25 N=9). Left: representative fEPSP responses to the first three bursts of 10 theta bursts in veh- (black) and Ro25- (blue, dashed) treated slices. **e, f)** Ro25 (horizontal bar) markedly reduced SC-CA1 LTP magnitude when delivering **e)** TBS at

threshold stimulation (4 TBS triplets, 90s intervals) ($t_8$=3.276, p=0.011; N=5/group) or **f)** a conventional 10-burst TBS ($t_{14}$=3.933, p=0.0015; veh N=7, Ro25 N=9). **g-h)** Slices received either control (con) low-frequency stimulation or 10 burst TBS in the presence of vehicle or Ro25. **g)** Images (left, arrows indicate F-actin labeling) and quantification (right) show TBS doubled numbers of spines with dense phalloidin, F-actin labeling in vehicle-treated slices, and this effect was completely blocked by Ro25 ($F_{2,39}$=16.81, $p$<0.0001, N=10-22/group, values normalized to con mean). **h)** Ro25 blocked the TBS-induced increase in numbers of $PSD95^+$ synapses with dense pSrc and pCaMKII but not pERK immunolabeling (pSrc: $F_{2,27}$=6.517, p=0.0049; N=5-17/group, pERK: $F_{2,36}$=14.36; $p$<0.0001, N=11-17/group; pCaMKII: $F_{2,24}$=5.111, p=0.0142; N=7-12/group). Scale bars: (**a, b**) 100µV, 20ms; (**c**) 50pA, 50ms; (**d**, **e, f**) 1mV, 10ms; (**g**) 5µm. Statistics: (**a, b, c**) two-tailed paired t-test, (**d**) repeated-measures two-way ANOVA (Interaction), (**e, f**) two-tailed unpaired t-test, (**g, h**) one-way ANOVA with post-hoc Tukey. White asterisks inside bars refer to experimental vs. control comparisons; black asterisks refer to comparisons between experimental groups. n.s. = not significant, *$p$<0.05, **$p$<0.01, ***$p$<0.001, ****$p$<0.0001. Mean ± s.e.m values shown.

**Females do not use GluN2B signaling for LTP stabilization.**

We investigated if and to what degree ionic and non-ionic NMDAR effects described for males are also present in female rats. Similar to the male result, in females MK801 infusion fully eliminated STP and LTP (LTP: vehicle vs. MK801: 152.3±6.1 vs. 104.5±5.8%, p=0.0008, two-tailed unpaired t-test; **Fig. 4.3a**) without evidence for depression relative to baseline. Furthermore, TBS-induced increases in spine F-actin were unaffected by MK801 but eliminated by APV (**Fig. 4.3b,c**). These results demonstrate that both sexes require NMDAR-gated calcium fluxes for LTP expression but not for the actin polymerization needed to maintain synapses in their potentiated state.

In striking contrast to males, Ro25 did not measurably affect TBS-induced increases in spine F-actin. TBS increased numbers of densely phalloidin-labeled spines to 215.4±19.8% of control values in slices infused with Ro25 (p=0.0041 vs. control), an increase comparable to that obtained in vehicle-treated slices (**Fig. 4.3c**). These results predicted that the disruptive effects of Ro25 in male LTP would be absent in female slices. In accord with this, Ro25 did not affect the magnitude of LTP elicited by TBS (vehicle vs. drug: 132.8±6.7% vs. 133.12±6.0%) in slices from females (**Fig. 4.3d**).

The negative results for MK801 and Ro25 effects on TBS-induced spine F-actin in females prompted us to examine another possible triggering mechanism for actin polymerization. Recent studies have shown that females, but not males, require estrogen receptor alpha (ERα) for TBS-driven signaling upstream from actin filament assembly, including phosphorylation (inactivation) of the actin severing protein cofilin (Wang et al., 2018a). Consistent with this, infusion of ERα antagonist MPP (3μM) prevented TBS-induced increases in F-actin enriched spines in females, but not in males (**Fig. 4.3e**). Possibly then females substitute local estrogen signaling for non-ionic NMDAR operations to mobilize processes that rapidly reorganize actin networks in mature spines.

The failure of Ro25 to disrupt actin polymerization and LTP in females raises the possibility of sex differences in the concentration or modulation of synaptic GluN2B subunits. We used FDT to evaluate the concentrations of GluN1, GluN2A, and GluN2B co-localized with the synaptic marker PSD95 in CA1 SR of males and females. Synaptic GluN1 levels were modestly higher in females (23.7±7.4%, $p<0.05$, two-tailed unpaired t-test) but densities of GluN2A and GluN2B subunits were comparable between the sexes ($p>0.05$) (**Fig. 4.3f**). Tyrosine phosphorylation of the NMDAR CTDs regulates receptor operations (Chen and Roche, 2007) and we accordingly measured the density of Tyr1472 phosphorylated GluN2B co-localized with PSD95. This value was significantly lower in females than males (84.0±4.2% vs. 100.0±3.1% respectively, $p=0.0041$). Given that the phosphorylation of GluN2B on the Tyr1472 site prevents endocytosis, thereby further increasing NMDAR-mediated current during LTP (Salter and Kalia, 2004; Trepanier et al., 2012), the difference in baseline phosphorylation suggests a plausible explanation for the more prominent role of GluN2B in LTP stabilization in males than is the case for females.

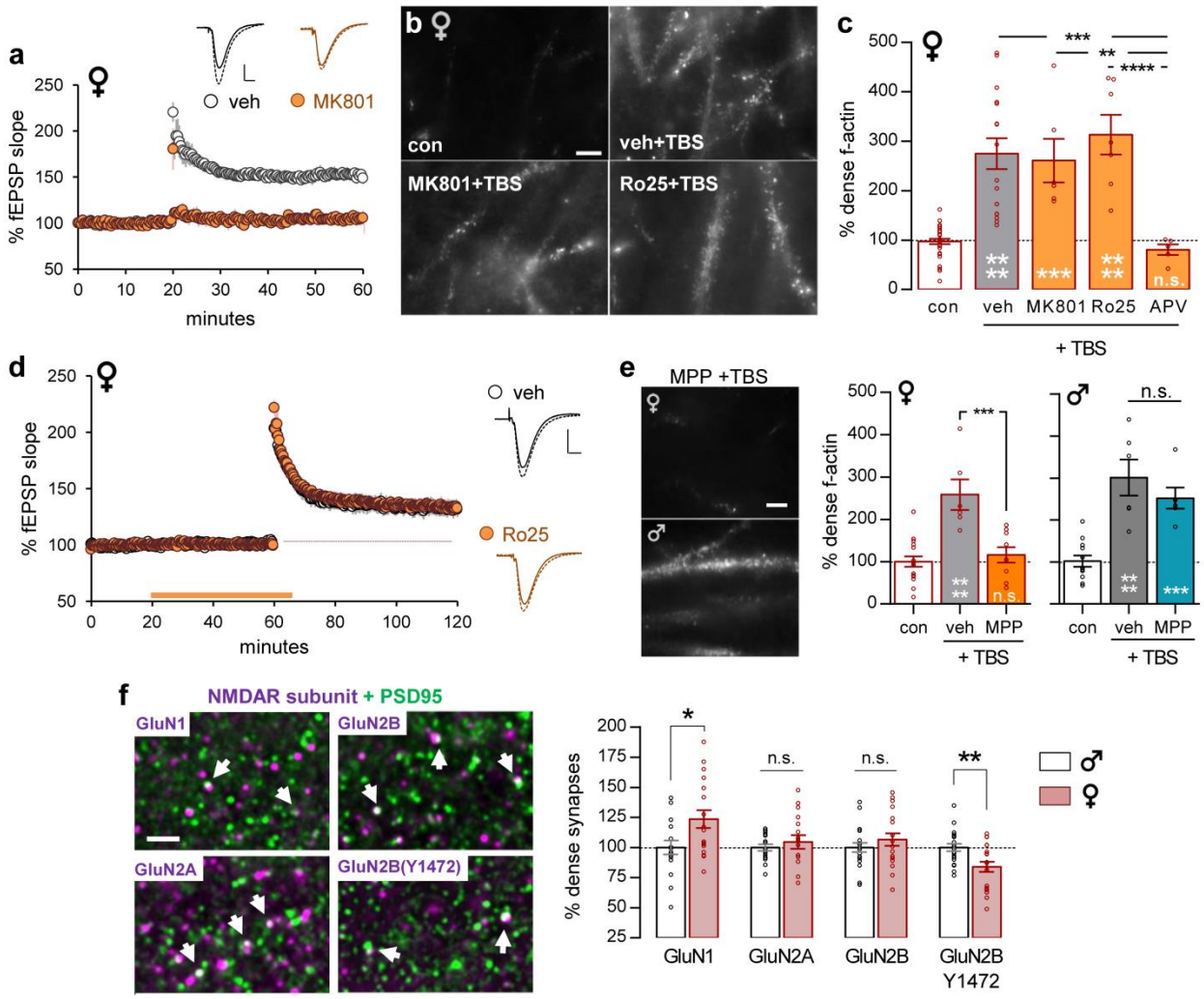


**Figure 4.3. The GluN2B antagonist Ro25-6981 does not block TBS-driven actin polymerization or CA1 LTP in females. a-e)** Stimulation and recording arrangements were as described in Fig 1. **a)** MK801 (30μM) eliminated female rat LTP induced by a 10-burst TBS train ($t_7$=5.563, p=0.0008; vehicle (veh) N=5, MK801 N=4). **b)** Representative images showing fluorescence-tagged phalloidin labeling in CA1 SR of a control (con) slice that received low frequency SC stimulation, and slices that received TBS in the presence of vehicle, MK801, or Ro25 (3 μM). **c)** Slices that received TBS in the presence of vehicle, MK801, or Ro25 showed robust increases in densely phalloidin labeled (F-actin enriched) spines relative to controls; this effect of TBS was blocked by NMDAR antagonist APV ($F_{4,62}$=22.88, $p$<0.0001; N=5-33, values normalized to control mean). **d)** Ro25 (bar) did not impair TBS-induced LTP in female slices ($t_9$=0.03626, p=0.9718; veh N=5, Ro25 N=6). Right: representative traces from before (solid) and 60 min after (dashed) TBS. **e)** In vehicle-treated slices, TBS robustly elevated the number of densely phalloidin labeled puncta above control values in both sexes; infusion of the ERα antagonist MPP (3μM, 1-3 hr) eliminated this TBS effect in females ($F_{2,29}$=16.02, $p$<0.0001; N=6-17) but not in males ($F_{2,21}$=20.28, $p$<0.0001; N=6-12). **f)** Dual-immunofluorescence for NMDAR subunits and PSD95 was quantified using FDT. Deconvolved images show the

localization of NMDAR subunits (magenta) and PSD95 (green) in CA1 SR; arrows indicate double-labeled profiles. In females as compared to males, percentage of $PSD95^{+}$ synapses had dense GluN1-ir ($t_{33}$=2.512, p=0.0171) whereas levels of GluN2A and GluN2B did not differ (N=17-20/group). Numbers of synapses with dense immunoreactivity for pGluN2B Tyr (Y) 1472 were lower in females than males ($t_{38}$=3.054, p=0.0041; N=17-20/group). Scale bar: (**a, d**) 1mV, 10ms; (**b, e**) 5µm; (**f**) 2µm. Statistics: (**a, d**) two-tailed unpaired t-test, **f**) two-tailed unpaired t-test Welch's correction, (**c, e**) One-way ANOVA with Tukey post-hoc tests. White asterisks inside bars denote comparison to controls; n.s. = not significant, **p*<0.05, ***p*<0.01, ****p*<0.001, *****p*<0.00001. Mean ± s.e.m values shown.

**Sex differences in episodic learning**.

Multiple lines of evidence indicate that the hippocampus plays a central role in the acquisition and retrieval of human episodic memory (Westmacott et al., 2001; Noulhiane et al., 2007; Dede et al., 2016). This also appears to be the case for encoding the basic elements of an episode by rodents (Dere et al., 2005; Eacott et al., 2005; Babb and Crystal, 2006). It is likely then that sex differences in NMDARs and hippocampal LTP will have consequences for acquisition of episodic information particularly given evidence that male rodents outperform females in remembering cue locations in an unsupervised episodic 'where' task (Le et al., 2022). Human studies point to the same conclusion but also suggest that women are superior to men in verbal learning and number of items remembered (Andreano and Cahill, 2009; Koss and Frick, 2017). Thus, sex differences in LTP thresholds may result in relative advantages and disadvantages with regard to encoding 'what', 'where', and 'when' components of episodic memory. We tested if female mice outperform males on one or more of these elements; to avoid effects of higher circulating estrogen, females were evaluated in stages outside of proestrus (Mukai et al., 2010) as was the case for the electrophysiological experiments.

To assess the cue identity ('what') element, we used a paradigm in which mice were presented with a sequence of 3 different odors (A-B-C; presented in paired jars with identical odors), followed by a test trial that paired one cue from the original series with a novel odor (A vs. D). Rodents have a strong proclivity for investigating novel stimuli and typically spend more time with a new relative to a previously sampled cue (Wang et al., 2018b; Cox et al., 2019). As with human episodic memory, there are no rewards or practice sessions in this paradigm. Both sexes preferred the novel odor and had similar retention scores (discrimination indices (DI) of male vs. female: 40.9±7.2 vs. 41.8±7.8; p=0.94; two-tailed unpaired t-test) (**Fig. 4.4a**, left). When presented with an additional 4$^{th}$ odor in the initial sequence, females maintained high retention scores but males did not (DI male vs. female: 7.3±4.2 vs. 35.3±4.5; p=0.0003, **Fig.**

**4.4a**, right). These results constitute the first evidence in a species other than humans for a robust adult female advantage in a fundamental component of unsupervised episodic memory. Next, we compared the sexes in a simultaneous 'what' paradigm in which the mice were given a single five-minute session with free access to four equally salient odors (A-B-C-D) in a large arena. One of the four cues was replaced with a novel odor in the retention trial (A-B-C-E). Females but not males exhibited a strong preference for the novel odor in tests conducted 48 hours after the initial encounter with the cues (**Fig. 4.4b**).

We then compared the sexes with regard to retaining information about the temporal order in which odors had been sampled (episodic 'when'). A previous study showed that male mice that had been presented with four series of odors (A-B-C-D) spent more time investigating the less recently experienced B than C in a subsequent test (Cox et al., 2019). This result was obtained when the odors were separated by 30 sec or 5 min during the initial sampling period, suggesting that the mice had acquired information about the sequence in which the cues had been presented (Cox et al., 2019). In the present study, the retention trial test cues were pushed further back in the original sequence to A vs. B. Under these conditions the males had no evident odor preference. In contrast, females spent more time with A than B and thus outperformed males in discriminating the less recent cue (**Fig. 4.4c**).

Finally, we tested the encoding of spatial relationships in an episode (i.e., episodic 'where') by allowing the mice to sample four odors for 5 min (as in panel B) and then testing if they recognized the odors switched to novel locations in the retention trial. Males investigated the relocated odors to a much greater degree than those left in their original positions. Females did not behave as though they remembered the initial positions of the cues (**Fig. 4.4d**). We summarized the results from the four behavioral tests by expressing retention for each male and female mouse as a z-score difference from the mean of the male group. This provided a relative advantage-disadvantage estimate for females for each assay. The group effect was highly

significant ($F_{3,21}$=49.11, $p$<0.0001; One-way ANOVA) with females exhibiting a strong advantage in the simultaneous 'what' test ($p$<0.015 or greater vs. the other tests, post-hoc Tukey) and a marked disadvantage in the 'where' problem ($p$<0.0001 vs. the other tests) (**Fig. 4.4e**). It is noteworthy that the same initial sampling period, used in the 'simultaneous what' and 'where' tasks, yielded the greatest sex differences depending on which aspect of learning – cue identity vs. spatial location – was tested.

There were no consistent systematic, cross-paradigm sex differences in the time spent sampling cues during initial exposure or retention test sessions. Similarly, speed of movement and distance traveled in the test arena during these two phases showed no consistent effects between sexes (**Supplementary Fig. 4.1a-d**).

The LTP results predict that blocking non-ionic NMDAR signaling will impair episodic encoding in males to greater degree than in females. We tested this by intraperitoneally injecting mice with vehicle or Ro25 (5mg/kg) 30 min prior to the start of the 3-odor serial 'what' and episodic 'where' paradigms, two tasks in which males have high retention scores. Episodic 'what' was modified to use a 10-minute initial sampling period so that females would also have positive, and comparable to male, retention scores. The GluN2B antagonist produced a profound encoding deficit for 'what' information by males without effect on performance in females (**Fig. 4.4f**). A similar result was obtained in the 'where' paradigm: vehicle-injected male mice spent considerably more time investigating the relocated odors compared to the stationary odors while Ro25-treated males did not. The antagonist had no effect on female performance in the 'where' paradigm (**Fig. 4.4g**). Ro25 treatment had no consistent effects on sampling times; although it increased locomotor activity in both sexes in the 'what' but not the 'where' episodic task (**Supplementary Fig. 4.1e-h)**.

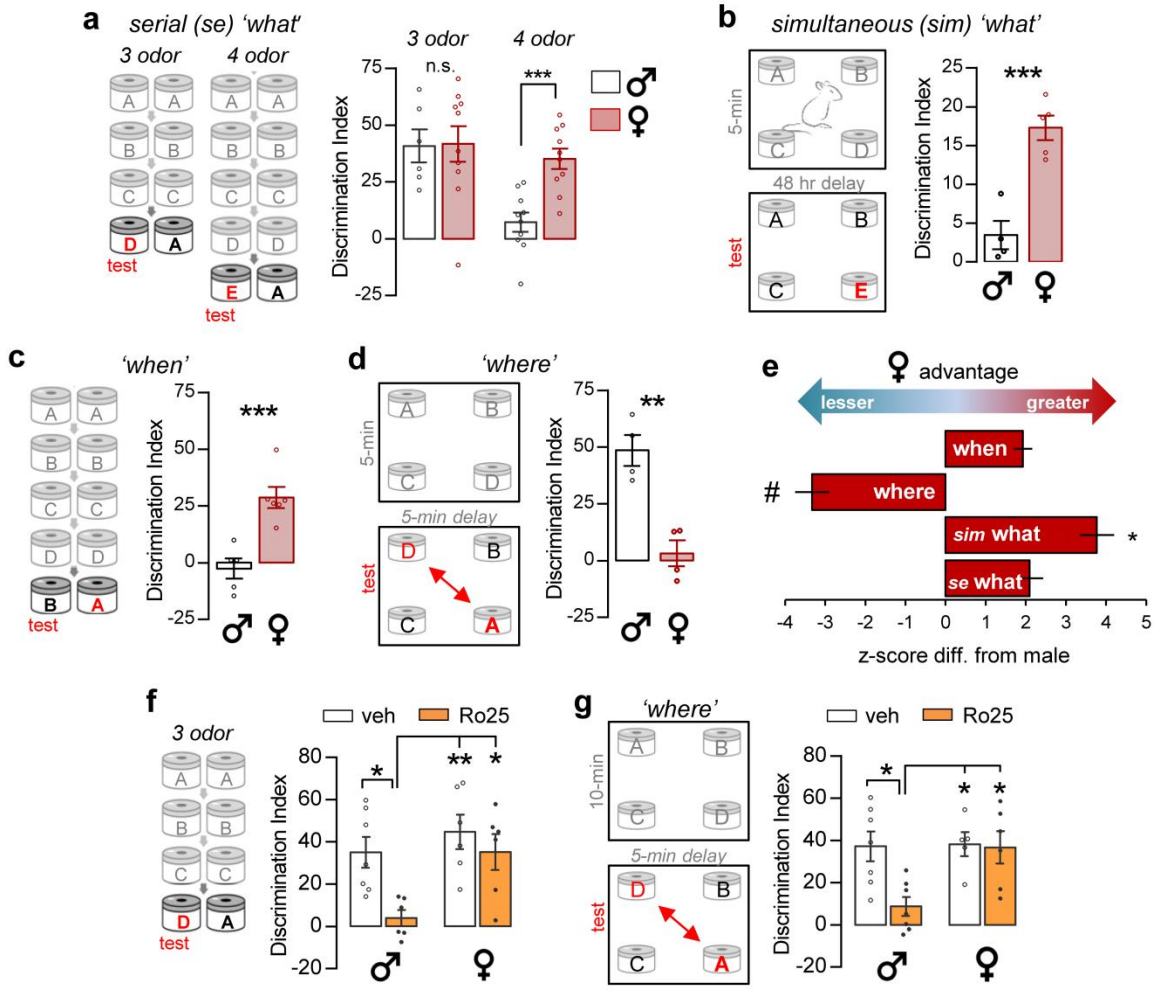


**Figure 4.4. Females outperform males in tests for episodic 'what' and 'when' encoding without GluN2B signaling. a)** Left: Schematic of serial 'what' task involving presentation of a series of 3 or 4 odor pairs before testing with a novel odor paired with the first cue in the sequence. Right: In the 3-odor task, mice preferentially explored the novel (D) vs. familiar (A) odor in the retention trial with no sex difference ($t_{14}$=0.0777, p=0.9392; male N=6, female N=10). The presence of four odors in the test sequence severely degraded performance in males but not females ($t_{18}$=4.526, p=0.0003; male vs. female, N=10/group). **b)** Simultaneous 'what' task: mice were exposed to four odors for 5 min, and returned to the chamber 48-hrs later with one odor exchanged for a novel odor. Females, but not males, distinguished the novel from the previously experienced odors ($t_7$=5.725, p=0.007; male N=4, female N=5). **c)** 'When' task: mice were given a series of 4 odor pairs, and then presented with the initial odor A versus more recent odor B. Females preferentially explored the least recently sampled odor whereas males did not ($t_9$=4.815, p=0.0021; male N=5, female N=6). **d)** 'Where' task: mice were given 5-min to sample four odors in an arena; after a 5-min delay they were tested with the positions of two of the odors switched. Males spent more time interacting with the novel-location odors whereas females did not ($t_6$=5.101, p=0.0022, N=4/group). **e)** Female performance expressed as a z-score difference (diff.) from the mean for the male group. The female advantage for

simultaneous ‘what’ was greater than for the other tests ($F_{3,21}$=49.11, $p$<0.0001; * $p$<0.15 Tukey post-hoc; N=4-10/group) and ‘where’ differed from the other three scores (# $p$<0.0001). **f,g)** Mice received Ro25 (5mg/kg) or vehicle 30 min before initial odor exposure in the 3 odor ‘what’ task and a version of the ‘where’ paradigm (10 min of initial sampling and 5 min delay to testing) in which females perform at a high level. **f)** Ro25 severely impaired male retention scores on the ‘what’ task but did not affect female performance ($F_{1,21}$=2.215, p=0.15; N=6-7/group). **g)** Vehicle-treated mice of both sexes performed well on the ‘where task’, but Ro25 markedly reduced retention scores in males but not females ($F_{1,21}$=4.375, p=0.0488; N=5-7/group). Statistics: (**a, b, c, d**) two-tailed unpaired t-test; (**e**) One-way ANOVA, post-hoc Tukey; (**f, g**) two-way ANOVA (interaction), post-hoc Tukey. n.s. = not significant, *$p$<0.05, **$p$<0.01, ***$p$<0.001). Mean ± s.e.m. values shown.

**Discussion.**

LTP stabilization passes through multiple stages, the most rapid of which begins within minutes of induction and involves reorganization of the spine actin cytoskeleton. Much of the machinery involved in this – integrins, multiple small GTPases, downstream effectors, actin polymerization and treadmilling (Krucker et al., 2000; Fontinha et al., 2008; Rex et al., 2009; Babayan et al., 2012; Yang and Liu, 2022) – is common to adhesion junctions. The synaptic variant includes specialized features such as the release and binding of the neurotrophin BDNF (Rex et al., 2007), various types of adenosine signaling (Rex et al., 2009), and glutamate release onto calcium permeant NMDARs (Rex et al., 2010; Lynch et al., 2013; Wang et al., 2018a; Gall et al., 2021). The present studies lead to the surprising conclusion that this complex collection of events, while dependent on NMDARs, can be completed without calcium flux through those receptors (**Fig. 4.5a**). Thus, in both males and females, blocking the NMDAR channel entirely eliminated SC LTP without disrupting the complex actin regulatory machinery required for stabilization of the potentiated state ('consolidation without potentiation').

There are many aspects of consolidation beyond the actin polymerization step (Kramár et al., 2006; Chen et al., 2010b; Lynch et al., 2013), including stabilization of newly formed filaments (Rex et al., 2009) and recovery of integrin signaling (Babayan et al., 2012), that are needed to maintain the potentiated state. Moreover, we cannot assume that F-actin assembly alone suffices to expand postsynaptic densities (Chen et al., 2007; Bosch et al., 2014) and indeed there are reasons to suspect that the transient increase in spine calcium required for LTP induction is required for this operation (Lynch et al., 1983; Malenka et al., 1988). At least two LTP-related effects have been linked to the cation: proteolysis of cytoskeletal anchoring proteins by calcium dependent proteinases (calpains) (Lynch and Baudry, 1984, 2015; Zhu et al., 2015) and CaMKII activation (Lisman et al., 2002; Cox et al., 2014). Proteolysis is thought to relax constraints on spine morphology, which could be a prerequisite for shape change,

whereas CaMKII is important for AMPAR movement into the synapse (Hayashi et al., 2000). The present studies confirmed that TBS activates synaptic CaMKII and this effect is reduced by MK801. In all, it seems likely that contributions by the ionic side of NMDAR operations are largely restricted to expression of LTP via expansion of the synaptic AMPAR pool.

The long CTD of GluN2B interacts with multiple factors that are critical for LTP stabilization (Shipton and Paulsen, 2014; Ishchenko et al., 2021) and numerous studies have implicated the subunit in metabotropic functions of the tetrameric receptor (Kessels et al., 2013). We found that, in males, the selective GluN2B antagonist Ro25-6981 disrupted TBS-induced actin polymerization and stabilization of SC LTP. The antagonist had minimal effects on NMDAR-mediated fEPSPs which accords with recent arguments that GluN2B di-heteromeric receptors are outnumbered within individual synapses by GluN2A-containing receptors (tri-heteromers and di-heteromers) (Rauner and Köhr, 2011). The present studies did not identify links between GluN2B and actin management but there are several likely possibilities. The subunit associates with the Ras/Rap GTPase activating protein SynGAP, which controls the activity of the small GTPase Ras and thereby regulates cofilin phosphorylation and actin polymerization (Carlisle et al., 2008). SynGAP also potently influences the activity of Rap (Krapivinsky et al., 2004), a GTPase that is intimately involved in integrin activation (Ortega-Carrion et al., 2016). The integrins regulate the actin cytoskeleton at many types of adhesion junctions and play a central role in initiating TBS-induced actin polymerization in hippocampus (Kramár et al., 2006; Wang et al., 2008).

Past studies showed that female rodents have a higher threshold for LTP induction than do males without significant differences in theta burst responses or their NMDAR mediated component (Wang et al., 2018a; Le et al., 2022). In striking contrast to its effects in males, Ro25-6981 had no detectable effect on TBS-induced actin polymerization or LTP in females. Our studies used gonadally intact females in lower estrogen phases of the estrous cycle (Mukai

et al., 2010) and it will be of interest to repeat the analyses when levels of the hormone are high (proestrus). In ovariectomized rats, estradiol effects on NMDAR EPSCs and LTP are reported to be mediated by GluN2B (i.e., are blocked by Ro25) (Smith and McMahon, 2006; Smith et al., 2009; Nebieridze et al., 2012). Whether estrogen effects on NMDAR-gated synaptic currents are accompanied by greater metabotropic signaling is unknown.

In all, our results indicate that NMDAR channel operations during theta bursts are comparable between the sexes but a fundamental difference exists in metabotropic signaling. As in males, TBS-induced spine actin polymerization in females was unaffected by the channel blocker MK801 but eliminated by APV, a competitive antagonist for glutamate binding to the NMDARs. These results, and the absence of an effect of Ro25, indicate that in females TBS-driven increases in F-actin assembly require non-ionic NMDAR signaling but not that mediated by the GluN2B subunit. One possibility is that GluN2A to a significant degree substitutes for GluN2B in females. This is not implausible given that the GluN2A CTD associates with multiple guanine exchange factors, along with other signaling molecules known to initiate actin-related signaling pathways (Sun et al., 2018). However, such a GluN2A effect is clearly not of itself sufficient to produce actin polymerization and LTP stabilization because in females these processes also require local estrogen signaling, as confirmed here with the ERα antagonist MPP. These arguments imply that there are sex differences in the status of NMDARs, and in accord with this we found higher levels of GluN2B Tyr1472 phosphorylation in males than females. The Tyr1472 residue is targeted by Src family tyrosine kinases, which are known to up-regulate NMDAR functions (Scanlon et al., 2017). The mechanisms responsible for differential phosphorylation are not known but there is evidence that estrogen can reduce phosphorylated GluN2B Tyr1472 (Waters et al., 2019), raising the possibility that the same local estrogen signaling needed for consolidation of female LTP tonically influences the operational state of GluN2B (**Fig. 4.5b**).

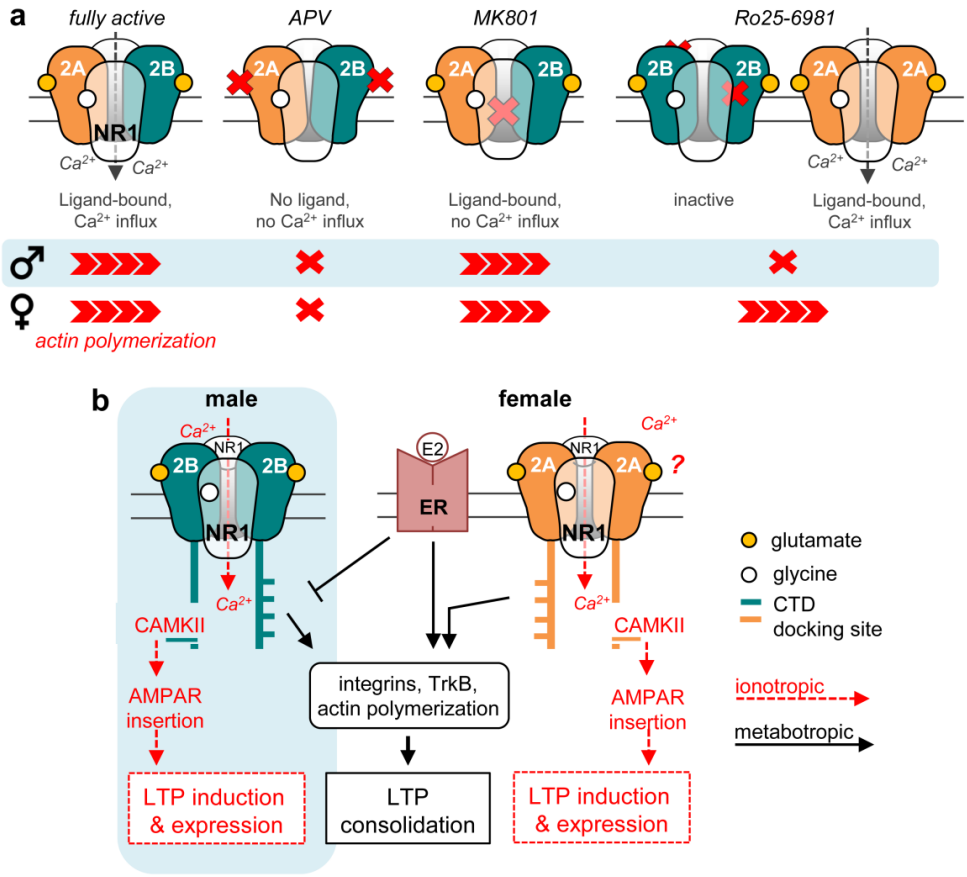


**Figure 4.5. Sex differences in the contributions of non-ionic NMDAR signaling to memory related synaptic plasticity. a)** The effects of three selective agents on ion flux through the NMDAR and observed consequences for actin polymerization, a critical late stage in LTP consolidation. The channel of the NMDAR opens and admits calcium into the cell when glutamate binds to the GluN2A or GluN2B subunits. Glutamate also triggers actin polymerization (chevrons) in both sexes. APV competes for the glutamate binding sites and prevents opening of the NMDAR ion pore. It also prevents actin polymerization ('X') in both sexes. MK801 binds within the channel and blocks calcium influx during transmission. Nevertheless, TBS drives actin polymerization in both sexes despite that absent calcium signal. Ro25-6981 binds to the interface between GluN1 and GluN2B. This does not significantly affect ion flux but does reduce actin polymerization in males but not females. **b)** Together the APV and MK801 results indicate that both sexes use non-ionic signaling to trigger actin polymerization and LTP consolidation. The actions of Ro25-6981 point to GluN2B as the NMDAR subunit subserving these non-ionic functions in males, presumably via the C-terminal domain ('CTD'). Females do not use the GluN2B mechanism to generate stable LTP. Rather they rely upon locally released estrogen and activation of synaptic estrogen receptors ('ER') to engage the same effectors as males. We hypothesize that the ERs tonically suppress GluN2B activities by reducing phosphorylation of the Tyr1472 site. As noted, the APV / MK801 results suggest that females use some type of non-ionic signaling from NMDARs to engage LTP consolidation machinery, likely via the GluN2A subunit.

The use in females of a complex synaptic signaling system of the type proposed here is plausibly related to why SC LTP threshold is higher in adult females relative to adult males. The observed sex differences also raise the question of whether there are adaptive advantages to a higher threshold for learning-related plasticity. While this is not intuitively likely, a higher threshold process for induction of LTP could serve to reduce the probability of acquiring irrelevant information in the noisy circumstances that characterize everyday life. People deal with the continuous flow of complex experience by constructing memories of episodes that minimally include information about the identities of multiple cues or events, their location, and the order in which they happened. Importantly, these elements are encoded routinely, along with contextual information, during a first-time encounter without practice, rehearsal, or explicit rewards (Tulving, 2002; Dede et al., 2016).

We compared males and females on hippocampus-dependent episodic-like memory and obtained results consistent with the idea that there are advantages to a higher encoding threshold. Female mice outperformed males on tests for acquiring the identities of multiple cues and the order in which cues were encountered (episodic ‘what’ and ‘when’). While this result is unprecedented for rodent studies, it does have correspondences in work with humans, including the observation that woman outperform men when dealing with extended lists (Youngjohn et al., 1991; Kramer et al., 1997; Rehnman and Herlitz, 2007). We found that female mice are similarly able to encode more cues than males. In the human case, there are necessary questions about whether sex differences in performance arise from other variables including experience and societal expectations for the two sexes (Cahill, 2014; Koss and Frick, 2017). Our results show that the female advantage is present when such considerations are absent, as was the male advantage in the episodic ‘where’ (Le et al., 2022) task. Indeed, the magnitude of male versus female differences described here, relative to those reported for humans, suggests that

education and related variables tend to minimize the consequences of sex differences in memory related plasticity (Voyer and Voyer, 2014; Voyer et al., 2017).

The GluN2B antagonist Ro25-6981 blocked episodic memory in males but not in females, a result that to our knowledge constitutes a first instance of drug not related to androgens disrupting episodic memory in males only. In previous work we obtained the opposite results using antagonists of estrogen receptors: severe episodic memory impairments in females with no detectable effect in males. The similarity between the effects of the treatments on LTP vs. episodic memory suggests that the synaptic events are contributors to the behavioral outcomes. If so, then the sex differences described here are likely to have a profound influence on the manner in which information is organized and used in higher cognitive operations.

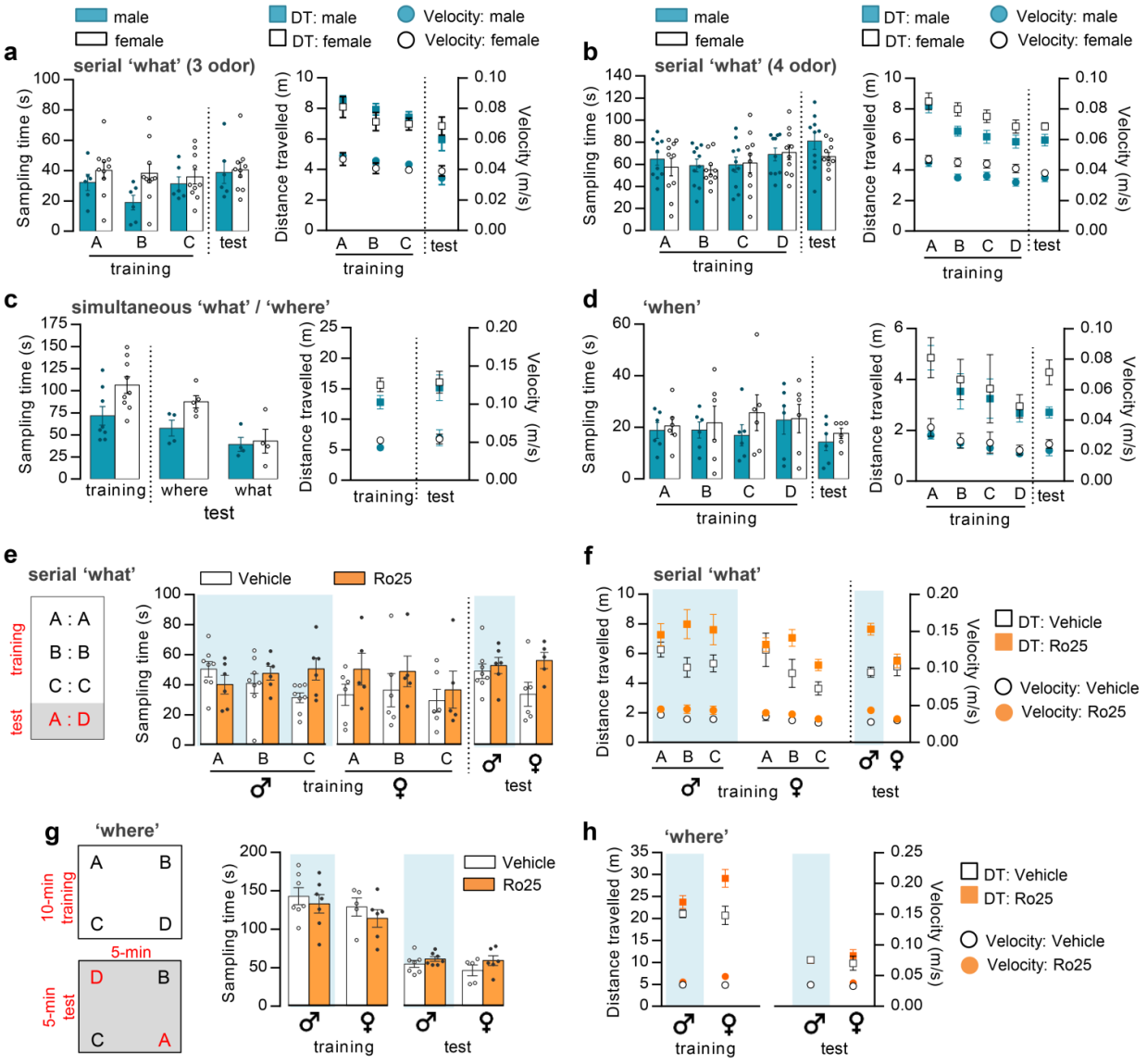


**Supplementary Figure 4.1. Detailed locomotor activity and sampling times in the behavior tasks. a)** Serial 3-odor 'what' task (presented in Figure 4a). *Left*: Sampling time of odors in the serial training (A-B-C) and test trials are similar across groups (interaction: p>0.05; two-way ANOVA). *Right*: Distance travelled (DT, squares) and velocity (circles) during each trial were also similar (interaction: p>0.05). **b)** Sampling and locomotor data for Serial 4-odor 'what' task (Fig 4a) (p>0.05). **c)** Sampling times and locomotor data during training for simultaneous 'what' and 'where' (from Fig 4b,d) were pooled together due to having the same initial (training) trial (p>0.05). **d)** Sampling and locomotor activity for 'when' task (from Fig 4c) (p>0.05). **e)** Serial 'what' (from Fig 4f) task sampling times were unaffected with the Ro25-6981 (Ro25) treatment during training trials within each sex or during testing. **f)** Distance travelled and velocity during the trials were increased in all animals receiving Ro25 ($p<0.05$). **g)** 'Where' task (from Fig 4g): Ro25 treatment did not affect sampling times or **h)** locomotor activity (note that the male Ro25 data are superimposed on the male vehicle data). For all panels, N=4-10/group.

**References**


Alonso M, Medina JH, Pozzo-Miller L (2004) ERK1/2 activation is necessary for BDNF to increase dendritic spine density in hippocampal CA1 pyramidal neurons. Learn Mem 11:172-178.

Andreano JM, Cahill L (2009) Sex influences on the neurobiology of learning and memory. Learn Mem 16:248-266.

Babayan AH, Kramár EA, Barrett RM, Jafari M, Häettig J, Chen LY, Rex CS, Lauterborn JC, Wood MA, Gall CM, Lynch G (2012) Integrin dynamics produce a delayed stage of long-term potentiation and memory consolidation. J Neurosci 32:12854-12861.

Babb SJ, Crystal JD (2006) Episodic-like memory in the rat. Curr Biol 16:1317-1321.

Baldi P, Vershynin R (2021) A theory of capacity and sparse neural encoding. Neural networks : the official journal of the International Neural Network Society 143:12-27.

Bender RA, Zhou L, Vierk R, Brandt N, Keller A, Gee CE, Schäfer MK, Rune GM (2017) Sex-Dependent Regulation of Aromatase-Mediated Synaptic Plasticity in the Basolateral Amygdala. J Neurosci 37:1532-1545.

Bosch M, Castro J, Saneyoshi T, Matsuno H, Sur M, Hayashi Y (2014) Structural and molecular remodeling of dendritic spine substructures during long-term potentiation. Neuron 82:444-459.

Cahill L (2014) Equal ≠ the same: sex differences in the human brain. Cerebrum 2014:5.

Cammarota M, Bevilaqua LR, Medina JH, Izquierdo I (2008) ERK1/2 and CaMKII-mediated events in memory formation: is 5HT regulation involved? Behav Brain Res 195:120-128.

Carlisle HJ, Manzerra P, Marcora E, Kennedy MB (2008) SynGAP regulates steady-state and activity-dependent phosphorylation of cofilin. J Neurosci 28:13673-13683.

Chen BS, Roche KW (2007) Regulation of NMDA receptors by phosphorylation. Neuropharmacology 53:362-368.

Chen LY, Rex CS, Casale MS, Gall CM, Lynch G (2007) Changes in synaptic morphology accompany actin signaling during LTP. J Neurosci 27:5363-5372.

Chen LY, Rex CS, Sanaiha Y, Lynch G, Gall CM (2010a) Learning induces neurotrophin signaling at hippocampal synapses. Proc Natl Acad Sci U S A 107:7030-7035.

Chen LY, Rex CS, Babayan AH, Kramár EA, Lynch G, Gall CM, Lauterborn JC (2010b) Physiological activation of synaptic Rac>PAK (p-21 activated kinase) signaling is defective in a mouse model of fragile X syndrome. J Neurosci 30:10977-10984.

Clarke RJ, Johnson JW (2006) NMDA receptor NR2 subunit dependence of the slow component of magnesium unblock. J Neurosci 26:5825-5834.

Cora MC, Kooistra L, Travlos G (2015) Vaginal Cytology of the Laboratory Rat and Mouse: Review and Criteria for the Staging of the Estrous Cycle Using Stained Vaginal Smears. Toxicol Pathol 43:776-793.

Cox BM, Cox CD, Gunn BG, Le AA, Inshishian VC, Gall CM, Lynch G (2019) Acquisition of temporal order requires an intact CA3 commissural/associational (C/A) feedback system in mice. Commun Biol 2:251.

Cox CD, Rex CS, Palmer LC, Babayan AH, Pham DT, Corwin SD, Trieu BH, Gall CM, Lynch G (2014) A map of LTP-related synaptic changes in dorsal hippocampus following unsupervised learning. J Neurosci 34:3033-3041.

Dede AJ, Frascino JC, Wixted JT, Squire LR (2016) Learning and remembering real-world events after medial temporal lobe damage. Proc Natl Acad Sci U S A 113:13480-13485.

Dere E, Huston JP, De Souza Silva MA (2005) Integrated memory for objects, places, and temporal order: evidence for episodic-like memory in mice. Neurobiol Learn Mem 84:214-221.

Dore K, Aow J, Malinow R (2015) Agonist binding to the NMDA receptor drives movement of its cytoplasmic domain without ion flow. Proc Natl Acad Sci U S A 112:14705-14710.
Dore K, Stein IS, Brock JA, Castillo PE, Zito K, Sjostrom PJ (2017) Unconventional NMDA Receptor Signaling. J Neurosci 37:10800-10807.
Eacott MJ, Easton A, Zinkivskay A (2005) Recollection in an episodic-like memory task in the rat. Learn Mem 12:221-223.
English JD, Sweatt JD (1997) A requirement for the mitogen-activated protein kinase cascade in hippocampal long term potentiation. J Biol Chem 272:19103-19106.
Ferreira JS, Papouin T, Ladépêche L, Yao A, Langlais VC, Bouchet D, Dulong J, Mothet JP, Sacchi S, Pollegioni L, Paoletti P, Oliet SHR, Groc L (2017) Co-agonists differentially tune GluN2B-NMDA receptor trafficking at hippocampal synapses. Elife 6.
Fischer G, Mutel V, Trube G, Malherbe P, Kew JN, Mohacsi E, Heitz MP, Kemp JA (1997) Ro 25-6981, a highly potent and selective blocker of N-methyl-D-aspartate receptors containing the NR2B subunit. Characterization in vitro. J Pharmacol Exp Ther 283:1285-1292.
Fontinha BM, Diógenes MJ, Ribeiro JA, Sebastião AM (2008) Enhancement of long-term potentiation by brain-derived neurotrophic factor requires adenosine A2A receptor activation by endogenous adenosine. Neuropharmacology 54:924-933.
Gall CM, Le AA, Lynch G (2021) Sex differences in synaptic plasticity underlying learning. J Neurosci Res.
Gray JA, Zito K, Hell JW (2016) Non-ionotropic signaling by the NMDA receptor: controversy and opportunity. F1000Res 5.
Hayashi Y, Shi SH, Esteban JA, Piccini A, Poncer JC, Malinow R (2000) Driving AMPA receptors into synapses by LTP and CaMKII: requirement for GluR1 and PDZ domain interaction. Science 287:2262-2267.
Hebb DO (1949) The Organization of Behavior. New York: Wiley.
Huang GZ, Woolley CS (2012) Estradiol acutely suppresses inhibition in the hippocampus through a sex-specific endocannabinoid and mGluR-dependent mechanism. Neuron 74:801-808.
Ishchenko Y, Carrizales MG, Koleske AJ (2021) Regulation of the NMDA receptor by its cytoplasmic domains: (How) is the tail wagging the dog? Neuropharmacology 195:108634.
Karakas E, Simorowski N, Furukawa H (2011) Subunit arrangement and phenylethanolamine binding in GluN1/GluN2B NMDA receptors. Nature 475:249-253.
Kessels HW, Nabavi S, Malinow R (2013) Metabotropic NMDA receptor function is required for β-amyloid-induced synaptic depression. Proc Natl Acad Sci U S A 110:4033-4038.
Koss WA, Frick KM (2017) Sex differences in hippocampal function. J Neurosci Res 95:539-562.
Kramer JH, Delis DC, Kaplan E, O'Donnell L, Prifitera A (1997) Developmental sex differences in verbal learning. Neuropsychology 11:577-584.
Kramár EA, Lin B, Rex CS, Gall CM, Lynch G (2006) Integrin-driven actin polymerization consolidates long-term potentiation. Proc Natl Acad Sci U S A 103:5579-5584.
Kramár EA, Chen LY, Brandon NJ, Rex CS, Liu F, Gall CM, Lynch G (2009) Cytoskeletal changes underlie estrogen's acute effects on synaptic transmission and plasticity. J Neurosci 29:12982-12993.
Krapivinsky G, Medina I, Krapivinsky L, Gapon S, Clapham DE (2004) SynGAP-MUPP1-CaMKII synaptic complexes regulate p38 MAP kinase activity and NMDA receptor-dependent synaptic AMPA receptor potentiation. Neuron 43:563-574.
Krucker T, Siggins GR, Halpain S (2000) Dynamic actin filaments are required for stable long-term potentiation (LTP) in area CA1 of the hippocampus. Proc Natl Acad Sci U S A 97:6856-6861.

Le AA, Lauterborn JC, Jia Y, Wang W, Cox CD, Gall CM, Lynch G (2022) Prepubescent female rodents have enhanced hippocampal LTP and learning relative to males, reversing in adulthood as inhibition increases. Nat Neurosci 25:180-190.
Li LJ, Hu R, Lujan B, Chen J, Zhang JJ, Nakano Y, Cui TY, Liao MX, Chen JC, Man HY, Feng H, Wan Q (2016) Glycine Potentiates AMPA Receptor Function through Metabotropic Activation of GluN2A-Containing NMDA Receptors. Front Mol Neurosci 9:102.
Lin B, Kramár EA, Bi X, Brucher FA, Gall CM, Lynch G (2005) Theta stimulation polymerizes actin in dendritic spines of hippocampus. J Neurosci 25:2062-2069.
Lisman J (1989) A mechanism for the Hebb and the anti-Hebb processes underlying learning and memory. Proc Natl Acad Sci U S A 86:9574-9578.
Lisman J, Schulman H, Cline H (2002) The molecular basis of CaMKII function in synaptic and behavioural memory. Nat Rev Neurosci 3:175-190.
Lisman J, Grace AA, Duzel E (2011) A neoHebbian framework for episodic memory; role of dopamine-dependent late LTP. Trends Neurosci 34:536-547.
Lisman J, Yasuda R, Raghavachari S (2012) Mechanisms of CaMKII action in long-term potentiation. Nat Rev Neurosci 13:169-182.
Lynch G, Baudry M (1984) The biochemistry of memory: a new and specific hypothesis. Science 224:1057-1063.
Lynch G, Baudry M (2015) Brain and memory: Old arguments and new perspectives. Brain Res 1621:1-4.
Lynch G, Larson J, Kelso S, Barrionuevo G, Schottler F (1983) Intracellular injections of EGTA block induction of hippocampal long-term potentiation. Nature 305:719-721.
Lynch G, Kramár EA, Babayan AH, Rumbaugh G, Gall CM (2013) Differences between synaptic plasticity thresholds result in new timing rules for maximizing long-term potentiation. Neuropharmacology 64:27-36.
Lynch G, Kramar EA, Rex CS, Jia Y, Chappas D, Gall CM, Simmons DA (2007) Brain-derived neurotrophic factor restores synaptic plasticity in a knock-in mouse model of Huntington's disease. J Neurosci 27:4424-4434.
Malenka RC, Kauer JA, Zucker RS, Nicoll RA (1988) Postsynaptic calcium is sufficient for potentiation of hippocampal synaptic transmission. Science 242:81-84.
Markram H, Gerstner W, Sjostrom PJ (2011) A history of spike-timing-dependent plasticity. Frontiers in synaptic neuroscience 3:4.
Minnella AM, Zhao JX, Jiang X, Jakobsen E, Lu F, Wu L, El-Benna J, Gray JA, Swanson RA (2018) Excitotoxic superoxide production and neuronal death require both ionotropic and non-ionotropic NMDA receptor signaling. Sci Rep 8:17522.
Miwa H, Fukaya M, Watabe AM, Watanabe M, Manabe T (2008) Functional contributions of synaptically localized NR2B subunits of the NMDA receptor to synaptic transmission and long-term potentiation in the adult mouse CNS. J Physiol 586:2539-2550.
Mukai H, Kimoto T, Hojo Y, Kawato S, Murakami G, Higo S, Hatanaka Y, Ogiue-Ikeda M (2010) Modulation of synaptic plasticity by brain estrogen in the hippocampus. Biochim Biophys Acta 1800:1030-1044.
Nabavi S, Fox R, Alfonso S, Aow J, Malinow R (2014) GluA1 trafficking and metabotropic NMDA: addressing results from other laboratories inconsistent with ours. Philos Trans R Soc Lond B Biol Sci 369:20130145.
Nabavi S, Kessels HW, Alfonso S, Aow J, Fox R, Malinow R (2013) Metabotropic NMDA receptor function is required for NMDA receptor-dependent long-term depression. Proc Natl Acad Sci U S A 110:4027-4032.
Nebieridze N, Zhang XL, Chachua T, Velíšek L, Stanton PK, Velíšková J (2012) β-Estradiol unmasks metabotropic receptor-mediated metaplasticity of NMDA receptor transmission in the female rat dentate gyrus. Psychoneuroendocrinology 37:1845-1854.

Nong Y, Huang YQ, Ju W, Kalia LV, Ahmadian G, Wang YT, Salter MW (2003) Glycine binding primes NMDA receptor internalization. Nature 422:302-307.
Noulhiane M, Piolino P, Hasboun D, Clemenceau S, Baulac M, Samson S (2007) Autobiographical memory after temporal lobe resection: neuropsychological and MRI volumetric findings. Brain 130:3184-3199.
Ortega-Carrion A, Feo-Lucas L, Vicente-Manzanares M (2016) Cell Migration. In: Encyclopedia of Cell Biology (Second Edition) (Bradshaw RA, Hart GW, Stahl PD, eds), pp 247-259. Oxford: Academic Press.
Paoletti P, Bellone C, Zhou Q (2013) NMDA receptor subunit diversity: impact on receptor properties, synaptic plasticity and disease. Nat Rev Neurosci 14:383-400.
Papouin T, Ladépêche L, Ruel J, Sacchi S, Labasque M, Hanini M, Groc L, Pollegioni L, Mothet JP, Oliet SH (2012) Synaptic and extrasynaptic NMDA receptors are gated by different endogenous coagonists. Cell 150:633-646.
Park DK, Stein IS, Zito K (2022) Ion flux-independent NMDA receptor signaling. Neuropharmacology 210:109019.
Park P, Volianskis A, Sanderson TM, Bortolotto ZA, Jane DE, Zhuo M, Kaang BK, Collingridge GL (2014) NMDA receptor-dependent long-term potentiation comprises a family of temporally overlapping forms of synaptic plasticity that are induced by different patterns of stimulation. Philos Trans R Soc Lond B Biol Sci 369:20130131.
Rauner C, Köhr G (2011) Triheteromeric NR1/NR2A/NR2B receptors constitute the major N-methyl-D-aspartate receptor population in adult hippocampal synapses. J Biol Chem 286:7558-7566.
Rehnman J, Herlitz A (2007) Women remember more faces than men do. Acta Psychol (Amst) 124:344-355.
Rex CS, Lin CY, Kramár EA, Chen LY, Gall CM, Lynch G (2007) Brain-derived neurotrophic factor promotes long-term potentiation-related cytoskeletal changes in adult hippocampus. J Neurosci 27:3017-3029.
Rex CS, Chen LY, Sharma A, Liu J, Babayan AH, Gall CM, Lynch G (2009) Different Rho GTPase-dependent signaling pathways initiate sequential steps in the consolidation of long-term potentiation. J Cell Biol 186:85-97.
Rex CS, Gavin CF, Rubio MD, Kramar EA, Chen LY, Jia Y, Huganir RL, Muzyczka N, Gall CM, Miller CA, Lynch G, Rumbaugh G (2010) Myosin IIb regulates actin dynamics during synaptic plasticity and memory formation. Neuron 67:603-617.
Salter MW, Kalia LV (2004) Src kinases: a hub for NMDA receptor regulation. Nat Rev Neurosci 5:317-328.
Scanlon DP, Bah A, Krzeminski M, Zhang W, Leduc-Pessah HL, Dong YN, Forman-Kay JD, Salter MW (2017) An evolutionary switch in ND2 enables Src kinase regulation of NMDA receptors. Nat Commun 8:15220.
Seeburg PH, Burnashev N, Kohr G, Kuner T, Sprengel R, Monyer H (1995) The NMDA receptor channel: molecular design of a coincidence detector. Recent progress in hormone research 50:19-34.
Seese RR, Wang K, Yao YQ, Lynch G, Gall CM (2014) Spaced training rescues memory and ERK1/2 signaling in fragile X syndrome model mice. Proc Natl Acad Sci U S A 111:16907-16912.
Shipton OA, Paulsen O (2014) GluN2A and GluN2B subunit-containing NMDA receptors in hippocampal plasticity. Philos Trans R Soc Lond B Biol Sci 369:20130163.
Singh VP, McNiven MA (2008) Src-mediated cortactin phosphorylation regulates actin localization and injurious blebbing in acinar cells. Mol Biol Cell 19:2339-2347.
Smith CC, McMahon LL (2006) Estradiol-induced increase in the magnitude of long-term potentiation is prevented by blocking NR2B-containing receptors. J Neurosci 26:8517-8522.

Smith CC, Vedder LC, McMahon LL (2009) Estradiol and the relationship between dendritic spines, NR2B containing NMDA receptors, and the magnitude of long-term potentiation at hippocampal CA3-CA1 synapses. Psychoneuroendocrinology 34 Suppl 1:S130-142.
Stein IS, Park DK, Claiborne N, Zito K (2021) Non-ionotropic NMDA receptor signaling gates bidirectional structural plasticity of dendritic spines. Cell reports 34:108664.
Stein IS, Park DK, Flores JC, Jahncke JN, Zito K (2020) Molecular Mechanisms of Non-ionotropic NMDA Receptor Signaling in Dendritic Spine Shrinkage. J Neurosci 40:3741-3750.
Sun Y, Xu Y, Cheng X, Chen X, Xie Y, Zhang L, Wang L, Hu J, Gao Z (2018) The differences between GluN2A and GluN2B signaling in the brain. J Neurosci Res 96:1430-1443.
Tanimura S, Takeda K (2017) ERK signalling as a regulator of cell motility. J Biochem 162:145-154.
Trepanier CH, Jackson MF, MacDonald JF (2012) Regulation of NMDA receptors by the tyrosine kinase Fyn. FEBS J 279:12-19.
Tulving E (2002) Episodic memory: from mind to brain. Annu Rev Psychol 53:1-25.
Vierk R, Glassmeier G, Zhou L, Brandt N, Fester L, Dudzinski D, Wilkars W, Bender RA, Lewerenz M, Gloger S, Graser L, Schwarz J, Rune GM (2012) Aromatase inhibition abolishes LTP generation in female but not in male mice. J Neurosci 32:8116-8126.
Vissel B, Krupp JJ, Heinemann SF, Westbrook GL (2001) A use-dependent tyrosine dephosphorylation of NMDA receptors is independent of ion flux. Nat Neurosci 4:587-596.
Volianskis A, Bannister N, Collett VJ, Irvine MW, Monaghan DT, Fitzjohn SM, Jensen MS, Jane DE, Collingridge GL (2013) Different NMDA receptor subtypes mediate induction of long-term potentiation and two forms of short-term potentiation at CA1 synapses in rat hippocampus in vitro. J Physiol 591:955-972.
Voyer D, Voyer SD (2014) Gender differences in scholastic achievement: a meta-analysis. Psychol Bull 140:1174-1204.
Voyer D, Voyer SD, Saint-Aubin J (2017) Sex differences in visual-spatial working memory: A meta-analysis. Psychon Bull Rev 24:307-334.
Wang W, Le AA, Hou B, Lauterborn JC, Cox CD, Levin ER, Lynch G, Gall CM (2018a) Memory-Related Synaptic Plasticity Is Sexually Dimorphic in Rodent Hippocampus. J Neurosci 38:7935-7951.
Wang W, Cox BM, Jia Y, Le AA, Cox CD, Jung KM, Hou B, Piomelli D, Gall CM, Lynch G (2018b) Treating a novel plasticity defect rescues episodic memory in Fragile X model mice. Mol Psychiatry 23:1798-1806.
Wang XB, Bozdagi O, Nikitczuk JS, Zhai ZW, Zhou Q, Huntley GW (2008) Extracellular proteolysis by matrix metalloproteinase-9 drives dendritic spine enlargement and long-term potentiation coordinately. Proc Natl Acad Sci U S A 105:19520-19525.
Warnet XL, Bakke Krog H, Sevillano-Quispe OG, Poulsen H, Kjaergaard M (2021) The C-terminal domains of the NMDA receptor: How intrinsically disordered tails affect signalling, plasticity and disease. Eur J Neurosci 54:6713-6739.
Waters EM, Mazid S, Dodos M, Puri R, Janssen WG, Morrison JH, McEwen BS, Milner TA (2019) Effects of estrogen and aging on synaptic morphology and distribution of phosphorylated Tyr1472 NR2B in the female rat hippocampus. Neurobiol Aging 73:200-210.
Weaver AM, Karginov AV, Kinley AW, Weed SA, Li Y, Parsons JT, Cooper JA (2001) Cortactin promotes and stabilizes Arp2/3-induced actin filament network formation. Curr Biol 11:370-374.
Weilinger NL, Lohman AW, Rakai BD, Ma EM, Bialecki J, Maslieieva V, Rilea T, Bandet MV, Ikuta NT, Scott L, Colicos MA, Teskey GC, Winship IR, Thompson RJ (2016)

Metabotropic NMDA receptor signaling couples Src family kinases to pannexin-1 during excitotoxicity. Nat Neurosci 19:432-442.
Westmacott R, Leach L, Freedman M, Moscovitch M (2001) Different patterns of autobiographical memory loss in semantic dementia and medial temporal lobe amnesia: a challenge to consolidation theory. Neurocase 7:37-55.
Yang Y, Liu JJ (2022) Structural LTP: Signal transduction, actin cytoskeleton reorganization, and membrane remodeling of dendritic spines. Curr Opin Neurobiol 74:102534.
Youngjohn JR, Larrabee GJ, Crook TH (1991) First-Last Names and the Grocery List Selective Reminding Test: two computerized measures of everyday verbal learning. Arch Clin Neuropsychol 6:287-300.
Zhu G, Liu Y, Wang Y, Bi X, Baudry M (2015) Different patterns of electrical activity lead to long-term potentiation by activating different intracellular pathways. J Neurosci 35:621-633.

# CHAPTER FIVE: Summary and Discussion

Work in this dissertation has identified sexually dimorphic features of the cellular cascades that produce the lasting, activity-driven synaptic modifications required for the encoding of episodic memory. Females, like males, utilize ion flux through NMDARs to shift synapses into their potentiated (LTP) state but then employ sex-specific, local estrogen signaling to generate the cytoskeletal adjustments needed to stabilize the changes. Males depend on newly discovered non-ionotropic (metabotropic) functions of NMDA receptors rather than steroids to reorganize the subsynaptic actin networks so as to consolidate LTP. The results also establish that earlier studies have over-estimated the role of calcium in LTP and that much, and likely most, of the machinery required for long term changes to synaptic strength is triggered by metabotropic actions.

The dramatic sex differences in substrates had were accompanied by clear differences in LTP thresholds: lasting potentiation in males was induced by a fewer number of theta bursts than is the case for females(Wang et al., 2018). This physiological effect was associated with rather surprising effects on episodic memory. Females were outclassed by males in spatial memory (episodic 'where') but acquired longer lists of cue identities ('what') and their temporal order ('when'). In all, there are profound differences in how the two sexes produce learning-related adjustments to their hippocampal synapses and these have major consequences for that form of memory routinely used to organize the flow of everyday experience.

**Contributions of Estrogen Receptors (ERs) to LTP Are Sex-Specific**

We will first consider how ERs are integrated into synaptic plasticity in female rodents, and how this additional machinery elevates the threshold for LTP induction and spatial encoding in females. Studies from our laboratory showed that stimulating the CA3-CA1 projections with theta bursts (TBS) activates signaling kinases that promote memory-related actin polymerization and stabilization(Gall et al., 2021). Much of the LTP-related substrate map overlaps with the actin cytoskeletal changes elicited by exogenous (infused) estrogen, an effect that appears to

be mediated by ERβ in both sexes(Kramár et al., 2009; Wang et al., 2016). Despite this, ERβ is not the primary trigger for female LTP, a role that is instead filled by membrane-associated ERα (see *Chapter Two*). Relatedly, females have greater density of synaptic ERα levels in the CA1 lamina than males. Outside of the estrogen-ER requirement in females, the downstream signaling pathways towards reorganization of the actin cytoskeleton are conserved in both sexes. Nonetheless, and of considerable functional significance, a higher threshold for induction accompanies the added, local estrogen step for LTP induction.

**LTP expression shifts with puberty**

If estrogen pools and ERs promote LTP in females, then the threshold for potentiation should be much higher prior to the estrogenic surge that occurs during puberty. But our studies produced the opposite result (see *Chapter Three*). As expected, prepubescent females (3-4 weeks old) had a reduced density of synaptic ERα in CA1 and lower circulating estrogen levels than sexually developed females (8+ weeks old). But in a startling negation of the above prediction, the immature animals --- though already dependent on ERα for induction --- had remarkably large LTP compared to young adult males or females. A search for factors that might produce the puberty related loss of function for plasticity led to an unexpected conclusion: a pronounced increase in both α5-containing synaptic $GABA_A$ receptors and related feedforward, shunting inhibition. The latter effect reduced depolarization during theta burst stimulation and thus the response of voltage-sensitive NMDARs. Inhibiting α5-containing $GABA_A$Rs restored LTP and spatial memory in adult females to levels found before puberty.

Puberty caused a marked decrease in the threshold for male LTP but this was not due to an opposite version of the events seen in females. Pre- and post-pubescent males had similar levels of shunting inhibition and synaptic α5-$GABA_A$R and were not different in this regard than adult females. Why the α5-$GABA_A$R puberty effect is restricted to females is unknown, but a study previously demonstrated that estrogen-induced enhancement of α5-$GABA_A$R localization

is female-specific in the spinal cord (Franco-Enzástiga et al., 2020). Future work should verify if this action is consistent in the hippocampus and regulated by the surge of circulating estrogen or a DNA modification triggered by puberty. Another developmental question of primary importance concerns the factors responsible for the dramatic gain of function for plasticity that occurs across male puberty. The size of the theta burst responses is similar during this period, which suggests that downstream factors are responsible for the enhanced LTP. Further information could be gained by a pre- vs. post-puberty analysis of the complex signaling events leading to the cytoskeletal adjustments that stabilize the potentiated state.

Two additional questions left unanswered by the work described in *Chapter Two* concern sex differences in thresholds: (i) why are female-NMDARs not sufficient to trigger LTP, thereby creating a need for co-activation of ERα, and (ii) why don't males utilize estrogen signaling during TBS despite having synaptic ERs (*Chapter 2*) and high levels of locally synthesized estradiol (Mukai et al., 2010)? We hypothesized that male LTP is not dependent on ERs because it employs a more efficacious form of NMDAR signaling than is found in females. In this scenario, the use of ERs allows females to compensate for weaker signaling by the glutamate receptors.

**Non-canonical, LTP related signaling via metabotropic NMDARs**

Work in *Chapter Four* suggested that the additional NMDAR-to-cytoskeleton link in males involves non-ionic (metabotropic: m-) signaling by the receptors, a feature that had been controversially connected to excitotoxicity and long-term depression (Park et al., 2022). A pivotal discovery from the early years of LTP research showed that calcium influx through NMDARs enables the response enhancement that defines LTP (Lynch et al., 1983; Larson and Lynch, 1988; Lin et al., 2005; Rex et al., 2009). It was tacitly assumed that the ionotropic feature of the NMDARs was in fact the primary initiator not only for LTP expression but also for the synaptic remodeling that consolidates the potentiated state. Specific pharmacological

manipulations of the NMDA receptors allowed us to parse the contributions of ionotropic and metabotropic NMDA operations to TBS-induced cytoskeleton reorganization. LTP is fully suppressed by an agent (MK801) that occludes the channel pore, but NMDAR-dependent actin polymerization and kinase activation persisted. The downstream signaling is engaged by ligand-bound NMDA receptors but not the accompanying calcium influx, hence 'metabotropic signaling'. We then traced this metabotropic feature to the GluN2B subunit which is known to have a long cytoplasmic tail domain (CTD) used as a docking site for several LTP-related effectors (e.g., CAMKII and Src) (Chen and Roche, 2007). Notably, infusion of the GluN2B antagonist, Ro25-6981, which prevents GluN2B-containing heterodimeric NMDARs from twisting into an active conformation, blocked calcium-independent activation of Src kinase, actin polymerization, and LTP consolidation in males. Conversely, GluN2B did not disrupt ERK activation by TBS, indicating a potential contribution from GluN2A or other receptors (e.g., TrkB) (Sun et al., 2018). Thus, it is evident that non-ionic signaling toward activity-induced actin cytoskeleton remodeling is mediated through the GluN2B subunit in adult male rat.

While we substantially enriched our understanding of the calcium-independent signaling set in motion by TBS, it remains the case that calcium influx is fundamental for LTP expression. We found that blocking the NMDAR channel prevents activation of CaMKII, a kinase that plays an essential role in LTP expression likely by promoting the addition of AMPARs to the postsynaptic pool (Lisman et al., 2012; Cox et al., 2014). There is also evidence that NMDAR-gated calcium influx activates the protease calpain, an event that appears to contribute to structural remodeling (Lynch and Baudry, 1984; Zhu et al., 2015).

In contrast to the male results, the GluN2B antagonist Ro25-6981 had no detectable effect on TBS-induced actin polymerization of LTP consolidation in young adult females. But as noted a compound that blocks ERα eliminated both effects. These results accord with the hypothesis that the estrogen receptors substitute for the metabotropic functions of the NMDAR

in females. However, the competitive antagonist APV disrupted both polymerization and LTP stabilization, two effects that as noted were left intact by suppression of ionic flux through the receptors. Accordingly, we propose that females employ two forms of metabotropic signaling, one via ERα and the other through GluN2A, which is known to have overlapping CTD sites with the GluN2B (Sun et al., 2018). Increased complexity is an evident disadvantage of the female system; its advantages are not obvious. An interesting possibility is that the combination of estrogen and glutamate signaling produces female-specific LTP effects of a type that were not detected in our studies to date. Work with male rodents has identified an array of LTP phenomena that have not been tested in females. These include delayed consolidation stages (Babayan et al., 2012) and a 'spaced trials' effect (Kramár et al., 2012) that appear to be involved in basic aspects of learning. Accordingly, the sex differences in LTP machinery described here could serve to influence behavior in ways yet to be examined. There is also the possibility that tying plasticity to estrogen generates a relationship between the estrous cycle and type of encoding. Such an effect could allow females to adjust learning to according to likely situational demands.

These points raise the question of whether there are benefits with regard to everyday learning associated one or the other of the two modes of producing LTP. The following section addresses this issue.

**Sex differences in LTP thresholds and Episodic Memory Encoding**

As described in *Chapter Two*, males outperform females on spatial memory problems when using a standard 5-min sampling period, a result that accords with their lower LTP threshold. Females learned the spatial problem with certain conditions when in the presence of high circulating estrogen (proestrus) or allowed to sample the cues for 10 minutes. The former condition links acquisition to the estrogen-ER mechanism because exogenous (to brain) E2 potently enhances LTP (Frick et al., 2018). It will as well be of interest to test the possibility that

high E2 phosphorylates the Src binding site on the GluN2B CTD to levels found in males and thereby engages the male metabotropic NMDAR signaling system. An intriguing prediction from this argument is that Ro25-6981, while ineffective during most of the estrous cycle, will disrupt female LTP during proestrus. In any event, the data so far collected for spatial learning accord with the assumption of a relatively simple relationship between LTP thresholds in CA1 and this form of encoding. But whether the male advantage extends to other forms of memory, and especially the everyday variants that are critical to cognition, is a question that has received surprisingly little attention. Work with humans strongly suggests that women outperform men on verbal problems, especially those involving sizeable numbers of items, and perhaps on certain aspects of episodic memory. Interpreting such results with regard to substrates is difficult because of differences in way the two sexes are treated during development and training – notably, the sex difference in spatial learning is common to mammals and so is assumed to have a neurobiological origin. The studies described in *Chapter Four* provided the first evidence from rodent studies for a female advantage in tests of episodic memory and thereby suggest that observed sex differences in humans for this type of encoding are biological rather than social in nature.

Female mice were able to acquire the identities of a series of four odors whereas males could only do three odor problems. The females were also able handle a larger number of cues in the episodic problem that required memory of the order in which these had been sampled. These results bear some resemblance to those for list learning by humans. But how does a higher LTP threshold in CA1 of females relate to better performance on the episodic ‘what’ and ‘when’ problems. One possibility is that rapid production of an LTP signal by CA1 terminates sampling and induction of synaptic changes at other sites in hippocampus. While formal comparisons have not been made, one has the strong impression that the CA3-CA1 connection has the lowest threshold for potentiation of any site within hippocampus. Perhaps then the

higher threshold in females ensures that cue sampling will continue long enough for synaptic changes to occur in, for example, field CA3 as well as in CA1. An equally speculative possibility is the conjoint ER-NMDAR used by females goes beyond the typical LTP fingerprint to produce adjustments that are favorable for the processing of large numbers of items. It should be possible in future studies to collect data pertinent to these ideas.

Males and females share a similar blueprint in activating the downstream kinases towards actin polymerization required for memory-related synaptic plasticity, but the critical initiators are clearly different between the sexes. These features and the changes that occur across puberty could provide insight on the etiology of various cognitive disorders including the critical question of why post-pubertal depression is so much more prevalent in girls than boys (Eid et al., 2019). The experiments also led us to reinterpret how low vs. high threshold LTP relate to different aspects of episodic memory, a finding that could have significant implications for learning theory.

The sexual dichotomy of hippocampal plasticity may reflect evolutionary pressures towards optimizing group level learning in real-world environments. Assuming guidance roles are freely exchanged between the sexes, then having ‘specialists’ for different types of circumstances will likely result in a more successful population. A lower threshold for spatial navigation would be advantageous for foraging males while slower acquisition by females could be advantageous in situations in which the signal-to-noise ratio for critical cues is low. If as we suggest these features are the shared inheritance of mammals, then it is interesting to speculate on how they may have influenced human society. As sometimes noted, the male advantage for episodic ‘where’ could have led men to likely prioritize the spatial awareness to hunt and return food to the community. Women, with their strong performance on episodic ‘what’ and ‘when’, could enhance socialization via complex stories and in general use cautionary tales to ensure the success of future generations. More broadly, psychologists have

described how episodic memories are used for deriving inferences thinking and in imaginative thinking (Beaty et al., 2020). The sex differences reported in *Chapter Four* thus raise the possibility of corresponding cognitive differences, something that again could prove to be of great value for group survival. Relatedly, it would be fascinating to consider how history would appear to us if it had been written by women. Comparing histories of the same era as written by women vs. men might be one way to gain insight into the human consequences of sex differences in synaptic plasticity.

**References**


Babayan AH, Kramár EA, Barrett RM, Jafari M, Häettig J, Chen LY, Rex CS, Lauterborn JC, Wood MA, Gall CM, Lynch G (2012) Integrin dynamics produce a delayed stage of long-term potentiation and memory consolidation. J Neurosci 32:12854-12861.

Beaty RE, Chen Q, Christensen AP, Kenett YN, Silvia PJ, Benedek M, Schacter DL (2020) Default network contributions to episodic and semantic processing during divergent creative thinking: A representational similarity analysis. Neuroimage 209:116499.

Chen BS, Roche KW (2007) Regulation of NMDA receptors by phosphorylation. Neuropharmacology 53:362-368.

Cox CD, Rex CS, Palmer LC, Babayan AH, Pham DT, Corwin SD, Trieu BH, Gall CM, Lynch G (2014) A map of LTP-related synaptic changes in dorsal hippocampus following unsupervised learning. J Neurosci 34:3033-3041.

Eid RS, Gobinath AR, Galea LAM (2019) Sex differences in depression: Insights from clinical and preclinical studies. Prog Neurobiol 176:86-102.

Franco-Enzástiga Ú, García G, Murbartián J, González-Barrios R, Salinas-Abarca AB, Sánchez-Hernández B, Tavares-Ferreira D, Herrera LA, Barragán-Iglesias P, Delgado-Lezama R, Price TJ, Granados-Soto V (2020) Sex-dependent pronociceptive role of spinal α. J Neurochem.

Frick KM, Kim J, Koss WA (2018) Estradiol and hippocampal memory in female and male rodents. Curr Opin Behav Sci 23:65-74.

Gall CM, Le AA, Lynch G (2021) Sex differences in synaptic plasticity underlying learning. J Neurosci Res.

Kramár EA, Chen LY, Brandon NJ, Rex CS, Liu F, Gall CM, Lynch G (2009) Cytoskeletal changes underlie estrogen's acute effects on synaptic transmission and plasticity. J Neurosci 29:12982-12993.

Kramár EA, Babayan AH, Gavin CF, Cox CD, Jafari M, Gall CM, Rumbaugh G, Lynch G (2012) Synaptic evidence for the efficacy of spaced learning. Proc Natl Acad Sci U S A 109:5121-5126.

Larson J, Lynch G (1988) Role of N-methyl-D-aspartate receptors in the induction of synaptic potentiation by burst stimulation patterned after the hippocampal theta-rhythm. Brain Res 441:111-118.

Lin B, Kramár EA, Bi X, Brucher FA, Gall CM, Lynch G (2005) Theta stimulation polymerizes actin in dendritic spines of hippocampus. J Neurosci 25:2062-2069.

Lisman J, Yasuda R, Raghavachari S (2012) Mechanisms of CaMKII action in long-term potentiation. Nat Rev Neurosci 13:169-182.

Lynch G, Baudry M (1984) The biochemistry of memory: a new and specific hypothesis. Science 224:1057-1063.

Lynch G, Larson J, Kelso S, Barrionuevo G, Schottler F (1983) Intracellular injections of EGTA block induction of hippocampal long-term potentiation. Nature 305:719-721.

Mukai H, Kimoto T, Hojo Y, Kawato S, Murakami G, Higo S, Hatanaka Y, Ogiue-Ikeda M (2010) Modulation of synaptic plasticity by brain estrogen in the hippocampus. Biochim Biophys Acta 1800:1030-1044.

Park DK, Stein IS, Zito K (2022) Ion flux-independent NMDA receptor signaling. Neuropharmacology 210:109019.

Rex CS, Chen LY, Sharma A, Liu J, Babayan AH, Gall CM, Lynch G (2009) Different Rho GTPase-dependent signaling pathways initiate sequential steps in the consolidation of long-term potentiation. J Cell Biol 186:85-97.

Sun Y, Xu Y, Cheng X, Chen X, Xie Y, Zhang L, Wang L, Hu J, Gao Z (2018) The differences between GluN2A and GluN2B signaling in the brain. J Neurosci Res 96:1430-1443.

Wang W, Kantorovich S, Babayan AH, Hou B, Gall CM, Lynch G (2016) Estrogen's Effects on Excitatory Synaptic Transmission Entail Integrin and TrkB Transactivation and Depend Upon β1-integrin function. Neuropsychopharmacology 41:2723-2732.
Wang W, Le AA, Hou B, Lauterborn JC, Cox CD, Levin ER, Lynch G, Gall CM (2018) Memory-Related Synaptic Plasticity Is Sexually Dimorphic in Rodent Hippocampus. J Neurosci 38:7935-7951.
Zhu G, Liu Y, Wang Y, Bi X, Baudry M (2015) Different patterns of electrical activity lead to long-term potentiation by activating different intracellular pathways. J Neurosci 35:621-633.